

International Council of Scientific Unions

Scientific Committee on Oceanic Research

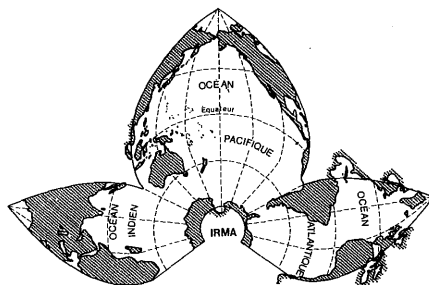
Royal Academy of Belgium

National Committee of Oceanology

Progress in Belgian Oceanographic Research

(Brussels, January 21–22, 1993)

Published with the support of the Royal Academy of Belgium
and the Ministry of Public Health and Environment by the
Institute of Marine Research and Air Sea Interaction (IRMA)



This volume of *Progress in Belgian Oceanographic Research* is dedicated to Professor Ivan Elskens, a pioneer of the development and success of oceanographic research in Belgium and a very dear friend.

Table of Contents

Pierre BRASSEUR and Jean-Michel BRANKART, <i>Reconstruction of Oceanic Data Fields and Data Assimilation</i>	9
J.M. BECKERS, J. HAUS, J.C.J. NIHOUL, R. SCHOENAUEN <i>Results of Metagnostic (system-oriented) and Diagnostic (process-oriented) Models</i>	23
É.J.M. DELHEZ, G. LACROIX, G. MARTIN, J.C.J. NIHOUL and R.A. VARELA <i>Development of Interdisciplinary Models of Ecosystems under Severe Hydrodynamic Constraints</i>	37
Jean LANCKNEUS, Guy DE MOOR, Linde VANDE VELDE, Els DE WINNE, Isabel SANCHEZ ALMAZO and Teresa GARRIDO MARTÍN <i>Morphodynamics and Sediment Dynamics in the Southern Bight, Belgium</i>	55
J. LANCKNEUS, G. DE MOOR, V. VAN LANCKER and G. DE SCHAEPMEESTER <i>The Use of the McLaren Model for the Determination of Residual Transport Directions on the Gootebank, Southern North Sea</i>	75
Patric JACOBS and Erwin SEVENS <i>Eocene Siliciclastic Continental Shelf Sedimentation in the Southern Bight North Sea, Belgium</i>	95
H. VAN MALDEREN, L. DE BOCK, J. INJUK, Ch. XHOFFER and R. VAN GRIEKEN <i>North Sea Aerosol Characterization by Single Particle Analysis Techniques</i>	119
M. ELSKENS, L. CHOU, P. DAUBY, M. FRANKIGNOULLE, L. GOEYENS, M. LOIJENS and R. WOLLAST <i>Primary Production and Nutrient Fluxes in the Gulf of Biscay</i>	137
Michel FRANKIGNOULLE, Marc ELSKENS, Michèle LOIJENS and Patrick DAUBY <i>Seawater pCO₂ Distribution and Air-Sea CO₂ Exchanges on the Atlantic European Shelf</i>	159
Patrick DAUBY, Willy BAEYENS, Renzo BIONDO, Jean-Marie BOUQUEGNEAU, Lei CHOU, Olivier COLLETTE, Frank DEHAIRS, Marc ELSKENS, Michel FRANKIGNOULLE, Michèle LOIJENS, Hugues PAUCOT and Roland WOLLAST <i>Distribution of particulate trace elements in the Northeastern Atlantic</i>	171
Jacques C.J. NIHOUL, P. ADAM, S. DJENIDI and É. DELEERSNIJDER <i>Modelling the Coastal Ocean's Complex Ecohydrodynamics. A case study: the Northern Bering Sea</i>	203

O. HAMERLYNCK, J. MEES, J.A. CRAEYMEERSCH, K. SOETAERT, K. HOSTENS, A. CATTRISSE and P.A. VAN DAMME <i>The Westerschelde Estuary: two Food Webs and a Nutrient Rich Desert</i>	217
J.-H. HECQ, P. BRASSEUR, A. GOFFART, G. LACROIX and L. GUGLIELMO <i>Modelling Approach of the Planktonic Vertical Structure in Deep Austral Ocean. The Example of the Ross Sea Ecosystem</i>	235
Anne GOFFART and J.H. HECQ <i>Control of Phytoplankton Development by Nitrate Availability in the Liguro-Provençal Basin (Western Mediterranean)</i>	251
J. GODEAUX <i>The State of the Art of Plankton Research in two Hyperhaline Bodies of Water, the Levantine Basin and the Arabian Gulf</i>	263
List of Participants	277
Program	285

Reconstruction of Oceanic Data Fields and Data Assimilation

Pierre BRASSEUR and Jean-Michel BRANKART

GHER, University of Liège

Abstract.

In the new generation of models conceived to understand and predict the evolution of marine systems, the assimilation of observations has an increasingly significant role to play. The reconstruction of data fields from scattered observations, or data analysis, appears as a key component of any complex data assimilation scheme. This strategy has promising implications, not only for physical, but also for biological, ecological and biogeochemical marine models.

Among a variety of methods, the Variational Inverse Model (VIM) is a mathematical/numerical analysis tool developed at the GHER with the aim of taking into account the peculiarities of oceanic data fields. The objectives of this new technique are multifold: on the one hand, it guides the interpretation of experimental data into their physical context; on the other hand, it provides the indispensable bodyguard that prevents primitive equation models from producing unrealistic results. The utility of the VIM in a global modelling perspective will be illustrated by three kinds of applications related to the modelling of the Mediterranean general circulation:

- (i) mathematical visualization of extensive sets of *in situ* observations (reconstruction of the hydrology at the climatological scale in the Mediterranean Sea);
- (ii) realistic initialization of primitive equation models designed to simulate dynamical processes (seasonal variability of the general circulation in the Western Mediterranean);
- (iii) optimal adjustment of boundary conditions (control of thermodynamic forcings in the Mediterranean);

The possible extensions of the VIM to intermittent and continuous data assimilation schemes will be discussed briefly.

1.— Introduction: why do ocean models need efficient analysis methods?

The assimilation of observations is more and more considered as an essential ingredient of most up-to-date ocean models (Robinson and Leslie, 1985). The reason of that tendency is quite evident: whatever the degree of sophistication reached, a series of deficiencies and weaknesses inevitably affect numerical models. Indeed, simplifications of the real world are required to make numerical models effective and tractable. On the other hand, the volume of oceanic observations has increased substantially, namely since more and more satellites are providing the scientists with high-resolution sea-surface properties (elevation, temperature, roughness, wind stress, ...).

The imperfections of models may have different sources: (i) structural undeterminations, when the structure of the model equations has been simplified, leaving some processes — unimportant at first insight — misrepresented; the hydrostatic assumption made in a majority of circulation models is a typical example of structural deficiency; (ii) statistical undeterminations, when the data base used to pilot the system's behaviour is inadequate, for instance when initial and boundary conditions, or even auxiliary parameters of the model, are poorly known (Wunsch, 1989).

For a given structure of the model equations, the model trajectory in the phase space depends on: (i) the initial conditions from which the evolution of the system starts, (ii) the boundary conditions used to reflect how the system interacts with the external world, and (iii) the various numerical parameters of the model equations. The trajectory will be different if one of these three types of settings is changed.

Usually, additional sets of observations relevant to the system itself are available, although not in a form suitable for direct integration in the model. On the one hand, initial and boundary conditions are seldom “observed” in the real ocean, as well as auxiliary parameters such as those taking place in a turbulent closure scheme. On the other hand, some state variables can be estimated from direct observations, but only within a certain accuracy. These estimations are indicative of the real trajectory of the model in the phase space.

Broadly speaking, data assimilation relates to techniques conceived to improve our estimation of the optimal trajectory in the phase space, taking into account both the model results and the direct observations on the state variables. It is customary to distinguish between variational and recurrent data assimilation schemes (Ghil and Malanotte-Rizzoli, 1991).

There are indeed two possibilities to approach the real trajectory. Variational data assimilation determines the “best” initial and boundary conditions, as well as the best model parameters, which are supposed to produce an optimal

trajectory, fitting the observations as much as possible. For instance, the adjoint technique, developed initially for meteorological applications, is a relatively complex and time consuming method: it requires the repeated integration of the model, forward and backward in time, in order to minimize some cost function measuring the distance between the trajectory and the observations.

Recurrent data assimilation schemes, like the well-known Kalman filter, proceeds differently: after a certain time integration of the model, the forecast is corrected according to the observed state of the system, producing in this way the best possible guess. This new guess is then used to reinitialize the model for a further time integration. The successive corrections, to be meaningful, require that both the model forecast and the observations are provided with a confidence level testifying their mutual accuracy.

The reconstruction of data fields from scattered observations, or data analysis, appears as a key component of any complex data assimilation scheme. Indeed, to operate one of the procedures mentioned hereabove, it is necessary to estimate, at the time of assimilation, the point in the phase space which is most consistent with the observations. Typically indeed, the observations provide only a fragmentary picture of the system, leaving some state variables unexplored. The purpose of data analysis, which is effectively a nowcasting procedure, is to reconstruct—from scattered observations—a comprehensive picture of the system's state at a given time.

Among various methods, the Variational Inverse Model (VIM) is a mathematical/numerical analysis tool derived from meteorological studies and adapted to the ocean at the GHER. The objectives of this new technique are multifold: on the one hand, it guides the interpretation of experimental data into their physical context; on the other hand, it provides the indispensable bodyguard that prevents primitive equation models from producing unrealistic results.

The mathematical formulation of the VIM has been developed in Brasseur (1990), Brasseur and Haus (1991) and Brasseur *et al.* (1993), and is summarized in table 1. Compared to standard objective analysis methods, the VIM has the major advantage of taking into account the peculiarities of oceanic domains and processes (introducing, for instance, the possibility of anisotropic correlation functions via kinematic constraints). Three different classes of applications will be described hereafter (only a few samples of the results produced by VIM will be shown here).

Table 1

Mathematical formulation of the Variational Inverse Model (VIM),
described in details in Brasseur (1991) and Brasseur and Haus (1991)

$$\begin{aligned}
 \bar{\varphi}(x_i, y_i, z_k) &\simeq d_i^k, & i &= 1, \dots, N_d^k \\
 \varphi(x, y, z_k) &= \varphi_k(x, y) = \sum_{m=1}^{N_m} q_m^k w_m(x, y) \\
 \Rightarrow \min J_k[\varphi_k(x, y)] &= \int \int_{\mathcal{D}} \{D^k[\varphi_k] + S[\varphi_k] + C^k[\varphi_k]\} dx dy \\
 D^k[\varphi_k] &= \frac{S}{N_d^k L^4} \sum_{i=1}^{N_d^k} \mu_k [\varphi_k(x, y) - d_i^k]^2 \delta(x - x_i) \delta(y - y_i) \\
 S[\varphi_k] &= \left(\frac{\partial^2 \varphi_k}{\partial x^2} \right)^2 + \left(\frac{\partial^2 \varphi_k}{\partial y^2} \right)^2 + 2 \left(\frac{\partial^2 \varphi_k}{\partial x \partial y} \right)^2 + \frac{\beta_1}{L^2} \left(\frac{\partial \varphi_k}{\partial x} \right)^2 + \frac{\beta_1}{L^2} \left(\frac{\partial \varphi_k}{\partial y} \right)^2 + \frac{\beta_0}{L^4} \varphi_k^2 \\
 C^k[\varphi_k] &= \frac{\gamma_k}{U^2 L^2} \left[u_k \frac{\partial \varphi_k}{\partial x} + v_k \frac{\partial \varphi_k}{\partial y} - \lambda \frac{\partial^2 \varphi_k}{\partial x^2} - \lambda \frac{\partial^2 \varphi_k}{\partial y^2} \right]^2
 \end{aligned}$$

2.- Data analysis and visualization of oceanic data fields.

One of the first motivations of data analysis is the “mathematical” or “scientific” visualization of huge observed data sets. Indeed, from a collection of historical data, it is necessary to reduce the information to only a few visible properties, highly suggestive and reflecting the global behaviour of the marine system. The aim of the example described below was to produce a three-dimensional numerical representation of the hydrology in the Mediterranean.

During the last decade, a lot of numerical and experimental studies have been conducted in the Western Mediterranean to identify and diagnose regional processes: among them, the deep water formation taking place in the Gulf of Lions at the end of the winter, the instability of the Algerian Current, the anticyclonic circulation associated with the Alboran Sea gyre, the exchange of water, heat and salt through the Gibraltar and Sicily straits, ... A vast amount of *in situ* measurements (mainly hydrographic data) emerged from the surveys of these local processes.

However, no exhaustive historical data bank has been compiled up to now with all *in situ* data collected in the Mediterranean Sea. Two major files containing a substantial part of the experimental work are available for the purposes of this study: the french BNDO (Bureau National des Données Océaniques, Brest, France) file containing exclusively hydrographic casts for the Mediterranean region, and the NODC (National Oceanographic Data Center, Washington, USA) file which is a subset of a larger world ocean data bank. These

two major sources have been merged to constitute the so-called MED data bank, and other smaller data sets, collected by regional institutions, will be considered for possible upgrade in the future.

The BNDO data set consists of about 17,000 STD casts taken in the Eastern and Western basin, the Black Sea and also the Atlantic region adjacent to the Strait of Gibraltar. These measurements were collected since 1911, but the data set is mainly representative of the period 1945–1978. The data point distribution is highly inhomogeneous in space and in time. In the Western basin, a lot of

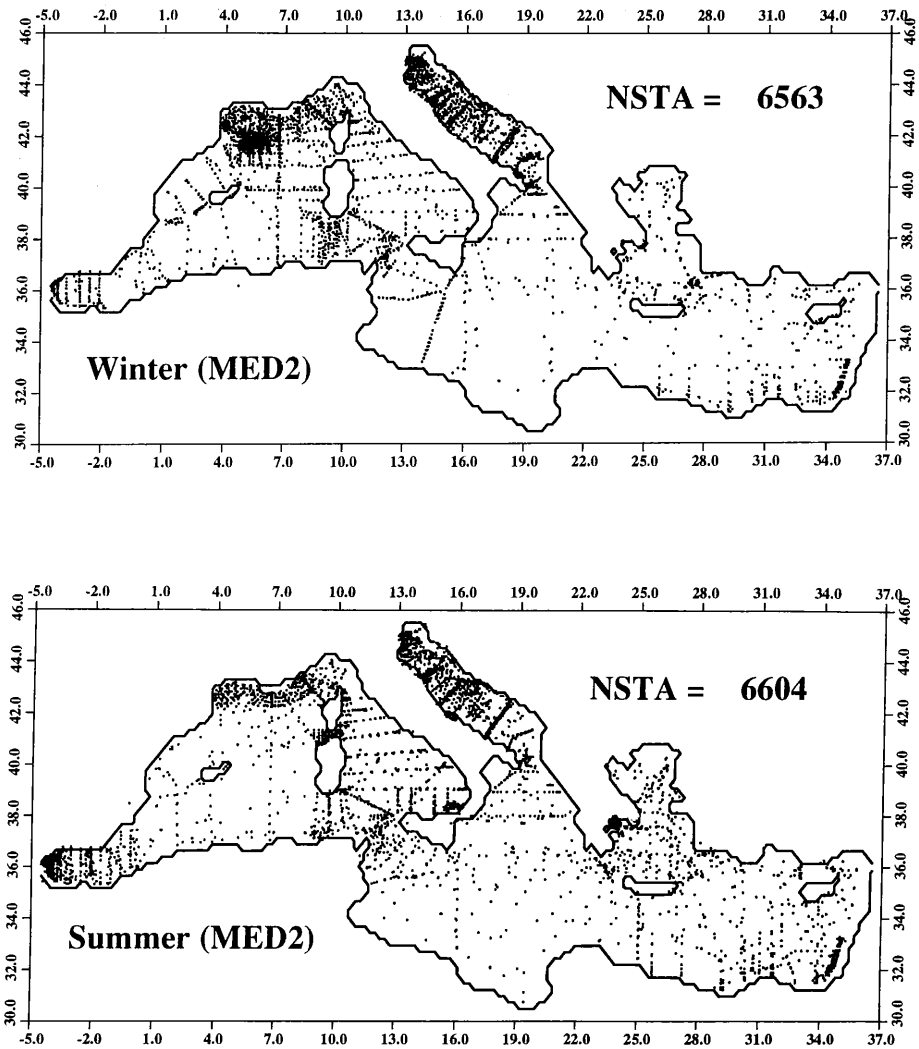


Fig. 1.— Spatial distribution of STD/CTD casts in the Mediterranean from 1911 to 1980, as recorded in the BNDO and NODC data banks: upper = winter, lower = summer.

stations are located in the Gulf of Lions during February, as a consequence of the survey of deep water formation processes. However, the density of data collected during the autumn and the winter is rather low, especially in the Eastern basin.

In the BNDO file, the temperature and salinity measurements are given at the original sampling depths, but in the NODC file, which contains more than 20,000 vertical profiles, the values are interpolated at standard levels. The coverage of the Eastern basin from NODC is much better than from the BNDO data file, as well as the southern part of the western basin, along the algerian coast. Even if some overlap exists between the two sets, the different spatial and temporal station distributions are complementary, so that one can expect a better representation of the hydrology from a merged version of the two original files.

The spatial distribution of data available at 10 m depth (for the winter and summer periods only) is shown in figure 1. The VIM has been applied to this data set to reconstruct the three-dimensional hydrological field in the Eastern and Western Mediterranean basin (annual-mean distribution). The trace of the temperature and salinity fields at 10 m depth is illustrated in figure 2. This picture could be considered as a climatological reference and should be compared (or, tentatively, assimilated) to the results of general circulation models.

Although very schematic, the patterns of figure 2 represent a synthetic view of the hydrology, obtained from the experimental work achieved sofar in the Mediterranean: this picture provides indeed a global and consistent representation of the hydrology, after reconstruction from numerous pieces of information.

More complex visualisation tools (three-dimensional color graphics, video-animations, ...) can also be used to highlight the 3 D structures appearing in the reconstructed fields (Haus, 1993): these technical tools are extremely useful to explore in details the interior of the ocean. Since the new generation of powerstations, the joined utilisation of efficient analysis procedures and scientific visualisation software will offer the possibility of a deeper exploitation of direct and remote observations.

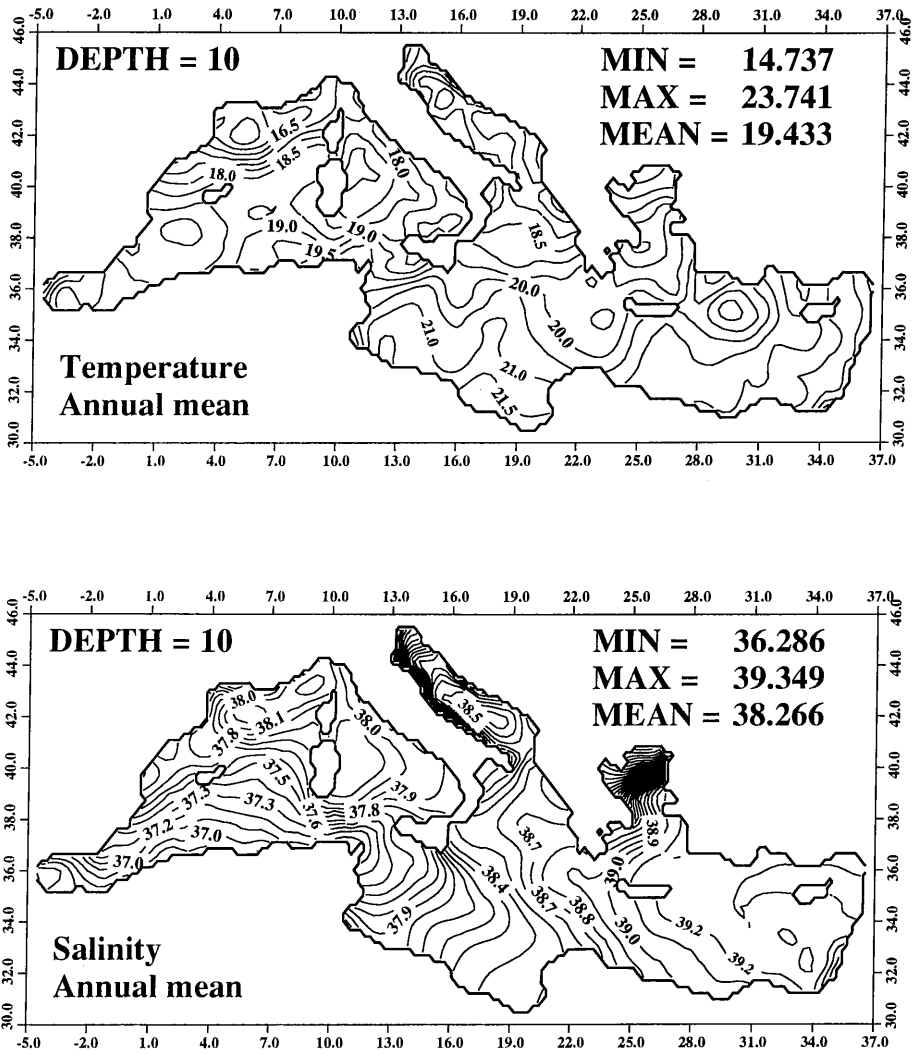


Fig. 2.— Temperature and salinity fields in the Mediterranean at 10 m depth (annual-mean distribution), reconstructed by the VIM from historical data.

3.— Data analysis and initialization of numerical models.

According to the classical picture, the Mediterranean sea can be considered as a “concentration” basin, where evaporation exceeds precipitation and river runoff. The budgets of salt and water masses are balanced by the inflow of Atlantic Water (AW) in the surface layer and the outflow of a mixture of Levantine Intermediate Water (LIW) and Mediterranean Deep Water (MDW)

through the Strait of Gibraltar. The mass of LIW originates in the Levantine region, enters the Western basin through the Sicilian Channel and then circulates at mid-depth between the light, modified AW and the pool of dense, deep water. The formation of MDW is subject to typical conditions encountered in the Gulf of Lions in late winter.

Within this very simple scheme however, the WMCE studies indicate a more complex circulation (La Violette, 1990). In particular, some features of the circulation display a strong seasonal signal and variability. One critical question concerns the main physical forcing mechanisms responsible for that behaviour.

As deep water formation is often thought to be one of the possible forcing mechanisms of the general circulation, the utilisation of numerical models based on the hydrostatic approximation (*e.g.*, Beckers, 1992) could be questioned. In the case of the Mediterranean, such approximations could actually prevent the models from reproducing some non-hydrostatic features of the circulation (or, at least, could imply an extremely long spin-up period) if the model initial conditions are too different from the real situation. For instance, if initial fields are characterized by a too weak stratification, vertical mixing, diffusion and deep water formation could be inhibited.

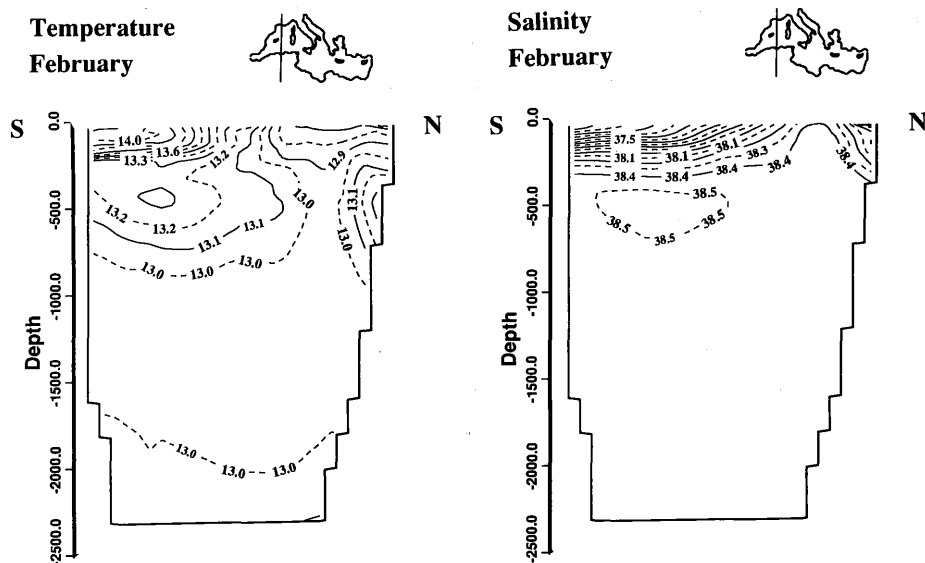


Fig. 3.— Vertical cross-section in the Western Mediterranean (South to North, longitude = 5° E); temperature (left) and salinity (right) fields reconstructed from data representative of the February month.

To avoid this problem, the VIM has been applied to monthly data sets to reconstruct realistic temperature and salinity fields, representative of one specific

period of the year. The February month is classically used to start a simulation, since the MED data bank has a very good coverage for that period. Figure 3 shows a vertical cross-section in the temperature and salinity fields through the Gulf of Lions: the analysis of *in situ* observations clearly demonstrates that the stratification is very weak in the Northern Mediterranean for that period.

These fields are injected as initial conditions in the GHER primitive equation model and are gradually adjusted to the surface heat and momentum fluxes. Beckers (1992) has shown that the response of the model initiated with monthly VIM results is much better than with annual mean fields (like those produced by Levitus, 1982).

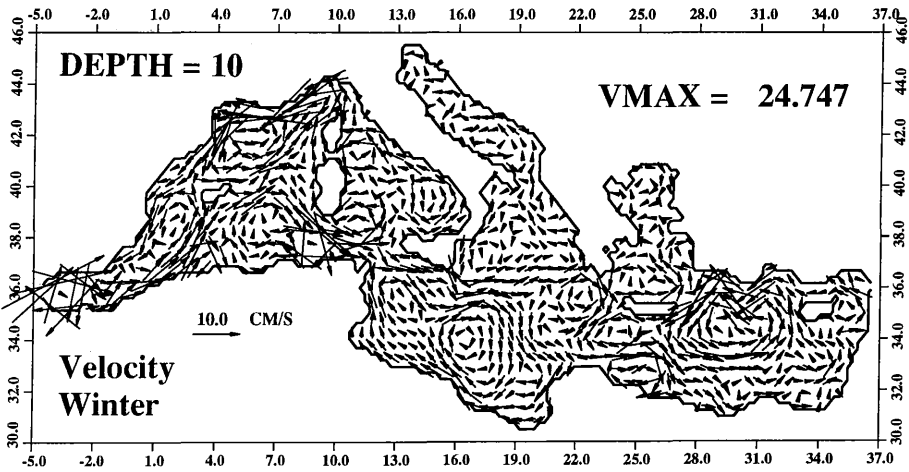


Fig. 4.— Geostrophic currents calculated from the winter density field (10 m depth). This advection pattern is subsequently used as kinematic constraint in the VIM.

Using the method proposed by Beckers and Brasseur (1993), the geostrophic currents are finally calculated from the winter density field (figure 4). Then, the advection constraint of the VIM can be implemented for improving the analysis procedure, especially in regions where the data distribution is very sparse.

4.- Data analysis and estimation of optimal boundary conditions.

Another weakness of numerical models concerns the sea-surface boundary conditions: heat fluxes, for instance, are often poorly known and their parameterization remains rather approximative. However, if *in situ* observations are reliable enough to reproduce the seasonal cycle of the temperature field in the upper layer, it is possible to estimate the distribution and intensity of heat fluxes which could reproduce the observed thermal field: this is typically an inverse problem.

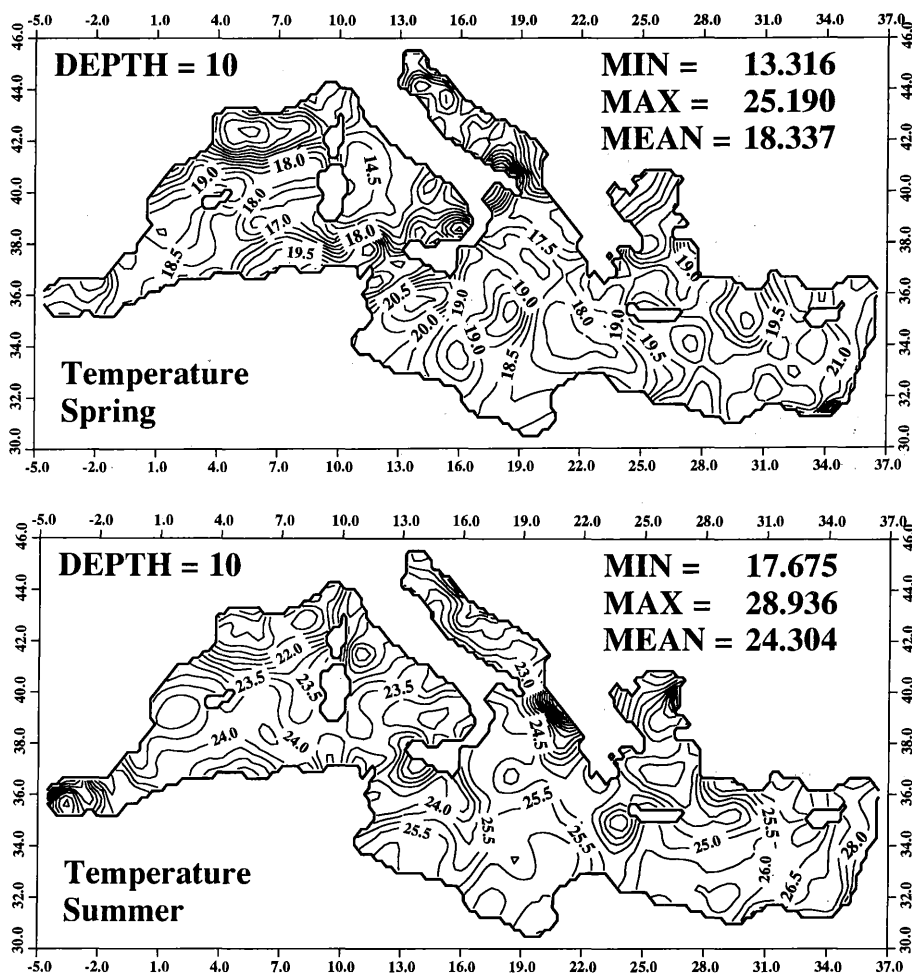


Fig. 5.- Seasonal cycle of the temperature field (10 m depth) in the Mediterranean reconstructed from *in situ* observations; snapshots representative of Spring and Summer.

As a tentative data assimilation experiment, the VIM has been used to reconstruct the seasonal cycle of the thermal field in the upper layer of the Mediterranean. Figures 5 and 6 shows four snapshots of the seasonal temperature field at 10 m depth in the Mediterranean. These VIM analyses have been exploited as a control of the surface heat fluxes in the primitive equation model (Beckers, 1992): when the surface temperature predicted by the model is lower (higher) than the observed values, heat fluxes are increased (reduced). This method, proposed by Beckers (1992), has been successfully applied to study the seasonal variability of the circulation in the Mediterranean. In particular, the predictions of the model with data assimilation

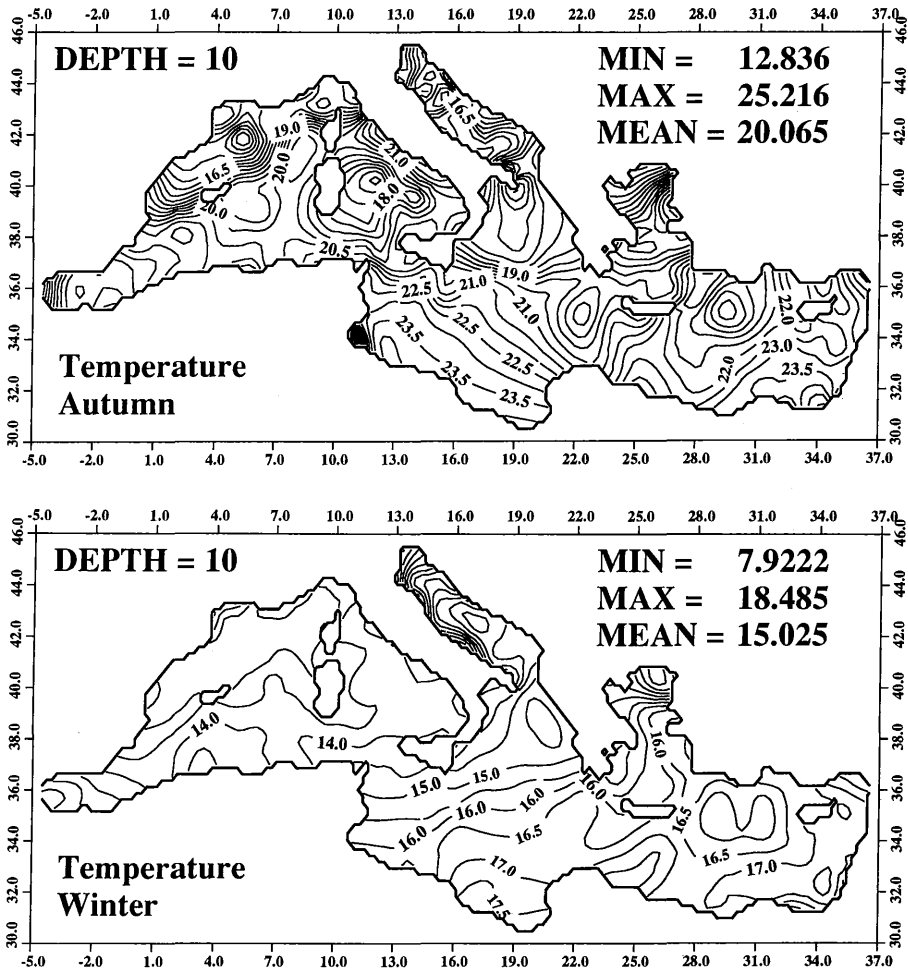


Fig. 6.– Seasonal cycle of the temperature field (10 m depth) in the Mediterranean reconstructed from *in situ* observations; snapshots representative of Autumn and Winter.

are in excellent agreement with the SSTs provided by remote sensing photographs.

Other applications of data analysis, in relation with model boundary conditions, could be investigated. For instance, the question of mass exchange through the Strait of Gibraltar is still under study. As climatological data are available in the Atlantic region adjacent to the Mediterranean basin, a numerical buffer zone just in front of the Gibraltar Strait could be introduced to match the model with climatological observations. In the case of narrow straits, this approach seems to give better results than the traditional open-sea boundary conditions.

5.— Conclusions.

Three different applications of a variational procedure for analysing oceanic data have been described in the context of the Mediterranean basins. The reconstruction of 3 D physical fields offers now the opportunity of more complex data assimilation systems. The main problem to solve remains the estimation of 3 D error fields, in order to make the data/model blending as consistent as possible.

The nudging of physical variables into primitive equation model is now under investigation: this quite simple assimilation scheme will allow the dynamic insertion of hydrographic data in the ocean's interior, in addition to the optimization of initial and boundary conditions.

Other perspectives are also foreseen: for instance, the availability of altimetric measurements from newly operational satellites (TOPEX-POSEIDON) will have an undisputable interest for controlling the sea surface elevation predicted by non rigid-lid models. The question how altimeter observations must be pre-processed and spatially interpolated before their actual assimilation into primitive equation model is far from being completely solved.

Acknowledgements.

The authors are very grateful to Dr. P.W. May for kindly providing his data on the atmospheric mechanical and thermodynamical forcing in computer usable form. The authors are indebted to the Ministry of Education and Research, the Ministry for Science Policy, the National Fund for Scientific Research (Belgium) and *IBM* for their financial and technical assistance in providing supercomputers facilities. The financial support of the European Communities in the scope of the program MAST-0043-C and MAS2-CT92-0041 (EUROMODEL) and the "EROS 2000" (European River Ocean System) project (contract EV4V-0111-F) is greatly acknowledged.

References.

- BECKERS, J.M. (1991). Application of a 3D model to the Western Mediterranean, *J. Mar. Syst.*, 1:315–332.
- BECKERS, J.M. (1992). *La Méditerranée occidentale : de la modélisation mathématique à la simulation numérique*, Ph.D. Dissertation, Liège University, 342 pp.
- BECKERS, J.M. and BRASSEUR, P. (1993). A New Method for Computing Optimal Geostrophic Currents, submitted to *J. Phys. Oceanogr.*
- BRASSEUR, P. (1991). A Variational Inverse Method for the Reconstruction of General Circulation Fields in the Northern Bering Sea, *J. Geophys. Res.*, 96 (C3), 4891–4907.
- BRASSEUR, P. and HAUS, J. (1991). Application of a Three-Dimensional Variational Inverse Model to the Analysis of Ecohydrodynamic Data in the Bering and Chuckchi Seas, *Journal of Marine Systems*, 1:383–401.
- BRASSEUR, P., BRANKART, J.M. and BECKERS, J.M. (1993). General Circulation in the Mediterranean Sea Reconstructed from Historical Data, in preparation for *J. Phys. Oceanogr.*
- GHIL, M. and MALANOTTE-RIZZOLI (1991). Data Assimilation in Meteorology and Oceanography, *Advances in Geophysics*, 33:141–265.
- HAUS, J. (1993). Visualisation of Real and Simulation Data in Physical Oceanography, *Proceedings of the BCS Conference on "Animation and Scientific Visualisation"*, IBM UK Scientific Center, UK.
- LA VIOLETTE, P.E. (1990). The Western Mediterranean Circulation Experiment (WMCE): Introduction, *J. Geophys. Res.*, 95 (C2), 1511–1514.
- ROBINSON, A.R. and LESLIE, W.G. (1985). Estimation and Prediction of Oceanic Fields, *Progr. Oceanogr.*, 14:485–510.
- WUNSCH, C. (1989). *Tracer Inverse Problems*, in: D.L.T. Anderson and J. Willebrand (Editors), *Oceanic Circulation Models: Combining Data and Dynamics*, Kluwer Academic Publishers, 605 pp.

Results of Metagnostic (system-oriented) and Diagnostic (process-oriented) Models

J.M. BECKERS, J. HAUS, J.C.J. NIHOUL, R. SCHOENAUEN

GHER, University of Liège

Abstract.

After a review of the Mediterranean system, and the justification of the scientific interest, we examine the type of model (scope, purview and resolution) used for the description and simulation of the Mediterranean circulation from a system-oriented view and a process-oriented view. These two aspects of mathematical simulations are then illustrated by two examples:

- a) The simulation of the month to month variability of the general circulation in the Western Mediterranean Sea shows the main physical features, but the choice of initial conditions is crucial for a realistic simulation, and an inverse model is proven to be absolutely necessary for a valuable prognostic model.
- b) Secondly, a high resolution simulation of the Algerian Current instability is performed. It is well known that the Atlantic water flows along the Algerian coast as a light water intrusion. This current is unstable, and mesoscale activities generate cyclones and anticyclones, but only the latter grow enough to get separated from the mean flow. Numerical simulations, in an idealized case, and reality show strong instabilities that are analyzed by energy budgets. It is suggested that the instabilities are primarily baroclinic, which is consistent with initial vertical movements at the front.

1.- Introduction.

Mathematical models of the marine system have considerably evolved since the early days of the hydrodynamic depth-integrated constant viscosity models of tides and storm surges on the shelf or the quasi-geostrophic models of ocean circulation in idealized basins.

Improvements include (i) progressive confluence of shelf and ocean models with in particular the extension of the former to three dimensions and the rallying of the latter to primitive equations, (ii) expansion of hydrodynamic models to biogeochemical and ecosystem models, (iii) refined parameterization of sub-grid

scale processes, in particular turbulent vertical diffusion, introducing new state variables like the turbulent kinetic energy k (e.g. Nihoul *et al.*, 1989), (iv) refined numerical methods and algorithms on supercomputers.

At this stage, one can rely on sound 3D $k - \ell$ models able to describe the so-called “weather” of the sea, from mesoscale processes like tides and storm surges, inertial oscillations, diurnal cycles (time scale: from a few hours to a few days) to synopticscale and macroscale processes like general circulation currents, seasonal cycles and associated frontal structures, upwellings, deep convection (time scales: from a few days to a few months).

Such a robust model, however, even restricted to its hydrodynamic sector, has a minimum of seven state variables: the three components of the velocity vector \mathbf{v} , pressure p , buoyancy b (or salinity S), temperature T and the turbulent kinetic energy k , described by time-dependent 3D partial differential equations.

It raises the questions of (i) the size of the database necessary to provide 3D initial and boundary conditions (see also the paper of Brasseur and Brankart, 1993, this volume), (ii) the required amount of computing power and the difficulty of designing simple, relevant, numerical tests, (iii) the volume of simulation outputs and the need to “sample” them intelligently, with the objectives of the model in mind.

Faced with all these difficulties, one is naturally tempted to simplify the model. But one can easily burn one’s fingers over drastic simplifications, made too lightly for the purpose of mathematical or numerical tests.

A sensible approach to the problem of reducing the size of the model is the restriction to the diagnostic study of one or a few, isolated and idealized, processes. Devised to investigate, in details, particular mechanisms, scrutinize the behaviour of specific state variables, elucidate fundamental questions ..., often very refined in their representation of, sometimes, rather subtle processes, *diagnostic* models are frequently content with very crude approximations of the physical world (constant depths, rectilinear coasts, infinite ocean, steady two-dimensional fronts, rigid sea surface, ...). In brief, the reduction, in this case, bears on the model’s ambition and realism, trying to conserve the “physical insight” of the process study.

Advantages of diagnostic models are readily listed: (i) reduced dependence on initial and boundary conditions, (ii) reduced computing cost of numerical tests and simulations, (iii) reduced complexity of simulation’s outputs, easier interpretation of results and better understanding of the process (at least, in its idealized form).

Disadvantages are quite as easily pointed out: (i) risk of misunderstanding the real process if it actually results from several interacting effects, (ii) risk, if

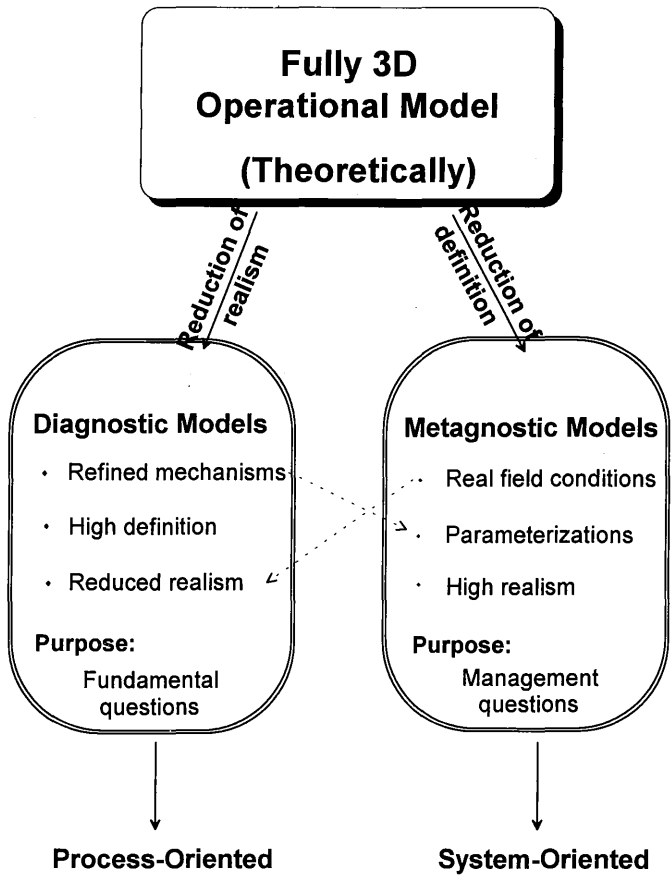


Fig. 1.– Diagnostic and metagnostic versions of a mathematical model.

the realism is prohibitively reduced, in applying the model's equations—which have been calibrated with real field data—to an idealized system to which they are not, actually, applicable, (iii) loss of accuracy and loss of pertinence to the questions posed to the physicists by co-workers in other disciplines and managers which were, probably, the initial motivations of the modelling enterprise.

Answer to these questions must be realistic and require the operation, on a routine basis, of a system-oriented (as opposed to process-oriented) *metagnostic* model.

Called upon to tackle a practical situation, a metagnostic model may not ignore real field conditions (depths, coastlines, actual atmospheric forcing, ...). Its aim however is to assess the consequences of particular events and provide the marine nowcasts and forecasts which will assist interdisciplinary field studies, planning and management. The model must be sound, expeditious and efficient

but is not required to provide detailed information on the delicate machinery subtending its parameterization scheme.

Advantages of a metagnostic model are obvious but its disadvantages should not be ignored: the critical need of many—many more than for process studies—reliable data to *calibrate*, *initiate* and *operate* the model and, accordingly, its unavoidable sensitivity to the quality as well as the quantity of the available data. The realism of a metagnostic model may be paid—as a result of shortage of data and limitations of computing facilities—by a reduction of the model’s definition and precision. Finally, the tremendous amount of data produced by such a model calls for an appropriate 3D visualization package.

In the present paper we will show two applications: one for the metagnostic approach, and the second for the diagnostic approach. These two different ways are summarized on figure 1.

2.— Methods and models.

The mathematical model on which rely the diagnostic and metagnostic versions, is a general primitive equation model with turbulent closure scheme based on the kinetic turbulent energy and an algebraic mixing length (depending on the local stratification) approach (*e.g.* Nihoul, 1988; Nihoul *et al.*, 1989).

The subsequent numerical resolution is prepared by a coordinate change that is a generalization of the classical σ -coordinate change (*e.g.* Cheng and Sommerville, 1975; Deleersnijder, 1989). This coordinate change introduced by Kasahara (1974) and recently revisited by Deleersnijder and Ruddick (1993) allows for an easy transformation of the primitive equations towards a conservative form.

It also enables the use of for energy budgets in the transformed space. These budgets are similar to those found in Orlanski and Cox (1973), but in our case, the definition of the mean current is *a priori* not given (Beckers, 1992). One can indeed deduce evolution equations for mean kinetic energy, eddy kinetic energy, mean barotropic potential energy, eddy barotropic potential energy, mean available potential energy and eddy available potential energy, all energies being defined in Beckers (1992b). The corresponding energy transfers can then be used to define the baroclinic instability (Orlanski, 1968) that will be investigated in the second application.

Finally, concerning the numerical resolution method (Beckers, 1992b), the partial differential equations are solved by a variant of the finite difference technique: a finite volume method on the Arakawa C-grid allows indeed for an efficient conservative computing. A constraining feature is the presence

of the free surface. It has the advantage of enabling the model to deal with mesoscale processes, but surface gravity waves impose a time step (Beckers and Deleersnijder, 1993) that is small compared to the rest of the time scales involved. In order to avoid a prohibitive computational cost, a mode-splitting technique (e.g. Sheng *et al.*, 1978; James, 1986; Blumberg and Herring, 1987; Killworth *et al.*, 1991) is implemented by integrating the 2D equations with the small time step over several steps before integrating the 3D equations with a larger time step.

3.– Applications.

In order to illustrate the system-oriented and process-oriented type of study, two applications are representative.

3.1.– The General Circulation in the Western Mediterranean.

The GHER metagnostic model is presently being applied to the simulation of a complete annual cycle, using the climatological forcing provided by May (1982) and assimilating new data supplied by the joint application of objective analysis and inverse modelling (Roussenov and Brasseur, 1989; Brasseur and Brankart, 1993). A complete annual cycle in climatological conditions will hopefully provide a much better set of initial conditions, on which realistic

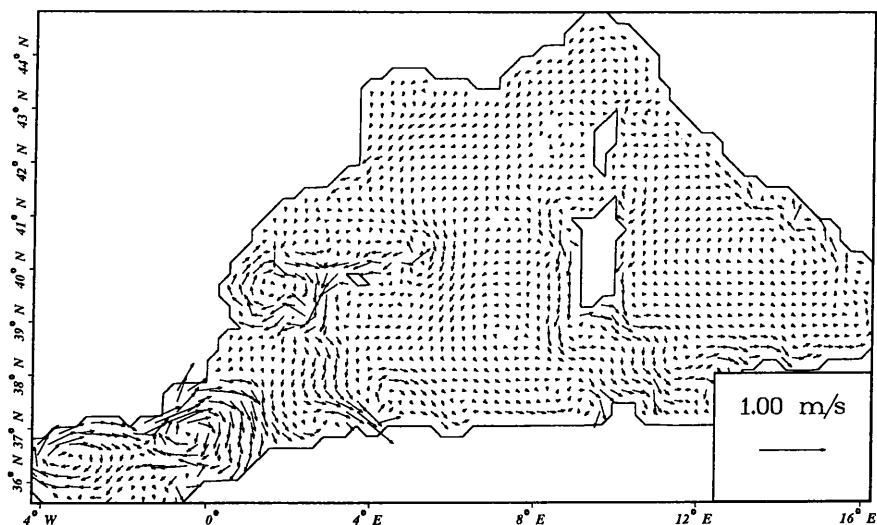


Fig. 2.– Surface currents in December, computed by the model.

metagnostic and prognostic modelling can be based. The model will then be run, on a routine basis, with boundary inputs supplied by a Meteorological Forecasting Model operated at the French Meteorological Office, with a view of exploiting the results, as a regular service in the scope of the EROS 2000 Project, to assist interdisciplinary field surveys, planning and management.

As a result of the excellent scope (*i.e.* the model's dimension in state space), the numerical grid is relatively coarse ($81 \times 47 \times 14$ grid points), but promising results have already been obtained with this grid. For example, the surface currents obtained for the month of December (figure 2) comply with the general idea of the circulation in the Western Mediterranean Sea: we can see the two anticyclonic gyres in the Alboran Sea, the generally cyclonic circulation in the central basin and the well defined Liguro-Provençal current.

A more quantitative comparison with observations can be based on mass fluxes through straits. As an example, figure 3 correlates the fluxes computed by the model and the measurements of Astraldi *et al.* (1990) in the Corsican Channel. The accordance between the two sources gives an idea of the potentialities of a metagnostic model, at least if accurate boundary and initial conditions are provided. The need of data is typical for metagnostic models, in opposition to the process-oriented studies as the following one.

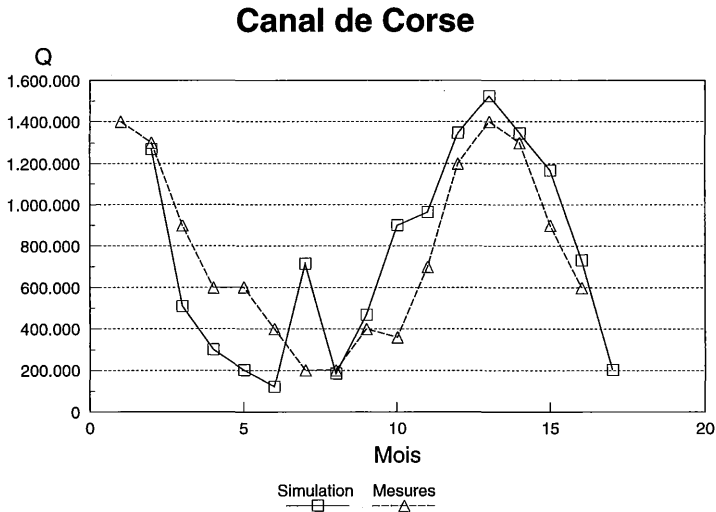


Fig. 3.— Comparison of computed fluxes through the Corsican Channel with the observations of Astraldi *et al.* (1990).

3.2.– The Algerian Current Instabilities.

In the general circulation pattern, one generally states that the Atlantic Water entering the strait of Gibraltar first exhibits an anticyclonic gyre in the western Alboran Sea. In the eastern Alboran Sea, a second and more variable anticyclonic gyre (Heburn and La Violette, 1990) leads to the Almeria-Oran front (Tintoré *et al.*, 1988). The fluctuations of the second gyre alter the fresh water flow that emerges from this gyre. Due to the Coriolis force, this creates a coastal current which is called the Algerian Current when he reaches 0° longitude. This Algerian Current is generally described as a narrow coastal current of less the 60 km width (*e.g.* Perkins and Pistek, 1990) which separates at the eastern Algerian coast. One branch flows then across the Sardinia and the Sicily strait, while the other one flows northward along the western coast of Sardinia.

But it is well known (*e.g.* Millot *et al.*, 1990), that the Algerian Current is subjected to various instabilities (especially in Summer) generating gyres which move eastward at a speed of a few kilometers per day. The anticyclones deviate the mean flow northward, which could explain the northern Balearic front (Millot, 1991). Afterward, the cyclones collapse, while the anticyclones grow to reach 100 km of diameter before they separate from the mean flow and propagate seaward.

The deviation from the nice relatively uniform coastal current has several significant consequences. Trivially, the spreading of Atlantic Water to the north modifies the hydrological situation, but more subtle interactions are possible with the underlying intermediate water that can be trapped at the bottom of one of those anticyclones (Millot *et al.*, 1990). It is also clear that the Algerian Current instabilities are of prime importance from an eco-hydrodynamic view. Indeed, the instabilities exhibit strong vertical motions that can be detected on satellite pictures (*e.g.* Arnone *et al.*, 1990). In the Algerian Current, for example, an upwelling is generally found upstream of the anticyclones (Martinez *et al.*, 1990).

In order to understand the evolution and effects of the Algerian Current, the question of the instability mechanism naturally arises and can be challenged by several methods.

A first insight in the instability mechanism can be achieved by using a reduced analytical gravity model (with a single moving upper layer). Several studies (*e.g.* Killworth and Stern, 1992; Paldor, 1982; Killworth, 1983; Paldor, 1983a, 1983b; Cushman-Roisin, 1985; Paldor and Ghil, 1990) show that criteria of instability or stability depend strongly on the initial base current. Furthermore, in the most simple case of a uniform coastal current, it has been shown that the current is stable in the scope of a reduced gravity model (Beckers, 1992a; Beckers

and Nihoul, 1992). This model doesn't seem very appropriate for the explanation of the Algerian Current instabilities.

It is thus tempting to look for another instability mechanism and turn towards the possibility of having a second moving layer that allow for baroclinic instabilities (e.g. Saltzman and Tang, 1975; Hart, 1979). The baroclinic instability mechanism has been put forward by Millot *et al.* (1990) to be responsible for the Algerian current's instabilities; this hypothesis has been supported by the laboratory experiments of Griffiths and Linden (1981), while other laboratory experiments (Chabert d'Hières *et al.*, 1992) suggest shear layer instabilities at the coast.

The aim of the present section is to prove that the instability of the Algerian Current is most probably due to the baroclinic instability mechanism. For this purpose, a numerical 3D primitive equation model is applied to a situation comparable to the one used in the analytical reduced gravity model of Beckers (1992a) and Beckers and Nihoul (1992). A uniform coastal surface current in a periodic channel (figure 4) is perturbed and the evolution of this perturbation computed by the model.

Figure 5 shows the surface currents exhibiting the propagating of wavelike features along the front in a first stage. The amplitude of this feature increases and leads to a detachment of the current from the coast where the wave has

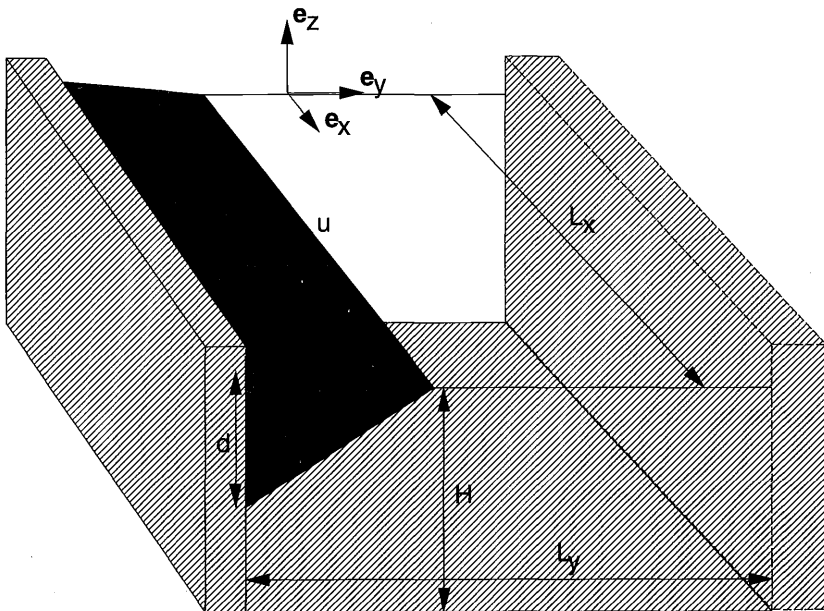


Fig. 4.— Base current whose stability is analysed.

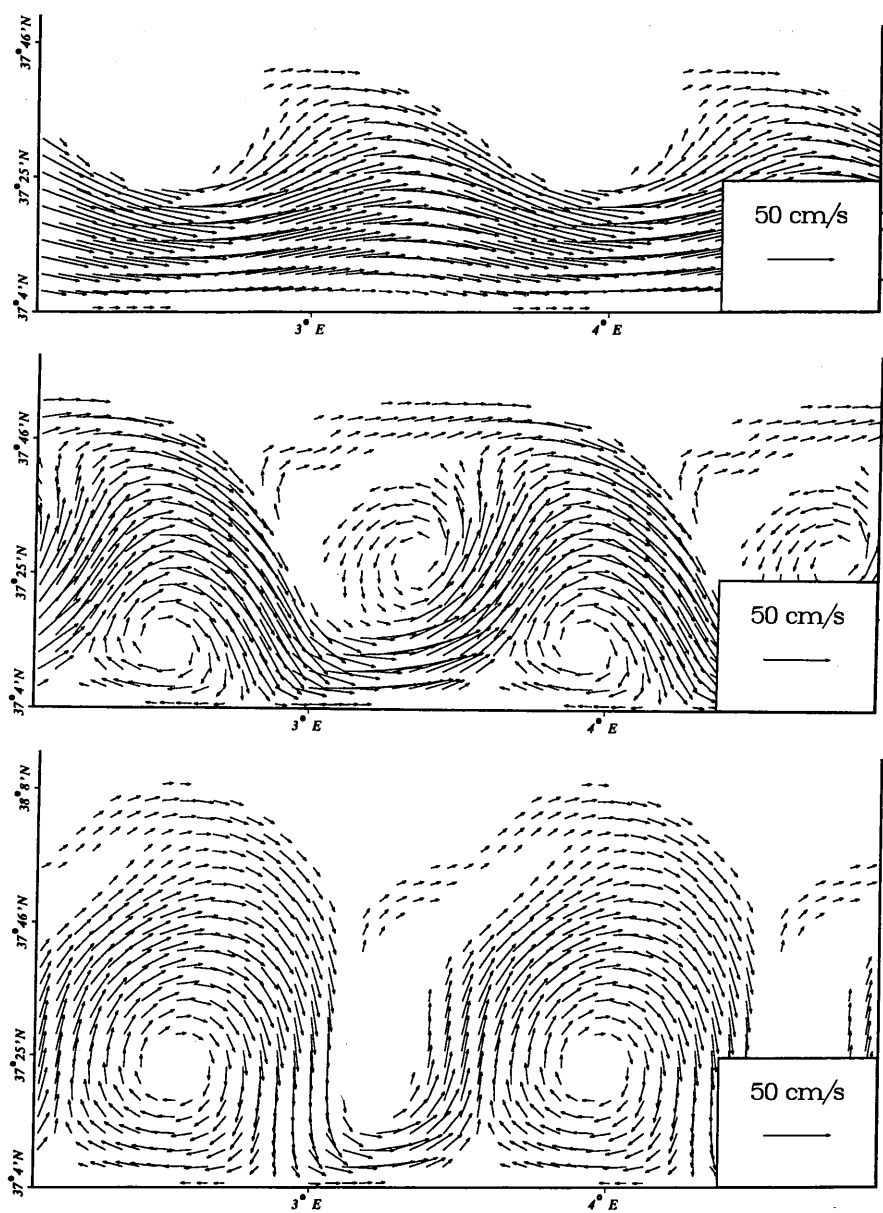


Fig. 5.– Evolution of the surface currents (days 30, 50 and 75).

its crest. This detachment allows for the development of an anticyclone at the coast, while at the wave trough, a strong cyclone appears. In the late stage of the instability, only the anticyclone grows, while the cyclone decays.

In order to verify the baroclinic instability hypothesis, we use the energy analysis of Beckers (1992a, 1993). To do so, we have to define a “mean” current. In the periodic case with an initially zonal current, the use of a zonal mean is indicated. Looking at the energy transfers, it can be shown that the condition of baroclinic instability are satisfied. We have thus a transfer of available potential energy towards the eddy kinetic energy. An interpretation of the vertical velocities is then possible by assuming that transfers are locally similar to mean transfers. One would then obtain an inequality that shows that an off-shore water parcel moving towards the front, will be downwelled. Similarly, a lighter particle moving from the coastal current towards the front will be upwelled. This phenomenon of upwellings downstream of the wave troughs and downwellings downstream of the wave-crest is the one shown on figure 6 and also observed in the Gulf Stream and atmospheric jets (Newton, 1978).

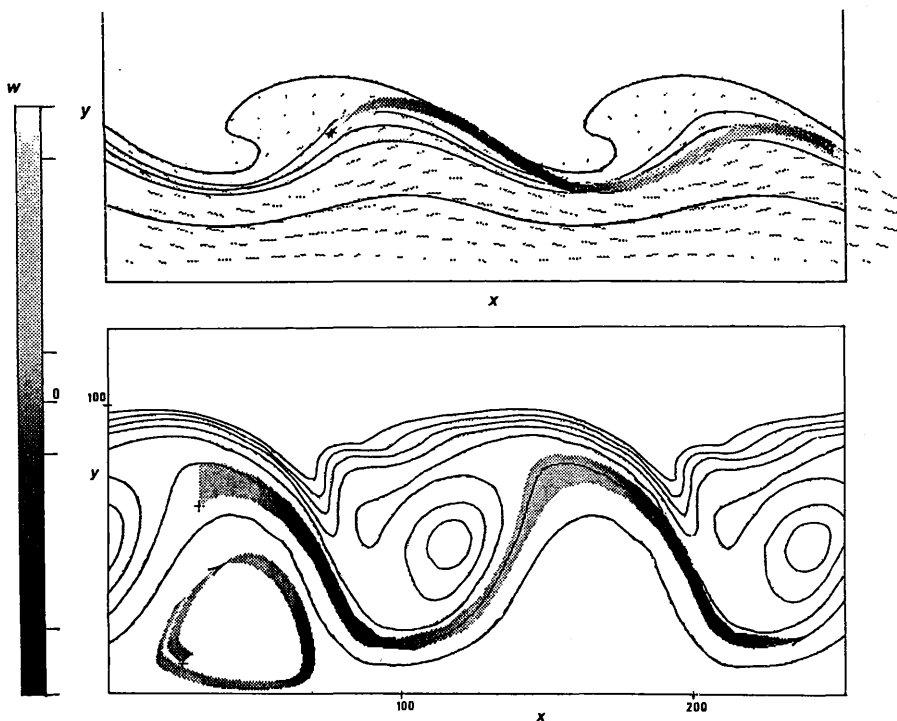


Fig. 6.— Down and upward motion during the baroclinic instability. The colour of the trajectory indicates the local vertical velocity.

To connect this diagnostic (process-oriented) study with the system-oriented one, we observe that, in a baroclinic instability, there is a transfer of eddy kinetic energy towards mean kinetic energy. The paradigm of the constant horizontal

eddy diffusivity is thus clearly inappropriate in a general circulation model. The possibility of negative eddy diffusion coefficients (computed eventually by a diagnostic model) should thus be included in the metagnostic model.

4.- Conclusion and perspectives.

On the few selected examples given above, one can see that the GHER metagnostic model reproduces well the main trends of the general circulation. More detailed process studies may be pursued with the model by investigating localized areas with finer grid diagnostic submodels operating in parallel with the basin metagnostic model; diagnostic studies providing useful information to refine the mathematical representation of dominant processes, metagnostic nowcasts and forecasts supplying a realistic overview of the system in which the individual processes are immersed and improved boundary conditions for the process studies.

The handicap of the metagnostic model remains however the complexity imposed by its realism. The model is very demanding in initial and boundary conditions and the qualitative and quantitative deficiency of reliable data may severely reduce the model's resolution and predictability.

A more thorough exploitation of the data—in particular, applying variational inverse methods to reconstruct complete data fields—and the operation of the model in a preliminary simulation with climatological forcing to reshape the initial conditions will hopefully bring significant improvements in this respect, in the near future.

Acknowledgements.

The authors are very grateful to Dr. P.W. May for kindly providing his data on the atmospheric mechanical and thermodynamical forcing in computer usable form. The authors are indebted to the Ministry of Education and Research, the Ministry for Science Policy, the National Fund for Scientific Research (Belgium) and IBM for their financial and technical assistance in providing supercomputers facilities. The financial support of the European Communities in the scope of the program MAST-0043-C and MAS2-CT92-0041 (EUROMODEL) and the "EROS 2000" (European River Ocean System) project (contract EV4V-0111-F) is greatly acknowledged.

References.

- ARNONE, R.A., WIESENBERG, D.A. and SAUNDERS, K.D. (1990). The Origin and Characteristics of the Algerian Current, *Journal of Geophysical Research*, Vol. 95, C2:1587–1598.

- ASTRALDI, M., GASPARINI, G.P., MANZELLA, G.M.R. and HOPKINS, T.S. (1990). Temporal Variability of Currents in the Eastern Ligurian Sea, *Journal of Geophysical Research*, Vol. 95, C2:1515–1522.
- BECKERS, J.M. (1992 a). De la stabilité d'un écoulement uniforme côtier dans un modèle à gravité réduite. *Comptes Rendus de l'Académie des Sciences*, t. 315, Série II, 783–789.
- BECKERS, J.M. (1992b). *La Méditerranée Occidentale: de la modélisation mathématique à la simulation numérique*, thèse de doctorat en sciences appliquées, Université de Liège, Collection des publications, 350 pp.
- BECKERS, J.M. (1993). A numerical investigation of the Algerian current instabilities, in preparation for *Journal of Physical Oceanography*.
- BECKERS, J.M. and DELEERSNIJDER, É. (1993). Stability of a FBTCs scheme applied to the propagation of shallow-water inertia-gravity waves on various space grids. Accepted for publication in *Journal of Computational Physics*.
- BECKERS, J.M. and NIHOUL, J.C.J (1992). Model of the Algerian Current's instability, *Journal of Marine Systems*, Vol. 3, 4/5:441–451.
- BLUMBERG, A. and HERRING, J. (1987). *Circulation Modelling using orthogonal curvilinear Coordinates*, in: J.C.J. Nihoul (ed.), *Three-Dimensional Models of Marine and Estuarine Dynamics*, Elsevier Publ. Co., Amsterdam, pp. 55–88.
- BRASSEUR, P. and BRANKART, J.M. (1993). *Reconstruction of Oceanic Data Fields and Data Assimilation*, this volume.
- CHABERT D'HIÈRES, G., DIDELLE, H. and OBATON, D. (1991). A Laboratory Study of Surface Boundary Currents: Application to the Algerian Current, *Journal of Geophysical Research*, Vol. 96, C7:12539–12548.
- CHENG, T.G. and SOMMERVILLE, R.C.J. (1975). On the Use of a Coordinate Transformation for the Solution of the Navier-Stokes Equations, *Journal of Computational Physics*, 17:209–228.
- CUSHMAN-ROISIN B. (1985). Frontal Geostrophic Dynamics, *Journal of Physical Oceanography*, 16:132–143.
- DELEERSNIJDER, É. and RUDDICK, K. (1993). A generalized vertical coordinate for 3D marine models, *Bulletin de la Société Royale des Sciences de Liège*, Vol. 61, 6:489–502.
- DELEERSNIJDER, É. (1989). Upwelling and Upsloping in three-dimensional marine models, *Applied Mathematical Modelling*, 13:462–467.
- GRIFFITHS, R.W. and LINDEN, P.F. (1981). The Stability of Buoyancy-Driven Coastal Currents, *Dynamics of Atmospheres and Oceans*, 5:281–306.
- HART, J.E. (1979). Finite Amplitude Baroclinic Instability, *Annual Review Fluid Mechanics*, 11:147–172.
- HEBURN, G.W. and LA VIOLETTE, P.E. (1990). Variations in the Structure of the Anticyclonic Gyres Found in the Alboran Sea, *Journal of Geophysical Research*, Vol. 95, C2:1599–1613.

- JAMES, I.D. (1986). A front-resolving sigma coordinate sea model with a simple hybrid advection scheme, *Applied Mathematical Modelling*, 10:87–92.
- KASHARA, A. (1974). Various vertical coordinate systems used for numerical weather predictions, *Monthly Weather Review*, 102:509–522.
- KILLWORTH, P.D. (1983). Long-wave instability of an isolated front, *Geophys. Astrophys. Fluid Dynamics*, 25:235–258.
- KILLWORTH, P.D., STAINFORTH, D., WEBB, D.J., PATERSON, S.M. (1991). The Development of a Free-Surface Bryan-Cox-Semtner Ocean Model, *Journal of Physical Oceanography*, 21:1333–1348.
- KILLWORTH, P.D. and STERN, M.E. (1982). Instabilities on Density-Driven Boundary Currents and Fronts, *Geophys. Astrophys. Fluid Dynamics*, 22:1–28.
- MARTINEZ, R., ARNONE, R.A. and VELASQUEZ, Z. (1990). Chlorophyll a and Respiratory Electron Transport System Activity in Microplankton From the Surface Waters of the Western Mediterranean, *Journal of Geophysical Research*, Vol. 95, C2:1615–1622.
- MAY, P.W. (1982). *Climatological flux in Western Mediterranean Sea*, Part one: Winds and wind stresses, NORDA Rep., 54, 56 pp.
- MILLOT, C. (1991). Mesoscale and seasonal variabilities of the circulation in the western Mediterranean, *Dynamics of Atmospheres and Oceans*, 15:179–214.
- MILLOT, C., TAUPIER-LETAGE, I., BENZOHRA, M. (1990). The Algerian Eddies, *Earth-Science Reviews*, 27:203–219.
- NEWTON, C.W. (1978). Fronts and Wave Disturbances in Gulf Stream and Atmospheric Jet Stream, *Journal of Geophysical Research*, Vol. 83, C9:4697–4706.
- NIHOUL, J.C.J. (1988). *Three-dimensional modelling of synoptic/mesoscale currents in the Northern Adriatic Sea*, in: B.A. Schrefler and O.C. Zienkiewicz (eds.), *Computer Modelling in Ocean Engineering*, A.A. Balkema Rotterdam, pp. 215–301.
- NIHOUL, J.C.J., DELEERSNIJDER, É., DJENIDI, S. (1989). Modelling the General Circulation of Shelf Seas by 3D $k-\epsilon$ Models, *Earth-Science Reviews*, 26:163–189.
- ORLANSKI, I. (1968). Instability of Frontal Waves, *Journal of Atmospheric Sciences*, 25:178–200.
- ORLANSKI, I. and COX, M.D. (1973). Baroclinic Instability in Ocean Currents, *Geophysical Fluid Dynamics*, 4:297–332.
- PALDOR, N. (1982). *Stable and unstable modes of surface fronts*, Ph.D. Dissertation, University of Rhode Island.
- PALDOR, N. (1983 a). Linear Stability and Stable Modes of Geostrophic Fronts, *Geophys. Astrophys. Fluid Dynamics*, 24:299–326.
- PALDOR, N. (1983 b). Stability and Stable Modes of Coastal Fronts, *Geophys. Astrophys. Fluid Dynamics*, 27:217–228.
- PALDOR, N. and GHIL, M. (1990). Finite-Wavelength Instabilities of a Coupled Density Front, *Journal of Physical Oceanography*, Vol. 20, 1:114–123.

- PERKINS, H. and PISTEK, P. (1990). Circulation in the Algerian Basin During June 1986, *Journal of Geophysical Research*, Vol. 95, C2:1577–1585.
- ROUSSENOV, V. and BRASSEUR, P. (1991). *A Comparative Analysis of Climatological Fields on the Mediterranean Sea*, Presses Universitaires de Liège.
- SALTZMAN, B. and TANG, C.H. (1975). Formation of Meanders, Fronts, and Cutoff Thermal Pools in a Baroclinic Ocean Current, *Journal of Physical Oceanography*, 5:86–92.
- SHENG, Y.P., LICK, W., GEDNEY, R.T., MOLLS, F.B. (1978). Numerical Computaion of Three-Dimensional Circulation in Lake Erie: A Comparison of a Free-Surface Model and a Rigid-Lid Model, *Journal of Physical Oceanography*, 8:713–727.
- TINTORÉ, J., LA VIOLETTE, P., BLADE, I., CRUZADO, A. (1988). A Study of an Intense Density Front in the Eastern Alboran Sea: The Almeria-Oran Front, *Journal of Physical Oceanography*, Vol. 18, 10:1384–1397.

Development of Interdisciplinary Models of Ecosystems under Severe Hydrodynamic Constraints

É.J.M. DELHEZ^{*1}, G. LACROIX², G. MARTIN^{*1},
J.C.J. NIHOUL¹ and R.A. VARELA¹

¹ GHER, University of Liège

² Laboratoire d'Écologie du Plancton Marin (L.E.P.M.), Université Pierre et Marie Curie – Paris VI

Abstract.

The need for reliable management models of the marine resources is large. In this paper, the problem of the mathematical modelling of ecosystems is approached mostly from the point of view of the physical oceanographer.

Hydrodynamic phenomena in the range of 10^5 s to 10^7 s (the weather of the sea) form the prescribed physical conditions in which ecosystems must develop. Sometimes, these phenomena result in important constraints (advection of new material, high flushing rate, vertical diffusion, ...) which must be taken into account as accurately as possible in any modelling attempt of the ecosystem. A detailed three-dimensional, time-dependent description of the currents and turbulence fields is thus prerequisite in such a case.

However, the complexity of mathematical models must be limited. Therefore, a trade-off must be found between the complexity of, respectively, the biological and the physical descriptions in agreement with the ultimate goals of the study.

A case study demonstrating the feasibility of ecosystem models combining complex hydrodynamics and simple biology is described. Results of both the hydrodynamic and biological sub-models of the North-Western European Continental Shelf (NWECS) are included.

* Research Assistant of the National Fund for Scientific Research (Belgium).

1.- Introduction.

During the last decades, great concerns have been raised about the health and the future of the world ecosystem. The development of our urban and industrialized society has led to unexpected short term and long term environmental problems at regional and larger scales (with long term problems usually associated to large physical dimensions and short term issues being only of local interest). In the field of oceanography, these problems have been studied extensively to be understood and, eventually, solved.

The pollution by heavy metals like zinc, lead, titanium, cadmium, mercury, ... has been identified as a serious problem affecting all the successive levels of the trophic chain. The transport of these toxic matters, their dispersion and transfer through the trophic chain with the probable accumulation of heavy metals in the higher trophic levels is now studied extensively (*e.g.* Abdullah and Royle, 1972; Balls, 1985; Dehairs *et al.*, 1985; Ackroyd *et al.*, 1986; Bouqueneau and Joiris, 1988).

The excessive riverine and aerial inputs of inorganic nutrients lead to drastic modifications in the nutrients balance and seriously affect the equilibrium of the classic food web. This results in the proliferation of toxic, or simply unwanted, species well beyond acceptable bounds (*e.g.* Lancelot *et al.*, 1987; Fraga *et al.*, 1988; Delgado *et al.*, 1990; Lancelot, 1990). Such phenomena are often very spectacular, like phaeocystis blooms, green tides and the accumulation of foam on the beaches, and have also a very negative impact on tourism. It is therefore economically relevant to determine the precise conditions likely to promote such phenomena to set up an efficient prevention policy.

The best solution to address the problems reported here-above is undoubtedly brought by the mathematical modelling of the ecosystems. Numerous ecosystem or water quality models, no matter how they are called, have been developed around the world to answer specific environmental questions (*e.g.* Tett *et al.*, 1986; Stigebrandt and Wulf, 1987; Radford *et al.*, 1988; Fransz *et al.*, 1991). Most of them result from the work done by biologists trying to understand, often through box-models, how the real ecosystem works. Many such initiatives have been crowned with success. However, such models usually lack some important aspects of the real natural systems like spatial variability and hydrodynamic forcing. Therefore, both the possibility to compare the results with field measurements and satellite pictures, and the predictive ability of the model are likely to suffer from such shortcomings.

The purpose of this paper is to show why and how hydrodynamic models should be combined with purely biological models to build reliable ecosystem models when severe hydrodynamic constraints exist.

2.- The common framework for biological and hydrodynamic models.

It may seem surprising to include the description of hydrodynamic processes in the study when addressing biological processes. However, as we will show, important links and interactions exist between these two sectors.

Biological systems can be studied at different length scales, from individual organisms to a whole population. However, most of the practical problems arise at the level of the ecosystem and so mathematical models focus on those time scales inherent of the ecosystem. This usually means periods of time from 10^4 s– 10^8 s, possibly narrowed to 10^5 s– 10^7 s, which correspond to characteristic cycles in the life of many pelagic and benthic populations (periods of diurnal, seasonal and annual oscillations) and to the rhythm of human activities interplaying with the marine system.

There are hydrodynamic processes in this range of time scales. These are (Table 1) the mesoscale (typical time scale t_c of a few hours), synopticscale (t_c = a few days) and seasonalscale (t_c = a few weeks) processes which are usually referred to as the *weather of the sea*. Therefore, these hydrodynamic processes are likely to interact significantly with the biological phenomena. In fact, motions at the time scale of the weather of the sea are resonant processes with the biological dynamics and maintain a permanent strain on the ecosystem, through the advection process. This mechanism tends to impose to the ecosystem the length scales of the synchronous physical mechanisms and is therefore often called the ecohydrodynamic adjustment (Nihoul and Djenidi, 1991).

Not only do biological and hydrodynamic processes have similar time scales and length scales, but also similar mathematical formulations. In fact, the equations describing the evolution in space and time of the state variables whether physical or biological, are all particular expressions of a unique basic equation (figure 1). This equation sets forth that the variations in time of any state variable at any given point, result from (i) local production-destruction according to the proper dynamics of the variable, (ii) advection by the fluid (flow) and (iii) diffusion by sub-window scale processes (flux).

There is thus a common framework for the development of ecosystem models combining hydrodynamic and biological processes in one single big model. However, a major simplification can be introduced here if one notices that biological processes are very often influenced by hydrodynamics while the reverse is seldom true, especially at large spatial scale. Therefore the hydrodynamic sub-model can be run prior to the simulation of the biological cycles. Indeed, biology can only influence hydrodynamics through two ways: (i) the modification of the bottom roughness, and hence friction, by the development of the benthic population, (ii) the modification of the baroclinic circulation because of modifications of the sea water temperature vertical structure arising from of a

Table 1
Schematic Representation of Marine Geohydrodynamic Variability (Nihoul and Djenidi, 1991)

	Climatic scale	•	Macroscale	•	Mesoscale	•	Mesial scale	•	Smallscale	•	Miniscale	•
Freq. (s^{-1})	10^{-9}	.	10^{-8}		10^{-7}		10^{-6}		10^{-5}		10^{-4}	
Time scale	decade		year		month		week		day		hour	
									min		sec	
				Rossby waves		Inertial oscillation	Internal waves		Surface waves		Acoustic waves	
					Storms/Tides							
			Seasonal variations		Weather variations	Diurnal variations		Langmuir cells	Wind mixing		Energy dissipation	
			Convective overturning restratification		Alternance of mixing and stratification in upper layer		Vertical microstructures/ 3D turbulence in mixed layers				Molecular diffusion	
			General circulation	Synoptic features								
			Deep circ., Gyres, Variability									
				Cross shelf exchanges								
				Fronts (Frontal currents, meanders, extrusions, ...)								

MARINE WEATHER
ECOHYDRODYNAMICS

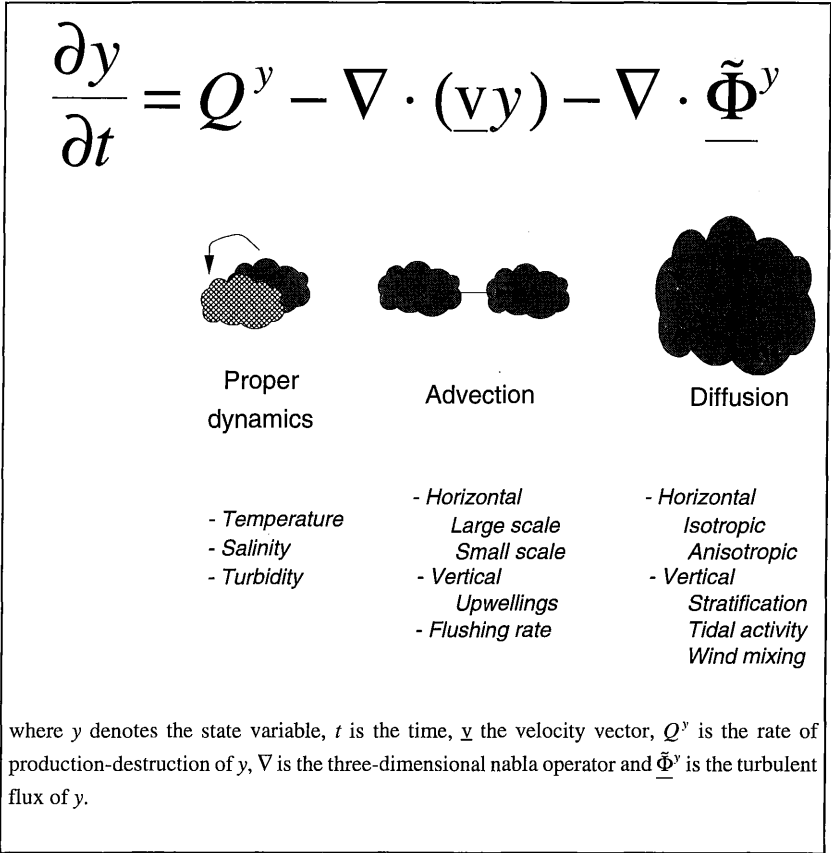


Fig. 1.— The general evolution equation of hydrodynamic and biological variables. Hydrodynamic influences on biological processes are listed under the corresponding terms.

biologically induced increase of the light extinction coefficient. These feedbacks from biology to hydrodynamics can only be significant at small scales in very particular situations (*e.g.* proliferation of *mucilagine* in the Adriatic Sea) and, in general, the hydrodynamic conditions form a prescribed environment for ecosystems. In the same way, the results of the hydrodynamic sub-model form imposed constraints to apply to the biological sub-model. This allows the separate and prior validation of the hydrodynamic sub-model and a considerable reduction in the required computer resources.

3.- The optimum ecosystem model.

The introduction of the three-dimensional hydrodynamic processes in biological models, and hence of the horizontal and vertical dimensions, is a huge theoretical benefit. However, its practical realization is far from obvious at this time. Indeed, lumping together in a giant model all the state-of-the-art in both biological and physical modelling will not result in an optimum ecosystem model. The reasons for such a remark are diverse.

First of all, it is clear that limited computer resources impose limitations on the number of state variables. Even if processors speed and storage facilities increase at an amazing rate, running complex coupled three-dimensional hydrodynamic and biological models involving as much as 40 state variables, as many biological box models do, at each grid point will still remain a dream for some time. Besides, there are also reliability and clarity constraints on the number of state variables. A model with many state variables incorporates at least as many different processes and interactions and involves a correspondingly large number of parameters and boundary conditions which cannot be evaluated from existing data bases without an inevitable margin of error. Because of the non-linear biological dynamics, the precise determination of the resulting error bounds is even often nearly impossible. On the other hand, the results of such a model, because of its increased sophistication and fallibility, can become impossible to be interpreted in terms of scientific diagnosis or management recommendations.

The bottom line is therefore that mathematical models must be simplified views of the natural system with simplifications derived from the precise objectives of the study. The model must have an appropriately fine resolution in physical and state space to describe adequately the system's behaviour but, on the other side, it must involve sufficiently few state variables for their evolution equations to be amenable to analysis. The ecological model derived through this approach appears as an optimum use of computer resources and accumulated knowledge about the ecosystem. Tractability and reliability are thus the main characteristics of this model.

The precise simplifications involved in the derivation of this optimum ecosystem model concern not only the representation of the proper dynamics of the biological system, but also the spatial and temporal resolutions and the representation of the interactions of this system with other sectors of the state space, like hydrodynamics, chemistry, economy ... In particular, hydrodynamic influences can be included with variable levels of aggregation when the full three-dimensional time-dependent description seems too complex, or irrelevant. In biological box-models, total flow rates derived from measurements or from the aggregation of the results of a hydrodynamic model can be included. In 1D vertically resolving models, the turbulent structure and the vertical profiles of the horizontal advective inflows of nutrients can be further incorporated.

Depth-mean horizontal currents at lateral boundaries and inside the domain must be prescribed in depth-averaged, horizontally resolving, biological models.

As stated in a previous section, the relevance of any physical or biological process must be appraised with respect to the goals of the investigation. Very often, ecosystem models are designed to become real management tools of the marine resources and/or anti-pollution warning systems. Such models should thus be able to determine the influence of the anthropogenic disturbances on the ecosystem. They should be fit for use in both diagnostic and prognostic modes. They should help evaluating the consequences and the possible success of any political decision designed to protect the environment prior to its real application. For such a purpose, it is particularly crucial to track pollutant patches and to be able to determine where the pollution is likely to develop, which area will be mostly affected and how. The inclusion of an accurate description of hydrodynamic processes is thus imperative.

On the other hand, biological models can be used as powerful research tools. They are often the only way to study how the ecosystem really works. Indeed, countless numerical experiments including simplifications, idealized scenarios and extreme forcings, can be carried out to test hypothesis and to validate or reject theories. In such a perspective, hydrodynamic processes seem less important. However, even then, because of the largely non-linear dynamics of ecosystems, a correct specification of the different fluxes, flushing rates and vertical diffusion processes is compulsory to appropriately model the system's behaviour. So, for such a purpose too, a trade-off must be found between the complexity of the real system and the necessary simplicity for the model to be amenable to analysis.

4.— Hydrodynamic constraints.

All the hydrodynamic constraints applying to the biological state variables are summarized in figure 1. To go into more details about these interactions, this paragraph will be illustrated with references to the North-Western European Continental Shelf.

The most obvious hydrodynamic constraint is the one produced by the advection of the biological properties and/or variables by the mean fluid velocity. In the same way that they are classified according to their origin and salinity, *water masses* (Atlantic water, Coastal waters, Baltic water, ...) are characterized by well-defined biological properties and nutrients concentrations (Lee, 1980). The general motion of these *water masses* forced by the general circulation on the NWECS determines thus the availability of nutrients, the off-shore influence of river loads, the bio-geo-chemical exchanges (nutrients, organic matter, ...)

between the different ecosystems of the shelf ... This advection constraint is obviously part of the explanation of the large scale distribution of active constituents like nitrate, phosphorus, silicate, phytoplankton cells, ...

Advection is also important at smaller scales. For instance, local gyres, often produced by non-linear interactions of the irregular bathymetry and large oscillating tidal currents, can sometimes be seen as biological spatial loops, with successive trophic levels spread along the stream (Nihoul and Hecq, 1984).

So far, the stress has been put on horizontal advection. However, very important biological events are associated with vertical motions. Particular combinations of bathymetric features and currents, or more frequently, particular wind forcing can produce coastal upwellings, or upslopings (Deleersnijder, 1989), which pump bottom nutrient rich waters into the euphotic layer and make thus nitrate, phosphorus, ... available for primary production. Wind induced upwellings are usually not very persistent features. They last only a few days. However, because of the huge primary production promoted by such a hydrodynamic phenomenon, and because of the possible repetition of such events along the year, upwellings are likely to account for a non negligible part in the total primary production budget (Brockmann *et al.*, 1990). Other vertical motions are associated with filaments. These hydrodynamic features were discovered very recently and are therefore much less known and understood. However, vertical velocities associated to such processes as high as 40 to 100 m day⁻¹ are now reported (Haidvogel *et al.*, 1991; Pollard and Regnier, 1992). Therefore, if such figures are confirmed, filaments would be of huge importance for biology.

In the previous paragraphs, advection was seen as a way to make nutrients available in a well-defined area or to carry organic matter from one location to another. However, apart from the movement itself, the hydrodynamic circulation pattern is also important in determining the flushing rate of open or close areas. The German Bight region, for instance, is well-known for its poor renewal of water (Van Westernhagen and Detlefsen, 1983; Rachor, 1990). Such a situation is known to be propitious to eutrophication problems (Cruzado, 1990). The large amounts of nitrate and other nutrients discharged by the river Elbe can promote a very high primary productivity which can, in turn, degenerate into severe problems because of a large oxygen consumption by degrading organic matter and a poor renewal of this oxygen. Tidally-induced gyres like the ones of Barfleur, St Brieuc, ... can have similar effects by increasing the residence time of pollutants and other constituents in restricted coastal areas. On the contrary, in the Southern Bight of the North-Sea, such eutrophication problems do not occur thanks to a small residence time of water masses, despite the high nitrate supply by the rivers Rhine, Meuse and Scheldt. So, advection does not only move away and disperse biological constituents leaving the dynamics of the ecosystem unchanged (if one takes a frame of reference moving with the water mass) but

also deeply influence the behaviour of the ecosystem. Hydrodynamic processes modify indeed the concentration of the biological variables and, because of the non-linearities of biological interactions, alter the rates of biological interactions.

Hydrodynamics can also influence biology through diffusion. The diffusion term accounts for the mean effect of all sub-window scale processes, *i.e.* processes not resolved by the velocity field, often with time-scales smaller than 10^5 s. The general assumption about these motions is that they contribute to the general spatial smoothing of the different properties. This occurs both horizontally and vertically.

Many biological models already include the vertical eddy diffusion profile as a control parameter (*e.g.* Wroblewski and O'Brien, 1976) or derived it from measurements (*e.g.* Tett *et al.*, 1986) or from a coupled 1D hydrodynamic model of the mixed layer (*e.g.* Lacroix, 1992; Varela *et al.*, 1992). The friction of tidal, wind-induced and other currents on the bottom and the surface wind action dissipate large amounts of energy which are then available for the vertical mixing of the water column. This turbulence is further inhibited by stratification. The actual vertical diffusive fluxes of matter result thus of a complex, and still not fully understood, combination of parameters like the local depth, the strength of the currents and of the wind field, the sharpness of the thermocline, the occurrence of internal waves ... (Kullenberg, 1983). Nevertheless, hydrodynamic processes control the rate of matter exchanges between the surface euphotic layer and the bottom layer and the possible formation of a nutricline. For instance, the rate at which nutrients, recycled in the bottom layer, can be made available in the euphotic layer and hence the phytoplankton growth, depend on the strength of the turbulent mixing, especially in open waters. This particular mechanism and the ratio of nutrients release and phytoplankton growth rates determine the formation of a deep-water chlorophyll maximum (DCM) and its location (Varela *et al.*, 1992). At some locations, the water column remains well-mixed all along the year, because of strong tidal currents, and the exchange between bottom sediments and the euphotic layer is always very effective. At some other locations, a sharp summer thermocline can develop and inhibit vertical exchanges so that surface and bottom layers remain uncoupled.

Horizontal diffusion also contributes to the flushing of marine areas. Very often, horizontal diffusion reflects the anisotropy of the original hydrodynamic processes. For instance, oscillating tidal currents result in an anisotropic horizontal diffusion of the constituents with preferential diffusion directions along the main axes of the tidal ellipse (Nihoul, 1972). The same situation occurs with the baroclinic instabilities of frontal structures (Simpson and James, 1986). Fronts are well known as regions of enhanced primary production. This mainly occurs because of frontal instabilities which inject nutrients rich waters from the unstratified side into the optimum euphotic layer at the stratified side. The

instabilities act thus like a one-dimensional diffusion perpendicular to the front, while the main stream remains nearly parallel to the front.

Finally, the development of a biological model can also take benefit of the simultaneous development or of the results of a three-dimensional, baroclinic, turbulent closure, hydrodynamic model for the accurate representation of the biological system's proper dynamics. Among the results of hydrodynamic models, some are indeed control parameters for the biological interactions. Temperature controls many biological processes. Salinity is an important criterion for the preferential proliferation of well-defined species. Turbidity determines the light extinction coefficient and hence the depth of the euphotic layer. So, an indirect effect can also be introduced at this stage as hydrodynamic features determine the temperature distribution which, in turn, influences the ecosystem.

5.— A case study: the NWECS.

As explained before, ecosystems models can be designed by including either many physical processes and a crude representation of the biological complexity, or many biological variables and a coarse spatial and physical description, or any reasonable trade-off. This section resolutely takes the part of complex physics and more simple biology to emphasize the influence of physical processes on the North-Western European Continental Shelf.

A very detailed description of hydrodynamic processes is provided by a three-dimensional, baroclinic, turbulent closure, mathematical model of the residual circulation on the North-Western European Continental Shelf (Delhez and Martin, 1992; Martin and Delhez, 1992). This model is designed to study the monthly-mean or seasonal circulation on the shelf, with a spatial discretization of $10'$ longitude \times $10'$ latitude and 10 vertical levels at each horizontal location. It provides the three-dimensional description of the velocity, temperature and salinity fields. Additional informations are brought through the residual free surface elevation and the three-dimensional turbulent kinetic energy fields. The model takes into account all the possible forcing of the residual circulation on the NWECS, *i.e.* the wind forcing, the exchanges with the Atlantic Ocean, the mean effect of the semi-diurnal lunar tide M_2 (the dominant tidal component on the NWECS, with a period of 12 h 25') the baroclinic forcing and the main river discharges. This model was run in typical summer and winter conditions to get summer (figure 2) and winter three-dimensional velocity fields, and turbulence conditions. Seasonal variations were then computed by fitting a sinusoidal curve between these data. In the same way, incident solar radiations were assumed to vary sinusoidally along the year with the peak value at the summer solstice. The diurnal cycle was not included. No spatial variation of this light input was

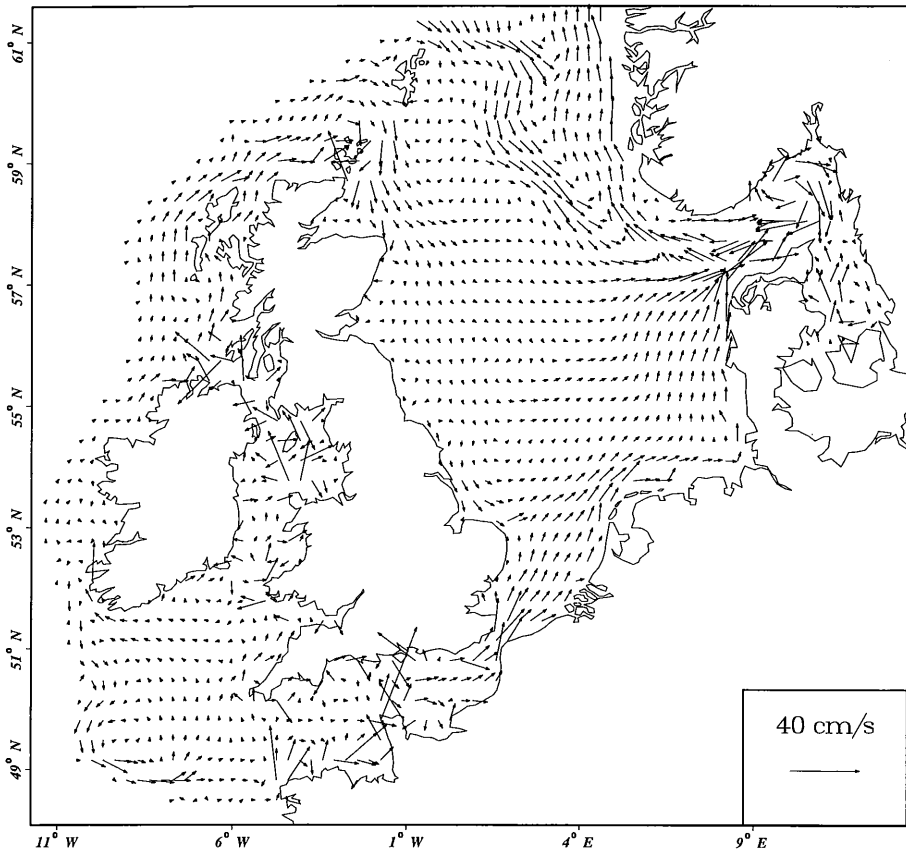


Fig. 2.— Depth-mean summer residual circulation on the NWECS computed with a 3D baroclinic model (Delhez and Martin, 1992).

introduced because of the lack of data about clouds cover above marine areas and because the different phytoplankton species present around the shelf were supposed equally adapted to their local light conditions. These annual cycles determine thus the prescribed physical conditions in which biological activity has to take place within the model.

The biological description must be simple to be included in a three-dimensional time-dependent hydrodynamic framework. A classic food web is assumed (figure 3). It involves one inorganic nutrient (nitrogen without distinction between nitrate, nitrite or ammonium), a phytoplankton variable, a zooplankton variable and the detritus. All the variables are expressed in nitrogen unit. The biological processes included are the light and food limited (product law) phytoplankton growth, the grazing by zooplankton, the zooplankton excretion and production of fecal pellets, the phytoplankton and zooplankton mortality and the

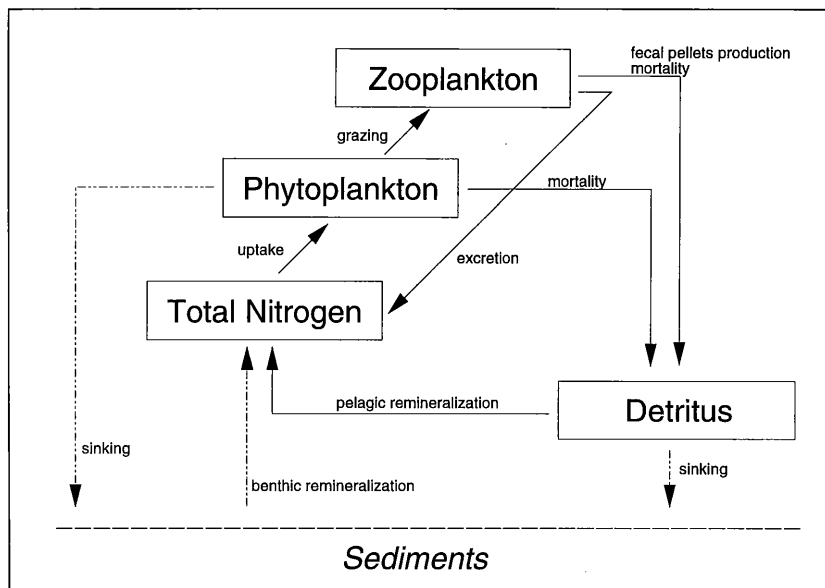


Fig. 3. – Schematic representation of the nitrogen cycle of the biological sub-model.

pelagic remineralization of the detritus. Phytoplankton and detritus are assumed to sink at constant vertical velocities. The subsequent benthic remineralization is not dynamically modelled but supposed instantaneous. The remineralized nitrogen is then injected in the bottom finite volume and further dispersed by currents and vertical diffusion. All these interactions are parameterized with first order laws or classic Michaelis-Menten-Monod formulations except for the boundary condition at the top of the food chain: zooplankton mortality follows a second order law. All the parameters involved in these formulations are adjusted in a one-dimensional, vertically resolving version of the full 3D ecosystem model. The small number of these parameters should allow their explicit determination with available field data. For this feasibility experiment, however, they were only tuned to get qualitatively satisfactory seasonal variations.

The first simulations are designed to test the feasibility of such a model and its potential achievements. Initial winter conditions are issued from published maps (Brockmann *et al.*, 1990) supplemented with qualitative data (Lee, 1980). For instance, the salinity field provided by the hydrodynamic model is used to identify high salinity Atlantic waters and fresher river plumes. Characteristic inorganic nutrients concentrations are then associated to these masses. Initial phytoplankton and zooplankton distributions are also derived from published maps and/or are assumed proportional to the initial local nitrogen concentration. No detritus is present at the beginning of the simulation.

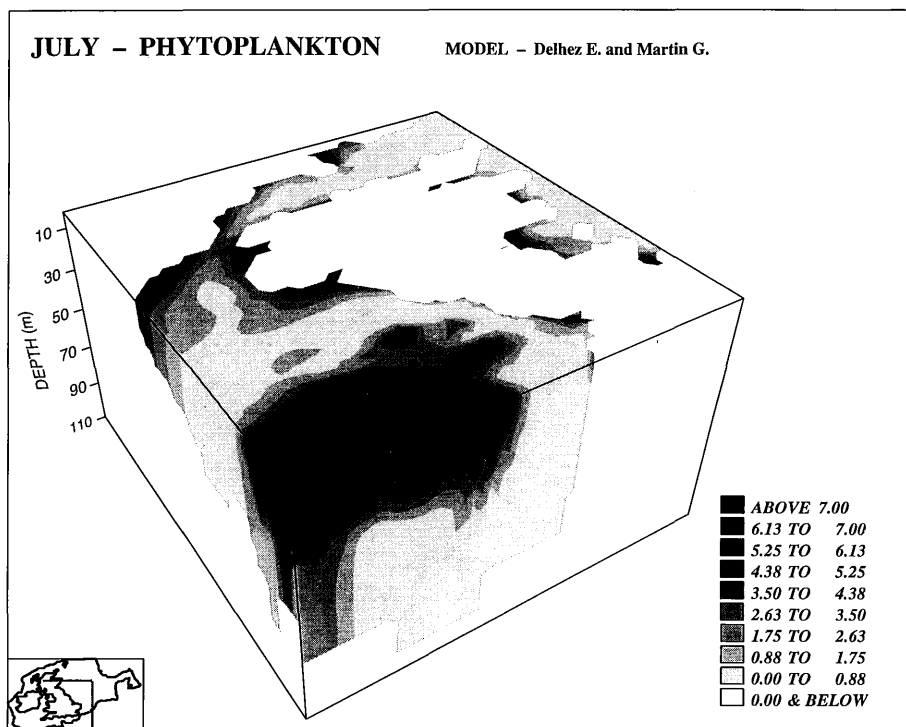


Fig. 4.– 3D view of the mid July phytoplankton concentration ($\mu\text{g at NI}^{-1}$) computed with the model.

Results exhibit a large sensitivity to initial conditions, especially in off-shore areas which undergo less important forcings than coastal systems. In fact, a fine analysis of these results has still to be carried out, but reasonable agreements can already be stressed. At first, the annual cycle seems well represented in many parts of the shelf, with a satisfactory evaluation of the bloom period. This kind of consideration, if confirmed, is rather promising for the application of biologically simple models to large spatial domains. It is indeed not obvious that a single simple biological model involving few parameters can be used to study the numerous different ecosystems living on the NWECS under a large range of physical and nutrients availability conditions. The reason for the observed satisfactory behaviour could be that the large aggregation of the plentiful phytoplankton species into very few compartments probably leads to simpler dynamics and laws than for the different species taken separately.

For what regards the purpose of this paper, figures 4 and 5 clearly display the importance of physical processes and spatial variations. They represent respectively the three-dimensional distribution of phytoplankton in central and southern North-Sea in mid July and the bottom concentration of detritus at the

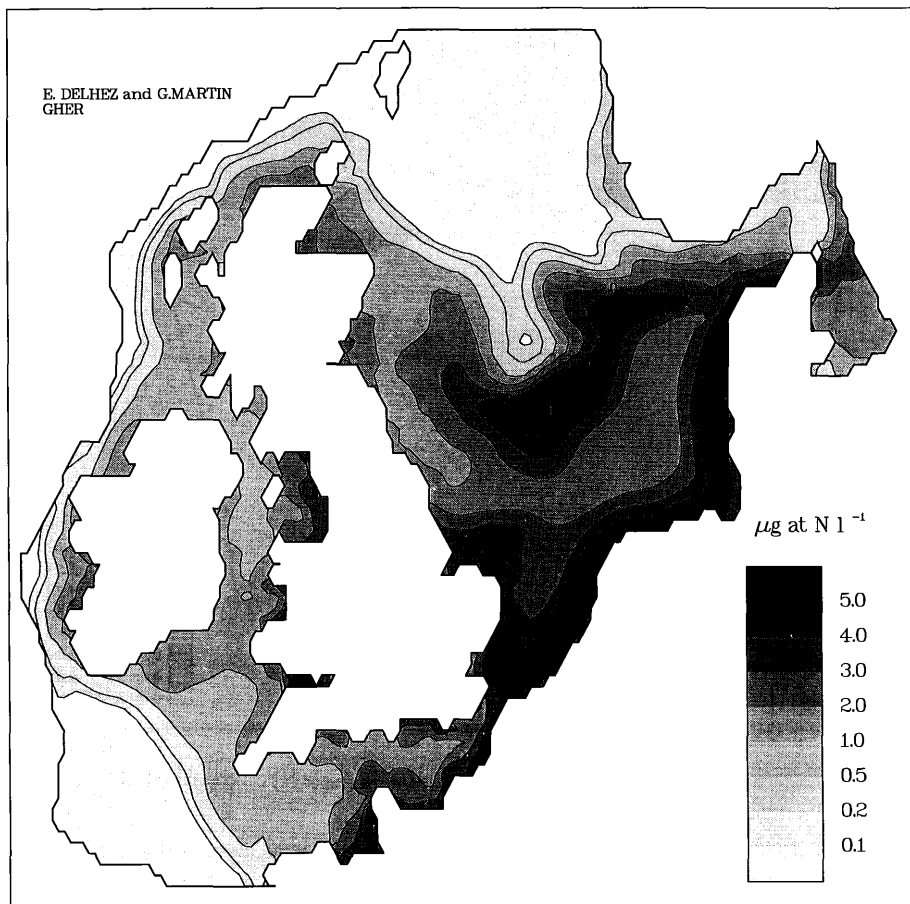


Fig. 5.— Bottom concentration ($\mu\text{g at N l}^{-1}$) of the mid July detritus computed with the model.

same time. High phytoplankton and detritus concentrations are found at the mouth of the main rivers because of their high nutrient supply and of smaller depths. The same reasons explain the earlier bloom in those regions. This remark applies to all the rivers of the NWECS to various degrees. The effect of a river is indeed not directly proportional to its mean flow rate or to its nutrient supply. For instance, the influence of the Rhine, Meuse and Scheldt is largely softened by the strong mixing and flushing along this part of the continental coast. On the other hand, the very modest river Humber, on the English side, can promote a high local phytoplankton maximum because of the weakness of the horizontal exchanges around the river mouth. In the German Bight, both large nutrient inputs and small renewal of the water account for a (too) large phytoplanktonic development.

Because of larger riverine nutrients supplies, primary production is also larger on the French side of the English Channel than on the English side. This effect is further enhanced by the existence along the French coast of the so-called “fleuve côtier” (coastal river) which prevents French coastal waters from spreading in the transverse direction of the Channel.

In the centre of figure 4, a phytoplankton maximum can be seen over the Dogger Bank. This well-known feature (*e.g.* Brockmann *et al.*, 1990) is produced by the shallowness of this area and the stratification of the neighbouring waters which ensure that phytoplankton cells remain in the euphotic layer (see the foreground of figure 4).

6.– Conclusions.

The mathematical modelling of ecosystems will certainly become the definite management tool of marine resources. However, to reach this goal, modellers will have to find a compromise between biological and physical complexity in a real interdisciplinary dialogue.

The application described in this paper demonstrates the feasibility of ecosystem models based on simple biology and complex physics. It shows that the hydrodynamic forcing induces three-dimensional constraints to the biological populations. Results also show that the simplification of horizontal homogeneity leading to one-dimensional vertically resolving biological models is a very poor representation of the reality in this case study.

However, at this time, it is still very difficult to answer the important question of the optimum complexity of ecological models. Nevertheless, it seems clear that, beside the number of biological state variables, the number of biological processes, the number of control parameters, the number of basic inorganic nutrients, the number of levels of the food chain, the number of compartments per level, the number of loops in the food web ... the accuracy of the description of hydrodynamic phenomena is an important point in the definition of the complexity of an ecosystem model.

Acknowledgements.

This study would not have been possible without the support of *IBM* and of the Ministry of Education and Research in the scope of the Program of Concerted Actions (no. 89/94-131).

The authors wish also to express their gratitude to the Belgian National Fund for Scientific Research.

Partial support for this work came from the European Communities grant no. 910645 in the frame of the MAST program and from the Spanish Ministry of Science under PF 49539257 grant.

References.

- ABDULLAH, M.J. and ROYLE, L.G. (1972). The determination of copper, lead, cadmium, nickel, zinc and cobalt in natural waters by pulse polarography, *Anal. Chim. Acta*, 58:283–288.
- ACKROYD, D.R., BALE, A.J., HOWLAND, R.J.M., KNOX, S., MILLWARD, G.E. and MORRIS, A.W. (1986). Distribution and behaviour of dissolved copper, zinc and manganese in the Tamar Estuary, *Est. Coas. Mar. Sci.*, 23:621–640.
- BALLS, P.W. (1985). Copper, lead and cadmium in coastal waters of the Western North Sea, *Mar. Chem.*, 15:363–378.
- BOUQUEGNEAU, J.-M. and JOIRIS, C. (1988). *The fate of stable pollutants—heavy metals and organochlorines—in marine organisms*, in: R. Gilles (Editor), *Advances in Comparative and Environmental Physiology*, 2:219–247.
- BROCKMANN, U.H., LAANE, R.W.P.M. and POSTMA, H. (1990). Cycling of nutrient elements in the North Sea, *Netherlands Journal of Sea Research*, 26 (2–4):239–264.
- CRUZADO, A. (1990). *Eutrophication of coastal areas*, in: H. Barth and L. Fegan (Editors), *Eutrophication-related phenomena in the Adriatic Sea and in other Mediterranean coastal zones*, Commission of the European Communities, Water Pollution Research Reports, 143–205.
- DEHAIRS, F., GILLAIN, G., DEBONDT, M. and VANDENHOUDT, A. (1985). *The distribution of trace and major elements in Channel and North Sea suspended matter*, in: R. Van Grieken and R. Wollast (Editors), *Progress in Belgian Oceanographic Research*, Brussels, March 1985. Published by the University of Antwerp, Antwerpen-Wilrijk, 136–146.
- DELEERSNIJDER, E. (1989). Upwelling and upsloping in three-dimensional marine models, *Applied Mathematical Modelling*, 13:462–467.
- DELGADO, M., ESTRADA, M., CAMP, J., FERNANDEZ, J.V., SANTMARTI, M. and LLETI, C. (1990). Development of a toxic *Alexandrium minutum* Halim (Dinophyceae) bloom in the harbour of Sant Carles de la Rapita (Ebro Delta, northwestern Mediterranean), *Scient. Mar.*, 54:1–7.
- DELHEZ, É. and MARTIN, G. (1992). Preliminary results of 3-D baroclinic numerical models of the mesoscale and macroscale circulations on the North-Western European Continental Shelf, *Journal of Marine Systems*, 3:423–440.
- FRAGA, S., ANDERSON, D.M., BRAVO, I., REGUERA, B., STEIDINGER, K.A. and YENTSCH, D.M. (1988). Influence of upwelling relaxation on dinoflagellates and shelf-fish toxicity in Ria de Vigo, Spain, *Est. Coas. Shelf. Sci.*, 27:349–362.
- FRANSZ, H.G., MOMMAERTS, J.P. and RADACH, G. (1991). Ecological modelling of the North Sea, *Neth. J. Sea. Res.*, 28 (1–2):67–140.
- HAIDVOGEL, D.B., BECKMANN, A. and HEDSTRÖM, K.S. (1991). Dynamical simulation of filaments formation and evolution in the Coastal Transition Zone, *J. Geophys. Res.*, 96 (C8):15017–15040.

- KULLENBERG, G. (1983). *Mixing processes in the North Sea and aspects of their modelling*, in: J. Sündermann and W. Lenz (Editors), *North Sea Dynamics*, Springer-Verlag, 349–369.
- LACROIX, G. (1992). *Extending the GHER 3D model to the modelling of ecosystems in Western Mediterranean Coastal zones: results from an exploratory study*, in: J.M. Martin and H. Barth (Editors), *Water Pollution Research Report no. 28, Proceedings of the third EROS 2000 Workshop on Research in the North Western Mediterranean Sea*, Texel, october 1991.
- LANCELOT, C. (1990). *Phaeocystis blooms in the continental coastal area of the Channel and the North Sea*, in: C. Lancelot, G. Billen and H. Barth (Editors), *Eutrophication and algal blooms in North Sea coastal zones, the Baltic and adjacent areas: prediction and assesment of preventive actions*, *Water Pollution Research Report no. 12*, Commission of the European Communities, 27–54.
- LANCELOT, C., BILLEN, G., SOURNIA, A., WEISSE, T., COLIJN F., VELDHUIS, M.J.W., DAVIES, A. and WASSMANN, P. (1987). *Phaeocystis blooms and nutrient enrichment in continental coastal zones of the Nort-Sea*, *Ambio*, 16 (1):38–46.
- LEE, A.J. (1980). *North-Sea: Physical Oceanography*, in: F.T. Banner, M.B. Collins and K.S. Massie (Editors), *The North Western European Shelf Seas: the Sea Bed and the Sea in Motion*, II. Physical and Chemical Oceanography and Physical Resources, Elsevier Oceanogr. Ser., 24B:467–494.
- MARTIN, G. and DELHEZ, É. (1992). Résultats récents sur la circulation tridimensionnelle sur le Plateau Continental Nord-Ouest Europééen, *Bulletin de la Société Royale des Sciences de Liège*, 61 (1–2):19–52.
- NIHOUL, J.C.J. (1972). Shear effect diffusion in shallow open seas, *Bulletin de la Société Royale des Sciences de Liège*, 41 (9–10):521–526.
- NIHOUL, J.C.J. and DJENIDI, S. (1991). Hierarchy and scales in marine ecohydrodynamics, *Earth Science Reviews*, 31:113–127.
- NIHOUL, J.C.J. and HECQ, J.-H. (1984). Influence of the residual circulation on physico-chemical characteristics of water masses and the dynamics of ecosystems in the Belgian coastal zone, *Continental Shelf Research*, 3 (2):167–174.
- POLLARD, R.T. and REGNIER, L.A. (1992). Vorticity and vertical circulation at an ocean front, *J. Phys. Oceanogr.*, 22:609–625.
- RACHOR, E. (1990). Changes in sublittoral zoobenthos in the German Bight with regard to eutrophication, *Netherlands Journal of Sea Research*, 25 (1–2):209–214.
- RADFORD, P.J., BURKILL, P.H., COLLINS, N.R. and WILLIAMS, R. (1988). *The validation and scientific assessment of an ecosystem model for the Bristol Channel*, in A. Marani (Editor), *Advances in Ecological Modelling, Proceedings of the ISEM Conference on Ecological Modelling* (Italy, 1987), Internations Society for Ecological Modelling, Elsevier, 427–442.
- SIMPSON, J.H. and JAMES, I.D. (1986). *Coastal and estuarine Fronts*, in: *Coastal and Estuarine Science-3*, AGU publications, 63–93.

- STIGEBRANDT, A. and WULF, F. (1987). A model for the dynamics of nutrients and oxygen in the Baltic, *Progr J. Mar. Res.*, 45:729–759.
- TETT, P., EDWARDS, A. and JONES, K. (1986). A model for the Growth of Shelf-Sea Phytoplankton in Summer. *Estuarine, Coastal and Shelf Science*, 23:641–672.
- VAN WESTERNHAGEN, H. and DETLEFSEN, V. (1983). North-Sea oxygen deficiency 1982 and its effects on the bottom fauna, *Ambio*, 12:264–266.
- VARELA, R.A., CRUZADO, A., TINTORÉ, J. and LADONA, E.G. (1992). Modelling the deep-chlorophyll maximum: A coupled physical-biological approach, *Journal of Marine Research*, 50:441–463.
- WROBLEWSKI, J.S. and O'BRIEN, J. (1976). A spatial model of phytoplankton patchiness, *Mar. Biol.*, 35:161–175.

Morphodynamics and Sediment Dynamics in the Southern Bight, Belgium

Jean LANCKNEUS, Guy DE MOOR, Linde VANDE VELDE,
Els DE WINNE, Isabel SANCHEZ ALMAZO and Teresa GARRIDO MARTÍN

Research Unit Marine and Coastal Geomorphology, University of Ghent

Abstract.

The Research Unit Marine and Coastal Geomorphology of the University of Ghent has been involved for 15 years in research projects dealing with the genesis, the present-day morphodynamics and sediment dynamics and the maintenance mechanisms of sandbanks. Such a research has, in addition to the scientific value, several applications in the field of offshore engineering, management of natural resources, coastal protection and environment policy, which are discussed in the present paper.

1.- Introduction.

Complex hydrodynamic processes in which tidal currents and meteo-marine conditions play the principal roles, are responsible for a continuous evolution of the seabottom topography. The study of these short and medium term changes and of the factors causing these modifications is the field of the marine morphodynamics. The sediment dynamics concern the study of the movement of surficial sediments and the analysis of the consequences of these displacements.

Research on morphodynamics and sediment processes has a fundamental significance in environmental studies evaluating for example the effects of waste disposal into the sea and of aggregate extraction. At the same time, all major engineering constructions in the offshore are preceded by a detailed cartography of the seafloor coupled to a morphodynamic evaluation of the bedforms. The practical interest of such a research will be demonstrated in this paper with the help of some examples.

2.– Dynamics of large dunes.

2.1.– Practical importance.

A morphodynamic analysis of large bedforms is of vital importance in the planning of proposed cable and pipeline routes. The Zeepipe transportation system is the longest (1,100 km) and largest diameter (1.20 m) system laid in the North Sea and connects the Norwegian Troll and Sleipner gas fields to the harbour of Zeebrugge. During construction no major problems were encountered between the gas fields and the area off Texel where the pipe was laid on the existing seafloor. However the presence of nearly 600 large dunes was detected near the border with the Belgian continental platform. Large dunes present a problem for construction of oil and gas pipes as they can cause over-stressing and freespanning with subsequent stability and safety repercussions. Pre-sweeping (flattening by dredging) of the large dunes was carried out along the planned route (Hartsuiker, 1992). A number of questions however remains, such as, will the large dunes grow back to their original height, and if this is the case, with what speed. At the same time, will the bedforms be subject to lateral migrations and how fast will they move. These questions can only be answered by a detailed analysis of the seafloor topography over a long time period. Time-series of recordings are in this case an essential tool to unravel the behaviour of large sand dunes.

2.2.– The large dunes on the Middelkerke Bank.

2.2.1.– Environmental setting.

A sediment dynamic study of bedforms is only possible if all geometric characteristics of the seafloor features can be carefully mapped and analysed. Such an analysis of the geographical distribution and characteristics of the bedforms on and near a tidal sandbank was performed on the Middelkerke Bank, southern North Sea (figure 1). This particular research project was partly financed by the European Commission in the framework of its MAST (Marine Science and Technology) programme and is known under its acronym RESECUSED (Relationship between Seafloor Currents and Sediment Mobility in the Southern North Sea; MAST contract 25-C) [Lanckneus *et al.*, 1991, De Moor *et al.*, 1993].

The Middelkerke Bank has a length of 12 km, a mean width of 1.5 km and an elevation above the seabottom varying from 15 m in the southwest to 8 m in the northeast. The bank's axis has a SW–NE orientation and runs obliquely to the coast line.

The hydrodynamics around the Middelkerke Bank are characterised by semi-diurnal tides with neap tidal ranges reaching only 65 % of the spring tidal

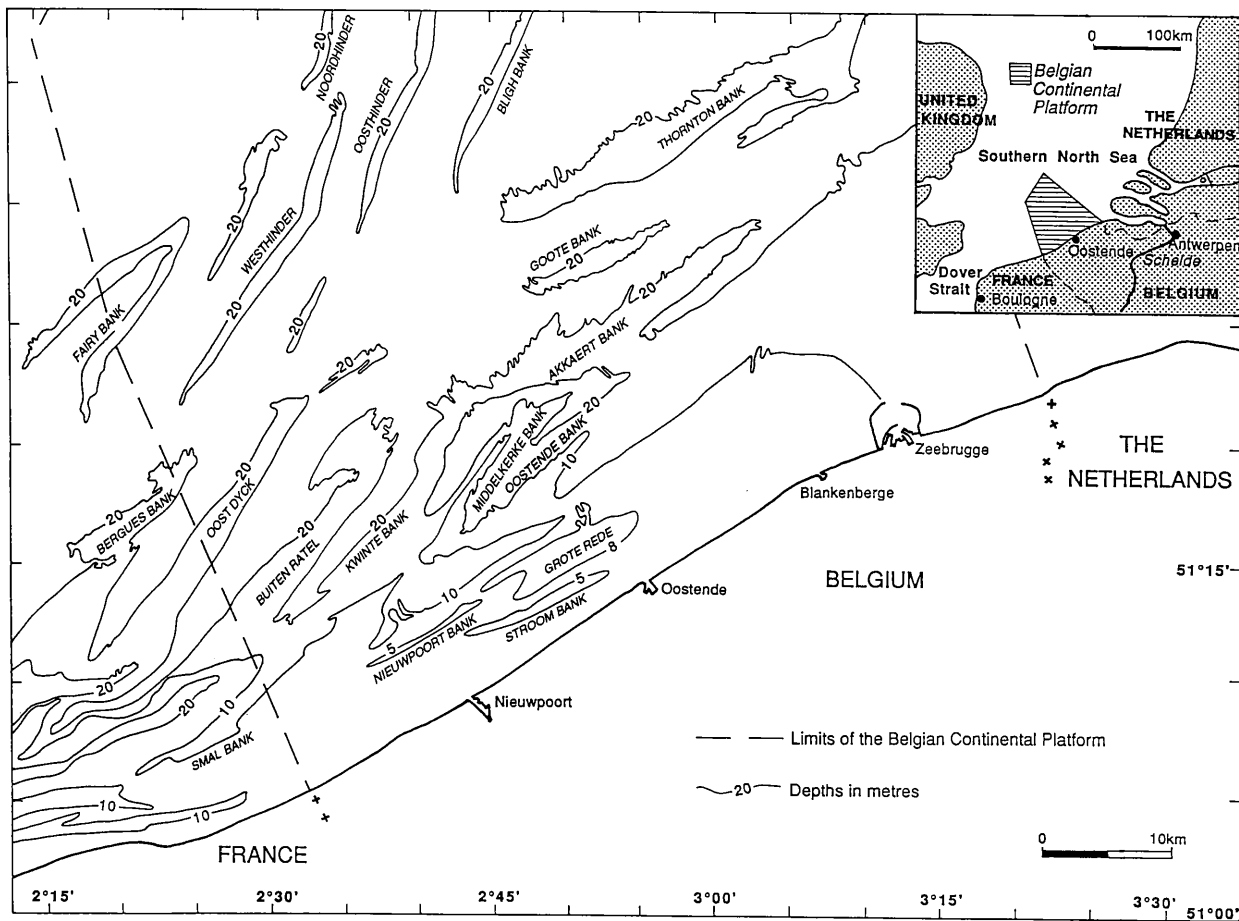


Fig. 1.- Location of the Middelkerke Bank and the Kwintebank on the Belgian continental platform

ranges. The mean tidal range near the coast is about 4.5 m. The average tidal movement corresponds to an elongated current ellipse. Peak flood and ebb currents are respectively directed towards the northeast and to the southwest. The velocity of the surface peak currents attains values of 1 m/s (Van Cauwenberghe, 1992).

2.2.2.– Cartography of the large dunes.

A detailed analysis of the bedforms on the bank and adjacent channels was carried out in May 1990 using a *Deso XX* echosounder and a *Klein* two-channel analog side-scan sonar recorder coupled with a high resolution 500 kHz transducer for the realisation of sonographs. Track lines were spaced such as to obtain complete sonar coverage of the entire bank for the purpose of attaining a sonograph mosaic. The side-scan sonar recordings were carried out with a maximum ship velocity of 4 Kts. All bedforms were mapped on a scale of 1/5,000.

The crest and the leeside troughs of the large dunes were mapped; asymmetries and heights were determined (figure 2). The large dunes occur on the flanks and summit of the bank and are completely absent in the two adjacent swales.

2.2.3.– Geometric characteristics.

The large dunes are not only mapped, but all their geometric characteristics are parameterized after which they are presented in a graphical way. Correlations between parameters are as well calculated and the results are confronted with results from theoretical equations (Lanckneus and De Moor, 1993).

The large dunes have a length of several hundreds of metres, a width of several tens of metres, a maximal height of 4.50 metres and a wavelength varying between 50 and 300 metres. The large dunes are straight to sinuous and their crests have an uniform orientation which is slightly oblique to the bank axis.

The slope of the large dunes is an important factor which affects directly the stability of man-made constructions. Figure 3 represents the angles of the steep slopes of each of the 95 dunes of the bank. Only one measurement per dune is retained corresponding to the value of the maximum observed height. In this specific case, angles are low and range between 1° and 10°, the most common value being 2° to 3°. Present-day large dunes are known to present slopes with small angles, but values of 10° are commonly found (McCave 1985). Berné (Berné *et al.*, 1989) even mentions values of 30° to 35° which were measured in several very large dune fields of the continental shelf around France.

The recordings allowed as well a detailed analysis of the asymmetry of the dunes (figure 2). All large dunes on both bank ends have their steep slopes dipping towards the northeast. The central area of the bank is characterised by

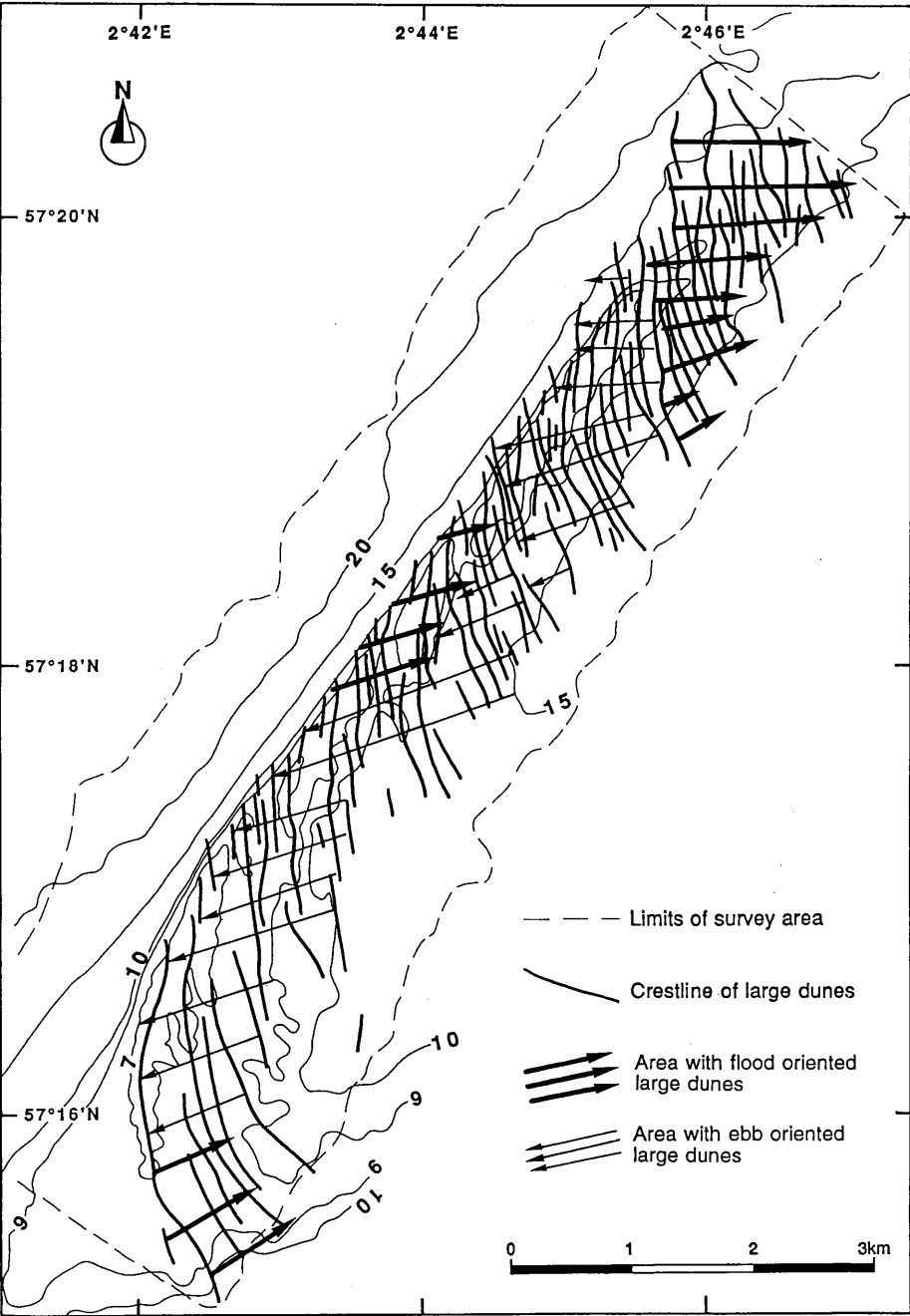


Fig. 2.- Crest lines and asymmetries of the large dunes on the Middelkerke Bank

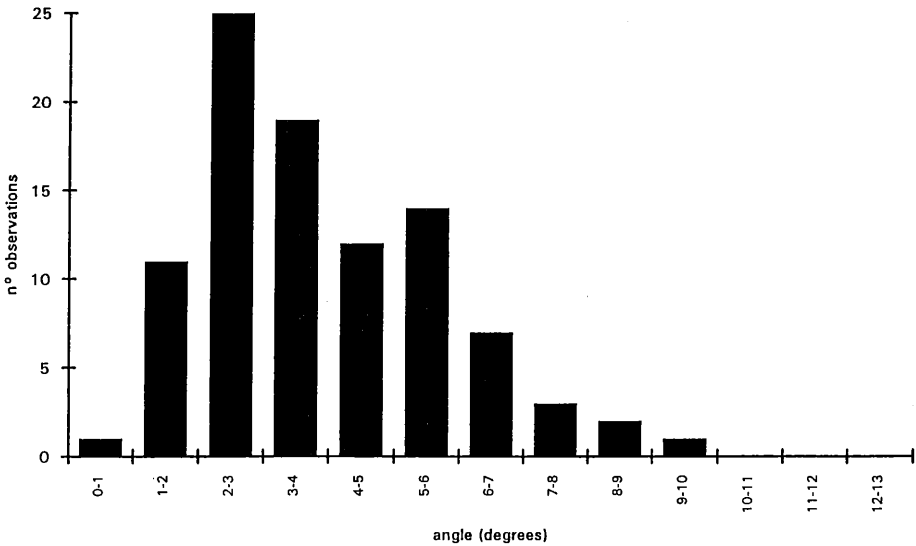


Fig. 3.— Histogram of the angle values of the steep slopes of the large dunes. Only one measurement per dune is retained.

large dunes with steep slopes dipping in opposite directions on both bank flanks towards the bank axis. Two areas with large dunes dipping toward the southwest are found between the central area and the two bank ends. Symmetric features occur especially on both bank flanks where large dunes are still relatively small. The asymmetry of one single large dune may invert along its course. Branching of crest lines was observed in several occasions.

The asymmetry of a large dune is linked to the long term hydrodynamic environment and in many cases this asymmetry can be considered as permanent (Dalrymple, 1984). This “permanent” character of asymmetry may explain the fact that few authors comment on medium-term reversal of asymmetry of large dunes. Figure 4 presents some corrected bathymetric profiles across the Middelkerke Bank along the same reference line (red Decca line H00) recorded in the period November 1987 to March 1992. Several changes in asymmetry can clearly be observed. Furthermore, it can be deduced that some large dunes reverse their asymmetry in a time span of a single month (between 22/02/1988 and 21/03/1988). Moreover, individual large dunes can disappear completely as it can be observed on 22/02/1988 and 23/03/1990. The bank however always seems to recover from such abrupt changes and to restore itself to a specific cross-profile, in this case characterised by four major large dunes.

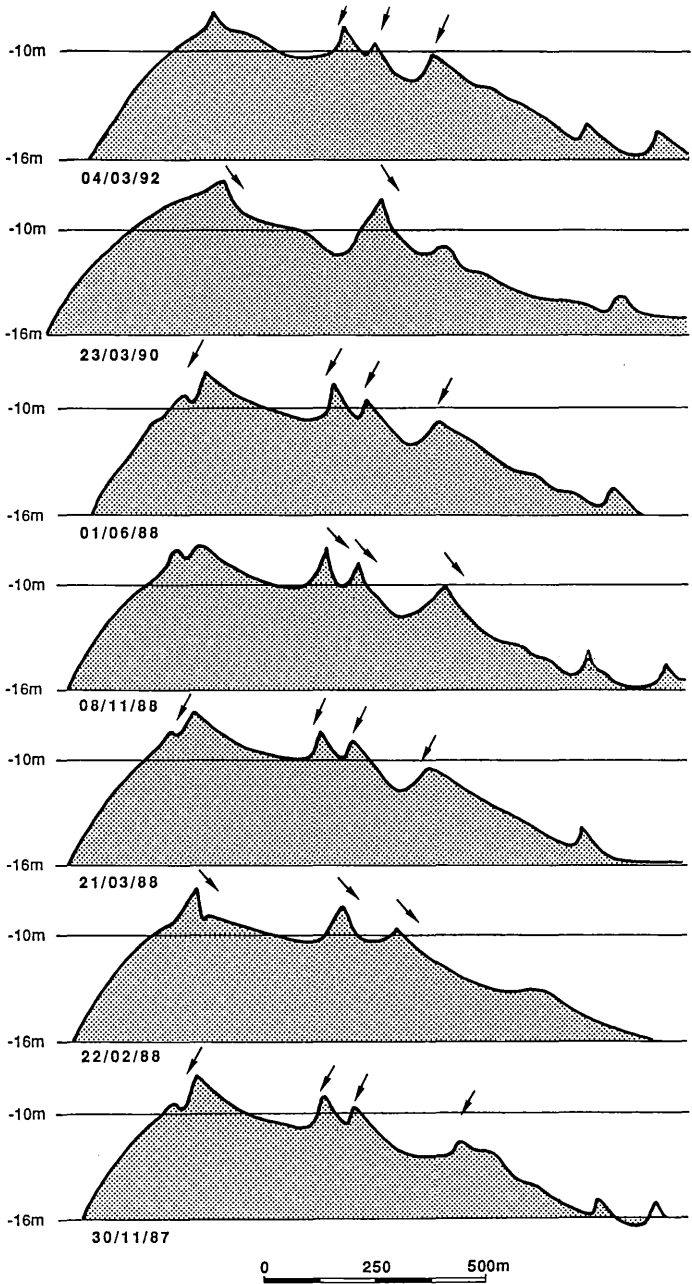


Fig. 4.– Corrected bathymetric profiles across the Middelkerke Bank along the red Decca line H00 recorded in the period November 1987–March 1992. The position of this profile can be visualized on figure 8.

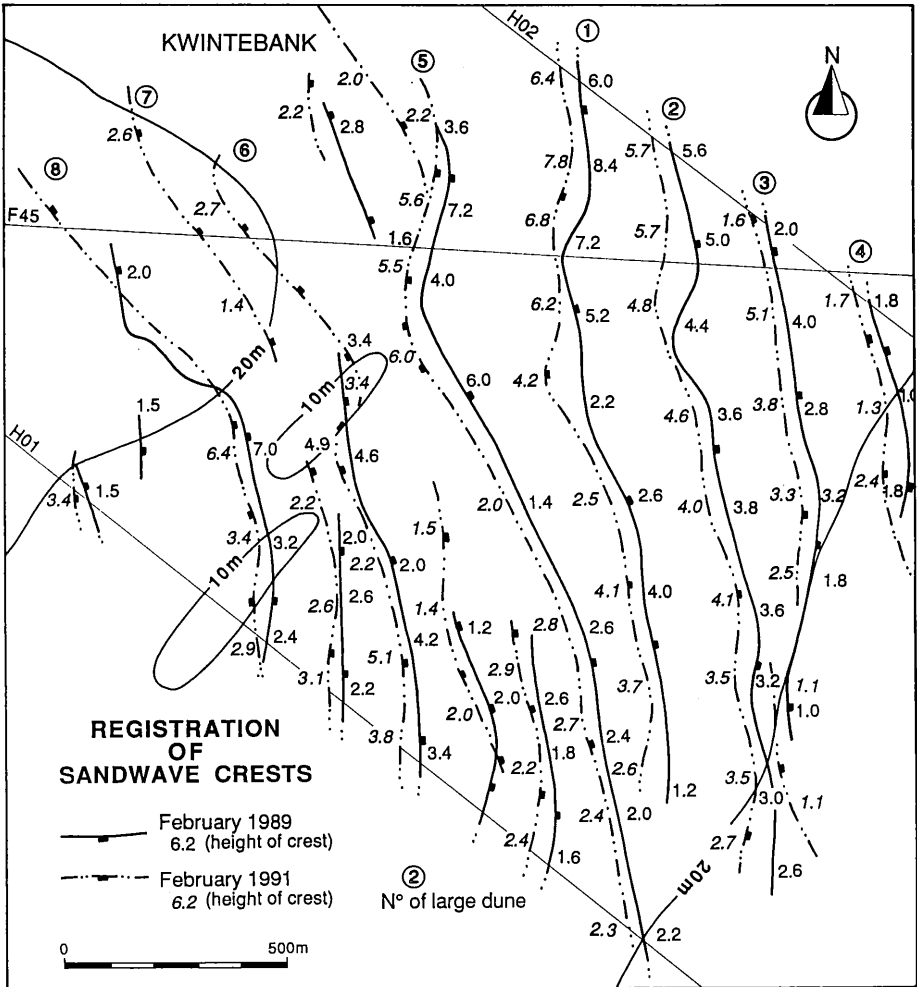


Fig. 5.— Position of the crest lines of large dunes on the northern Kwintebank in February 1989 and February 1991.

2.3.— Displacement of large dunes on the northern Kwintebank.

Analysis of the displacement of large dunes has been carried out since five years on the northern Kwintebank (De Moor, 1985) [figure 1] a bank located westward of the Middelkerke Bank. Two different techniques have been used in this aspect. First, side-scan sonar recordings were made along tracks 141 m apart allowing a complete sonograph coverage of an area of 5,500 m by 1,500 m. Position of the crest lines and of the leeside troughs, the height of the crests and the asymmetry of the large dunes were drawn on maps of a scale of 1/5,000.

Such maps representing the position of the large dunes on different moments can be superposed allowing a first evaluation of the crest's displacements. Figure 5 displays for example the net movement of the large dune's crests in the period between February 1989 and February 1991. The changes the large dunes suffered in this two-year period are minor and consist of a shifting of the crest lines towards the west of the order of some tens of metres. In the western part of the study area a new large dune (no. 7) appeared with a recorded maximum height of 2.6 m. The length of the northern extremities of two large dunes (no. 6 and 8) increased several hundreds of metres into the western swale. The height of the large dunes increased in a general way with a mean value of 0.5 m.

Furthermore, bathymetric profiling was carried out on several occasions along a number of reference lines. As positioning and depth data were digitally stored twice per second, it was possible to deduce exactly the position of the crest of the large dunes along the sailed track lines.

This technique does not allow a cartographic representation of the crest lines as only intersections between the large dune's crests and the sailed reference line are obtained. The method is however less time-consuming as registrations can be carried out at 10 Kts and processing is mainly done by the computer.

Figure 6 presents a depth profile along the reference line H00 across the northern Kwintebank sailed on 4 March 1992.

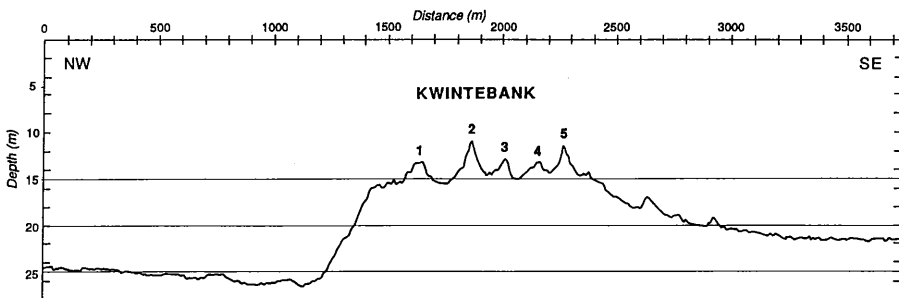


Fig. 6.- Corrected depth profile along the reference line rH00 across the northern Kwintebank recorded on 4 March 1992. The position of this profile can be visualized on figure 8.

Subsequent profiles were obtained on 5 May 1992, 9 September 1992 and 23 February 1993. The exact position of the crests along the reference tracks were calculated and plotted on a digitised crest line map of the Kwintebank which was obtained with the help of a set of side-scan sonar recordings. These data make it possible to deduce the displacements of the large dune's crests which are represented in table 1.

The information of table 1 shows that the large dunes are subject to oscillations in direction of both steep and stoss slopes. The values of displacement

Table 1
Displacement of large dune's crest lines based on echosounding
recordings carried out on 04/03/92, 05/05/92, 09/09/92 and 23/02/93

	Displacement of crest between 04/03/92 and 05/05/92	Displacement of crest between 05/05/92 and 09/09/92	Displacement of crest between 09/09/92 and 23/02/93
Large dune n° 1	35 m to W	10 m to W	30 m to E
Large dune n° 2	25 m to W	20 m to W	25 m to E
Large dune n° 3	20 m to W	25 m to W	25 m to E
Large dune n° 4	— *	— *	— *
Large dune n° 5	20 m to W	15 m to W	25 m to E
Mean value	25 m to W	17 m to W	25 m to E

* Values for large dune n° 4 could not be calculated as the large dune disappeared after the registration of 4 March 1992.

are low and after 2 years the large dunes returned more or less to the same position they initially had. Interesting to note is that along this reference line, the asymmetry of the large bedforms remained unchanged which means that several large dunes moved in the direction of their gentle slope, while keeping their original asymmetry (Lanckneus and De Moor, 1991).

3.— Impact of aggregate extraction.

3.1.— Practical importance.

Sand and gravel have been exploited in the past decades mainly on land. A continuous increase of the demand together with a growing environmental protection policy are responsible for the fact that in Belgium, like in many other countries, an interest grew up for the exploitation of the continental shelf. Extraction of marine aggregates on the Belgian continental platform started in 1979. In the first 10 years, exploitation was limited to 0.5 million m³ a year. This quantity doubled however from 1989 on and extraction in 1991 reached the figure of 1.4 million m³ (Pichot and Lauwaert, 1993a). Sand is used principally for the building industry, construction of roads and for beach nourishment. The exact impact of the extraction of marine aggregates on the environment is still a matter of debate. However, several studies demonstrate clearly that an effective management of these valuable natural resources is an absolute necessity.

Harris *et al.* (1990) mentions the case of the dredging activities on a section of the Middle Banks, Queensland, Australia, where 14 million tons of sand were dredged in 1983 for the construction of Brisbane Airport. Survey work in 1989 indicated that the bank, which had been dredged to 17 m, had been completely

rebuilt. The question which can be asked is of course, like Harris states it: "where did the sand come from?" It has been suggested, based on studies of sandbanks in other areas, that there exists a balance in sand flux between offshore sandbanks and the coastline (Pattiaratchi, 1986). A fact is that the shoreline of Moreton island, in front of the Middle Bank, has been shown to undergo erosion, to supply, possibly the dredged bank section, although no definite evidence was found to corroborate this hypothesis.

Sutter *et al.* (1989) illustrated the need to determine optimum dredging configurations if deleterious effects of utilisation of offshore sand are to be minimised. A preliminary assessment of the consequences of using sand from a large shore-parallel feature for beach nourishment on the coast of Louisiana indicated that the shoal serves to attenuate storm waves. Removal of this feature would result in increased erosion of the adjacent shoreline.

Migniot and Viguier (1980) emphasise as well the need for respecting precise dredging conditions of sand in the offshore if damaging consequences of these extractions on the coast line are to be avoided. Studies in flumes and wave tanks point out that in areas with severe waves extraction has to be carried out at a minimum depth of 20 m under the lowest low water level to obtain negligible sand movements on gently sloping bottoms.

Bruun (1964) studied the impact of sand extraction on the beach and stressed the fact that removal of bottom material in the nearshore and offshore will interfere with the stability of the beach and sea bottom.

3.2.– The case of the Kwintebank.

Sand is extracted by private companies on the Kwintebank, Buiten Ratel and Oost Dyck (figure 1). More than 70% of the sand is exploited on the Kwintebank (De Moor and Lanckneus, 1991) which can be explained by the fact that the characteristics of the sand on the northern part of this bank suit the best the official prevailing standards for the use of sand in public works. As the most important part of the exploitation is carried out in a specific section of a single bank, questions arise concerning the stability of the seafloor in this part and the possible relationship with coastal erosion phenomena. The Flemish Banks play after all an important role in the protection of the coast as the energy of the waves is weakened by their presence. A lowering of the bank top would without doubt lead to stronger erosion of the beach area.

The evolution of the bank volume of the Flemish Banks has been monitored since more than a decade in order to study the morphological and sedimentological impact of the sand extraction.

3.2.1.– Methodology.

Volumetric monitoring of the bank volume (De Moor *et al.*, 1989) is carried out through bathymetric registrations, recorded along a number of reference tracks situated across the bank and sailed three to five times a year. After corrections for tidal movements and variations in ship's velocity and heading, net depth profiles are plotted in relation to a zero level. Different profiles sailed along the same reference track can then be compared. The numeric processing of the depth data comprises the calculation of unit volumes along the reference tracks which are delimited by the bank profile and by a reference level which can be situated at intervals of 2.5 m beneath the zero reference level. Examples of such unit volumes are the top slice volume (defined at the bottom by the highest reference plane intersecting the bank) and the total bank volume (defined at the bottom by the lowest reference plane intersecting the bank above the highest base concavity) [figure 7].

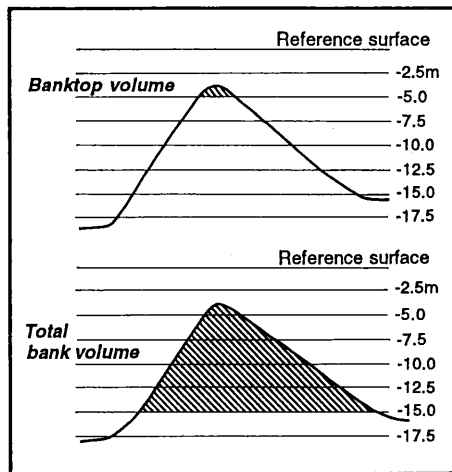


Fig. 7.– Definition of the bank top volume and the total bank volume

All calculated values can be expressed in absolute values ($\text{m}^3/\text{m}/\text{year}$) and in relative values ($\%/ \text{year}$). These relative values are obtained by normalising the absolute values in relation to a reference unit volume. After having sailed several times a reference track, a time-series of unit volumes is obtained on which a regression analysis is applied. Results of this analysis allows to deduce the present volumetric trend which can be towards erosion, accumulation or stability.

3.2.2.– Results.

Bank top volume.

Analysis of the relative trend of the bank top volume (figure 8a) shows clearly that the northern part of the bank is subject to a sediment loss which amounts up to 10%. This zone corresponds to the area in which aggregate extraction is carried out intensively. South of this area, a section exists with relative high gains. The central and southern part of the bank are characterised by areas of relative stability alternating with areas of light sediment loss. A precise correlation study between exploited sand and sediment loss is however not possible as precise data concerning the exact place and amount of extracted sediment lack.

It is interesting to mention in this respect that the impact of sand extraction on the erosion energy near and on the Flemish Banks was studied with the help of hydrodynamical models (Pichot and Lauwaert, 1993b). Results of a simulation taking into account a 3 year period of sand extraction, proved that the erosion energy would increase with 1 to 2% on the northern part of the Kwintebank.

Total bank volume.

The significance of the above mentioned sediment losses in function of the total sand reserve can be appreciated on figure 8b. The general trend of the total bank volume points to a tendency of stability as the mean annual volumetric change ranges for nearly the entire bank between -1% and $+1\%$. The severe sediment loss of the top volume in the northern part of the bank is however still reflected in the total bank trend which indicates in this section a weak decrease in volume (up to -2%). Similarly an area of light accumulation is found in the central part of the bank.

4.– Fluxes of sand.

If the total bank volume remains more or less stable in spite of a high rate of extraction, it is clear that a maintenance mechanism has to exist which is responsible for a sediment supply towards the bank top. Such a mechanism was in a similar way responsible for the rebuilding of the Middle Banks, as it was mentioned in a former paragraph.

An analysis of the residual transport paths along which net sediment fluxes occur can be performed with several techniques (Lanckneus *et al.*, 1992a).

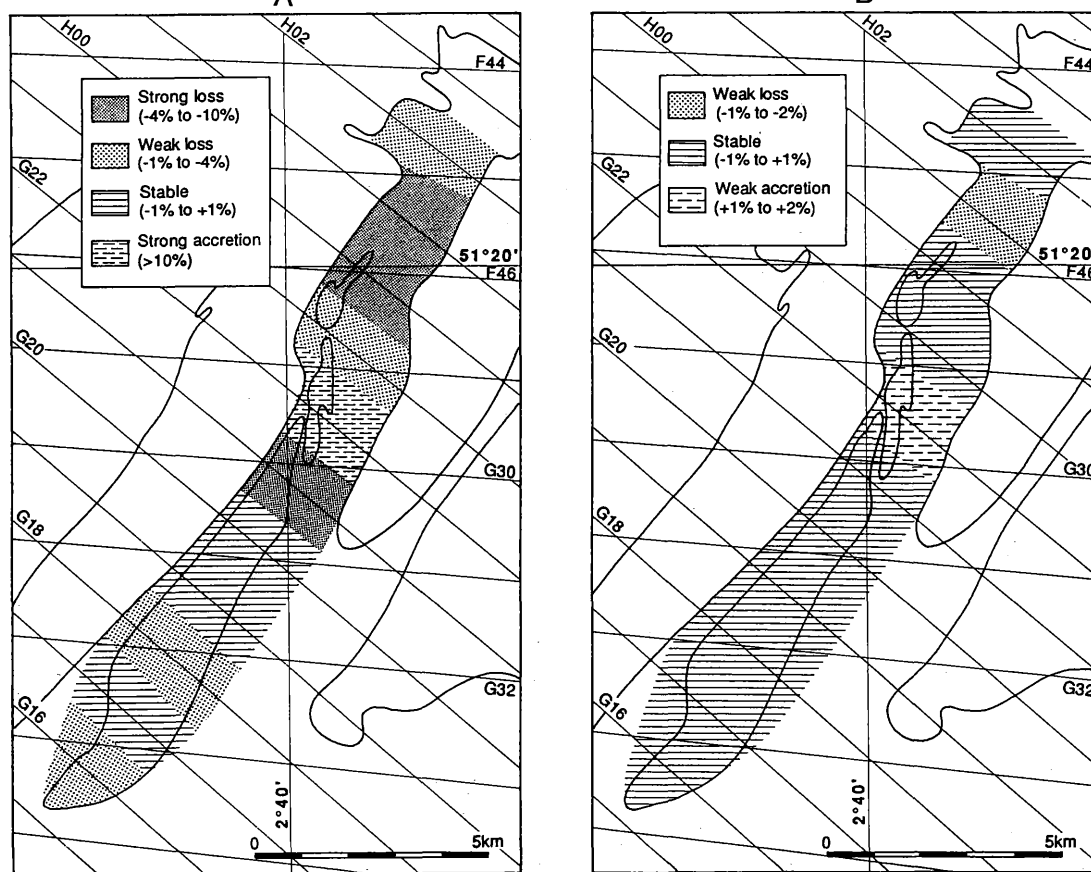


Fig. 8.- Mean annual trends expressed in relative values of the banktop volume (a) and of the total bank volume (b) based on bathymetric data recorded in the period 1983–1992.

4.1.– Methodology.

Cartography of these paths can be based on the study of the geometric characteristics of bedforms such as large (Caston, 1972) and small dunes (McCave and Langhorne, 1982). Former studies on the Flemish Banks based on sonographs and current meter results (Lanckneus *et al.*, 1992a) showed that only the small dunes are oriented perpendicular to the direction of the peak currents.

As the direction of the net sediment displacement generally corresponds to that of the more intense current (Johnson *et al.*, 1981), residual transport path research on the Flemish Banks is always based on small dunes (Lanckneus *et al.*, 1989). Mapping the bedforms on the Flemish Banks is carried out several times a year with the help of side-scan sonar equipment.

4.2.– Results.

Sonographs make it possible to visualise the sediment fluxes on the sandbanks. The general model of these transport paths implies a sediment supply from both adjacent swales towards the bank top in opposite directions (figure 9). The western flank of the Kwintebank receives sand from the southwest transported by the peak flood current. The residual transport on the eastern flank is commanded by the peak ebb current from the northeast.

The sediment contributions from both swales can however vary significantly through time and time-series of sonographs proved that the dominant sediment supply can come either from the southwest or from the northeast (Lanckneus *et al.*, 1992b).

This supply mechanism is responsible for the maintenance of the bank and has the effect that the bank regenerates after erosional phases caused by heavy storms or sand extraction. The origin of the sediment and the possible morphological evolution of the source area remain however unknown. These questions arise the problem of the origin of the intensive beach erosion which ravages some sections of the Belgian coast. Data lack however in this stage to associate coastal erosion phenomena to maintenance mechanisms of sandbanks. These questions will be tackled in the framework of a new research project which will emphasise on the analysis of sediment interactions between beach, nearshore and offshore.

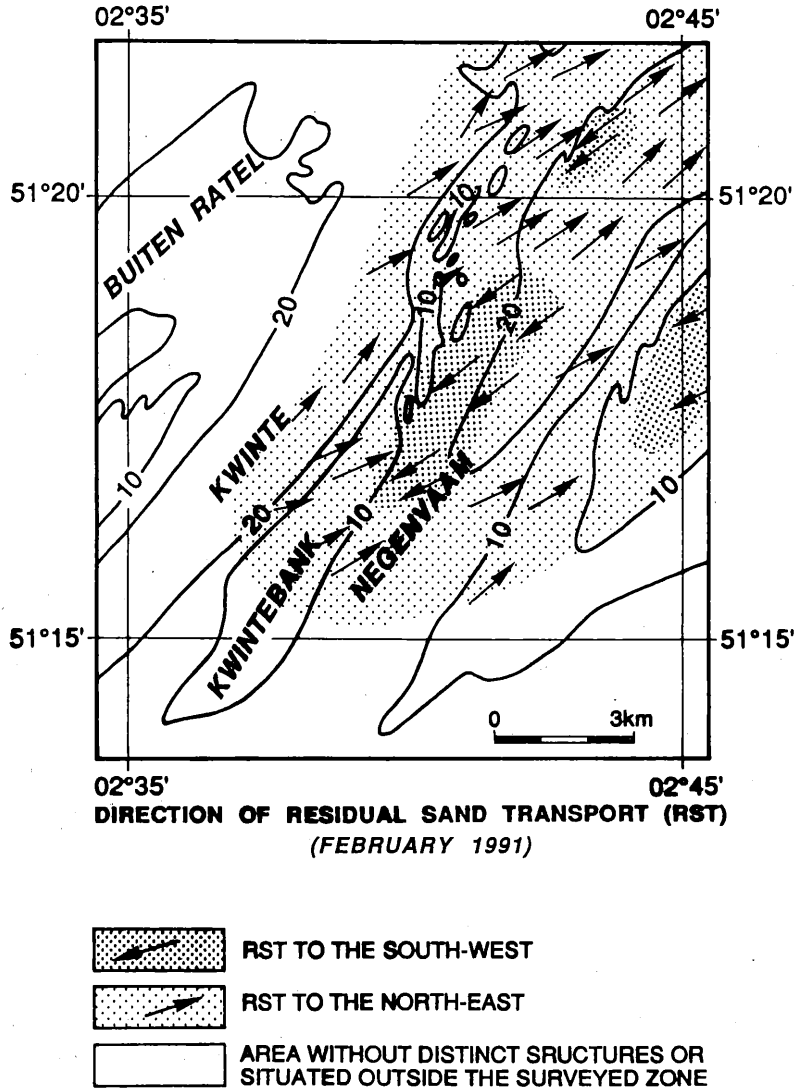


Fig. 9.- Directions of residual sand transport on and near the Kwintebank based on sonographs recorded in February 1991.

5.- Conclusions.

Extraction of marine resources such as aggregates will without doubt increase in future times due to a growing environmental protection policy on land. It is therefore an absolute necessity to monitor carefully the areas where exploitation is being carried out in order to maintain a sustainable extraction rate

of these valuable resources. The major lack in our knowledge nowadays concerns the exact location of the sites where extraction of offshore sand is carried out. However, installation in a near future of a black box aboard the dredgers, which will record the ship's position and the volume of the extracted sediment, will without doubt be a major improvement.

At the same time the fluxes of sand responsible for the maintenance mechanism of the sandbanks have to be analysed on a larger scale. Mapping the sediment transport paths by acoustic teledetection techniques or by sedimentological approaches has to be carried out towards the nearshore. The establishment of the exact relationship between coastal erosion phenomena and offshore processes will be a great challenge for future years.

Finally the evolution of bedforms such as large dunes has to be analysed on a time-scale of various years. Emphasis will be put in future research on the link between prevailing meteo-marine conditions and the migrational trends of large bedforms.

Acknowledgements.

This research was supported by the European Commission in the framework of its MAST programme, the Belgian Ministry of Economic Affairs and by the Management Unit of the Mathematical Models North Sea. We are grateful for the logistic support provided by the National Fund for Scientific Research. The authors wish to thank the entire crew of the oceanographic vessel Belgica for their constant help and co-operation during the survey activities.

References.

- BERNÉ, S., ALLEN, G., AUFFRET, J.P., CHAMLEY, H., DURAND, J. and WEBER, O. (1989). Essai de synthèse sur les dunes hydrauliques géantes tidales actuelles, *Bull. soc. géol. France*, V, 6:1145-1160.
- BRUUN, P. (1964). Offshore dredging, Influence on Beach and bottom stability, *The Dock and Harbour Authority*, XLV, 530:241-247.
- CASTON, V.N.D. (1972). Linear sand banks in the southern North Sea, *Sedimentology*, 18:63-78.
- DALRYMPLE, R.W. (1984). Morphology and internal structure of sandwaves in the Bay of Fundy, *Sedimentology*, 31:365-382.
- DE MOOR, G. (1985). *Shelfbank Morphology off the Belgian Coast. Recent methodological and scientific developments*, in: M. Van Molle (Editor), *Recent trends in Physical Geography in Belgium. Liber Amicorum L. Peters*, VUB, Study series of the Vrije Universiteit Brussel, New series, 20:149-184.

- DE MOOR, G., LANCKNEUS, J., VAN OVERMEIRE, F., VAN DEN BROECK, P., and MARTENS, E. (1989). *Volumetric analysis of residual sediment migration on continental shelf sand banks in the Southern Bight (North Sea)*, Intern. Comm. Explor. Seas, Hydrography Committee, Den Haag Meeting 1989, CM 1989/C, 43:1–25.
- DE MOOR, G. and LANCKNEUS, J. (1991). *Zand- en grindwinning op het Belgisch Continentaal Plat en monitoring van de eventuele gevolgen voor de bodemstabiliteit*, Colloquium Oppervlaktedelfstoffen problematiek in Vlaanderen, Gent, 23 oktober 1991, Genootschap Gentse Geologen, *Proceedings*, 188–214.
- DE MOOR, G., LANCKNEUS, J., BERNÉ, S., CHAMLEY, H., DE BATIST, M., HOUTHUYS, R., STOLK, A., TERWINDT, J., TRENTESAUX, A. and VINCENT, C. (1993). *Relationship between sea floor currents and sediment mobility in the southern North Sea*, Symposium MAST Days, Brussels 15–17 March 1993, Project Reports, 1:193–207.
- HARRIS, P.T., PATTIARATCHI, C.B., KEENE, J.B. and COLE, A. (1990). *Modelling the Evolution of a Linear Sandbank Field, Moreton Bay, Queensland: Report of Results Obtained During the Cruise of A.M. Brolga in July, 1989*, Ocean Sciences Institute, The University of Sidney, 41, 172 pp.
- HARTSUIKER, F.E.A.P. (1992). *Mariene Geodesie: Praktische Toepassingen*, in: *The Hydrographic Society, Benelux Branch (Editor) Mariene Geodesie, Meten op Zee*, 35–45.
- JOHNSON, M.A., STRIDE, A.H., BELDERSON, R.H. and KENYON, N.H. (1981). *Predicted sand wave formation and decay on a large offshore tidal-current sand-sheet*, in: S.D. Nio, R.T.E. Schüttenhelm and T.C.E. Van Weering, (Editors), *Holocene marine sedimentation in the North Sea Basin*, 247–256.
- LANCKNEUS, J., DE MOOR, G., DE SCHAEPMEESTER, G. and LIBEER, L. (1989). *Acoustic teledetection of shelf bedforms and their meaning for sediment dynamics*, in: G. Pichot (Editor), *Progress in Belgian Oceanographic Research 1989*, Brussels, 147–163.
- LANCKNEUS, J. and DE MOOR, G. (1991). *Oceanologica Acta*, Vol. SP. 11, 123–127.
- LANCKNEUS, J., DE MOOR, G., BERNÉ, S., CHAMLEY, H., DE BATIST, M., HENRIET, J.P. and TRENTESAUX, A. (1991). *Cartographie du Middelkerke Bank : dynamique sédimentaire, structure géologique, faciès sédimentaires*, International Symposium Ocean Space Advanced Technologies European Show, Brest, September 24–27 1991, 11 pp.
- LANCKNEUS, J., DE MOOR, G., DE SCHAEPMEESTER, G., MEYUS, I., SPIERS, V. (1992a). *Residual sediment transport directions on a tidal sand bank, Comparison of the "McLaren Model" with bedform analysis*, *Bull. de la Soc. belge d'Études Géog.*, 2:425–446.
- LANCKNEUS, J., DE MOOR, G., DE SCHAEPMEESTER, G., MEYUS, I. and SPIERS, V. (1992b). *Monitoring of a tidal sandbank: evolution of bedforms, volumetric trends, sedimentological changes*, Hydro'92, Eight Biennial International Symposium of the Hydrographic Society (Copenhagen, 30 November – 3 December 1992), *Proceedings*, 19 pp.

- LANCKNEUS, J. and DE MOOR, G. (1993). *Bedforms on the Middelkerke Bank, Southern North Sea*, Special Publication International Association of Sedimentologists (in press).
- MCCAVE, I.N. and LANGHORNE, D.N. (1982). Sand waves and sediment transport around the end of a tidal sand bank, *Sedimentology*, 29:95–110.
- MCCAVE, I.N. (1985). *Recent shelf clastic sediments*, in: Brenchley and Williams (Editors), *Sedimentology, recent developments and applied aspects*, 49–65.
- MIGNIOT, C. and VIGUIER, J. (1980). Influence de l'extraction des granulats en mer sur l'équilibre du littoral, *La Houille Blanche*, 3:177–194.
- PATTIARATCHI, C.B. (1986). *Offshore sandbanks and coastal erosion implications for the dredging industry*, in: M.K. Gandy and A.J. Williams (Editors), *The Future of the Aggregates Industry in Wales*, published by the Prince of Wales Committee, 49–75.
- PICHOT, G. and LAUWAERT, B. (1993a). *Evolutie van de zand- en grindontginningen*, in: *Effecten op het marien leefmilieu van de zand- en grindontginningen op het Belgisch continentaal plat*, Syntheseverslag opgesteld door de stuurgroep zand- en grindontginningen, opgericht door het Ministerie van Economische Zaken, Brussel (in press).
- PICHOT, G. and LAUWAERT, B. (1993b). *Modelisatie van erosie-energie*, in: *Effecten op het marien leefmilieu van de zand- en grindontginningen op het Belgisch continentaal plat*, Syntheseverslag opgesteld door de stuurgroep zand- en grindontginningen, opgericht door het Ministerie van Economische Zaken, Brussel (in press).
- SUTTER, J.R., MOSSA, J., PENLAND, S. (1989). Preliminary assessments of the occurrence and effects of utilization of sand and aggregate resources of the Louisiana Inner Shelf, *Marine Geology*, 90:31–37.
- VAN CAUWENBERGHE, C. (1992). *Stroomatlas 1992 Noordzee Vlaamse Banken*, Dienst der Kusthavens, Hydrografie Oostende, Ministerie van de Vlaamse Gemeenschap, Leefmilieu en Infrastructuur, 26 pp.

The Use of the McLaren Model for the Determination of Residual Transport Directions on the Gootebank, Southern North Sea

Jean LANCKNEUS, Guy DE MOOR,
Vera VAN LANCKER and Geert DE SCHAEPMEESTER

Research Unit Marine and Coastal Geomorphology, University Ghent

Abstract.

Sixty samples were collected on the Gootebank to assess the application of the McLaren sediment transport model on a tidal sandbank environment. Residual sediment transport directions were deduced and compared with the results of a detailed bedform analysis obtained by side-scan sonar recordings. Results show that when sediments become finer and better sorted, the corresponding skewness becomes more positive which is in contradiction with the sediment transfer function of McLaren and Bowles (1985). Comparison of the directions of residual sediment transport deduced from bedform analysis and from the sediment trend analysis shows that a good similarity is reached in the adjacent swales and that an offset of 90° exists on the bank. The transversal grain-size differentiation is explained by the formation of a lag deposit induced by an upslope increase in maximum current speed from the swale to the bank crest.

1.- Introduction.

Several techniques have been developed to study the residual currents and the residual sediment transport (Lanckneus *et al.*, 1992). Bedforms, especially their asymmetry, can be used to determine the residual direction of bedload transport. On such ground Johnson and Baldwin (1986) drew dominant sand transport paths on the Northwest European Shelf. They advance two directions of residual sand movement off the Belgian coast; a northeastward transport in a narrow coastal section and a southwestward transport more offshore.

Recent developments in sedimentology unfolded the possibility of the use of variations in the areal pattern of grain-size parameters for the determination of residual sediment transport paths (McLaren, 1981; McLaren and Bowles, 1985). The latter advance that in a downstream direction, sandy sediments

become either finer, better sorted and more negatively skewed ("case B transport") or coarser, better sorted and more positively skewed ("case C transport"). McLaren's model has been applied chiefly in coastal, fluvial and lacustrine environments. Published studies on the applicability of the McLaren model in a tidal shelf environment where currents are continuously changing in direction and velocity are still rare. The Research Unit Marine and Coastal Geomorphology of the University Ghent has been critically analysing the possibilities of this technique on several tidal banks (Lanckneus *et al.*, 1992) of the Belgian continental platform. The present paper presents the results of a study carried out on one of these banks, the Gootebank which has been the object of a scientific monitoring programme for several years as the bank is subject to aggregate extraction.

2.- Environmental setting.

The Gootebank is a shelf sand bank located on the Belgian continental platform (figure 1). The bank belongs to the Zeeland Ridges, a group of banks whose orientation is parallel to the coastline and which are mainly located in Dutch territorial waters. The Gootebank has a length of 15 km and a maximum width of 2 km. It shows a relative elevation above the seafloor of 6 m at the ends and up to 10 m at the centre which corresponds with a low water depth of 12 m. Its height is, in comparison with the Flemish Banks, less pronounced although they occur at approximate similar water depths. The topography of the bank is not very explicit, but in general, it has very mild slopes to the NW and a more steeper slope to the SE. According to Houbolt (1968) and to Laban and Schüttenhelm (1981), the Zeeland Ridges are originated by a sand accumulation around small pre-existing sediment bodies.

The hydrodynamics around the Gootebank are characterised by semi-diurnal tides of megatidal range which differ considerably between neap and spring tide. The mean tidal range near the coast, situated at about 22 km reaches 4.5 m. The average tidal movement corresponds to an elongated current ellipse. The general directions of the flood peak and ebb peak currents are approximately from southwest to northeast and from northeast to southwest respectively. Information from a nearby current meter indicates a slightly stronger ebb peak current which amounts up to 1 m/s (Van Cauwenberghe, 1992).

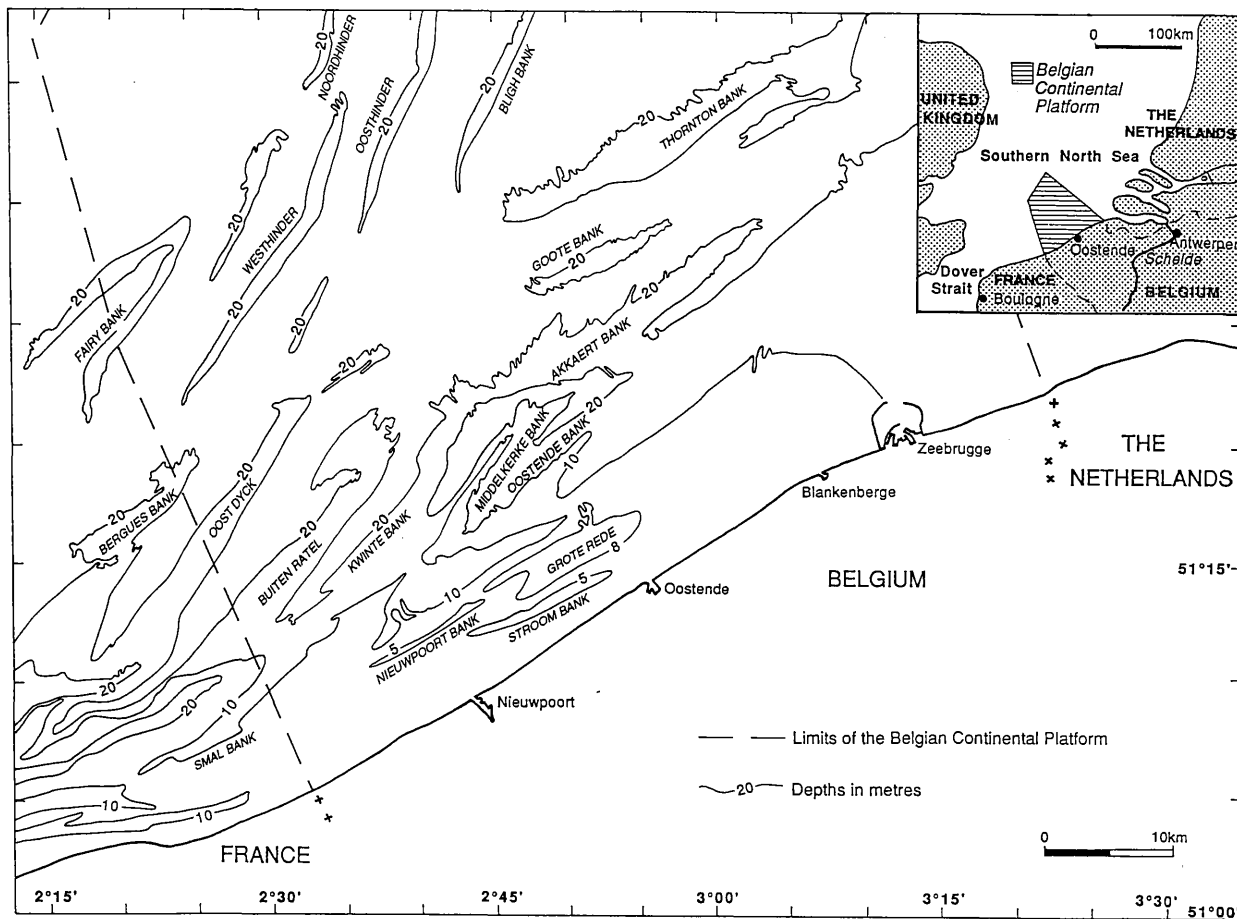


Fig. 1.- Location of the Gootebank Bank on the Belgian continental platform

3.- Acquisition of field data.

On the 9th and 10th of June 1992 sixty bottom samples were collected on the central part of the Gootebank using a Van Veen bottom sampler with an average spacing of 600 m (figure 2). This grab sampler has a penetration of more or less 10 cm in the sea bottom and does not allow the sampling of individual laminae of sediment. This is however not a disadvantage as the use of a more global sample of the superficial sediment is more adequate for sediment trend interpretations on a regional scale (McLaren, 1981) and certainly on a longer term.

The samples, consisting of ± 2 kg of sediment, were dried at room temperature. A small representative sample of 200 g was separated with the help of a sample splitter. Fractions coarser than 4 mm and finer than 50 mm were separated respectively by dry and wet sieving. Fines have an average value of 1% of the total sample. Sediments were decalcified by acid dissolution after which the sand fraction was further analysed by dry sieving. The grain-size analysis can be carried out on the natural as on the decalcified sample. Decalcification was carried out to improve results in the sediment trend analysis. Sand consists indeed of quartz particles and shell fragments. Both types of grains have a different density and a different morphology as the shell fragments present mostly a flat shape quite different from the rounded quartz grains. This will cause the two types of particles to react in a different way to the sorting processes which act upon them. It is therefore preferable to work exclusively with quartz grains as shell fragments could bias the grain-size parameters. The following grain-size parameters were calculated according to Folk and Ward (1957):

— Mean Size

$$M = \frac{\phi_{16} + \phi_{50} + \phi_{84}}{3}$$

— Standard deviation:

$$\sigma = \frac{\phi_{84} - \phi_{16}}{4} + \frac{\phi_{95} - \phi_5}{6.6}$$

— Skewness:

$$Sk = \frac{\phi_{16} + \phi_{84} - 2\phi_{50}}{2(\phi_{84} - \phi_{16})} + \frac{\phi_5 + \phi_{95} - 2\phi_{50}}{2(\phi_{95} - \phi_5)}$$

The position of the samples and the values of the above mentioned grain-size parameters are presented in table 1.

The next day geosonic survey operations were carried out on the same site. A *Deso XX* echosounder was used for bathymetric recordings and sonographs were realised with a Klein digital dual channel side-scan sonar recorder coupled with a 500 kHz transducer. During these operations a slant range of 75 m was maintained. Navigation and positioning were performed by the Syledis system with a geographical position accuracy of 5 m. The recordings were made along tracks 141 m apart (figure 3) which allowed a coverage of an area of 3 km². The

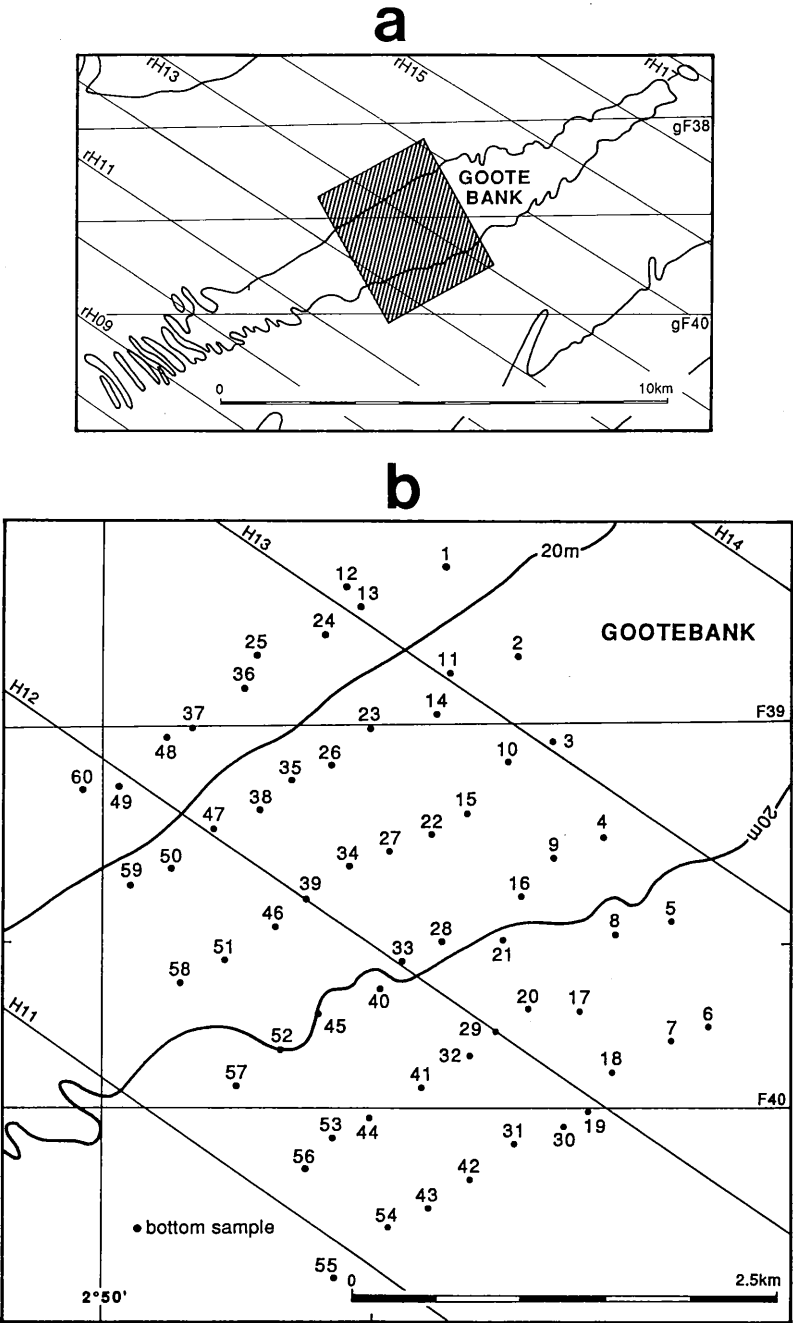


Fig. 2.– Location of sampled area (a) and of samples taken on the central Gootebank in June 1992 (b)

Table 1

Position and grain-size parameters of the decalcified samples of the central part of the Gootebank taken on the 9th and 10th of June 1992

Sample	Position Lat.	Position Long.	Mean ϕ	Sorting ϕ	Skewness
1	51 28 06.88	02 51 43.97	2.07	2.14	0.451
2	51 27 51.60	02 52 06.23	1.60	0.39	0.057
3	51 27 36.20	02 52 16.61	1.90	0.29	0.230
4	51 27 18.78	02 52 31.65	1.82	0.35	0.078
5	51 27 04.29	02 52 53.60	1.53	0.50	- 0.091
6	51 26 45.42	02 53 04.41	1.92	0.43	0.175
7	51 26 42.48	02 52 52.33	1.92	0.44	0.102
8	51 27 01.82	02 52 34.32	1.22	0.69	0.069
9	51 27 15.12	02 52 15.41	1.79	0.30	0.112
10	51 27 32.75	02 52 02.20	1.94	0.28	0.240
11	51 27 48.70	02 51 45.47	1.63	0.68	0.250
12	51 28 03.84	02 51 13.14	1.65	0.61	0.005
13	51 28 00.43	02 51 18.12	1.59	0.55	0.061
14	51 27 41.38	02 51 41.66	1.28	0.69	- 0.290
15	51 27 23.49	02 51 51.09	1.92	0.31	0.140
16	51 27 08.68	02 52 07.27	1.70	0.34	0.030
17	51 26 48.34	02 52 25.11	1.97	0.34	0.240
18	51 26 37.49	02 52 34.31	1.93	0.38	0.202
19	51 26 29.55	02 52 27.01	1.91	0.42	0.070
20	51 26 48.50	02 52 08.23	1.89	0.40	0.150
21	51 27 00.99	02 52 01.77	1.86	0.40	0.004
22	51 27 19.94	02 51 40.17	1.82	0.40	- 0.075
23	51 27 38.71	02 51 21.32	1.62	0.43	- 0.003
24	51 27 55.42	02 51 07.30	1.67	0.59	0.018
25	51 27 51.48	02 50 47.36	1.44	0.55	0.046
26	51 27 32.19	02 51 09.83	1.82	0.38	0.097
27	51 27 16.85	02 51 27.26	1.80	0.40	- 0.084
28	51 27 00.69	02 51 43.41	1.83	0.39	- 0.017
29	51 26 44.56	02 51 59.77	1.93	0.33	0.250
30	51 26 27.75	02 52 19.91	1.94	0.42	0.101
31	51 26 24.71	02 52 04.96	1.99	0.75	0.003
32	51 26 40.51	02 51 51.84	1.88	0.38	0.159
33	51 26 57.00	02 51 31.28	1.86	0.41	- 0.051
34	51 27 14.10	02 51 15.10	1.88	0.35	0.034
35	51 27 29.47	02 50 57.85	1.73	0.46	0.124
36	51 27 45.01	02 50 43.34	1.54	0.64	0.014
37	51 27 37.90	02 50 26.85	1.76	0.68	0.014
38	51 27 23.42	02 50 47.62	1.80	0.33	0.113
39	51 27 07.42	02 51 01.28	1.82	0.36	- 0.032
40	51 26 52.38	02 51 24.32	1.69	0.54	- 0.226
41	51 26 34.34	02 51 37.51	1.84	0.42	0.187
42	51 26 17.96	02 51 52.23	2.02	0.52	0.263
43	51 26 12.23	02 51 39.01	2.29	2.66	0.586
44	51 26 28.27	02 51 20.44	1.83	0.40	0.141
45	51 26 46.86	02 51 05.63	1.80	0.40	0.018
46	51 27 03.19	02 50 52.06	1.53	0.48	- 0.157
47	51 27 20.05	02 50 33.27	1.63	0.40	0.072
48	51 27 37.04	02 50 18.95	2.01	0.53	0.120
49	51 27 28.19	02 50 04.28	2.04	0.77	0.232
50	51 27 12.95	02 50 21.26	1.01	0.98	- 0.461
51	51 26 56.61	02 50 37.66	1.58	0.40	- 0.122
52	51 26 41.63	02 50 54.19	1.67	0.51	- 0.099
53	51 26 25.47	02 51 10.16	1.90	0.38	0.176
54	51 26 09.57	02 51 26.87	1.60	0.39	0.028
55	51 26 00.07	02 51 09.24	1.84	0.56	0.140
56	51 26 20.27	02 51 01.51	1.86	0.48	0.185
57	51 26 34.38	02 50 40.11	1.58	0.45	- 0.012
58	51 26 52.56	02 50 23.30	1.71	0.35	- 0.036
59	51 27 10.10	02 50 07.47	1.76	0.75	- 0.342
60	51 27 26.83	02 49 52.88	1.92	0.54	0.013

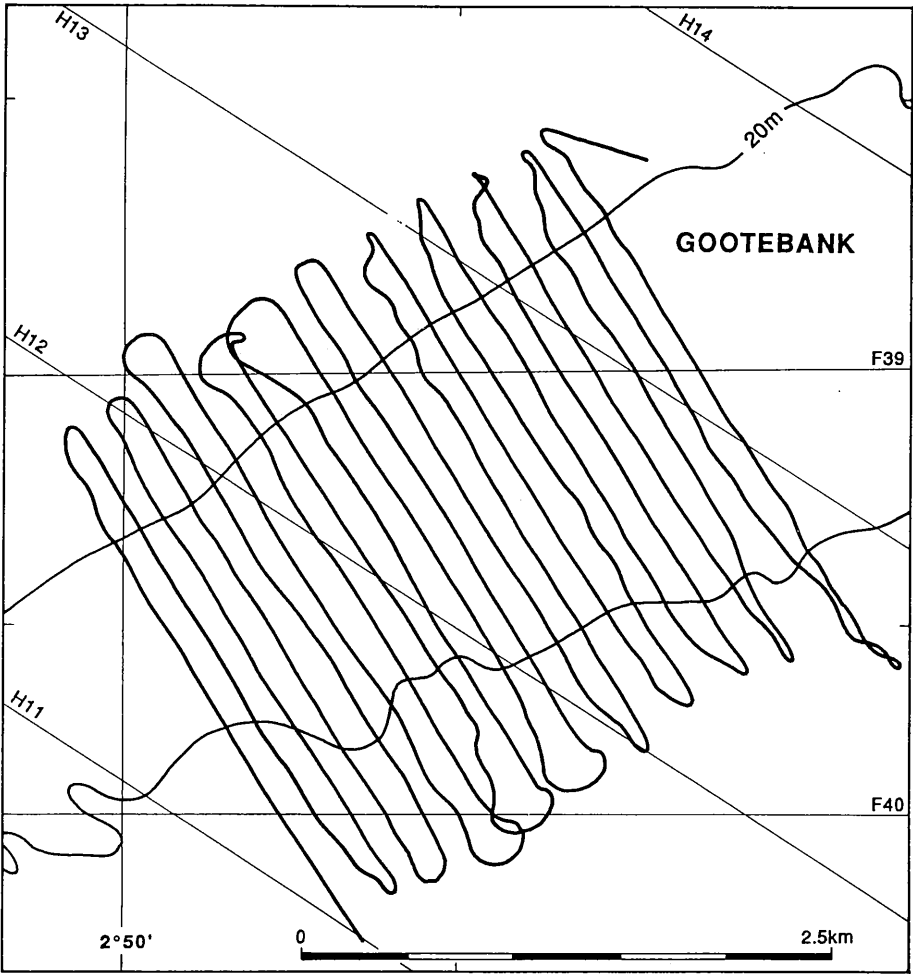


Fig. 3.— Sailed tracks across the central Gootebank

sonographs were processed according to Flemming (1976) and a bedform map was drawn on a scale of 1/5,000 (De Moor and Lanckneus, 1988).

4.– Residual sediment transport directions by bedform analysis.

4.1.– Bedforms.

The central section of the Gootebank, selected for this study, is completely covered with flow transverse bedforms, which can be classified as very large, large, medium and small dunes according to Ashley (1990).

The large to very large dunes (both defined hereafter as large dunes) [figure 4] occur on both flanks and summit of the bank and are absent in the northern and southern swales. They display a good lateral continuity and the large ones are traceable from one flank of the bank to the other over a distance of 2.3 km. The large dunes have a strike of N 50° W which locate them slightly oblique to the bank's axis. They have a height ranging from 0.5 m to 5.40 m and a wavelength varying between 25 and 300 m. All large dunes have a pronounced cross-sectional profile. In most cases they have their steep slope dipping towards the southwest, although along some sections steep slopes point to the opposite direction.

Small to medium dunes (defined hereafter as small dunes) cover the flanks and summit of the bank. They superpose both flanks of all large dunes. They are 2-dimensional and present a wavelength ranging from 1 to 10 m. The small dunes occurring on the northern bank flank have as a general rule a shorter wavelength than the remaining ones. All small dunes have a strike of approximately N 30° W. This means that they are completely perpendicular to the bank and that they are oriented at an oblique angle to the large dunes with a clockwise angle offset of 20°. The same offset value was found on the Kwintebank, a bank situated 8 km to the southwest, although its flow transverse bedforms present different orientations than on the Gootebank. The steep slopes of all detected small dunes are dipping towards the southwest which is the direction of the peak ebb current.

4.2.– Residual sediment dynamics.

Most sediment dynamic studies carried out in the Southern North Sea agree that in the coastal section of the Belgian coast residual sand movement is to the northeast. Although this movement may be correct on a regional scale, much more complex movements occur near sandbanks (De Moor, 1985). Several models have been proposed to explain the near-bed currents and the related sediment movements which would be responsible for the formation and maintenance of linear sand banks on continental shelves. Pattiaratchi and Collins (1987) provide an overview of these models.

Residual transport paths can be deduced from the strike and the steep slope direction either from large dunes (Caston, 1972) or from small dunes (McCave & Langhorne, 1982; Lanckneus *et al.*, 1989). As the direction of the net sediment

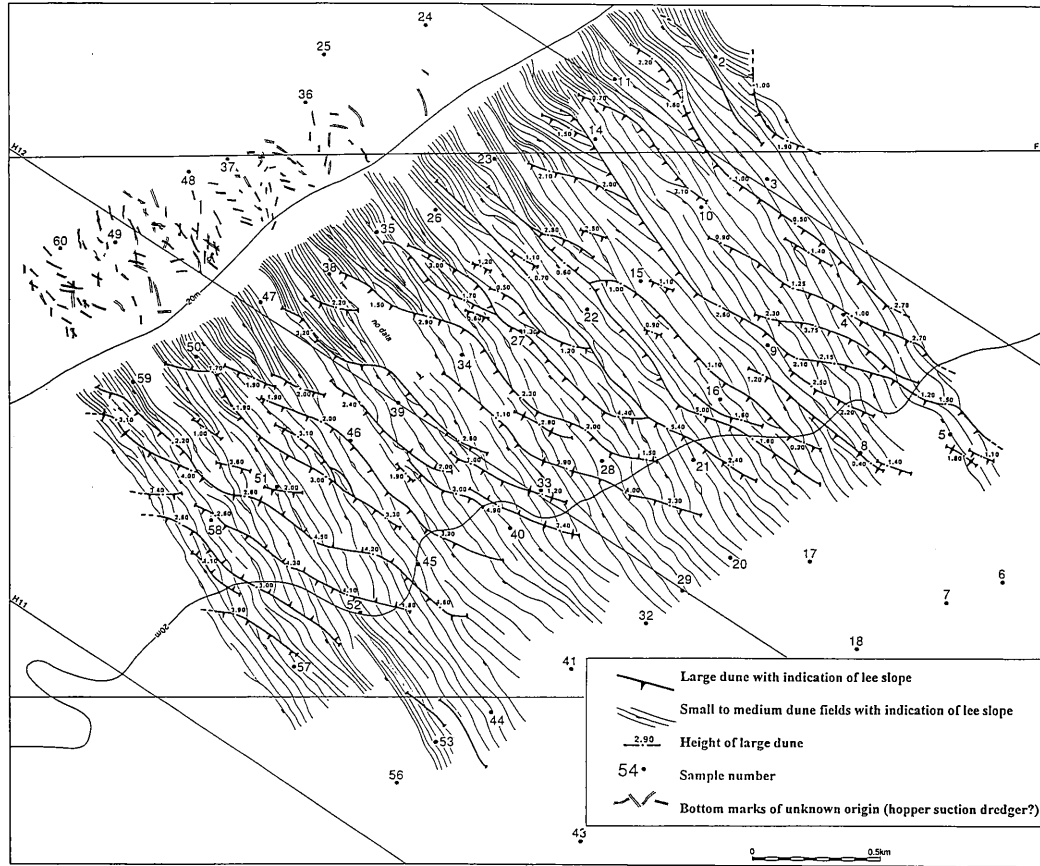


Fig. 4.- Bedform map of the central Gootebank deduced from sonographs recorded in June 1992

displacement generally corresponds to that of the more intense current (Johnson *et al.*, 1981), directions of flood peak and ebb peak currents were compared with the characteristics of the bedforms, using information from a current meter positioned on an adjacent sandbank, the Kwintebank (Lanckneus *et al.*, 1992). These data show clearly that the peak currents are completely perpendicular to the small dunes. Small dunes are therefore used to derive the directions of the residual sediment transport (figure 5).

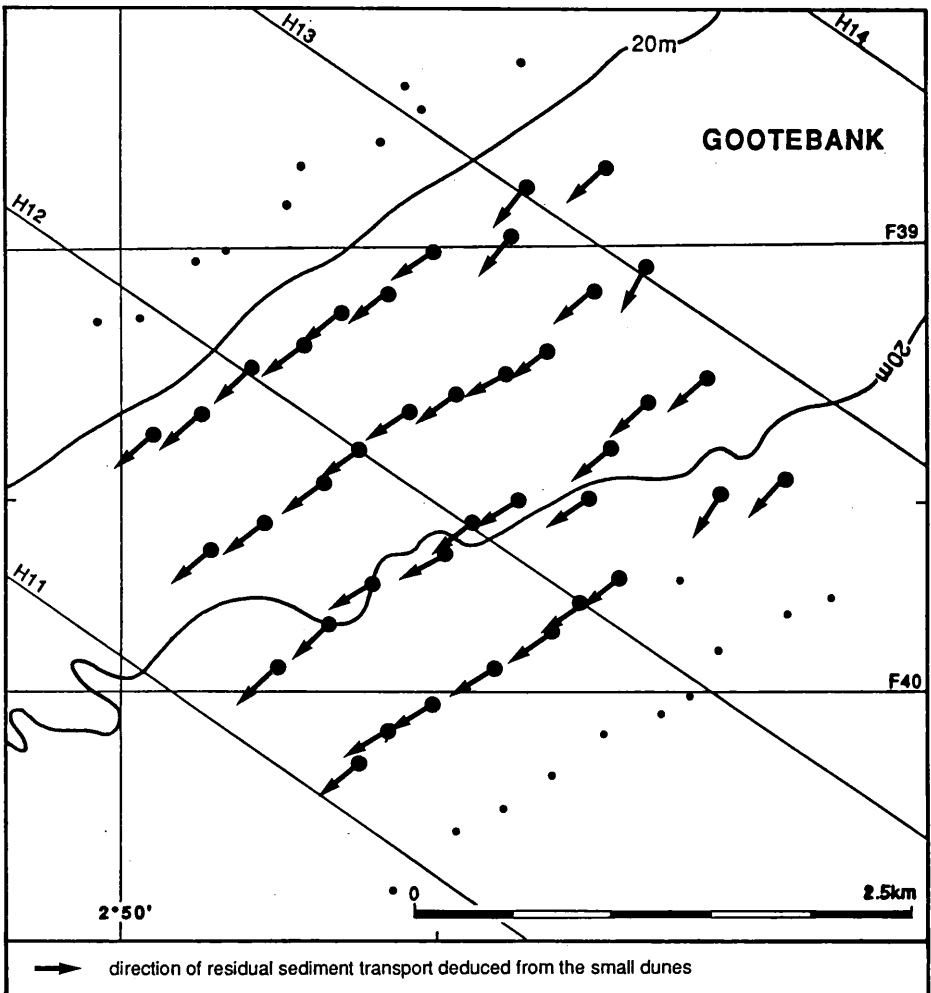


Fig. 5.— Directions of residual sediment transport deduced from strike and asymmetry of small dunes

5.– Residual transport directions by sediment trend analysis.

5.1.– The McLaren Model.

McLaren and Bowles (1985) elaborated a statistical approach to determine the sediment transport directions along a line by examining the sedimentological parameters of all possible pairs of samples on a sample line. This line-by-line approach is however difficult to use in the case of samples taken in a grid if no information about the directions of the residual transport is available. In this case it is impossible to know the direction along which pairs of samples have to be examined.

Therefore, a two-dimensional approach, as the one proposed by Gao and Collins (1990) can be used to reduce the bias implied in the selection of the sampling tracks. The first step in this procedure is to compare coarseness, sorting and skewness of each sample with the same parameters of its eight neighbouring samples and to draw a unit length vector for each direction corresponding to a specific defined transport trend. Several types of transport trends can occur and some discrepancy seems to exist between theory and field data.

5.2.– Types of transport trends.

McLaren suggested in 1981 that if sediments in transport undergo selective deposition, the resultant deposit can either be finer (case III A) or coarser (case III B) than the source, but the sorting will always be better and the skewness more positive. Both transport trends are illustrated by McLaren by means of several data-sets.

McLaren and Bowles however introduced in 1985 a sediment transfer function which defines the relative probability that a grain within each particular class interval will be eroded and transported. The introduction of these function demonstrates that, according to the authors, when sediments become finer, the skewness must become more negative (case B). At the same time, the transport trend III B (coarser, better sorted, more positive skewness) is redefined as the case C trend.

Harris *et al.* (1990) studied the regeneration of a section of Middle Banks, Moreton Bay, Queensland, which was severely dredged to provide sand for the construction of Brisbane Airport. The McLaren model was used to investigate the sources of the sand and the directions of the residual sand transport. Harris mentions in several cases a decrease of mean grain-size with corresponding more positive skewness. Following the ideas of McLaren, he attributes this “erroneous” trend to the fact that the samples are not fully representative of the different environments.

The existence of transport trends was studied in detail on another tidal sandbank of the Belgian continental platform, the Kwintebank by Lanckneus *et al.* (1992). These authors found that neither case B nor case C trends occur dominantly on the northern section of the bank where, on the contrary, directions along which sediments become finer, better sorted and more positively skewed (case III A) prevail. The residual transport directions derived from this trend were compared with the transport directions deduced from the geometric characteristics of bedforms mapped with the help of sonographs. A good similarity between the results of the two methods was obtained and the sediment trend analysis proved its capability to distinguish between the flood and ebb dominated areas.

So it seems that a contradiction exists between the transport trends derived from more theoretical considerations and the one actually found on tidal sandbanks. New results on another sandbank of the Belgian continental platform, the Gootebank, will be used to study the existing types of transport trends.

5.3.– 2D sediment trend analysis on the Gootebank.

All publications agree to the fact that sediments, undergoing selective deposition, can either be finer or coarser and that they seldom become more poorly sorted (McLaren and Bowles, 1985).

So, in theory, compared to sample 1, sample 2 can theoretically be

- (1) finer (F), better sorted (B) and more positively skewed (+);
- (2) F, B and more negatively skewed (–);
- (3) coarser (C), B, + and
- (4) C, B, –.

Let us now examine which of these trends occur on the Gootebank and in which percentage. Table 2 presents the number of occurrence of each of the four here above defined sediment transport trends between each sample and its eight neighbouring samples.

Table 2

Number of occurrence of each of the four considered sediment transport trends

Transport trend	F, B, +	F, B, –	C, B, +	C, B, –
No of pairs of samples producing a specific transport trend	115	15	25	39
No of pairs of samples expressed in %	59.3 %	7.7 %	12.9 %	20.1 %

It is clear once more, that the transport trend F, B, + is dominant and that the F, B, - transport trend is insignificant. The abundance of F, B, + cases points to the fact that when samples become finer and better sorted, the corresponding skewness can become more positive. We take in our sediment trend analysis only into account the transport type F, B, + as it is the most wide-spread trend.

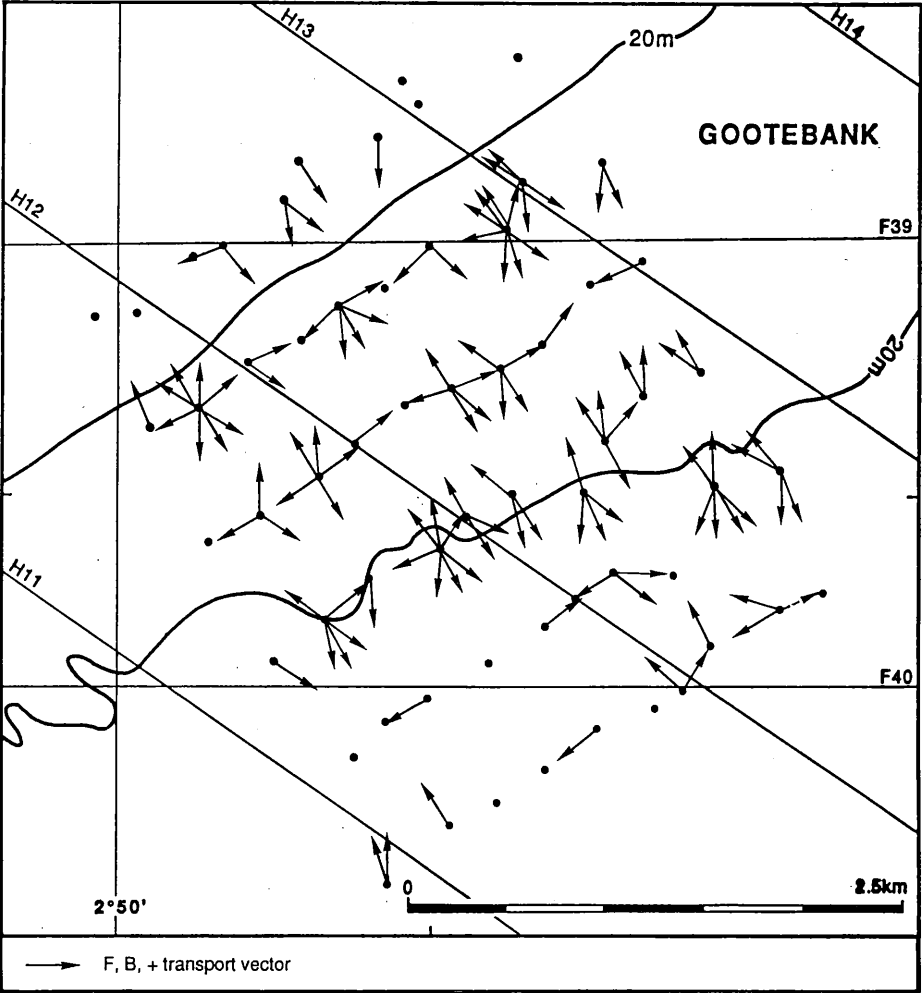


Fig. 6.– Unit length vectors for each F, B, + (finer, better sorted, more positively skewed) trend

We already mentioned that, in order to realise a 2D sediment trend analysis, unit length vectors have to be drawn for each direction corresponding to the prevailing transport trend, which in this case is the F, B, + trend. Figure 6 displays

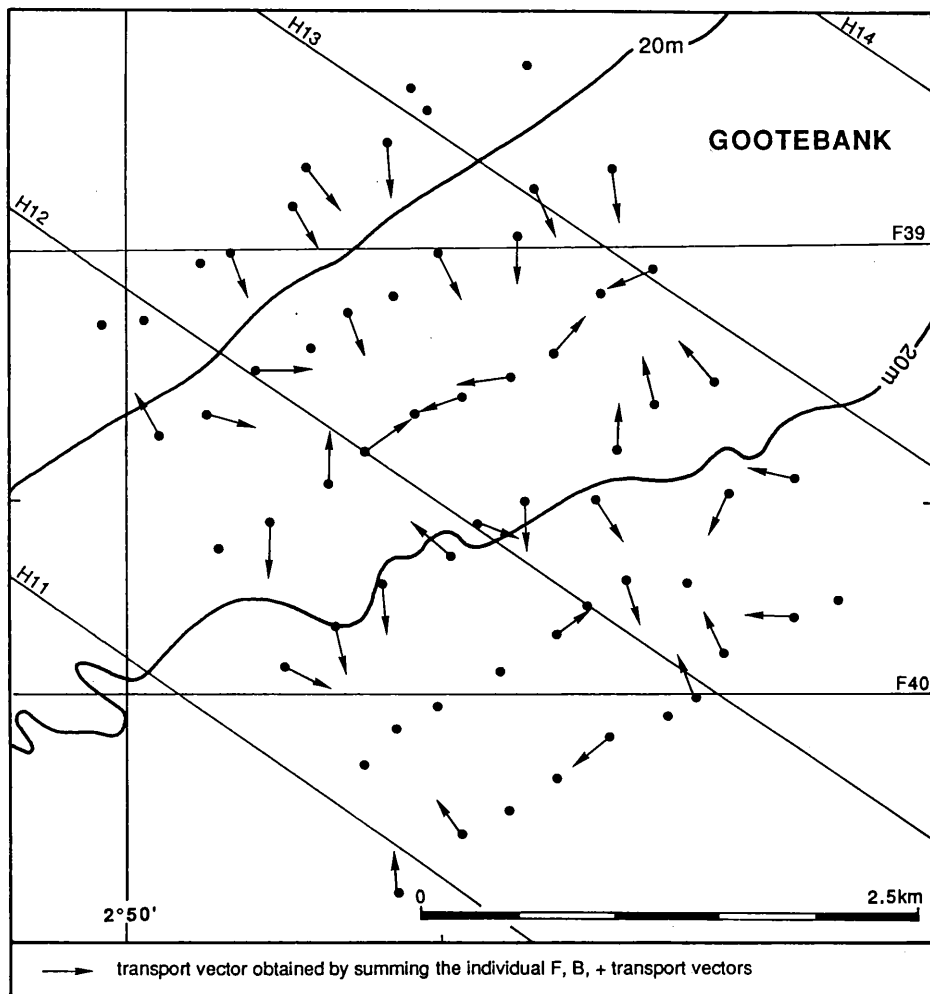


Fig. 7.— Result vector obtained by summing all unit length vectors in each point

all length vectors, corresponding to the F, B, + trend which can be drawn between each point and its eight neighbouring samples.

The direction of the vector points towards the sample with the best sorting. All unit length vectors occurring in each single point are then summed by vectorial computation so that only a single direction vector is left for each sampling site (figure 7). If only one length vector is present in a sampling point, the direction of the original vector is retained.

To easy the computations a full menu driven DOS environment programme was designed to calculate the result vector of up to eight user defined vectors.

All entered vector data are stored into a special designed database file. This structure gives the user the freedom to add records to the file or to modify a record already entered. After data entry the result vector is calculated and its length and direction is stored in a record field. Output of the programme can be alpha-numeric and consists in this case of the sample number, the length and the direction of the result vector. A DXF-file (*AutoCad* Data eXchange Format), can also be created allowing a graphical representation of both the initial and the result vectors. As the Easting and the Northing are available for each measurement, the points can be precisely located, and superposed on a digital bathymetric map.

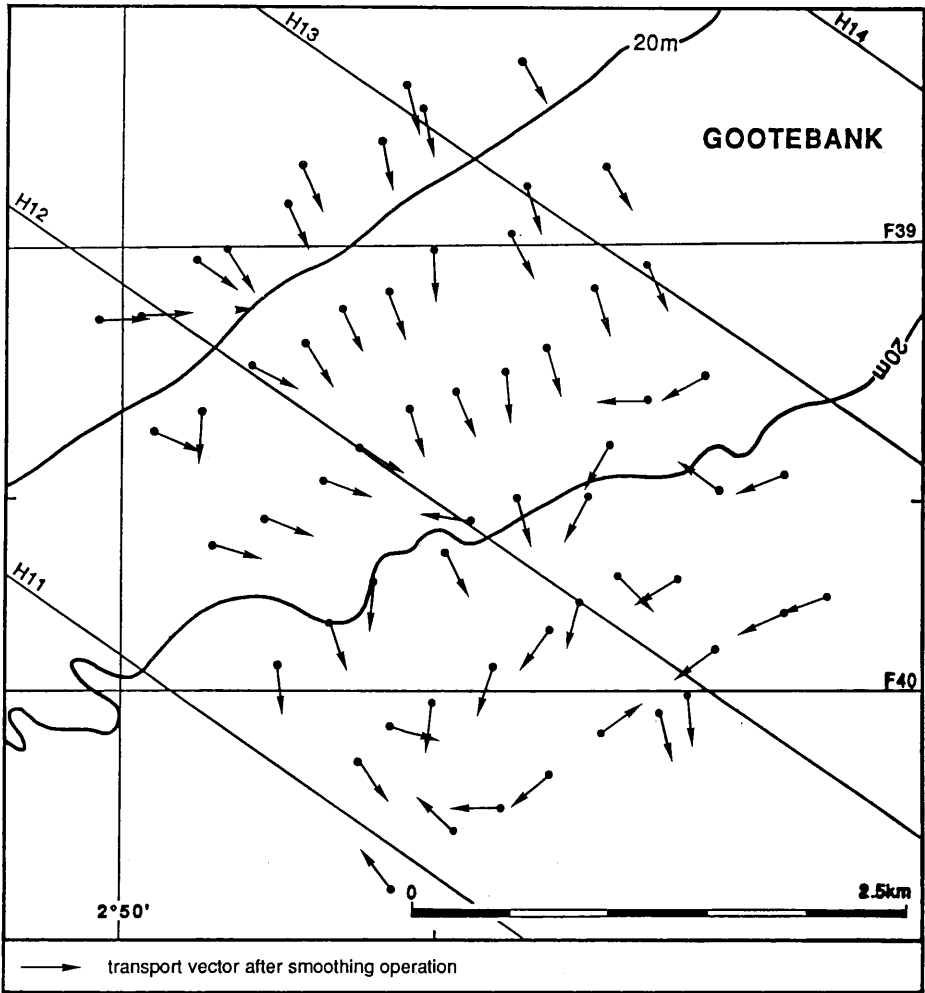


Fig. 8.– Smoothing operation carried out on the vectors displayed in figure 7

Finally, a smoothing operation is performed to reduce “noise” in the data by averaging the directions of the vectors of each sampling point and its neighbouring points (figure 8).

The results of the trend analysis suggest that:

- (1) sediment transport on the bank occurs perpendicular to the bank’s axis from north to south;
- (2) in the southern swale sediments move residually parallel to the bank from NE to SW.

6.– Conclusions — Confrontation with the sonograph results.

The results of a sediment trend analysis on a tidal sandbank has been compared to the findings of a bedform analysis based on sonograph interpretation. In a 24 hour period a total of 60 bottom samples were collected on a central section of the Gootebank followed by side-scan sonar registrations in mosaic form of the sampled area. Grain-size parameters were calculated and a bedform map was drawn. Residual sediment transport directions from both the sediment trend analysis and the bedform analysis were deduced. Similarities and dissimilarities between both methods can be resumed as follows (figure 9).

In the southern swale the small dunes indicate a clear residual sand movement towards the SW, which is in good agreement with the results from the trend analysis. On the bank itself however, the small dunes suggest a from NE to SW transport which is almost perpendicular to the movement derived from the McLaren model. It is striking that similar results were obtained on the Kwintebank (Lanckneus *et al.* 1992) where a good similarity between the two methods was reached in the adjacent swales and an offset of 90° was found on the bank itself.

How can these phenomena be explained? It is rational to accept that the flow transverse bedforms (as the name itself says) have their orientation more or less transversal to the dominant currents. But in this case, why do the expected variations in the areal pattern of the grain-size parameters not occur in a similar way? First, we have to consider the fact that those variations in the direction of the bank’s axis exist. Former sedimentological studies on adjacent banks like the Kwintebank (Lanckneus, 1989) and the Middelkerke Bank (Lanckneus *et al.*, 1991), show clearly that grain-size variations are found in the direction of the bank’s axis (coarsening towards the northern bank end) and transversal to the bank (coarser sand on the western bank flank). When sampling operations are however restricted to a section of the bank, it is normal that the longitudinal grain-size variations, as they are spread over the entire length of the bank, are masked by the more marked transversal grain-size differentiation.

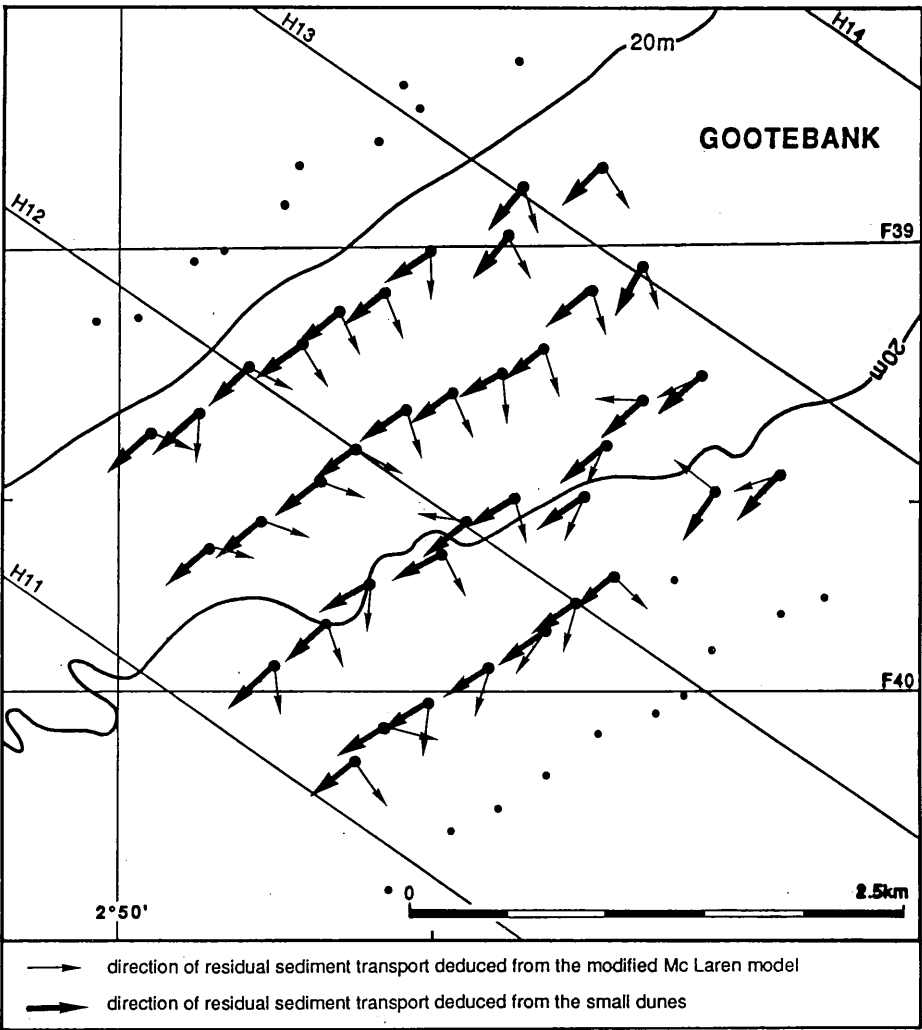


Fig. 9.– Comparison between residual transport directions deduced from the modified McLaren model and from the analysis of small dunes

Nevertheless, an additional process has to be introduced to explain the similarity of the results obtained in the swales with the two above mentioned methods and the offset of 90° found on the bank itself. As it is well known, tidal currents change continuously in direction and velocity. The bottom velocity on a specific moment of the tidal cycle is however not identical on the entire bank flank as there is a clear upslope increase in current speed from the swale to the crest (De Moor *et al.*, 1993). This simultaneous existence of different current velocities is responsible for the formation of a lag deposit on the western flank of the bank

where coarse sediments occur which become finer over the bank top towards the eastern bank flank. This effect does not exist in the swales where a constant depth prevails, which explains the similarity of results, obtained with the bedform analysis and the sediment trend analysis.

We can note as well that the offset between the directions of residual sediment transport deduced from the sediment trend analysis and from the bedform analysis is smaller (70°) if large dunes are considered instead of small dunes. Former research however (Lanckneus and De Moor, 1993) gave clear evidence to the fact that large dunes are not suited for the definition of residual sediment transport paths.

Discrepancy of the results obtained on the sandbank between the sediment trend analysis and the bedform analysis shows clearly that the definition of residual transport paths in a tidal environment has to be carried out cautiously. In order to gain a deeper insight in the existing sedimentological processes, new techniques will be used in future research including the use of high resolution flow models and hydrodynamic measurements with the help of current meters and instrumentation platforms.

Acknowledgements.

This research was supported by the Belgian Ministry of Economic Affairs and by the Management Unit of the Mathematical Models North Sea. We are grateful for the logistic support provided by the National Fund for Scientific Research. The authors wish to thank the entire crew of the oceanographic vessel Belgica for their constant help and co-operation during the sampling programme and survey activities.

References.

- ASHLEY, G.M. (1990). Classification of large-scale subaqueous bedforms: a new look at an old problem, *Journ. of Sed. Petrol.*, 60,1:160–172.
- CASTON, V.N.D. (1972). Linear sand banks in the southern North Sea, *Sedimentology*, 18:63–78.
- DE MOOR, G. (1985). *Shelfbank Morphology off the Belgian Coast. Recent methodological and scientific developments*, in: M. Van Molle (Editor), *Recent trends in Physical Geography in Belgium. Liber Amicorum L. Peters*, VUB, Study series of the Vrije Universiteit Brussel, New Series, 20:149–184.
- DE MOOR, G. and LANCKNEUS, J. (1988). Acoustic teledetection of seabottom structures in the Southern Bight, *Bull. de la Soc. Belge de Géol.*, 97,2:199–210.
- DE MOOR, G., LANCKNEUS, J., BERNÉ, S., CHAMLEY, H., DE BATIST, M., HOUTHUYS, R., STOLK, A., TERWINDT, J., TRENTESAUX, A. and VINCENT, C. (1993). *Relationship between sea floor currents and sediment mobility in the southern North Sea*, Symposium MAST Days, Brussels 15–17 March 1993, Project Reports, 1:193–207.

- FLEMMING, B.W. (1976). Side scan sonar: a practical guide, *The International Hydrographic Review*, LIII, 1, 27 pp.
- FOLK, R.L. and WARD, W.C. (1957). Brazos river bar: a study in the significance of grain-size parameters, *Journ. of Sedimentary Petrology*, 27,1:3–26.
- GAO, S. and COLLINS, M. (1990). A Critique of the “McLaren Method” for defining sediment transport paths. Discussion, *Journ. of Sedimentary Petrology*, 61,1:143–146.
- HARRIS, P.T., PATTIARATCHI, C.B., KEENE, J.B. and COLE, A. (1990). *Modelling the Evolution of a Linear Sandbank Field, Moreton Bay, Queensland: Report of Results Obtained During the Cruise of A.M. Brolga in July, 1989*, Ocean Sciences Institute, The University of Sidney, 41, 172 pp.
- HOUBOLT, J.J.H.C. (1968). Recent sediments in the Southern Bight of the North Sea, *Geologie en Mijnbouw*, 47,4:245–273.
- JOHNSON, M.A., STRIDE, A.H., BELDERSON, R.H. and KENYON, N.H. (1981). Predicted sand wave formation and decay on a large offshore tidal-current sand-sheet, in: S.D. Nio, R.T.E. Schüttenhelm and T.C.E. Van Weering (Editors), *Holocene marine sedimentation in the North Sea Basin*, 247–256.
- JOHNSON, H.D. and BALDWIN, C.T. (1986). *Shallow Siliclastic Seas*, in: H.G. Reading (Editor), *Sedimentary Environments and Facies*, Blackwell Scientific Publications, 229–282.
- LABAN, C. and SCHÜTTENHELM, R.T.E. (1981). Some new evidence on the origin of the Zeeland Ridges, *Spec. Publs. int. Ass. Sediment.*, 5:239–245.
- LANCKNEUS, J. (1989). *A comparative study of sedimentological parameters of some superficial sediments on the Flemish Banks*, in: J.P. Henriët and G. De Moor (Editors), *The Quaternary and Tertiary Geology of the Southern Bight, North Sea*, 229–241.
- LANCKNEUS, J., DE MOOR, G., DE SCHAEPMEESTER, G. and LIBEER, L. (1989). *Acoustic teledetection of shelf bedforms and their meaning for sediment dynamics*, in: G. Pichot (Editor), *Progress in Belgian Oceanographic Research 1989*, Brussels, 147–163.
- LANCKNEUS, J., DE MOOR, G., BERNÉ, S., CHAMLEY, H., DE BATIST, M., HENRIËT, J.P. and TRENTESAUX, A. (1991). *Cartographie du Middelkerke Bank: dynamique sédimentaire, structure géologique, faciès sédimentaires*, International Symposium Ocean Space Advanced Technologies European Show, Brest, September 24–27, 1991, 11 pp.
- LANCKNEUS, J., DE MOOR, G., DE SCHAEPMEESTER, G., MEYUS, I. and SPIERS, V. (1992). Residual sediment transport directions on a tidal sand bank; Comparison of the “McLaren Model” with bedform analysis, *Bull. de la Soc. belge d’Études Géog.*, 2:425–446.
- LANCKNEUS, J. and DE MOOR, G. (1993). *Bedforms on the Middelkerke Bank, Southern North Sea*, Proceedings Tidal Clastics, Special Publication International Association of Sedimentologists (in press).
- MCCAVE, I.N. and LANGHORNE, D.N. (1982). Sand waves and sediment transport around the end of a tidal sand bank, *Sedimentology*, 29:95–110.

- MCLAREN, P. (1981). An interpretation of trends in grain-size measures, *Journ. of Sedimentary Petrology*, 51,2:611–624.
- MCLAREN, P. and BOWLES, D. (1985). The effects of sediment transport on grain-size distributions, *Journ. of Sedimentary Petrology*, 55,4:457–470.
- PATTIARATCHI, C. and COLLINS, M. (1987). Mechanisms for Linear Sand bank Formation and Maintenance in relation to Dynamical Oceanographic Observations, *Prog. Oceanog.*, 19:117–176.
- VAN CAUWENBERGHE, C. (1992). *Stroomatlas 1992, Noordzee Vlaamse Banken*, Dienst der Kusthavens, Hydrografie Oostende, Ministerie van de Vlaamse Gemeenschap, Leefmilieu en Infrastructuur, 26 pp.

Eocene Siliciclastic Continental Shelf Sedimentation in the Southern Bight North Sea, Belgium

Patric JACOBS and Erwin SEVENS

University of Gent, Renard Centre of Marine Geology

Abstract.

Eocene sedimentation in the Southern Bight of the intracratonic North Sea Basin is determined by its ramp margin setting. Lithofacies analysis of siliciclastic shallow marine sediments enables reconstruction of sedimentation model in relation to relative sea level changes.

Two major sedimentary cycles composed of sequences of metric to decametric thickness can be discerned. The lower transgressive/regressive cycle evidences 3 sedimentary environments. Lowermost Eocene sediment units are mainly clayey, display an overall fining upward trend and are deposited on a mud shelf. A delta prograding out on the continental shelf deposits middle to upper Lower Eocene units, gradually becoming more sandy. Middle Eocene sediments are mainly sandy, contain calcarenite horizons, coarsen upward and are predominantly of tidal and lagoonal origin.

The upper cycle is composed of only 2 sedimentary environments. Lower Upper Eocene sediment packages consist of a succession of 4 gradually fining upward sandy to clayey sediment units of distal (pro)delta origin, while the Uppermost Eocene has a more sandy character and is of tidal sand flat origin.

The general sedimentation model is that of an advancing and retreating mainly deltaic sedimentation system, consisting of onlapping and shallowing upward sediment units, gradually infilling the Southern Bight of the North Sea Basin due to constant sediment supply of southern origin.

1.- Introduction.

Tertiary sedimentation in the shallow Southern Bight of the intracratonic North Sea Basin occurs within a ramp margin shelf setting. As shown in figure 1, siliciclastic shallow marine beds gently dip to the NNE (less than 0.5%) in a series of onlapping parallel WNW-ESE orientated units, with an outcrop pattern related to the Tertiary topography modelled by Quaternary erosion.

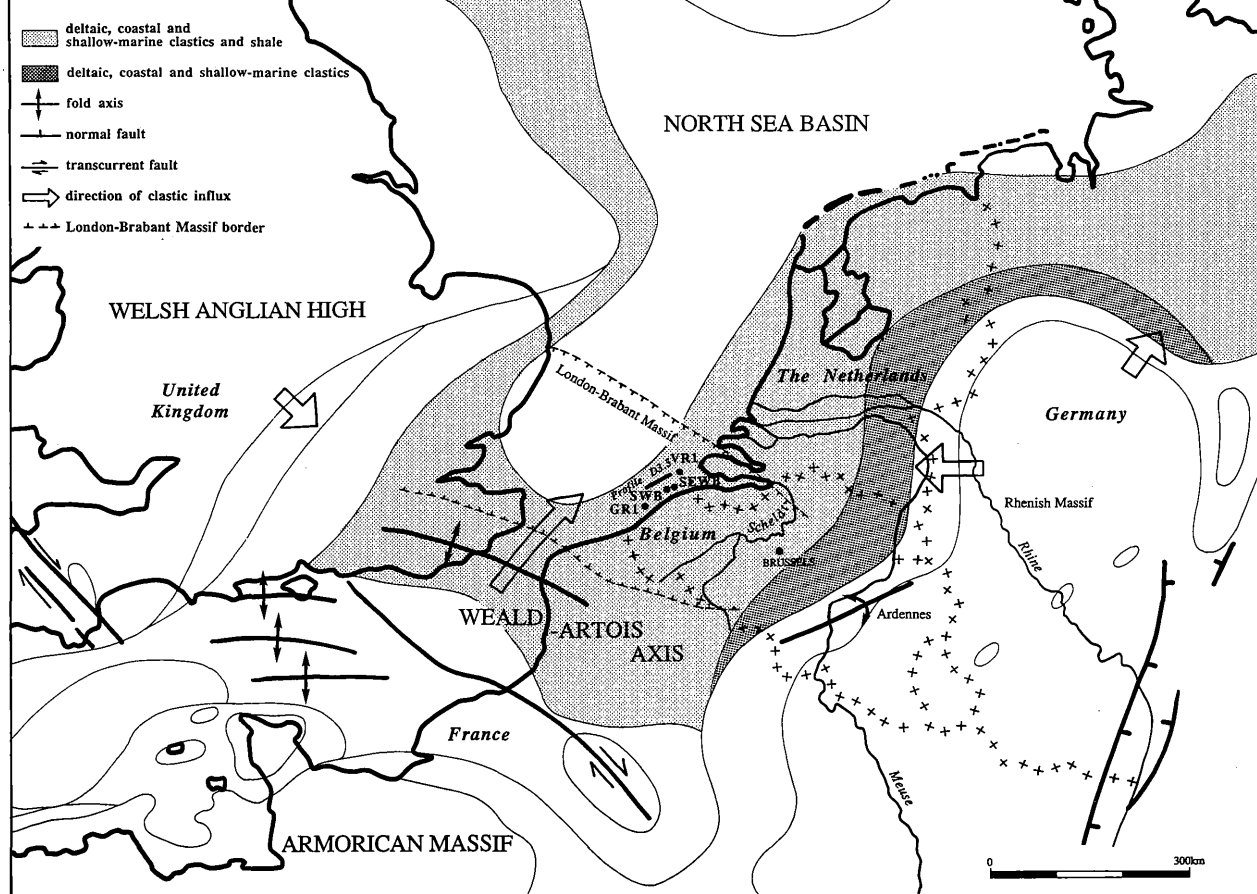


Fig. 1.— Late Eocene palaeogeography (after Ziegler, 1982) and situation of the study area in the Southern Bight of the North Sea, with indication of location of the cored holes GR1, SWB, SEWB and VR1.

Table 1

Chrono-, bio- and lithostratigraphy of the onshore Belgian Eocene; biostratigraphy mainly after Steurbaut; lithostratigraphy after the new proposal of Maréchal and Laga, 1988.

CHRONO	BIO	LITHO			Units (this paper)		
EPOCH	ZONES	GROUPS	FORMATIONS	Members	Number	Lithology	Thickness
L. EOCENE	NP 18-21	TONGEREN	ZELZATE	Watervliet Bassevelde	28-30		> 13 m
L. EOCENE	NP 16	MALDEGEM		Onderdijke	27		7 m
				Buisputten	26		4.5 m
				Zomergem	25		11.5 m
				Onderdale	24		3.5 m
				Ursel	23		19 m
M. EOCENE	NP 15			Asse	22		5.5 m
				Wemmel	21		6 m
M. EOCENE	NP 15	ZENNE	LEDE			not studied	
	NP 14		BRUSSEL	Chaumont-Gistoux/ Bois de la Houssière Neerijse/Diegem/ Archennes		not studied	
	NP 14		AALTER	Oedelem Beernem	17-20 15-16		20 m 7.5-10 m
E. EOCENE	NP 14	IEPER	GENT	Vlierzele	13-14		6.5 m
	NP 13			Pittem	10-12		6.5 m
				Merelbeke	9		11 m
	NP 13		TIELT	Egem Kortemark	7-8 6		9-22 m 7.5-13.5 m
	NP 11-12		KORTRIJK	Aalbeke Moen Saint-Maur Mont-Héribu	3-5 2 1		> 12 m 11.5 m > 10 m

The Eocene stratigraphy of onshore northwestern Belgium has been established by Rutot (1882, 1883), Murlon (1888), Leriche (1912, 1922) and more recently by Gulinck (1965, 1969a, 1969b), while the lithostratigraphy of the Upper Eocene and of the transitional layers between the Eocene and the Oligocene has been revised by Jacobs (1975). The Palaeogene lithostratigraphy (Table 1) was summarized by Maréchal and Laga (1988) based on contributions by different authors.

In order to study the offshore Lower Eocene to Lower Oligocene seismic stratigraphic units observed by De Batist (1989) on high resolution seismic reflection lines in the Southern Bight, four cored borings (figure 3) were drilled by the Belgian Geological Survey in front of the Belgian Coast (figure 2). These borings cut through a 200 m thick series of Eocene marine sediment units (figure 4), roughly forming a SW–NE/S–N dip section. Sedimentary facies analysis, grain size trends and sediment genetic interpretation of the GR1, SWB, SEWB and VR1 borings were used to reconstruct the sedimentation model. As no biostratigraphic study has been undertaken yet, age control had to rely on data (King, 1990; Steurbaut, 1990) obtained from correlatable sediment series in nearby onshore cored borings (11E/138 and 22W/276) [figure 3].

3.– Lithostratigraphy.

3.1.– Kortrijk Formation.

In the GR1 boring (figure 5) a stacked pattern of fining upward sediment units 1 to 4, each 5 to 10 m thick of the Kortrijk Fm of Early Eocene age forms a 35 m thick massive grey green clay, with some thin silt laminae and fine sand nests. Jarosite and pyrite concretions occur, sometimes with a fossil as nucleus. A 5 cm thick disturbed black clay layer with a high organic content marks an anoxic event representing a condensed section (Van Bavinchove, 1993), while horizontal layering reflects changes in organic material content. The bioturbated horizon in unit 3 represents a hiatus. Fine sandy layers are sometimes sideritized. In the VR1 boring (figure 12), the massive clay unit 4 is bioturbated (mostly chondrites) and covered by an 8 m thick bioturbated sandy clay with thick sand lenses (unit 5). Correlation is however based on geometrical arguments and thus still uncertain by lack of marker horizons.

Units 1 to 4 of transgressive character are deposited on an offshore mud-shelf, in the quiet setting of a deepening shelf characterized by very low sediment accumulation rates of about 1.5 cm/1,000 years (Jacobs and Sevens, 1988), and practically completely below storm wave base. The thin silt laminae and fine sand solitary migrating ripples indicate sporadically higher energy conditions which rework and redeposit sediment, indicating the rate of sea level rise slows down.

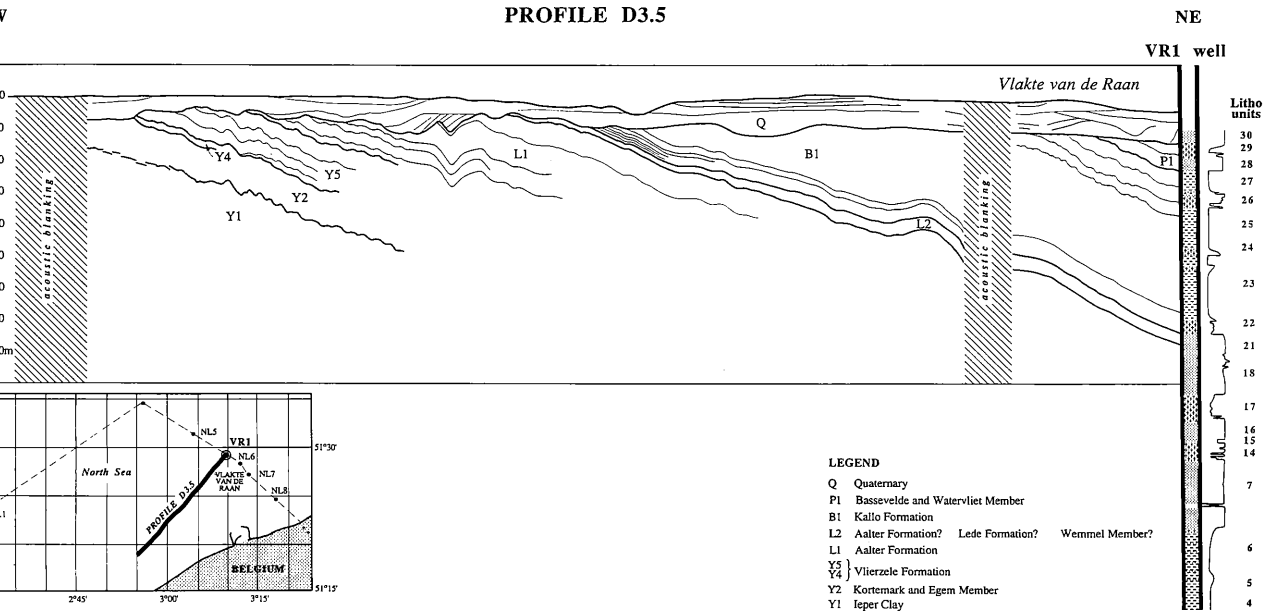


Fig. 2.- Seismic profile D3.5 (line drawing) illustrates correlation of De Batist's seismostratigraphical units and the VR1 boring litho units (Courtesy M. De Batist, 1989). Insert shows location.

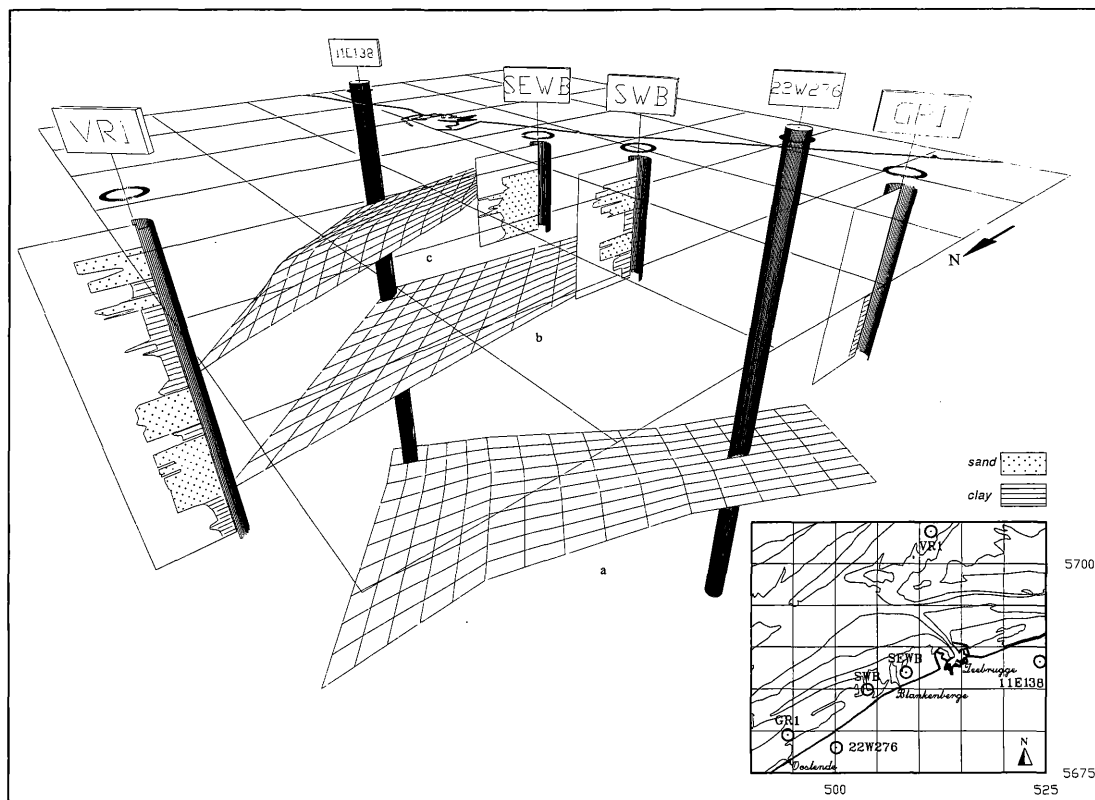
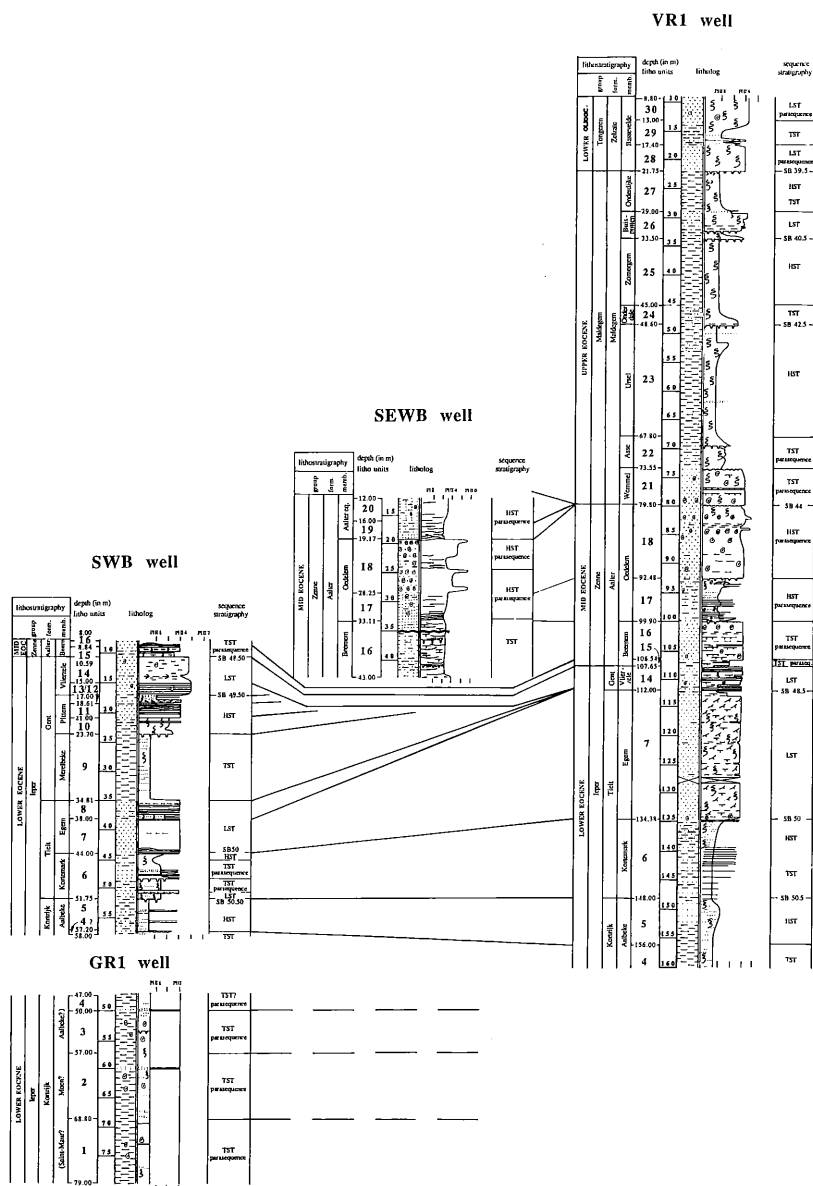


Fig. 3.— Lithologs of the four offshore cored holes and of two onshore borings of the Belgian Geological Survey (11E/138 and 22W/276) with lower boundary surface of the clayey Kortrijk Formation base (a), upper boundary surface of the clayey Kortemark Member top (b) and lower boundary surface of the clayey Asse Member base (c). Insert shows location of borings.



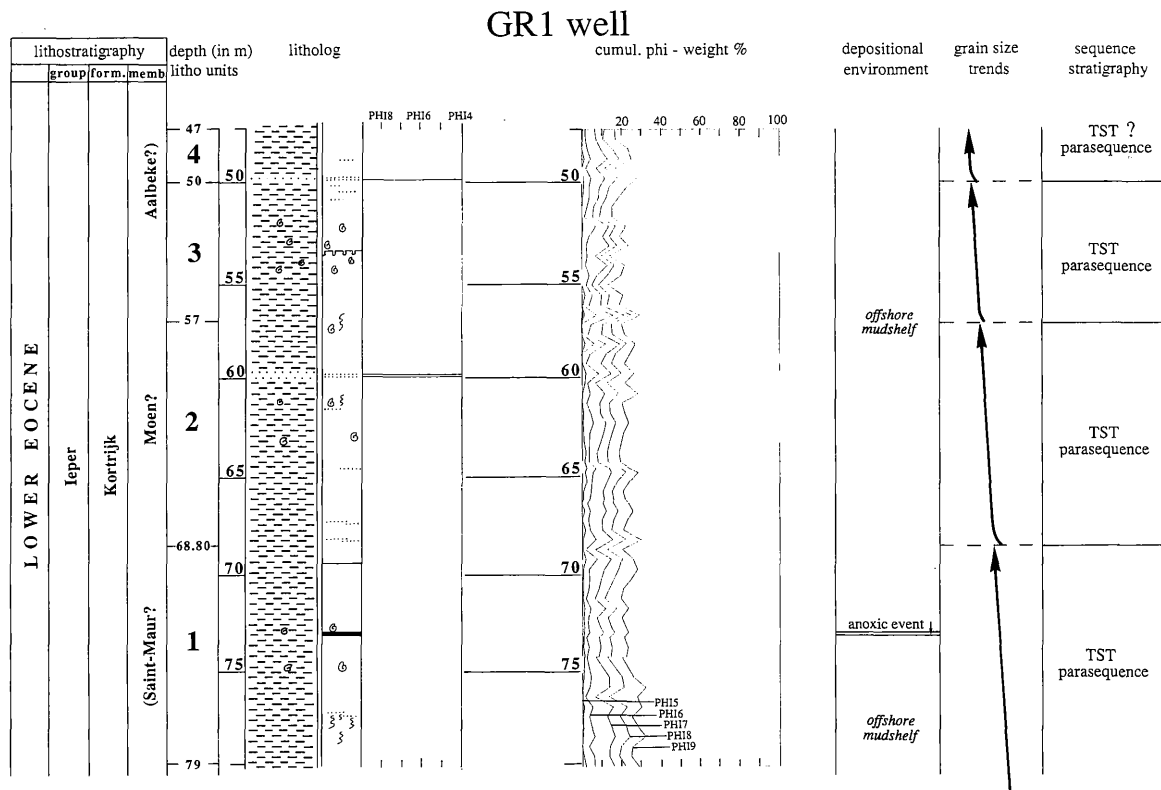
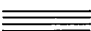
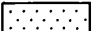
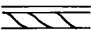
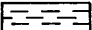

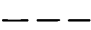


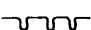






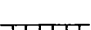
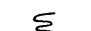







Fig. 5.— Detailed litholog with lithostratigraphy, sediment genetical and sequence stratigraphical interpretation of the GR1 boring.

Legend

	parallel lamination		sand
	low angle cross stratification		clay
	hummocky cross stratification		
	rhythmic interlayered bedding		
	flaser lamination		
	ripples		
	burrowed horizon	HST	highstand systems tract
	horizon with wood fragments	TST	transgressive systems tract
	mud drapes	LST	lowstand systems tract
	clay clasts	SB	sequence boundary
	sideritized fine sand		
	erosive contact		
	anoxic event		
	calcarenite horizon		
	bioturbations		no recovery
	silica cementations		"
	shells		
	nodules		

[figure 6] (Jacobs *et al.*, 1990) the 6 m thick basal unit 5 is composed of a lenticular clay with burrows at the top and with centimetric fining upward silty sand laminae (figure 7), indicating the offshore mudshelf to come under heavy storm influence.



On opposite page:

Fig. 6.— Detailed litholog with lithostratigraphy, sediment genetical and sequence stratigraphical interpretation of the SWB boring.

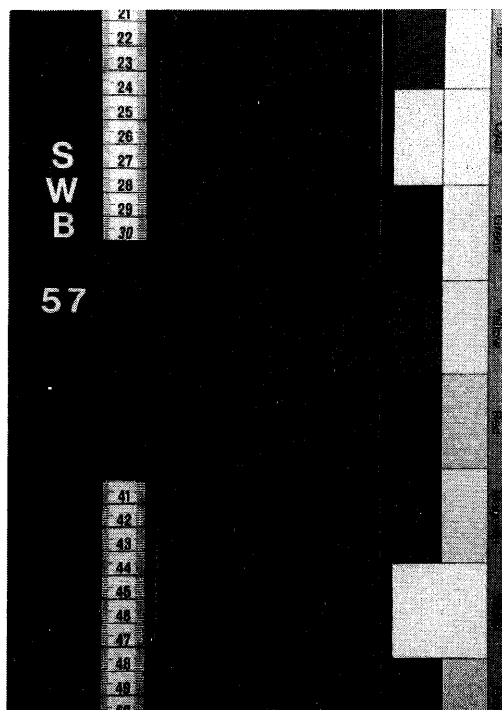


Fig. 7.— SWB boring 57 m 36: centimetric fining upward storm deposited silty sand laminae.

3.2.— Tiel Formation.

The Kortrijk Formation is overlain in the SWB boring by a sharp-based 8 m thick grey green bioturbated silty clay, containing thick sand laminae and burrows. This unit 6 is represented in boring VR1 by a 14 m thick grey clay with two centimetric yellowish clay lenses (consisting of bothroid and phramboid siderite), towards the top passing into a strongly bioturbated fine sandy clay due to an increasing number of thickening upward sand lenses. A sharp contact separates it from a glauconitic fine sand, with low angle cross bedding at the base in boring SWB. The thickness in the VR1 boring increases dramatically from 6 to 12 m, where this unit 7 shows fine laminations, ripples and flaser lamination (mud drapes), and contains bioturbations, dispersed shell clasts and local silica cementations. Sedimentation is here characterized by a deltaic regime:

the massive fine sand unit with low angle cross bedding is deposited on a delta front, and passes into a sedimentation near a delta front as indicated by the 3 m thick alternation of horizontal laminated fine sand and strongly bioturbated clayey fine sand (unit 8, only present in boring SWB).

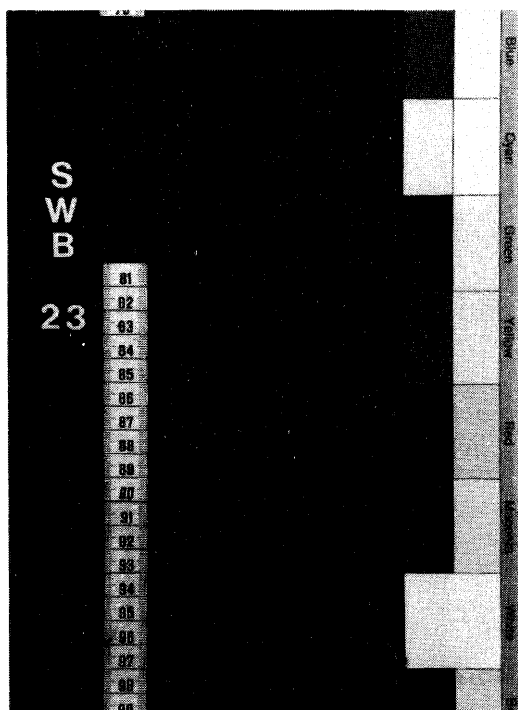


Fig. 8.– SWB boring 23 m 70–90: grey green silty clay top with large horizontal and vertical burrows and with an overall bioturbated clay matrix.

3.3.– Gent Formation.

The rapid transition to an 11 m thick lenticular silty clay (unit 9 in the SWB boring) indicates the retreat of the delta and the consequent redeepening of the basin towards an offshore mudshelf.

These muds with sand filled burrows at the top (figure 8) are abruptly overlain by an upward coarsening regressive sand (units 10 to 15). The lowermost 3 m of this sand (unit 10) is fine-grained, muddy and bioturbated. The overlying sand exhibits low angle cross bedding (unit 11) and rhythmic interlayered bedding (unit 12) [figure 9] topped by a strongly bioturbated lenticular clay with clay clasts. This middle portion is interpreted as deposition on a delta plain in lagoonal mud flats and sand shoals with sporadic wave influence.

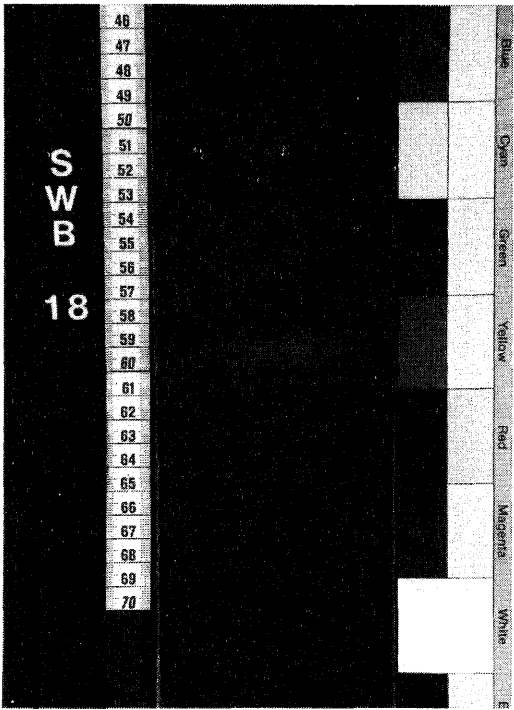


Fig. 9.– SWB boring 18m61: sand with rhythmic inter-layered bedding sharply topped by a grey green lenticular clay.

In the SWB boring units 13 and 14 form a 6 m thick sediment package consisting of green glauconitic fine sand. The lowermost 2 m show low angle parallel lamination (unit 13) with a brown clayey matrix and wood fragments (pedogenesis?). Deposition took place on intertidal to supratidal wave influenced sand shoals, with vegetation in the proximity. Due to lateral facies variations unit 14 is represented in boring VR1 by 3 coarsening upward sequences, in total 5 m thick, each composed of grey clay (sometimes with an erosive base) gradually passing into strongly bioturbated fine sand and at the top green glauconitic fine sand with parallel lamination and local cementations.

3.4.– Aalter Formation.

The Aalter Formation shows vertically and laterally the greatest facies diversity, reflecting highly varying sedimentary environments. All sediments are from base to top of Middle Eocene age (Jacobs *et al.*, 1990).

Unit 15 (SWB boring) is a sharp based 2 m thick fine sand with clay laminae, local silica cementations and bioturbated coarse interlayered bedding transitioning into rhythmic interlayered bedding with decreasing bioturbation. The top

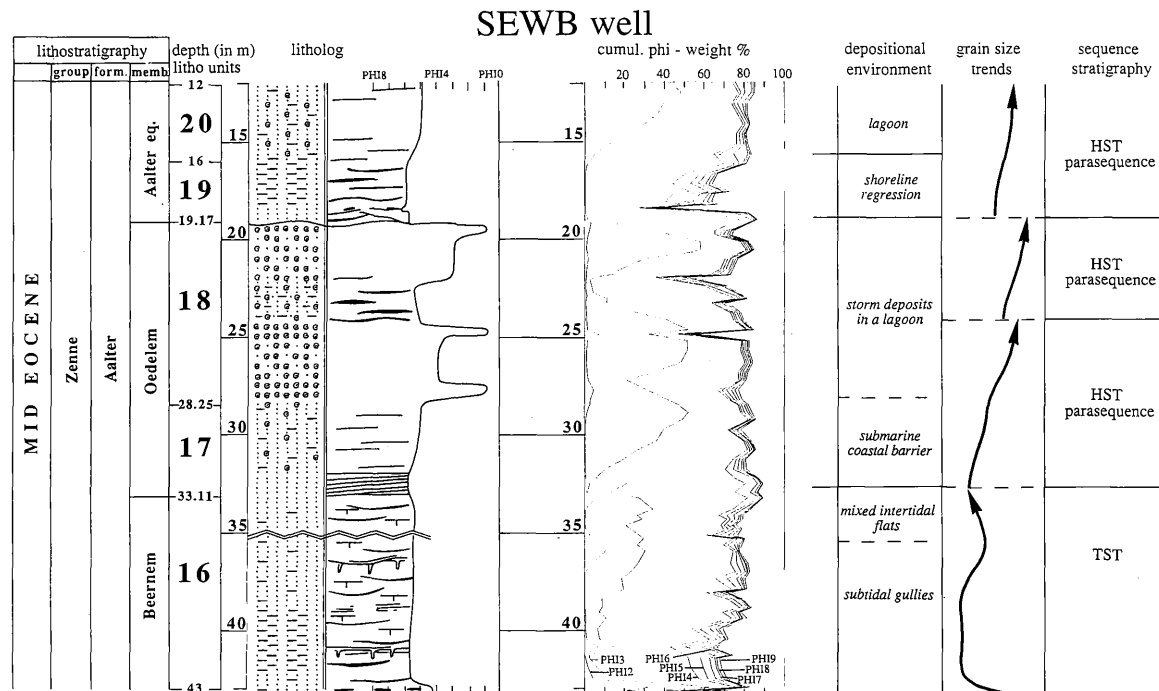


Fig. 10.– Detailed litholog with lithostratigraphy, sediment genetical and sequence stratigraphical interpretation of the SEWB boring.

(represented by unit 16, but incomplete in boring SWB) shows parallel lamination. Deposition might therefore have taken place in a subtidal environment, wave influenced at the top. In northeastern direction (boring VR1) unit 15 consists of 2 sequences of bioturbated grey clay, coarsening upward into grey green glauconitic fine sand with some clay, strongly bioturbated and locally silica cemented; the first sequence has an erosive base. Here the complete unit 16 reaches more than 6 m thickness, is also composed of grey green bioturbated glauconitic fine sand with millimetric clay lenses and local cementations, but contains shell fragments at the base and large specimen of the bivalve *Cardita planicosta* at the top, normally absent in the strongly bioturbated glauconitic medium fine sands of the SEWB boring. The 10 m thick basal but incomplete part of unit 16 (figure 10) starts with a thin fining upward sequence at the base, gradually coarsens upward, contains also local silica cementations, but displays vertical burrows (figure 11) which depart from erosion surfaces and penetrate into parallel laminated fine sands. The basal sediments in this succession are deposited in subtidal gullies, the top sediments in a mixed intertidal flat environment.

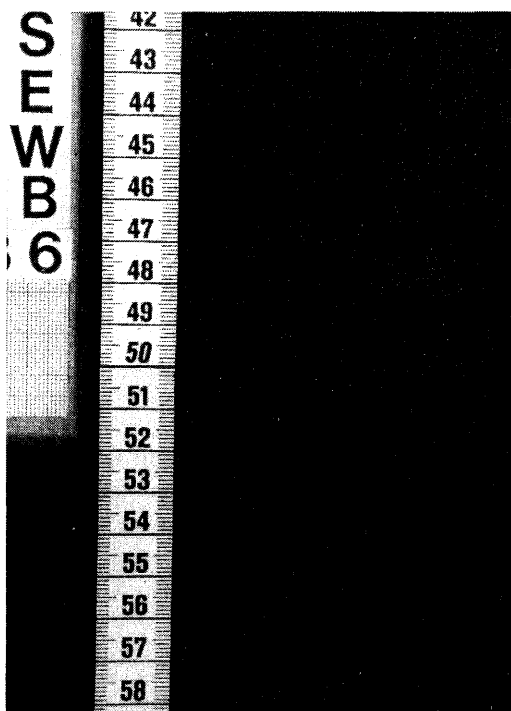


Fig. 11.— SEWB boring 36 m 50: vertical burrow departing from a reactivation surface; varying degree of bioturbation is caused by alternating periods of slack water and current activity.

In the SEWB boring no sharp boundary can be observed between units 16 and 17, which consists of a glauconitic fine sand, 5 m thick. The flaser lamination obliterated by bioturbation points towards the submarine facies of a coastal barrier, of which the laminated sand was deposited in shallow water and the clay layers in deeper water. More to the northeast (VR1 boring) unit 17 becomes somewhat thicker and more clayey, and is characterized by an irregular but sharp lower boundary with clay clasts and burrows backfilled with sand. This lenticular grey green sandy to silty clay is fossiliferous, bioturbated and contains millimetric as well as metric lenses affected by bioturbation and small scale faulting.

Like most of the Aalter Formation sediments in the northeastern part of the study area, the base of unit 18 has an erosional character with burrows backfilled with sand, in contrast to the gradual transition in boring SEWB. This 10 to 12 m thick grey green glauconitic fine sands to clayey sands with some centimetric clay layers, and displaying flaser lamination and bioturbations, are interpreted as storm deposits in a lagoonal environment. The abundant shells (mainly gastropods like *Turritella* but also *Cardita planicosta*) sometimes reworked and concentrated in coquinas indicate the position of the chenier itself.

The sharp basal contact of the overlying 3 m thick glauconitic fine sands (unit 19, SEWB boring) suggests erosion and incision due to very high energy conditions, while the hummocky cross stratification, the basal mud drapes and low angle cross bedding with mud drapes of this fine sands with clay clasts on erosive contacts represents repeated channel incision and infill with lateral migration. The glauconitic clayey fine sand facies with intensive bioturbation on top can be related to backstepping of the shoreline. The slightly coarsening upward 4 m thick slightly clayey glauconitic fine sands of unit 20 are interpreted as a lagoonal sedimentation, because of faintly visible horizontal burrows and uniformly dispersed shells due to complete sediment reworking.

3.5.– Maldegem Formation.

The Maldegem Formation of Upper Eocene age shows an overall fining upward trend from unit 21 to 27 and is only present in the VR1 boring (figure 12), as this is situated in the northeastern part of the study area. The succession begins with glauconitic slightly clayey sands, 7 m thick, slightly fining upward, with clay coated burrows, bioturbations, 2 calcarenite horizons, weathered shell fragments and a sharp but irregular top (unit 21).

It is overlain by 3 stacked fining upward cycles (units 22–23, 24–25 and 26–27), each about 10 m thick. All depart from erosion surfaces with sandfilled burrows (figure 13, top of unit 23) and are completely bioturbated. The lowermost unit 22 starts with a highly glauconitic clayey sand, covered by an alternation of clayey sands and sandy clay with bioturbations (mostly chondrites) and burrows

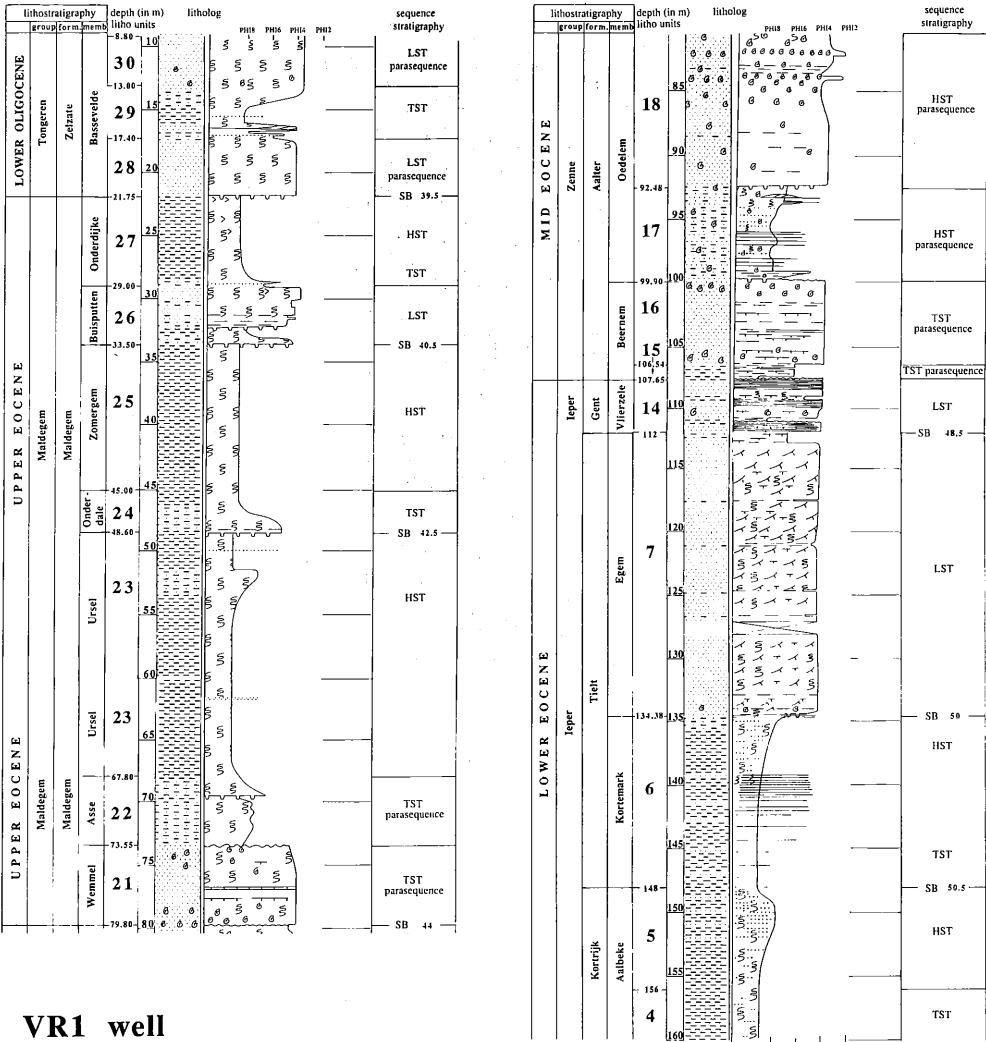


Fig. 12.— Detailed litholog with lithostratigraphy, sediment genetic and sequence stratigraphical interpretation of the VR1 boring.

which fine upward into clayey sands and silty clay, moderately glauconitic. After major erosion and a hiatus favouring glauconite formation, unit 22 is deposited in a prodeltaic low energy environment of a shelf sea. A blue grey bioturbated clay (unit 23) with millimetric fine burrows filled with sand or with organic rich clay, contains pyrite concretions, pyritized sand spots, small scale faults, and progressively fining and thinning upward sand laminae is deposited in a somewhat deeper part of the continental shelf. A transitional zone with a coarsening upward silty clay to sandy clay, covered at the top by a blue green massive clay with pyritized

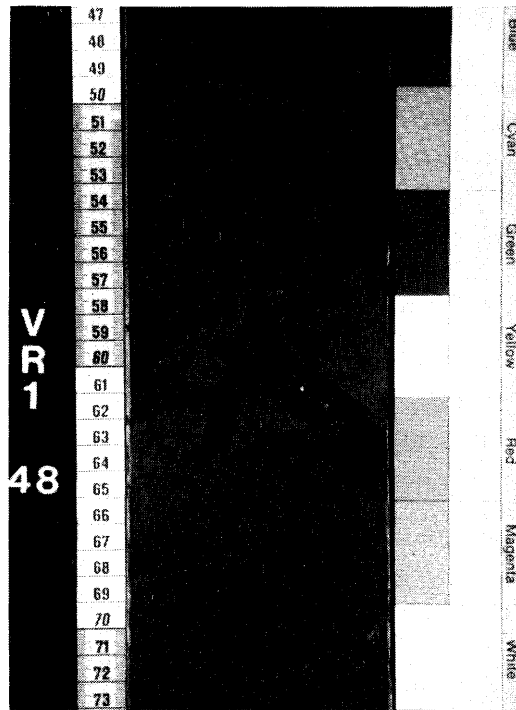


Fig. 13.— VR1 boring 48 m 60: bioturbated blue green clay with centimetric burrows at the top.

sand spots and millimetric burrows suggests prodeltaic deposition in a nearshore continental shelf environment, followed by a marked deepening.

Departing from a burrowed lower boundary, the middle cycle (unit 24) consists of moderately clayey sands with coarse interlayered and flaser bedding (figure 14), fining upward into a strongly bioturbated blue green clay, with sporadic pyritized sand spots, organic rich laminae and millimetric fine burrows backfilled with clayey sand. After a period of renewed erosion, relatively higher energy conditions alternated with relatively low energy conditions characterized by slow sedimentation rates of a deepening deltaic setting.

The third cycle (unit 26) is composed of strongly bioturbated clayey sands passing into a silty clay, covered by grey green glauconitic slightly clayey sands with flaser lamination and clay filled burrows. On top of a 50 cm thick alternation of sandy clay and clayey sands, a silty clay to blue green massive clay, strongly bioturbated (mostly chondrites) with large pyritized sand spots and nodules is deposited. Outside the study area thin peat detritus layers have been recorded in the top of this unit 27 (Gulinck, 1969a; Jacobs, 1975). The nearshore continental shelf sedimentation, reinstalled after a third erosion phase, deepens towards

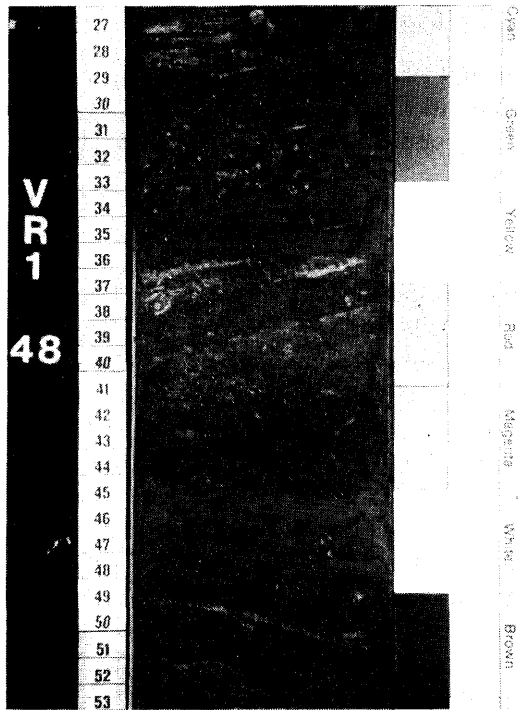


Fig. 14.– VR1 boring 48 m 25–55: medium fine sand, strongly bioturbated, with coarse interlayering and flaser lamination.

a continental shelf sea sedimentation, characterized by the deposition of a prodeltaic massive clay.

3.6.– Zelzate Formation.

The terminal Eocene succession in boring VR1 starts with 4 m of glauconitic clayey fine sands, with a mottled texture and locally containing carbonized plant remains; it is moderately to strongly bioturbated and has a burrowed lower boundary. This unit 28 is deposited in a mixed intertidal flat environment with rhythmic high energy conditions, after a major erosion phase. The alternations of fine sandy clay and mottled clayey fine sands, strongly bioturbated and containing chondrites, are interpreted as washover deposits in a lagoon protected by the presence of a (probably sandy) barrier. Sedimentation in the lagoon itself is characterized by a blue green silty clay coarsening upward into glauconitic slightly clayey fine sands. This 4 m thick unit 29 is topped by grey green glauconitic slightly clayey fine sands with a mottled texture, moderately to strongly bioturbated and containing few shell grit at the base, as the lagoon transitions into an intertidal flat. Unit 30 is incomplete in the VR1 boring.

4.– Sedimentation Model.

Facies analysis and stratal patterns allow reconstruction of the evolution with time of the depositional environment (figure 15) of the siliciclastic sedimentary system in the Southern Bight in relation to relative sea level changes.

Stage 1.

During Earliest Eocene times, distal Kortrijk Formation sediments were deposited on an open offshore mud shelf. The black clay layer with high organic content indicates restricted basin conditions in the Southern Bight of the North Sea at the moment the uplift of the Artois-Weald axis accelerated causing the separation of the Southern Bight from the opening North Atlantic (Ziegler, 1982). Restricted (or even absent) water circulation causes stratification, and consequent oxygen depletion in the bottom water layers (anoxic or suboxic conditions). The black layer representing a condensed section corresponds to a maximum flooding event in the basin. As the overlying top of unit 1 is slightly coarsening upward, the anoxia is broken up due to a change in water circulation pattern, probably because of the reinforcement or the installation of a southward longshore current system east of the British Isles oxygenating the Southern Bight bottom waters as relative sea level slowly lowers.

Because of their overall fining upward pattern, the first 4 litho units form stacked transgressive (para)sequences indicating a constantly rising relative sea level, but with sediment supply balancing subsidence thus creating stable shoreline positions. This succession is topped by a regressive unit 5 where the offshore mud shelf comes under storm influence as the rate of sea level rise slows down with time.

Stage 2.

In middle to late Early Eocene times, global lowering of relative sea level forced deposition of a delta complex (unit 6) in a more proximal position closer to the coast, as indicated by shoreline progradation. The relative sea level drop must have been considerable as indicated by characteristic sharp based "blocky sands" of the following sequence, as units 7 and 8 represent the progradation of a new delta front. The temporal reinstallation of the offshore mud shelf during a limited period of locally greater water depths (basal part of unit 9) points towards a short sea level rise forcing the delta to retreat (forced regression), but the delta sedimentation (with lagoonal mud flats and sand shoals) is restored already as sea level starts to lower again, depositing the regressive top portion of unit 9 and units 10 to 12 of the prograding delta.

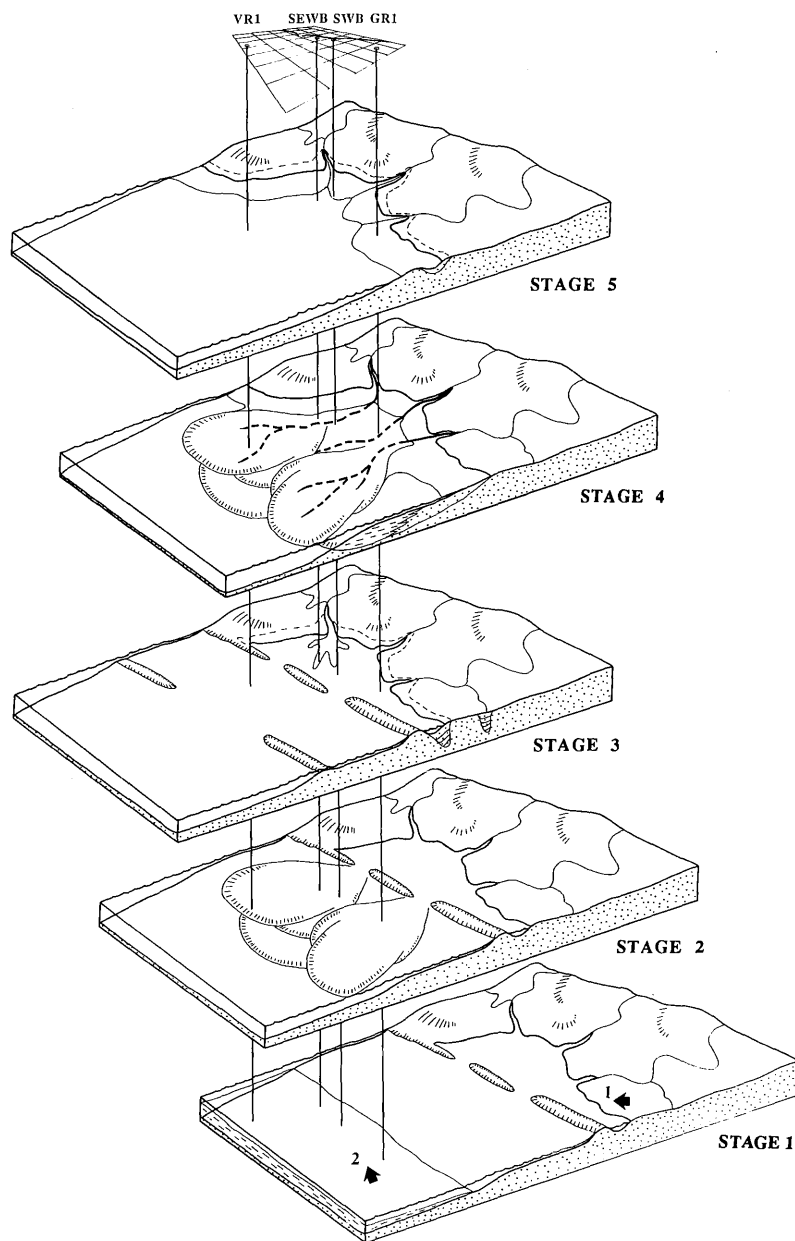


Fig. 15.— Evolution in time and space of the siliciclastic sedimentary system in the Southern Bight of the North Sea during the Eocene. Arrows indicate North (1) and main current direction (2).

Stage 2 sedimentation is characterized by deltas prograding onto the shelf, fed by a fossil proto-Rhine-Meuse-Scheldt fluvial drainage system, with a south-

ern sediment supply caused by the Alpine uplift of the hinterland as indicated by heavy-mineral provenance studies (Jacobs, in press). At the end of Early Eocene times (units 13 and 14) tidal influence became prominent with deposition of wave influenced subtidal sand shoals after further lowering of relative sea level, resulting in loss of accommodation space.

Stage 3.

In Middle Eocene times sedimentation shifts even closer to the coast towards its most proximal position, indicating higher energy conditions. Higher wave energy and longshore currents build up a series of barriers protecting a lagoon with estuaries and tidal flats. Large coarse sediment supply and loss of accommodation space due to further relative sea level lowering were responsible for the deposition of wave influenced subtidal and intertidal sediments with subtidal gullies and mixed intertidal flats (units 15 and 16), and the outbuilding of submarine coastal barriers (unit 17) protecting a lagoon (units 18 and 20) open to the sea (storm deposits), giving rise to stacked (para)sequences indicating shallowing of the basin and constant shoreline regression by excess of sediment supply.

Stage 4.

Late Eocene sedimentation of the 4 predominantly fining upward clayey layers takes place on a nearshore continental shelf progressively deepening towards a continental sea. Relative sea level rise is prominent but stepwise as indicated by the 4 basal erosional surfaces which represent consequent transgressive surfaces of stacked (para)sequences. Aggradation produces rather thick (on a scale of a few to ten meters) sedimentary sequences with a regular geometric architecture, regionally correlatable and predicting very gentle intrabasinal relief.

In comparison to the sediments of Stage 3, the units 21 to 27 are deposited in greater water depths under less energetic conditions. After the relative sea level drop terminating the deposition of unit 20, sea level must have risen considerably as much finer grained transgressive sediments are deposited. Unit 21 marks the onset of a new depositional regime of distal deltaic character that is fully installed with the deposition of 3 stacked cycles (units 22 to 27), each induced by a sea level rise but separated by a discrete relative sea level drop.

Stage 5.

A new relative sea level drop exposes part of the upper shelf and is responsible for the development of the thin detrital peat layers and the burrows backfilled with peaty sand in the top of unit 27. Terminal Eocene units 28

to 30 constitute stacked (para)sequences as the intertidal sand flat and lagoonal sedimentation is reinstalled in slightly shallower water conditions in comparison to Stage 4 as indicated by its more sandy sediment character.

5.— Conclusion.

Facies analysis and stratal patterns of Eocene siliciclastic shallow marine sediments in the Southern Bight of the North Sea enable sedimentation model reconstruction in relation to relative sea level changes. Two major transgressive/regressive cycles can be discerned, the lower one of Lowermost to Middle Eocene age evidencing 3 sedimentary environments. Lowermost Eocene sediments (Stage 1) are mainly clayey, display an overall fining upward trend and are deposited on a mud shelf. A prograding delta outbuilding on the continental shelf (Stage 2) deposits middle to upper Lower Eocene sediments, gradually becoming more sandy. Middle Eocene sediments are mainly sandy, contain calcarenite horizons, coarsen upward and are mostly of tidal and lagoonal origin (Stage 3).

The upper transgressive/regressive cycle of Upper to Uppermost Eocene age is composed of only 2 sedimentary environments. Upper Eocene strata consist of an alternation of sandy and clayey sediments of distal deltaic origin, gradually fining upward into a prodeltaic sedimentation, with slow sedimentation rates (Stage 4), while the Uppermost Eocene is more sandy and of intertidal sand flat and lagoonal origin documenting renewed delta progradation (Stage 5).

The gradual infilling of the Southern Bight of the North Sea Basin is provoked by the constant sediment supply of southern origin, poured into the basin by a mainly deltaic sedimentation system, giving rise to onlapping and shallowing upward sediment series. In vast lowland areas with practically no relief, lateral and vertical facies distribution documents even minor relative sea level fluctuations as shoreline migrations are marked and sediment supply balances or exceeds subsidence.

References.

- DE BATIST, M. (1989). *Seismostratigrafie en Structuur van het Paleogeen in de Zuidelijke Noordzee*, Ph.D. Thesis, Rijksuniversiteit Gent.
- GULINCK, M. (1965). Le passage du Bartonien au Rupélien dans la région Boom-Malines, *Bulletin de la Société belge de Géologie*, LXXIV:115–120.
- GULINCK, M. (1969a). Coupe résumée des terrains traversés au sondage de Kallo et profil géologique NS passant par Woensdrecht-Kallo-Halle, *Mémoires Explicatives des Cartes Géologiques et Minières de la Belgique*, 11:3–7.

- GULINCK, M. (1969 b). Le passage Oligocène-Eocène dans le sondage de Kallo et le Nord de la Belgique, in *Colloque sur l'Eocène, Mémoires du Bureau de Recherches Géologiques et Minières de France*, 69:193–195.
- JACOBS, P. (1975). *Bijdrage tot de litostratigrafie van het Boven-Eoceen en het Onder-Oligoceen in Noordwest België*, Ph.D. Thesis, Rijksuniversiteit Gent.
- JACOBS, P. (in press). Western Belgian Eocene sediment supply determined through heavy mineral distributions, *Geologie en Mijnbouw*.
- JACOBS, P. and SEVENS, E. (1988). *Sedimentation around the Eo-Oligocene boundary in the Belgian Basin*, in: *LAS 9th European Regional Meeting. Excursion Guidebook*, Leuven, Belgian Geological Survey, pp. 48–50.
- JACOBS, P., SEVENS, E., DE BATIST, M. and HENRIET, J.P. (1990). Grain size-, facies and sequence analysis of West Belgian Eocene continental shelf deposits, *Zentralblatt für Geologie und Paläontologie*, Teil I, 8:931–955.
- KING, C. (1990). Eocene stratigraphy of the Knokke borehole (Belgium), in *The Knokke boring (11E/138), Mémoires Explicatives des Cartes Géologiques et Minières de la Belgique*, 29:67–102.
- LERICHE, M. (1912). L'Éocène des bassins parisien et belge (Livret-guide de la réunion extraordinaire de la Société géologique de France), *Bulletin de la Société géologique de France*, (4), XII:692–724.
- LERICHE, M. (1922). *Les terrains tertiaires de la Belgique*, in: *Congrès géologique international. Livret-guide pour la XIII^e Session. Excursion A4*, Bruxelles.
- MARÉCHAL, R. and LAGA, P. (1988). *Voorstel lithostratigrafische indeling van het Paleogeen*, Belgian Geological Survey, 208 pp.
- MOURLON, M. (1888). Sur l'existence d'un nouvel étage de l'Éocène moyen dans le bassin franco-belge, *Bulletin de l'Académie royale de Belgique*, (3), XVI:252–276.
- RUTOT, A. (1882). Résultats de nouvelles recherches dans l'Éocène supérieur de la Belgique. IV.– Résolution de la question du Tongrien et du Wemmélien. Création du système Asschien, *Annales de la Société royale Malacologique de Belgique*, vol. XVII, Bulletin des séances, pp. CLXXXI–CLXXXV.
- RUTOT, A. (1883). Résultats de nouvelles recherches dans l'Éocène supérieur de la Belgique. II.– Constitution géologique des collines tertiaires comprises entre Bruges et Eecloo, *Annales de la Société royale Malacologique de Belgique*, vol. XVII, Bulletin des séances, pp. CLXXVIII–CLXXIX.
- STEURBAUT, E. (1990). Calcareous nannoplankton assemblages from the Tertiary in the Knokke borehole, in *The Knokke boring (11E/138), Mémoires Explicatives des Cartes Géologiques et Minières de la Belgique*, 29:47–62.
- VAN BAVINCHOVE, B. (1993). *Event stratigrafie van het Onder-Eoceen*, *Belgisch Continentaal Plat*, M.Sc. Thesis, Universiteit Gent.
- ZIEGLER, P.A. (1982). *Geological Atlas of Western and Central Europe*, Shell Internationale Petroleum Maatschappij, Elsevier Amsterdam, 130 pp., 40 encl.

North Sea Aerosol Characterization by Single Particle Analysis Techniques

H. VAN MALDEREN, L. DE BOCK, J. INJUK,
Ch. XHOFFER and R. VAN GRIEKEN

Department of Chemistry, University of Antwerp (UIA)

1.— Introduction.

Since some 10 years, direct deposition from the atmosphere has been recognized as a potentially major input source for contaminants into the North Sea. Though not fully quantified, this pathway is expected to be about as important as all others combined. But the few existing experimental values show significant discrepancies, certainly when compared with calculated values from deposition models.

The major differences between modeled and experimental deposition fluxes and also among them, are related to uncertainties in particle size distributions. The largest particle fraction, the so-called “giant” aerosols (these are particles with aerodynamic diameters larger than $2\text{ }\mu\text{m}$) have nearly always been neglected hitherto. Yet, it should be emphasized that, while giant particles are indeed numerically very scarce in the atmosphere, a particle of *e.g.* $10\text{ }\mu\text{m}$ has 1000 times more mass than a $1\text{ }\mu\text{m}$ particle and, additionally, its deposition velocity is *ca.* 100 times higher. The presence of only a few of these giant particles will therefore influence the deposition flux enormously.

The major problem in nearly all previous aerosol deposition studies over the North Sea in the past, is precisely that the large particle fraction has not been adequately assessed, because of the extreme difficulties in sampling these particles representatively. In order to achieve this, the particles should be sampled in an isokinetic way. This means that the linear velocity of the particles in the atmosphere should exactly be the same as the air inlet speed in the sampling device. This problem has always been overlooked for various reasons, but mainly because the large particle fraction has always been thought of as negligible. Recently collection of aerosols in wind tunnels under isokinetic conditions has been performed with both total filters and cascade impactors to collect the

atmospheric aerosols, including the largest fractions, as a function of particle size, under different atmospheric conditions and during different seasons.

Since quite some years, our research group has studied the North Sea environment intensively, where we focused our efforts primarily on the heavy metal concentrations and physical and chemical characterization of individual North Sea particles.

2.– Recent North Sea sampling campaigns.

Ships provide a stable platform for long-term sampling of marine aerosols over large areas. However samples taken from a ship can easily be contaminated *e.g.* by sea spray under high wind conditions, and by the ship itself or motor exhausts. Aerosols sampling with aircrafts has the technical possibility of both sampling at high altitudes and at very low altitudes, down to 15–20 m above the sea level, so that vertical profiles can be acquired. Ideally, the combined use of research vessels and aircrafts for aerosol sampling offers the possibility of sampling over large areas, to obtain vertical profiles and avoid contaminations of local sources.

In the last eight years, our group participated in numerous extensive sampling campaigns, both with ships and aircrafts. Over a period of four years (1984–1987), aerosols samples were collected on board of the research vessel *R/V Belgica* during various cruises over the North Sea, the English Channel and the Celtic Sea for analysis by energy-dispersive X-ray fluorescence (EDXRF), electron probe X-ray microanalysis (EPXMA) and laser microprobe mass analysis (LAMMA) [Bruynseels *et al.*, 1988; Xhoffer *et al.*, 1991, 1992; Otten, 1991].

From September 1988 to October 1989, a set of 108 aerosol samples was collected with the aid of an aircraft over the Southern Bight of the North Sea. Detailed information on sampling instrumentation and sampling strategy can be found elsewhere (Otten *et al.*, 1989). Briefly, after localizing the inversion layer, six horizontal tracks were flown at six different altitudes and equally spaced between sea surface and the inversion layer. Particulate matter was sampled and deposited on various substrates and impactors for analysis with different techniques such as EPXMA, LAMMA, EDXRF and anodic stripping voltammetry (ASV). Special attention was given to the collection of giant aerosol particles. They were collected with a special sampling device, consisting of a cylindrical impaction surface (diameter 1 cm) covered with a particle-free sticky tape and supported by a vertical bar, which was exposed outside the airplane perpendicularly to the streamlines of the airplane and directed upwind. Results of this sampling campaign can be found in publications by Rojas and Van Grieken (1992), Injuk *et al.* (1992), Van Malderen *et al.* (1992) and Rojas *et al.* (1993).

In September 1991, an extensive ship-based sampling programme was set up, covering the central area of the North Sea. Two research vessels (*R/V Belgica* and *F/S Alkor*) were continuously positioned downwind from each other, on a circle of about 200 km diameter. An identical sampling scheme was thus performed at 200 km intervals in the same air masses as they were crossing the North Sea. This allowed to study the changes in the aerosol and rainwater composition due to deposition processes and chemical reactions. Approximately every 8 h, new ship positions were taken on the operating circle. Special attention was given to the isokinetic sampling of the aerosols, by making use of a wind tunnel in which the impactors and filter units were placed. The samples were analyzed by several X-ray emission techniques (EDXRF, EPXMA and proton-induced X-ray emission analysis or micro-PIXE) both for bulk and individual particle analysis. Preliminary results can be found elsewhere (Injuk *et al.*, 1993).

During 1993, we will participate in 5 cruises with the *R/V Belgica* on the North Sea. Special attention will be given to the sampling under isokinetic conditions, collection of North Sea aerosols for individual particle analysis by techniques such as Fourier transform infrared microscopy, secondary ion mass spectrometry and Raman spectroscopy, which have never been invoked in this context before, and to suspended particles in rainwater and seawater.

3.- Potential of single particle analysis.

Most of the studies on particulate atmospheric matter have been based on bulk analysis. Micro-analysis, however, allows to characterize the composition and the morphology of individual particles. By investigating the presence of particular elements, it is possible to discriminate between specific particle types. It is possible to follow their abundance as a function of relevant parameters (*e.g.* wind direction, wind speed, location, humidity, ...) and to identify their origin and sources. Additional information on reactions that particles undergo in the atmosphere may be inferred from micro-analytical techniques capable of measuring selectively the surface layer composition.

Of all micro-analytical techniques, EPXMA is by far the most commonly used. When automated, EPXMA is a very efficient tool for analyzing a large number of individual particles within a reasonably short time. In our laboratory, several hundred particles can be analyzed in a few hours by a JEOL Superprobe JXA-733 EPXMA unit, which is automated by a system for automated particle recognition and characterization. An electron beam scans the sample until it detects a signal above a certain threshold value. The beam excites various signals which can be used for morphology studies, while X-ray detectors permit to obtain information about the chemical composition of the analyzed particle. The main

disadvantage of EPXMA is in the poor relative detection limits of about 0.1%. But combined with cluster analysis and/or multivariate techniques, EPXMA is a powerful tool for single particle analysis. With this method approximately 100,000 individual North Sea aerosols have been analyzed the last few years.

The very low Bremsstrahlung in a Scanning Proton Microprobe (SPM or micro-PIXE) permits detection limits down to 10 ppm, *i.e.* 100 to 1000 times better than in EPXMA. In SPM, a proton beam with an energy of 1 to 3 MeV is focused to a diameter of 0.5 to 10 μm by means of magnetic quadrupoles and/or electrostatic lenses. In a very similar way as in EPXMA, X-rays are generated and elemental maps of particles are obtained. This technique is still young and therefore not automated. Only a very limited number of particles has been measured with this technique up to now.

An alternative technique is LAMMA. The principle of LAMMA is based on vaporization and ionization of a particle by a focused laser beam. LAMMA has some interesting features: it can detect all elements, has very low detection limits compared to other techniques and it can give information about organic compounds. On the other hand, the results are rather irreproducible and because of the low mass resolution, results are sometimes difficult to interpret. To overcome these problems, a new Fourier-transform Ion Cyclotron Resonance Mass Spectrometer (FTIR-ICR-MS) with a 100 to 1000 better mass resolution has been acquired. Thousands of spectra have been measured by LAMMA over the last 10 years, but the new spectrometer is still in the experimental stage.

4.— Results and discussion.

The combination of these three different and in some ways complementary micro-analysis techniques, EPXMA, micro-PIXE and LAMMA, allows us to have a better and more quantitative understanding of the sources and behaviour of these particles. The fully automated EPXMA provides us with such an enormous amount of data in a short time, that the results can be statistically interpreted, but for this some way of data reduction is needed. This is done by performing multivariate techniques as hierarchical and non-hierarchical clustering techniques and principal factor analysis (PFA) on the thousands of generated spectra. LAMMA and micro-PIXE are not so automated and therefore a much more labour-intensive. Hence not so many data can be collected in a short time, but these techniques provide us with additional data, which cannot be collected by the fast EPXMA. Together they give us a good and clear insight in the North Sea aerosol. We will now elaborate more on the results for each of the techniques.

4.1.— Results of Electron Probe Micro Analysis.

For the processing of the EPXMA data, we need the help of multivariate techniques. The data reduction and interpretation of our results was based on hierarchical and non-hierarchical cluster algorithms combined with PFA with orthogonal Varimax rotations. Details and theoretical background of these multivariate techniques can be found elsewhere (Rojas, 1991).

4.1.1.— EPXMA: results of hierarchical clustering.

The EPXMA results after hierarchical cluster analysis of both the ship- and the aircraft-based measurements generally reveal about 10 major particle types. Differences in particle type abundances are observed for the various sampling campaigns since the chemical composition of the airborne particulate matter strongly depends on the meteorological conditions and the back trajectories of the air masses, but also on the sampling location and altitude of sampling. We shall discuss the identified particle types separately with special reference to their formation mechanisms and the chemical changes during their life-time in the atmosphere and to their specific emission sources.

Seasalt.

The breaking of waves is the main process for the generation of fresh seasalt into the atmosphere. The contribution of NaCl in the aerosol is more pronounced under more remote sampling conditions or when the backtrajectories of the sampled air came from far over the Atlantic Ocean without continental interferences.

Transformed seasalt.

This particle type is rich in S and Cl but also mixtures of NaNO_3 , Na_2SO_4 and NaCl are possible (Bruynseels *et al.*, 1988). These S- and Cl-rich particles are formed by the conversion of NaCl into Na_2SO_4 by SO_2 or H_2SO_4 , implying halogen displacement reactions in seasalt particles (Hitchcock *et al.*, 1980; Clegg and Brimblecombe, 1985). The contribution of S enrichment in seasalt aerosols is more and clearly pronounced in samples for which an important anthropogenic influence on the marine atmosphere is expected. In the aerosol samples collected during prevailing continental influence, pure seasalt particles are no longer detected. The formation of mixed seasalt/mineral aerosols can be explained by cloud coalescence processes between mineral and seasalt containing particles (Andreae *et al.*, 1986). Sometimes nitrate enrichment was observed in LAMMA spectra. Up to 49% of the total giant particles detected in marine air masses above the Southern Bight of the North Sea were identified as seasalt and aged seasalt. Principal factor analysis (PFA) performed on the giant particle dataset (Van Malderen *et al.*, 1992) showed that the marine source (high loadings

observed for Na, Mg, S and Cl) is slightly anti-correlated with altitude. This could be expected from the mechanism by which major and trace elements are injected from the sea into the atmosphere.

Sulphur-rich particles.

This particle type contained no other detectable elements with $Z > 11$ than S. High particle type abundances were observed during sampling campaigns for which the air masses had long residence times over industrial regions (*e.g.* South of England or from above Eastern European countries). Consequently, emissions must be related to industrial and automotive sources all over Europe. Most of these S-rich particles have a diameter in the submicrometer range. A number of secondary reactions can take place on particulate sulphur (Harrison and Sturges, 1984; Van Borm *et al.*, 1989). Neutralization reactions can occur between NH_4^+ (often present in continental aerosols) and H_2SO_4 with the formation of various ammonium salts such as $(\text{NH}_4)_2\text{SO}_4$, $(\text{NH}_4)\text{HSO}_4$ and $(\text{NH}_4)_3\text{H}(\text{SO}_4)_2$ (Charson *et al.*, 1978). A smaller fraction of the S-rich particles have a marine origin, as is the case for dimethyl sulphoxide (DMSO) and derived compounds. Low particle number concentrations were detected at the most westerly sampling locations, where only pure marine conditions are encountered. In open ocean waters, the predominant volatile sulphur compound is dimethyl sulphide (DMS), representing almost 90% of the marine sulphur emissions (Kolaitis *et al.*, 1989).

Calcium sulphate particles.

These particles are very often found in both marine and continental aerosols. Andreae *et al.* (1986) postulated some possible marine formation mechanisms such as fractional crystallization of marine aerosols or interaction processes between marine or terrestrial airborne CaCO_3 with atmospheric SO_3 and/or H_2SO_4 *e.g.* within clouds. However for the North Sea atmospheric environment, these mechanisms are of minor importance since the major abundances for CaSO_4 particles were present in the samples influenced by the continent. NaCl was virtually absent then. It was remarkable that all CaSO_4 -rich filters sampled above the North Sea were influenced by continental air masses travelling from over the South of England. Thus important sources for CaSO_4 particles above the North Sea are combustion processes and eolian transport. Note that large quantities of CaCO_3 and $\text{Ca}(\text{OH})_2$ are used in thermal power plants, as a desulphurization agent, to favour the oxidation of SO_2 and neutralize the SO_3 ; this leads to sulphates. Though commonly observed, the exact origin of these gypsum particles is still uncertain. In the near future this particle type will be investigated more closely and its abundances as a function of several parameters (position, wind direction, meteorological parameters, ...) will be examined.

Calcium-rich particles.

This particle type shows only Ca as detectable element in the X-ray spectrum. They are assigned to CaCO_3 (C and O cannot be detected in conventional EPXMA) and they can, just as CaSO_4 , originate from both marine and continental sources. In some Ca-rich particles, sulphur was detected. Yet, these were not classified into the CaSO_4 group because of too low S-characteristic X-ray intensities. This particle type may represent the initiation of Ca-S-rich particle formation from CaCO_3 and/or derived components with atmospheric SO_2 or H_2SO_4 . According to the obtained data set, Ca-rich particles above the North Sea cannot unambiguously be apportioned to one specific source type.

Aluminosilicate particles.

This mineral type of particles finds its origin on the continent. The major elements are Al, Si, S, K, Ca and Fe and the minor ones Ti, Cr, Mn, Ni and Zn. From morphology studies, smooth and nearly spherical particles could be identified as fly-ash and therefore be differentiated from soil dust. These typically shaped particles were frequently observed on filters when the sampled air masses were mainly influenced by Eastern European emissions. Positive LAMMA spectra of these spherical aluminosilicates also show the presence of trace elements as V, Ga, Rb, Cs, Ba, Pb, etc. However, one must realize that the distinction between soil dust and flyash is still dubious.

The giant aluminosilicate particle fraction, consisting of both wind blown dust and flyash, is positively correlated with altitude what could be explained by the presence of a long-range transported mineral aerosol at high altitudes. The size distribution of the giant aluminosilicates shows a bimodal character with maxima of the average diameters centred around 4 μm and 15 μm . This suggests two completely different sources and morphology studies confirmed the existence of smaller spherical particles (flyash derived) and a larger irregularly shaped fraction.

Silicon-rich particles.

These mineral quartz particles are irregularly shaped. They can be derived from soil dust or emitted into the atmosphere during the combustion of coal in power plants. Therefore, they are frequently found in the presence of aluminosilicates. The fact that these particles, just as the Fe-rich particles, are found in the smallest size range (below 1 μm) could strengthen the hypothesis that they are formed during combustion processes.

Titanium-rich particles.

For some North Sea samples, rather high Ti-rich particle abundances were observed. The main source for Ti-release into the atmosphere is pigment spray,

but minor pollution processes and sources as soil dispersion, asphalt production and coal-fired boilers and power plants have also been recognized (Hopke, 1985). Sometimes contributions of Cr, Si, Zn, Pb and Ba are observed in this particle type.

Iron-rich particles.

These particles show a spherical shape with a mean diameter of 0.6 μm and they are quite common at all heights over the Southern Bight airshed. They are mostly associated with siderurgical activities in Northern France (Bruynseels, 1987). Within the Fe-rich cluster three different Fe-rich fractions can be recognized. The first and second subgroup, characterized by Fe and Fe-Zn-Mn, respectively, are mainly produced by ferrous metallurgy processes. Very often S is associated with Fe-rich particles and this represent the third subgroup. These are pyrite and iron sulphate, probably formed by reaction between iron oxide and sulphuric acid during or after their release in ferrous metallurgy related combustion processes.

Miscellaneous particle types.

Each of the miscellaneous particle types observed, accounted for less than 10% of the total aerosol abundance in a sample. These particle types were not always present in air masses above the North Sea. They are often characterized by the presence of some heavy metals. Variations within these groups are mainly due to different meteorological conditions and seasons during which the sampling took place. Although their abundances are quite low compared to the other groups, the presence of these rather rare particles can sometimes be apportioned to one specific source. For example, higher abundances of heavier elements like Pb and Br together with Cl were detected. These Pb-rich particles originate from automobile exhaust emissions. Indeed, Pb is added to the gasoline together with ethylene dihalide compounds (Br, Cl). The emitted lead halides can readily be converted to lead sulphates by reaction with SO_2 , H_2SO_4 , or $(\text{NH}_4)_2\text{SO}_4$ with the loss of HBr (Sturges and Harrison, 1986). However, none of the transformed lead halide particles showed associations with S in spite of the very high S concentrations present in the corresponding sampled air masses.

Characteristic X-ray spectra showed that P was sometimes associated with S and Cl or with an organic fraction. The organic phosphorus fraction is primarily formed through biological activities. Bubble bursting in the sea can cause enrichment of P in the seasalt aerosols by fractionation out of the sea surface microlayer (Graham *et al.*, 1979). Chen *et al.* (1985) found that the major sources for particulate P in marine aerosols of New Zealand were soil particles containing both naturally occurring and fertilizer-derived P, as well as seasalt particles and industrial emissions. Na, Al and V can be associated with P as

markers for a marine source and an anthropogenic pollution source (burning of biological material). However, for the North Sea samples, no associations to these markers were observed and hence these P-rich particles probably have a marine origin. Also, Ca and P were often observed to present in the same particles. This particulate fraction can be fertilizer derived or is a residual from biological material (e.g. pollen) and can be transported over the North Sea by wind action. Ca- and P-rich particles, although with different elemental X-ray intensities, were identified in aerosol samples taken above the equatorial Pacific Ocean where only marine influences were expected (Xhoffer, 1987).

Heavy metal concentrations of Cu and Zn emitted by metallurgical processes were confirmed to reach maxima with East-Southeast winds (Injuk et al, 1990) as previously reported by Kretzschmar and Cosemans (1979). Also burning processes of either organic material or of municipal waste in incinerators are responsible for the emission of K- and Zn-chlorides.

Table 1a

Particle types identified for sampling flights with little continental influence

Group Number	Abundance (%)	Average Diameter (μm)	Elements Detected	Identification
1	31	3.5	Na,Cl,S	S enriched seaspray
2	18	3.3	Na,Cl	Seaspray
3	16	2.9	Ca,S	Gypsum
4	10	2.0	Fe	Fe-rich
5	8	3.9	S,Cl	Sulphates
6	6	3.1	Ca,S,Cl	Cl enriched Gypsum
7	5	3.2	Al,Si,Cl	Aluminosilicates
8	5	3.1	none	Organic
9	1	1.9	Na	Na-rich

Table 1b

Particle types identified for sampling flights with strong continental influence

Group Number	Abundance (%)	Average Diameter (μm)	Elements Detected	Identification
1	36	3.1	Ca,(Si,P)	Ca-rich
2	17	2.1	none	Organic
3	12	3.3	Ca,S	Gypsum
4	11	4.3	Al,Si	Aluminosilicates
5	4	2.7	K,Cl,(Zn)	K,Zn-chlorides
6	4	3.7	Cl,Na	Seaspray
7	3	3.6	Fe	Fe-rich
8	2	2.6	Si	Quartz

Particles with no major X-ray intensities were denoted as organic. They seemed anti-correlated with altitude and could therefore be related to biogenic material as pollen, spores and bacteria. Sometimes, V and Pb are associated to organic matter. The chemical complexity of these particles indicates that several atmospheric interaction processes can be involved in the formation.

As an example the results of the hierarchical clustering on the data set for giant North Sea aerosols is shown in Table 1a and 1b. The results are given for flights with both little and strong continental influence. More detailed information can be found elsewhere (Van Malderen *et al.*, 1992).

4.1.2.- EPXMA: results of nonhierarchical clustering.

In order to obtain an overall view on the particle types collected in a complete data set (*e.g.* all samples in one sampling campaign), we perform a nonhierarchical clustering. This is done by first clustering all particles in each separate sample by a hierarchical clustering (Ward's method). The average elemental abundances obtained from all the separate samples are then clustered again, what provides us with average elemental abundances, but for all samples together now. These are further used as centroids for the nonhierarchical clustering. Again as an example the results of a nonhierarchical clustering for the giant North Sea aerosols are shown in Table 2.

From Table 2, it appears that 22% of the detected particles consist of Ca-rich (61% Ca) particles. Nearly as much (21%) of the North Sea giant aerosols are seasalts, while 20% of the particles are found to be CaSO_4 -particles. Group 4 can be identified as K,Zn-chlorides, but since the sum of relative composition for all the elements does not make 100% and the abundance (18%) is very high compared to the results obtained from the hierarchical clustering, it is likely that they have been mixed up with particles without major X-ray intensities, previously identified as organic particles. Group 5 is characterized by high contents of Al, Si, Ca and Fe (8%, 28%, 6% and 5%, respectively) and therefore it can be ascribed to aluminosilicates (14%). Group 6 contains Fe-rich (60% Fe) particles (5%), while the low abundance group (1%) is identified by a high content of Na (69% Na). The size of the particles varies between 2.2 μm for the Na-rich particles and 4.2 μm for the seasalts.

4.1.3.- EPXMA: Principal factor analysis.

Beside hierarchical and nonhierarchical cluster analysis, also other multivariate techniques like principal component analysis can be useful to gain extra information from automated individual particle analysis. To identify the different sources for giant aerosols, principal factor analysis (PFA) with orthogonal Varimax rotation was performed on the data set. The objective of PFA is to take

Table 2

composition and size for the groups found by nearest centroid sorting performed on EPXMA-analyzed North Sea Giant particles

Group no	Group Abun (%)	Diam. (μm)	Na	Mg	Al	Si	P	S	Cl	K	Ca	Cr	Fe	Ni	Cu	Zn	O
			Relative abundance per element (in %)														
1	22	3.2	0.6	0.5	0.6	2.7	0.6	1.3	1.1	0.1	61	0	0.9	0	0	0	31
2	21	4.2	14	1.0	0.1	0.8	0	3.7	75	1.6	2.3	0	0.3	0	0	1.1	0
3	20	3.0	0.9	1.5	0.7	2.2	0.1	21	2.0	0.7	22	0.1	2.4	0.3	0.1	0.1	46
4	17	2.7	1.6	4.0	2.7	4.2	3.1	6.7	11	10	5.0	0.4	5.7	0.6	1.1	11	32
5	14	3.8	0.1	0.5	8.1	28	0.1	1.6	1.2	2.0	6.1	0	4.7	0	0	0.1	47
6	5	2.6	0	0.3	0.3	1.7	0.1	0.1	1.4	0.2	1.5	1.8	60	0.6	0	0.2	31
7	1	2.2	69	0	0	0	0	2.1	0.8	0.4	0	0	0	0	0.3	0	27

p variables and find linear combinations of these to produce uncorrelated new variables, which are ordered in decreasing order of importance so that the first one explains the largest amount of variance. In the second stage of the factor analysis, the first few new variables are rotated in order to find new factors that are easier to interpret. Here the data matrix consisted of 13 variables (Na, Mg, Al, Si, P, S, Cl, K, Ca, Fe, Cu, Zn and height of collection). An element was considered to be detected if an X-ray intensity of the element was found in one of the 500 analyzed particles for each sample. One of the most important problems of PFA is the decision of the dimensionality of the model. The decision on how many factors should be retained is often rather subjective. But it is usually a "rule of thumb" to retain as many factors as there are eigenvalues greater than unity. More detailed information on the strategy to perform PFA on EPXMA data can be found elsewhere (Rojas and Van Grieken, 1992; Van Malderen *et al.*, 1992). Results are shown in Table 3.

Table 3
Varimax rotated factor loading matrix for 25 North Sea giant aerosol samples

Variable	Factor 1	Factor 2	Factor 3	Factor 4	Communality	Standard Deviation
Na	- 0.42	0.69	0.36	-	0.814	0.09
Mg	-	0.75	-	-	0.627	0.13
Al	0.95	-	-	-	0.928	0.06
Si	0.96	-	- 0.18	-	0.956	0.05
P	- 0.40	- 0.85	-	-	0.913	0.06
S	-	0.86	-	-	0.878	0.08
Cl	- 0.31	0.73	-	0.46	0.883	0.07
K	- 0.28	-	-	0.84	0.822	0.09
Ca	0.59	- 0.60	-	-	0.773	0.10
Fe	0.90	-	- 0.26	-	0.887	0.07
Cu	- 0.30	-	0.83	0.25	0.867	0.08
Zn	-	-	0.85	-	0.813	0.09
Height of sampling	0.38	- 0.35	0.36	- 0.52	0.672	0.11
Eigenvalue	4.74	3.54	1.39	1.16		
% variance explained	36.3	27.1	10.6	8.9		
Source Identification	Alumino-Silicates	Marine	Industrial	Combustion processes		

Only factor loadings greater than three times their standard deviation are shown, because only these are considered as statistically significant. The four factors together explain 83% of the total variance. Communalities are high for all variables, except for Mg, Ca and "height". Factor 1 has high loadings for Al, Si, Ca and Fe.

Aluminosilicates, both wind blown soil-dust and fly-ash, which have similar chemical compositions with respect to many elements, probably correspond to this factor. Factor 1 is positively correlated with height, what could be explained by the presence of a long-range transported mineral aerosol at high altitudes. Factor 2 is most likely representing marine impact. Furthermore, this marine source is slightly anti-correlated with height. If one considers the mechanism by which matrix and trace elements are injected from the sea into the atmosphere, high concentrations of Na, Mg, S and Cl are to be expected at lower altitudes, as observed. Factor 3 has high loadings for Cu and Zn, suggesting the existence of an industrial source for Cu and Zn. Generally, Zn is emitted evenly in Europe, whereas emissions of Cu are rather attributed to Central and Eastern Europe. Heavy metal concentrations in the atmosphere were reported to reach maxima with East-Southeast winds and should therefore be mainly found in flights with continental air mass history. Cl and K, which characterize factor 4, are probably the result of combustion processes. The burning of organic material leads to emission of K, but also the burning of municipal waste in incinerators leads to K and Zn-chlorides. In summary, PFA on 13 variables distinguished 4 classes of giant aerosol sources; aluminosilicates (Al, Si, Ca, Fe), marine aerosols (Na, Mg, S, Cl), industrial processes (for Zn and Cu) and combustion processes (for K, Cl).

4.2.– Results of Laser Microprobe Mass Analysis.

All the particle types that are previously discussed for the EPXMA analysis were also found by LAMMA. However, here the particles often appear as internal mixtures: the image of this aerosol, as obtained with much more sensitive LAMMA, is therefore much more complicated.

LAMMA was applied to a number of representative particles from the previously discussed particle types in order to elaborate trace element contents and surface layer composition. Applying low energy laser shots to the spherical fly-ash particles revealed typical spectra that were interpreted as fingerprints for the desorption of polynuclear aromatic hydrocarbons (PAH). Spectra of pure seasalts are dominated by Na, K and typical Na/K/Cl cluster ions. Often, seasalt particles are found to have been transformed to some extent; in that case, nitrate and sulfate coatings are readily detectable (Bruynseels and Van Grieken, 1985). Bruynseels *et al.* (1985) found the amount of nitrate-coated seasalt particles to increase significantly from a beach site towards an industrialized area, 30 km downwind from the ocean. Another advantage of LAMMA in aerosol research is its ability to detect ammonium compounds, which are very interesting from an environmental point of view. Otten *et al.* (1987) found the relative abundances of ammonium-rich particles in the North Sea aerosol to increase dramatically

Table 4
Elemental composition of North Sea aerosols as obtained by Micro-PIXE, with values in ng cm^{-2}

Sample	S	Cl	K	Ca	Ti	V	Cr	Mn	Fe	Zn	Pb
B-18-2	118 \pm 4	900 \pm 80	23 \pm 2	24 \pm 3	—	—	—	—	—	—	—
B-18-2	53 \pm 9	350 \pm 30	12 \pm 1	14 \pm 1	—	—	—	—	—	—	—
B-18-2	27 \pm 5	220 \pm 20	7 \pm 1	7 \pm 1	—	—	—	—	—	—	—
B-18-2	76 \pm 17	720 \pm 60	15 \pm 2	9 \pm 1	0.8 \pm 0.3	—	16 \pm 1	—	0.7 \pm 0.1	—	—
B-18-2	86 \pm 11	300 \pm 30	11 \pm 2	57 \pm 4	—	—	24 \pm 2	—	2.2 \pm 0.2	—	—
A-18-2	23 \pm 3	92 \pm 6	3 \pm 1	4 \pm 1	—	—	16 \pm 1	—	0.6 \pm 0.1	—	—
A-17-4	—	12800 \pm 900	16 \pm 4	—	—	—	—	—	—	330 \pm 30	—
A-17-4	430 \pm 40	66 \pm 14	510 \pm 40	—	—	—	—	—	4.1 \pm 0.5	320 \pm 20	—
A-17-4	350 \pm 30	104 \pm 8	30 \pm 4	400 \pm 30	0.9 \pm 0.3	—	—	0.7 \pm 0.4	33 \pm 3	107 \pm 8	—
A-17-4	95 \pm 9	310 \pm 22	85 \pm 6	64 \pm 4	3.9 \pm 0.5	—	—	1.8 \pm 0.4	106 \pm 7	185 \pm 13	—
A-17-2	132 \pm 21	1600 \pm 100	—	9900 \pm 700	—	—	—	10 \pm 1	42 \pm 3	—	—
A-17-4	182 \pm 14	330 \pm 30	103 \pm 7	187 \pm 13	3.2 \pm 0.5	—	2.2 \pm 0.3	5 \pm 1	400 \pm 30	310 \pm 20	—
A-17-1	1460 \pm 120	780 \pm 60	—	8600 \pm 600	10 \pm 2	2.9 \pm 0.6	5.2 \pm 0.7	48 \pm 4	480 \pm 30	26 \pm 3	28 \pm 8
A-17-1	260 \pm 20	65 \pm 5	—	949 \pm 3	5.7 \pm 0.6	2.2 \pm 0.5	20 \pm 2	270 \pm 20	890 \pm 60	14 \pm 1	—
A-18-1	—	39 \pm 7	10 \pm 1	1200 \pm 100	—	—	—	—	—	—	—
A-18-1	—	240 \pm 20	10 \pm 1	160 \pm 10	—	—	—	—	—	—	—

under the influence of polluted air masses. Examining the relative abundances of several compounds as a function of size and wind direction allowed some clear trends to be interfered. Ammonium was mainly present in the smallest particles, seasalt exhibited its typical size profile and predominated with marine, air masses while aluminosilicates and KCl prevailed for continental air masses. More detailed information can be found in a publication by Dierck *et al.* (1992).

4.2.— Results of micro-PIXE analysis.

The results involving micro-PIXE analysis on 16 North Sea aerosol particles are presented in Table 4. At this preliminary stage, the elemental concentrations are expressed in ng cm^{-2} . The sea-salt aerosol particles are clearly predominating with Cl and usually S, K and Ca as major components and with several trace elements like Ti, V, Cr, Mn, Fe, Zn and Pb. Based on this data set, four different particles group can be distinguished. The first group is characterized by particles containing Cl as a major element with S, K and Ca as minor components. The second group contains particles with Cl as a major element, again, but enriched with S, Cr and Ca. The presence of Cr in the North Sea troposphere seems significant. In the third particle group, Ca is the predominant element but the particles are enriched with notable concentrations of Fe and heavy metals. They may partially correspond to the fly-ash particles found also by EPXMA and defined by their invariably high Al, Si and Fe content (Si and Al were not measured in micro-PIXE); trace elements cannot be found by EPXMA because of its high detection limits. Finally, particles containing only Ca, Cl and K form a fourth group; they are probably also of marine origin. Here it must be stressed that only a limited number of particles were analyzed by micro-PIXE and therefore, statistical analysis was impossible. Undoubtedly, the type and quality of information acquired by all different techniques is quite dissimilar but complementary. More detailed information on micro-PIXE results can be found elsewhere (Injuk *et al.*, 1993).

Acknowledgements.

This work was partially supported by the Belgian State—Prime Minister's Services—Science Policy Office, in the framework of the Impulse Programme in Marine Sciences (under contract MS/06/050) and of EUROTRAC (under contract EU7/08), and by the Belgian Ministry of Public Health and the Environment.

References.

- ANDREAE, M., CHARLSON, R., BRUYNSEELS, F., STORMS, H., VAN GRIEKEN, R. and MAENHAUT, W. (1986). Internal mixture of sea salt, silicates, and excess sulphate in marine aerosols, *Science*, 232:1620–1623.

- BRUYNSEELS, F. and VAN GRIEKEN, R. (1985). Direct detection of sulfate and nitrate layers on sampled marine aerosols by laser microprobe mass analysis, *Atmos. Environ.*, 19:1967–1974.
- BRUYNSEELS, F., STORMS, H., TAVARES, T. and VAN GRIEKEN, R. (1985). Characterization of individual particle types in coastal air by laser microprobe mass analysis, *Int. J. Environ. Anal. Chem.*, 23:1–14.
- BRUYNSEELS, F. (1987). *Application of laser microprobe mass analysis in aerosol research*, Ph.D. Dissertation, University of Antwerp (UIA).
- BRUYNSEELS, F., STORMS, H., VAN GRIEKEN, R. and VAN DER AUWERA, L. (1988). Characterization of North Sea aerosols by individual particle analysis, *Atmos. Environ.*, 22:2593–2602.
- CHARLSON, R., COVERT, D., LARSON, T. and WAGGONER, A. (1978). Chemical properties of tropospheric sulphur aerosols, *Atmos. Environ.*, 12:39–53.
- CHEN, L., ARIMOTO, R. and DUCE, R. (1985). The sources and forms of phosphorus in marine aerosol particles and rain from the Northern New Zealand, *Atmos. Environ.*, 19:779–787.
- CLEGG, S. and BRIMBLECOMBE, P. (1985). Potential degassing of hydrogen chloride from acidified sodium chloride droplets, *Atmos. Environ.*, 19:465–470.
- DIERCK, I., MICHAUD, D., WOUTERS, L. and VAN GRIEKEN, R. (1992). Laser microprobe mass analysis of individual North Sea aerosol particles, *Environ. Sci. Technol.*, 26:802–808.
- GRAHAM, W., PIOTROWICZ, S. and DUCE, R. (1979). The sea as a source of atmospheric phosphorus, *Mar. Chem.*, 7:325–342.
- HARRISON, R. and STURGES, W. (1984). Physico-chemical speciation and transformation reactions of particulate atmospheric nitrogen and sulfur compounds, *Atmos. Environ.*, 18:1829–1833.
- HITCHCOCK, D., SPILLER, L. and WILSON, W. (1980). Sulfuric acid aerosols and HCl release in coastal atmospheres: Evidence of rapid formation of sulfuric acid particulates, *Atmos. Environ.*, 14:165–182.
- HOPKE, P. (1985). *Receptor Modelling in Environmental Chemistry*, John Wiley & Sons, New York.
- INJUK, J., OTTEN, Ph., ROJAS, C., WOUTERS, L. and VAN GRIEKEN, R. (1990). *Atmospheric deposition of heavy metals (Cd, Cu, Pb and Zn) into the North Sea*, Final Report to Rijkswaterstaat, Dienst Getijdewateren, s'Gravenhage, The Netherlands, in the framework of project NOMIVE*2 task No DGW-920, University of Antwerp.
- INJUK, J., OTTEN, Ph., LAANE, R., MAENHOUT, W. and VAN GRIEKEN, R. (1992). Atmospheric concentrations and size distributions of aircraft-sampled Cd, Cu, Pb and Zn over the Southern Bight of the North Sea, *Atmos. Environ.*, 26A:2499–2508.
- INJUK, J., VAN MALDEREN, H., VAN GRIEKEN, R., SWIETLICKI, E., KNOX, J. and SCHOFIELD, R. (1993). EDXRS study of aerosol composition variations in air masses crossing the North Sea, *X-Ray Spectrometry*, in press.

- KOLAITIS, L., BRUYNSEELS, F. and VAN GRIEKEN, R. (1989). Determination of methanesulfonic acid and non-seasalt sulfate in single marine aerosol particles, *Environ. Sci. Technol.*, 23:236–240.
- KRETZSCHMAR, J. and COSEMANS, G. (1979). A five year survey of some heavy metal levels in air at the Belgian North Sea coast, *Atmos. Environ.*, 13:267–277.
- OTTEN, Ph., BRUYNSEELS, F. and VAN GRIEKEN, R. (1987). Study of inorganic ammonium compounds in individual marine aerosol particles by laser microprobe mass spectrometry, *Anal. Chim. Acta*, 195:177–183.
- OTTEN, Ph., ROJAS, C., WOUTERS, L. and VAN GRIEKEN, R. (1989). *Atmospheric deposition of heavy metals (Cd, Cu, Pb and Zn) into the North Sea*, Second Report to Rijkswaterstaat, Dienst Getijdewateren, s'Gravenshage, The Netherlands, in the framework of project NOMINIVE task No DGW-920, University of Antwerp.
- OTTEN, Ph. (1991). *Transformation, concentratins and deposition of North Sea aerosols*, Ph.D. Dissertation, University of Antwerp (UIA).
- ROJAS, C. (1991). *Study of the concentration and deposition of tropospheric aerosols using X-ray emission techniques*, Ph.D. Dissertation, University of Antwerp (UIA).
- ROJAS, C. and VAN GRIEKEN, R. (1992). Electron microprobe characterization of individual aerosol particles collected by aircraft above the Southern Bight of the North Sea, *Atmos. Environ.*, 26A:1231–1237.
- ROJAS, C., INJUK, J., VAN GRIEKEN, R. and LAANE, R. (1993). Dry and wet deposition fluxes of Cu, Cd, Pb and Zn into the Southern Bight of the North Sea, *Atmos. Environ.*, 27A:251–259.
- STURGES, W. and HARRISON, R. (1986). Bromine in marine aerosols and the origin, nature and quantity of natural atmospheric bromine, *Atmos. Environ.*, 20:1485–1496.
- VAN BORM, W., ADAMS, F. and MAENHAUT, W. (1989). Characterization of individual particles in the Antwerp aerosol, *Atmos. Environ.*, 23:1139–1151.
- VAN MALDEREN, H., ROJAS, C. and VAN GRIEKEN, R. (1992). Characterization of individual giant aerosol particles above the North Sea, *Environ. Sci. Technol.*, 26:750–756.
- XHOFFER, C. (1987). *Electronenprobe microanalyse van vlieg-as en partikels uit het marine milieu*, M.Sc. Thesis, University of Antwerp (UIA).
- XHOFFER, Ch., BERNARD, P., VAN GRIEKEN, R. and VAN DER AUWERA, L. (1991). Chemical characterization and source apportionment of individual aerosol particles over the North Sea and the English Channel using multivariate techniques, *Environ. Sci. Technol.*, 25:1470–1478.
- XHOFFER, Ch., WOUTERS, L. and VAN GRIEKEN, R. (1992). Characterization of individual particles in the North Sea surface microlayer and underlying seawater: comparison with atmospheric particles, *Environ. Sci. Technol.*, 26:2151–2161.

Primary Production and Nutrient Fluxes in the Gulf of Biscay

M. ELSKENS¹, L. CHOU², P. DAUBY³, M. FRANKIGNOULLE³,
L. GOEYENS¹, M. LOIJENS² and R. WOLLAST²

¹ Laboratorium voor Analytische Scheikunde, Vrije Universiteit Brussel

² Laboratoire d'Océanographie Chimique, Université Libre de Bruxelles

³ Laboratoire d'Océanologie, Université de Liège

Abstract.

Since the roles of continental shelves and coastal areas in the global biochemical carbon cycle are nowadays a leading concern in oceanographic research programmes, this study aims to define the specific effect of nutrients on the onset and development of the phytoplankton bloom at the ocean margins. Comparison experiments of the carbon, nitrogen and phosphorus assimilation rates were carried out from 1989 to 1991 in the English Channel and the Gulf of Biscay. New production were obtained from the traditional approach using f -ratio values, *i.e.* the ratios of directly measured nitrate to carbon uptakes and/or the ratios of nitrate to nitrate plus ammonium uptakes. Values of f agree well on the shelf, slope and deep basin regions of the Gulf of Biscay but are most likely overestimated in the coastal zone of the English Channel. The C/N/P uptake ratios exhibit, furthermore, great spatial variability that can reflect variations in the nutrient status of phytoplankton during its growth.

1.- Introduction.

The measurement of ^{14}C primary production alone is generally insufficient to assess the capacity of phytoplankton to support production at higher levels in the food web. This shortcoming and the need to understand the processes shunting transfer and behaviour of organic matter and the pelagic food web led to the introduction and development of the concepts of "new" and "regenerated" production. Their difference is based on the partitioning of primary production according to the nitrogen source (Dugdale and Goering, 1967). New production is the fraction of autotrophic production sustained by an external input of N-nutrients, mainly nitrate, while regenerated production refers to the uptake of *in situ* recycled nutrients, mostly ammonium and urea. Both ecological categories are not strictly separated in nature, but confine the frame for an

adequate understanding of the oceanic productivity (Goldman, 1988). The relative contributions of new and regenerated nitrogen to primary production are commonly estimated by the so-called *f*-ratio, *i.e.* the ratio of ^{15}N -nitrate to ^{14}C carbon uptakes (Eppley, 1989). A similar and almost equivalent expression uses the sum of nitrate and ammonium based production in stead of the ^{14}C primary production. This second equation refers to an open ocean system, where nitrate is the main allochthonous nitrogen source and ammonium the main autochthonous one. It should be pointed out, however, that while new production is usually supported by nitrate, the basic distinction is between nitrogen supplied by local photic zone regeneration and that supplied from elsewhere. For instance, near sewage outfall, considerable new production could be supported by ammonium (Eppley *et al.*, 1979), while in coastal and shelf regions, depending on the rate of nitrification, a significant part of the recycled nitrogen may be released as nitrate + nitrite and not as ammonium (Wollast, 1993). Therefore, *f*-ratio expressions may vary according to each situation or context (Harrison *et al.*, 1987; Knauer, 1993).

There are at least four general methods of measuring new production (Eppley, 1989; Knauer, 1993): (a) sediment traps at the bottom of the photic zone, (b) incubation experiments for assessing nitrate and carbon dioxide assimilation rates, (c) nutrient, oxygen, carbon dioxide and tracer gas distributions in the context of circulation models, and (d) the disequilibrium ratio of dissolved $^{234}\text{Thorium}/^{238}\text{Uranium}$. Besides incubation measurements, the increasing number of literature concerning the ^{15}N methodology, updated in a review by Harrison (1983), gives evidence on the present interest of stable isotope techniques. On the other hand, the use of radioactive phosphorus (^{32}P) on natural marine samples has also shown to provide easy measurements of the regenerated production by isotopic dilution techniques (Sorokin, 1985; Veldhuis *et al.*, 1991). Unlike nitrogen studies, use of radioactive phosphorus (carrier-free) may be less subject to methodological problems related to the addition of large amounts of stable isotopes and the analytical difficulties in measuring low ambient concentrations of substrate such as ammonia. Furthermore, since there is a close relationship between nitrogen and phosphorus in the production of organic matter (Codispoti, 1989), combined studies of both nitrogen and phosphorus assimilation rates may lead to the understanding of the role of these nutrients in the regulation of the carbon cycle.

In the present paper, short-time measurements of ^{15}N , ^{32}P and ^{14}C uptake rates by phytoplankton are used to illustrate the concepts of new and regenerated production in the Gulf of Biscay. The area, investigated during September 89, July 90 and June 91 in the framework of the Belgian Impulse Programme Global Change, allows the sampling in shelf, slope and deep basin regions and, therefore, presents a potential for the evaluation of exchanges at the ocean

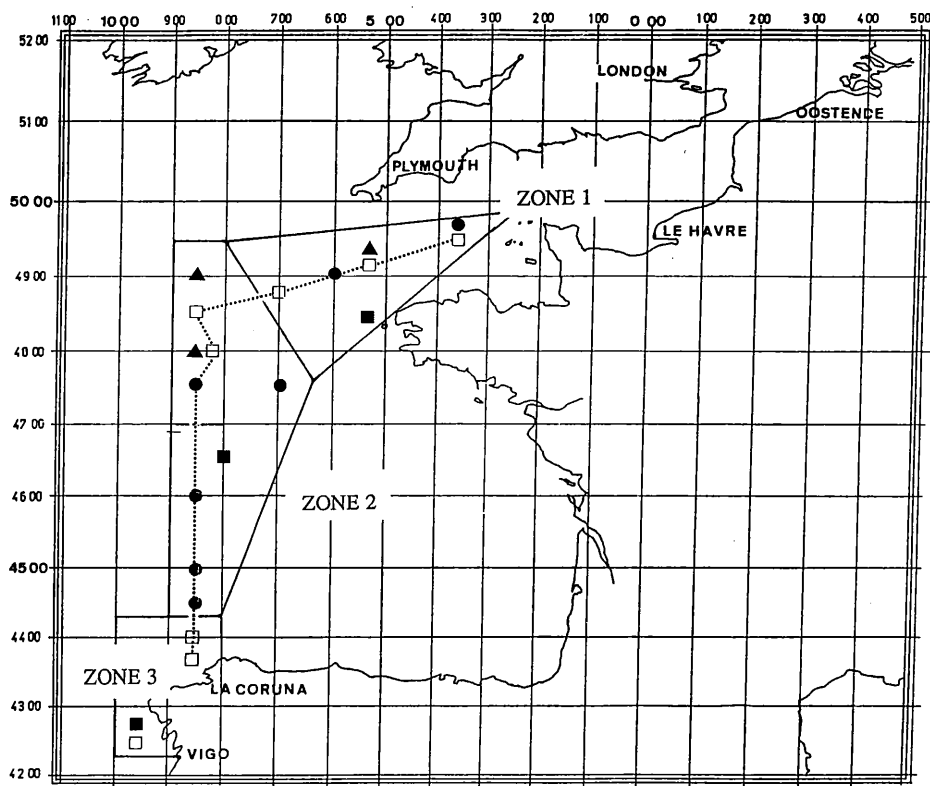


Fig. 1.— Cruise track (□) and location of the sampling stations during September 89, July 90 and June 91: (●) ^{14}C , (▲) ^{15}N , ^{14}C and (■) ^{32}P , ^{15}N , ^{14}C .

margins (figure 1). In the first section, a comparison of the nitrogen (nitrate and ammonium) and carbon uptake regimes in different functional subunits of the Gulf of Biscay, based on chlorophyll *a* and nutrient distribution patterns, is presented. The second section is mainly devoted to the problematic aspect of the measurements of phosphorus incorporation.

2.— Methods.

2.1.— C, N, P assimilation experiments.

For the carbon and phosphorus assimilation rates, samples were incubated in 600 ml flasks, spiked respectively with 0.6 (^{14}C) or 3.3 (^{32}P) Mbq. After incubation, samples were filtered using GF/F glass-fibre filters and the particulates were analyzed for ^{14}C or ^{32}P by liquid scintillation. The incubations for the nitrogen assimilation rates were started immediately after the addition of ^{15}N labelled nitrate or ammonium (99% ^{15}N) to samples in 2.7 l polycarbonate bottles. Spike solutions increased the ambient concentrations by about 10%. The particulate material was collected using Whatman GF/F glass fiber filters and the particulate nitrogen was subsequently converted to N_2 by a modified Dumas method according to Goeyens *et al.* (1985). The $^{14}\text{N}/^{15}\text{N}$ ratio was measured by emission spectrometry.

2.2.— Nutrient analyses.

The analysis of nutrients was carried out immediately on board after sampling. Ammonium was determined according to the manual method of Koroleff (1969) with a detection limit of $\pm 0.05 \mu\text{M}$. Nitrate, nitrite and phosphate were measured using the automated method described by Elskens and Elskens (1989) with detection limits of $\pm 0.1 \mu\text{M}$ for NO_3 and PO_4 .

2.3.— Calculation of productivity, nutrient stock concentrations, f -ratios and relative preference index.

A simple model, considering the evolution of light intensity, nutrient concentrations and the depth of the mixed layer was used to estimate the primary production measured by the ^{14}C and ^{15}N isotopic methods, in terms of $\text{mg}(\text{C or N}) \text{m}^{-2} \text{d}^{-1}$. Mean values for the global solar irradiance and the extinction coefficient were obtained from quantametric profiles performed during the different cruises according to Parsons *et al.* (1984). The influence of nutrients was taken into account by carrying out incubation experiments at at least two different depths (-10 and -40 m). Assimilation rates of nitrogen and carbon were corrected with respect to the mean value of the light intensity at these depths using field calibration curves of productivity *versus* light intensity. Values of primary production, chlorophyll a , and nutrient concentrations were finally integrated over the thickness of the mixed layer, whose depth was determined from the density data.

Two different expressions of the f -ratio have been used throughout this study. The first one is based upon results obtained from both $^{15}\text{NO}_3$ and ^{14}C incubation experiments according to the definition of Eppeley (1989). It assumes

Table 1

Primary production in the Gulf of Biscay. ρ represent the absolute uptake rate in nM h^{-1}

Stations	Primary production		<i>f</i> -ratios		$\text{RPI}_{(\text{NH}_4)}$	$\text{RPI}_{(\text{NO}_3)}$
	$\text{mg C m}^2 \text{ d}^{-1}$	$\text{mg N m}^2 \text{ d}^{-1}$	$\frac{\rho_{\text{NO}_3} * 6.6}{\rho_{^{14}\text{C}}} \text{ (1)}$	$\frac{\rho_{\text{NO}_3}}{\rho_{\text{NO}_3} + \rho_{\text{NH}_4}} \text{ (2)}$	$\frac{\rho_{\text{NH}_4} / (\rho_{\text{NO}_3} + \rho_{\text{NH}_4})}{\text{NH}_4 / \Sigma \text{N}_{\text{inorg.}}} \text{ (3)}$	$\frac{\rho_{\text{NO}_3} / (\rho_{\text{NO}_3} + \rho_{\text{NH}_4})}{\text{NO}_3 / \Sigma \text{N}_{\text{inorg.}}} \text{ (4)}$
Station 1	500 – 900 816 ± 117	95 – 187 140 ± 70	0.56	0.78 – 0.82 0.80	1.5 – 2.3 1.9	0.9 – 1.0 0.95
Station 2	47 – 220 123 ± 54	17 – 135 76 ± 58	0.12 – 0.95 0.46	0.12 – 0.95 0.48	1.0 – 7.8 3.5	0.8 – 1.4 1.0
Station 3	2100	744	> 1	0.93	0.9	0.9

a constant Redfield ratio of 6.6 by atoms for the C/N uptake rates (Eqn. 1, Table 1). The second one, defined as the ratio of nitrate to the total inorganic nitrogen transport rates (Eqn. 2, Table 1), provides a better insight regarding the nitrogen uptake regime (Eppley and Peterson, 1979). As will be discussed later, the comparison of both f -ratio values allow us to derive an estimate of the recycled production supplied by the dissolved organic nitrogen which is not measured in this study. f -ratios inform on the relative importance of the nitrogen source for the phytoplankton nutrition, the preference of the phytoplankton for one nutrient or another is indicated by the relative preference index RPI (McCarthy *et al.*, 1977). This index is defined as the ratio of the f value for the particular nutrient to its concentration fraction (Eqns 3 and 4, Table 1). A RPI value greater than 1 indicates preference, smaller than 1 rejection, and equal to 1 reflects that utilization of the nutrient is equitable with its availability.

2.4.– Nitrate depletions.

Summer stratification in the upper layer is usually characterized by seasonally warmed and high salinity surface waters with low amounts of nutrients. The integrated differences, over the thickness of the mixed layer, between the winter nitrate level and the *in situ* observed concentrations are defined as depletions. The term depletion signifies in this context the amount of nitrate removed from the water column during the ongoing growth season and leads to an estimate of the seasonally integrated new production. The winter reference levels of nitrate in the surface waters were taken from Morin *et al.* (1991). It should be stated that this winter value is usually in good agreement with the *in situ* value measured at the base of the photic zone.

3.– Carbon and nitrogen assimilation.

During September 1989, vertical distributions of salinity and dissolved inorganic nitrogen from a north to south transect (September 1989) along 8°30' W demonstrated the existence of a central high salinity lens with significantly decreased surface nitrate and ammonium concentrations, which extended approximately from 48° N to 45° N (figure 2). The potential temperature data shows that the northern border agrees with the summer thermal front of Ushant (Pingree *et al.*, 1975) and follows almost the outline of the haline fronts identified by Morin *et al.* (1991). The origin of these haline fronts resides mainly in the outflow, towards the English Channel, of the river Loire on the South Brittany shelf. In the winter, a conservative mixing is observed between the offshore waters with low nutrient concentrations and the coastal waters enriched by the river inputs (Morin *et al.*, 1991). To the south, the high salinity and low nitrogen surface

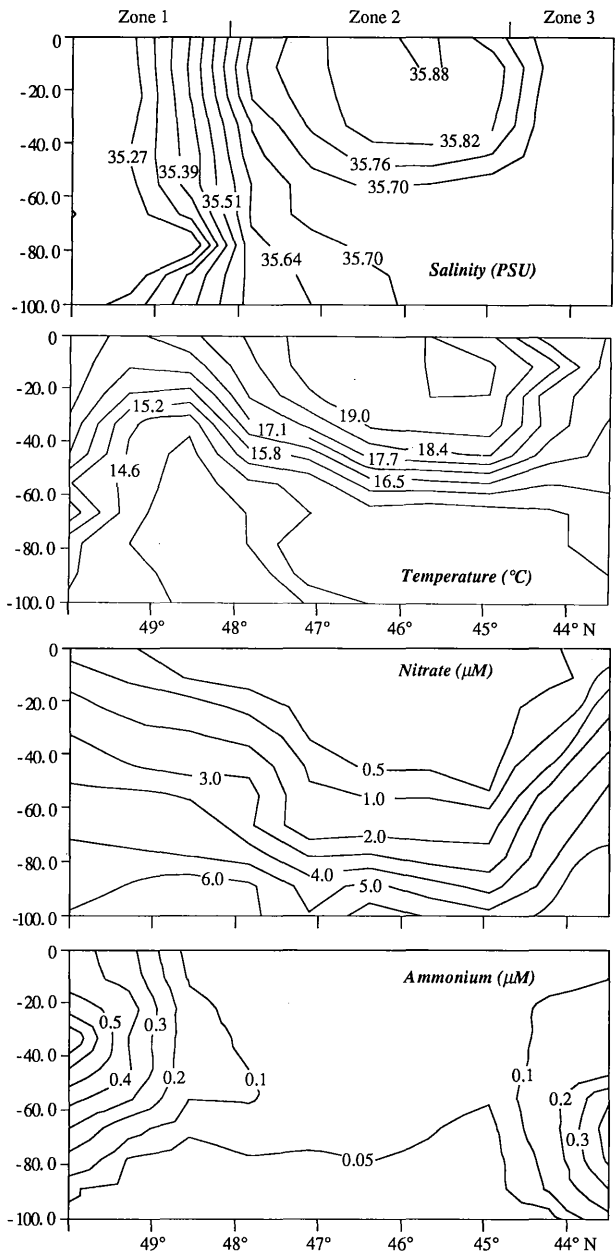


Fig. 2.— Vertical distributions of salinity (psu), potential temperature ($^{\circ}\text{C}$), nitrate (μM) and ammonium (μM) along a north to south transect $8^{\circ}30' \text{W}$ (Global Change Cruise September 1989). The cruise track is illustrated in figure 1.

water lens is confined by intense upwelling processes occurring in the vicinity of the Northern Spanish coast.

During July 1990 and June 1991, similar spatial variabilities were pointed out for the distribution of nutrients, salinity and temperature. Therefore, the Gulf of Biscay was divided into three different functional subunits according to the scheme of figure 1.

Zone 1 represents stations located at the Channel entrance on both sides of the Ushant front. In the summer, the vertical distribution of chlorophyll *a* shows a broader maximum with stock concentrations usually exceeding 60 mg m^{-2} . Primary production measurements average $816 \pm 177 \text{ mg C m}^{-2} \text{ d}^{-1}$ and $140 \pm 70 \text{ mg N m}^{-2} \text{ d}^{-1}$, that classify zone 1 among eutrophic ecosystems (Table 1). The maximum value remains lower than that observed in the Bay of Brest ($1200 \text{ mg C m}^{-2} \text{ d}^{-1}$, Quéguinier and Tréguer, 1986), but is close to the estimated yearly average production for continental shelves ($800 \text{ mg C m}^{-2} \text{ d}^{-1}$, Wollast, 1991). In the summer, nitrate was the main source of nitrogen production, although the relative preference index (RPI) showed that ammonium is apparently the preferred nutrient for phytoplankton. It should be noted that our *f*-ratios for the uptake of inorganic nitrogen (0.78–0.82, Eqn. 2, Table 1) are high in comparison with those reported for coastal waters (0.30–0.46) by Eppeley and Peterson (1979). On the other hand, they are in good agreement with those (0.70–0.80) measured in the Bay of Brest during the spring bloom (Dauchez *et al.*, 1991). Such high values can be related to relatively high inputs of new nitrogen (nitrate) in zone 1. However, one cannot exclude the possibility that dissolved organic nitrogen (DON) represents a significant fraction of the total nitrogen assimilation. It has been reported that urea uptake accounts on an annual basis for about 25% of the total nitrogen utilization in Californian coastal waters (McCarthy *et al.*, 1977) and supplies approximately 27% of the nitrogen requirement for the surface water community in the Southern Ocean during autumn (Probyn and Painting, 1985). Therefore, if urea uptake occurs in similar proportion in the Channel entrance area, our *f*-ratio would be lowered to ± 0.6 . This value is close to the mean annual value of ± 0.5 documented for the coastal regions and upwelling areas (Paasche, 1988) and even closer to the *f*-ratio of 0.58 calculated from the nitrogen and carbon assimilation experiments (Eqn. 1, Table 1). From these results and the comparison of both *f*-ratio values, it is suggested that about 58, 20 and 22% of the nitrogen production are supplied by nitrate, ammonium and DON, respectively (see also figure 3).

The inorganic nitrogen stock concentrations in the mixed layer remain in the summer close to $2.6 \pm 0.7 \text{ g N m}^{-2}$, so that any limitation of the phytoplankton production by this nutrient can probably be ruled out in this zone. For July 1990 and September 1989, the calculated nitrate depletions range from 2.3 to 3.9 mg N m^{-2} . Assuming that the growth season begins in March and neglecting

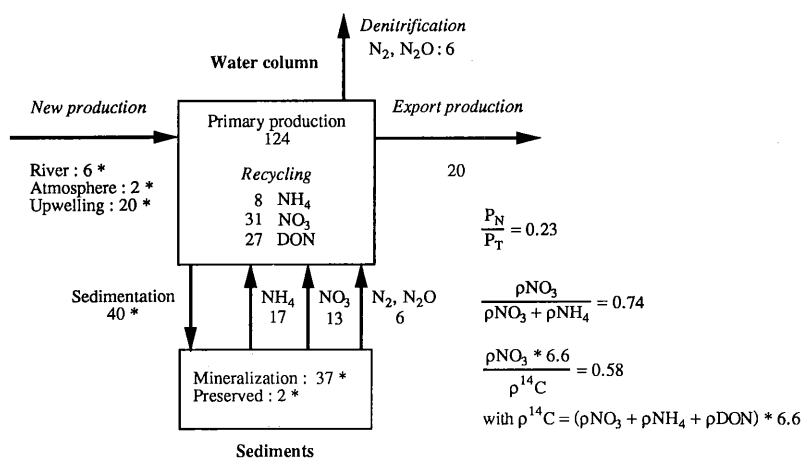


Fig. 3.— Tentative N-budget for zone 1. Fluxes are given in $\text{mg N m}^{-2}\text{d}^{-1}$. The incoming fluxes (*) at the boundaries of the system are taken from Wollast (1993).

effects such as nitrification and turbulent diffusion through the mixed layer, a daily nitrate deficit of $21 \pm 5 \text{ mg N m}^{-2} \text{d}^{-1}$ was calculated for the different sampling periods. On the basis of a Redfield ratio of 6.6 by atoms, the corresponding new production rate of $118 \text{ mg C m}^{-2} \text{d}^{-1}$ represents less than 15% of the instantaneous primary production measurements in zone 1 and, as a consequence, is significantly lower than the value predicted by the f -ratio of 0.58. This suggests that primary production in the Channel entrance has to be sustained by continuous inputs of new or recycled nitrate at the boundaries of the system. Considering the average yearly fluxes of nitrogen in the coastal zone calculated by Wollast (1993) from the continental, benthic, atmospheric and oceanic sources and combining these data to the measurements of primary production in zone 1, a tentative N-budget was established. According to the fluxes presented in figure 3, new production would account for about 25% of the total primary production, the remaining 75% being supported by recycling processes. Approximately 50% would be supplied by recycled nitrogen in the water column and 25% by the sediments. In the latter case, since most of the remineralization occurs close to the water-sediment interface and as the nutrients released are rapidly available for photosynthesis, it seems reasonable to incorporate these fluxes, for both nitrate and ammonium, in the evaluation of the regenerated production and not as an external source of nutrients (Jickells, 1991). The nitrogen speciation was calculated to fit the experimental values for both expressions of the f -ratios (figure 3). The recycled amounts of nitrate and ammonium in the water column were then estimated by subtraction knowing the incoming fluxes at the boundaries of the system (Wollast, 1993). It is interesting to note that the value obtained for nitrate, using this approach, is consistent

with the mean annual rate of nitrification of $12 \text{ g N m}^{-2} \text{ y}^{-1}$ given for the coastal zone by Henriksen and Kemp (1988). Moreover, the exported production flux, required to maintain the system at steady state, is almost equal to the rate of new production. A distinctive property of this cycle, as compared to the open ocean, is the intensive recycling of nitrogen derived from the sediments. In this study a daily flux of $30 \text{ mg N m}^{-2} \text{ d}^{-1}$ was used according to the value selected by Wollast (1993). It should be stressed that this flux may be overestimated in regions where the water column is seasonally stratified. Since most of the stations in zone 1 appear to be in regions where summer stratification occurs, exchanges between the superficial and bottom waters could be reduced because of the presence of the thermocline. Nevertheless, to balance our N-budget in zone 1, as the benthic flux decreases, primary production has essentially to be sustained by larger inputs of new nitrogen at the boundaries of the system. Under extreme conditions, assuming a benthic flux equal to zero and keeping the remineralization rate in the water column at $66 \text{ mg N m}^{-2} \text{ d}^{-1}$, new production would then represent $58 \text{ mg N m}^{-2} \text{ d}^{-1}$, *i.e.* practically 46% of the total production. Since the total flux of nitrate in the system is $72 \text{ mg N m}^{-2} \text{ d}^{-1}$ ($P_T \times 0.58$, figure 3), the amount of nitrate recycled in the water column by nitrification is $14 \text{ mg N m}^{-2} \text{ d}^{-1}$. Although this N-budget is rather speculative, it illustrates the complexity of the nitrogen cycle in the coastal zones. It suggests, furthermore, that with a benthic flux varying seasonally between 0 and $30 \text{ mg N m}^{-2} \text{ d}^{-1}$, new production would represent 46 to 23% of the total primary production in zone 1. The most important conclusion is certainly that in both situations, the regenerated production is underestimated by use of classical expressions of the *f*-ratio (Eqns 1 and 2, Table 1) and that the importance of the discrepancy increases depending on the nitrification rate.

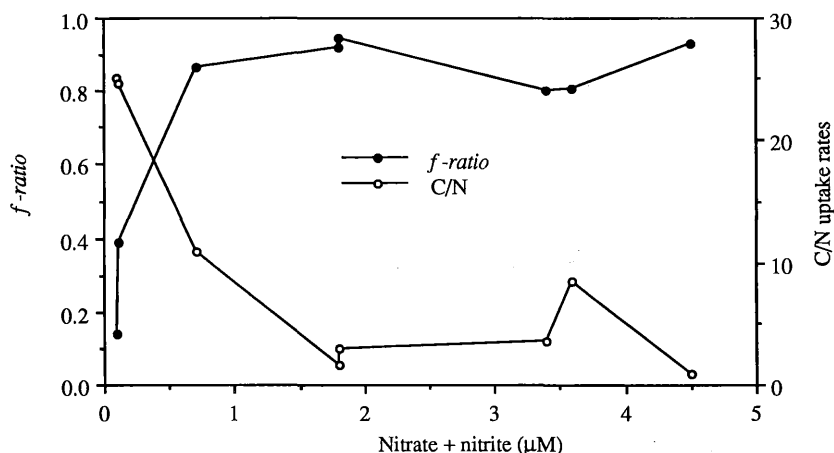


Fig. 4.— Evolution of the *f*-ratio (Eq. 2) and the C/N uptake rates *versus* nitrate concentrations for each incubation depth in zone 2. Combined data from July 1990 and June 1991.

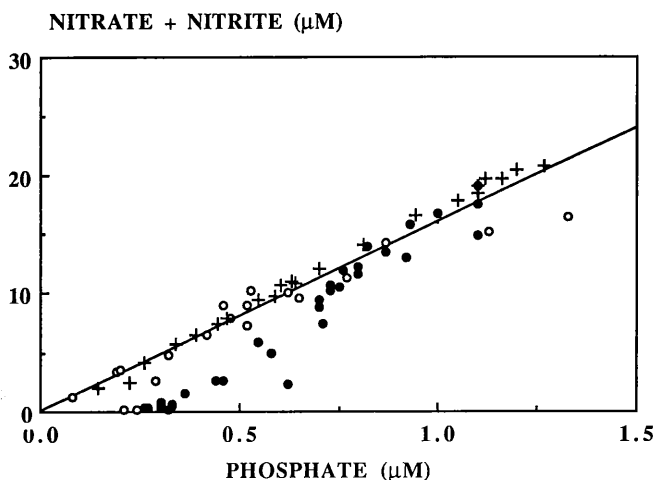


Fig. 5.— Evolution of nitrate + nitrite *versus* phosphate concentrations in zone 2: (●) September 89, (○) July 90, (+) October 92 and (—) Redfield ratio.

Zone 2 groups stations located in the vicinity of the margin on the shelf, slope and deep basin region. In the summer, it appears as a typical oligotrophic system with an average production of $123 \pm 54 \text{ mg C m}^{-2} \text{ d}^{-1}$ (Table 1). At these stations, extremes in concentrations and gradients occur within shallow subsurface depth intervals, located between 30 and 70 m (figure 2). Chlorophyll *a* and O_2 maxima are overlapping in the 60 to 65 m intervals, located just above the thermocline, in the nutricline. Stock concentrations of chlorophyll *a* average at $20 \pm 8 \text{ mg m}^{-2}$. Considerable fluctuations were observed for the nitrogen assimilation rates (17 to $135 \text{ mg N m}^{-2} \text{ d}^{-1}$) and the nitrogen uptake regime (*f*-ratios ranging from 0.1 to 0.9). Both of them were strongly influenced by the nutrient dynamics of the environment. The evolution of the *f*-ratio *versus* nitrate concentration shows clearly a system shift from new to regenerated production when the concentration of nitrate falls below $1 \mu\text{M}$ (figure 4). One should stress that the half-saturation constant for nitrate assimilation, is usually close to $1 \mu\text{M}$ (Collos and Slawyk, 1980). In September 1989, surface waters (above 100 m) typically showed a nitrogen deficit relative to the values predicted by the Redfield ratio N/P (16/1 by atoms) which applies for depths below 100 m (figure 5). Within the photic zone, extreme nitrogen to phosphate ratios can occur when either available P or N is exhausted, or is close to exhaustion. The tendency for a general low photic N/P ratio in most of the oceanic surface layers has been reported (Codispoti, 1989). Under N-limiting conditions, higher specific uptake rates of ammonium are found, but the absolute transport rates of total nitrogen decrease drastically. In these conditions, the C/N assimilation ratios reach a maximum of 20–25. Such high values are to be expected in nitrogen-limited environments

(Carpenter and Dunham, 1985) and have been reported in the Bay of Brest at the end of the spring bloom when the ambient concentration of nitrate fell below $1.6 \mu\text{M}$ (Dauchez *et al.*, 1991). When nitrogenous nutrients are non-limiting, N-production essentially originates from new production and the C/N uptake ratios approach values close to the C/N composition of the particulate organic matter (figure 4). No significant differences are detected between the two expressions of the f -ratio (Table 1) suggesting that the contribution of DON is negligible. This requires, however, further investigation. The nitrogen budget calculation within zone 2 is much more difficult to establish because little information is available. Nevertheless, the results presented here suggest that, during spring, the ecosystem evolves from a first phase where new production predominates into a second one dominated by regenerated production. The relationship between productivities (in $\text{mg C m}^{-2} \text{ d}^{-1}$), biomasses (Chl. *a* in mg m^{-2}) and nutrient stock concentrations (NO_3 and NH_4 in mg N m^{-2}) for the different sampling periods is illustrated in figure 6. On an average basis, the highest productivity and biomass are observed in July 1990 with a system running on new production (f -ratios > 0.5). June 1991 is characterized by a system shift from new to regenerated production (f -ratios ≤ 0.5) and by the highest accumulation of ammonium, an indication of intensive heterotrophic activity. During these productive periods, the nitrate uptake rate amounts on average to $50 \pm 20 \text{ mg N m}^{-2} \text{ d}^{-1}$ and the nitrate depletions, calculated as previously mentioned, range from 1.3 to 3.7 g N m^{-2} (average of 2.7 ± 0.9). Assuming that the nitrate uptake rate remains constant during this time, the length of the new production period is estimated to about 60 days from the nitrate depletions to the uptake rate ratio. Since nitrate is almost totally exhausted in the surface water (0–20 m) at the end of the spring time, it can be assumed that the initiation of the phytoplankton bloom, in zone 2, would start in mid-April. As will be discussed later, this is consistent with the model of Morin *et al.* (1991) for the prediction of the growth season development on the Armorican shelf. During September 1989, the low biomass and productivity were paralleled with low inorganic nitrogen stocks (figure 6), but the decline in primary production has also to be related to the day length and light.

Zone 3 groups stations located in the vicinity of the Northern coastal area of Spain (figure 1). As already stated, this area is seasonally influenced by intense upwelling processes occurring along the Spanish and Portuguese Atlantic coast. Regarding the T, S diagram for near-shore stations (Vigo), sampled in July 1990, the water column can be divided into three different layers: (1) the photic zone (0–80 m) where the variation of the salinity gradient is possibly due to fresh water inputs from the rias Vigo and Arosa, (2) an intermediate layer (80–400 m) where temperature and salinity are closely related and vary more or less linearly with depth, and (3) a deep layer (400–800 m) characterized by an inversion of

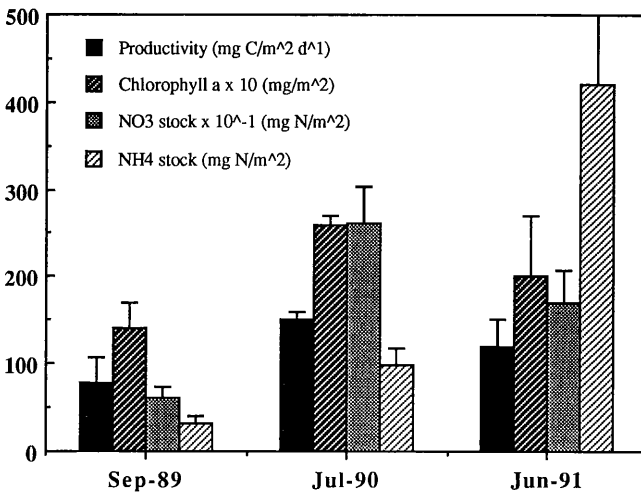


Fig. 6.— Mean values of productivity, biomass and nitrogen stock concentrations for the different sampling periods in zone 2.

the salinity and thermic gradients. At 800 m, salinity and temperature amount to 36‰ and 11.44°C respectively (figure 7a). The origin of this water mass probably resides from the outflow of Mediterranean waters through the Gibraltar Strait. Similar conclusions can be drawn from a plot of nutrients *versus* salinity. It should be stressed, however, that in July 1990, neither the thermocline, nor the nutricline were marked. A conservative behaviour of nutrients with temperature is found between 0 and 400 m (figure 7b). The N/P ratio remains almost constant on the whole profile of the water column and the slope of 16.8 ± 1 is in agreement with data reported in the literature (figure 7c). Due to the upwelling processes, stock concentrations of nitrate in the surface water in July 1990 are extremely high, ranging from 2.9 to 4.5 mg N m⁻². They support considerable biomass (136 mg Chl. *a* m⁻²) and productivity (2100 mg C m⁻² d⁻¹). The *f*-ratio for the uptake of inorganic nitrogen amounts to 0.9 indicating a major importance of the nitrate assimilation (Table 1). However, its value calculated from the nitrogen and carbon assimilation experiments is greater than 1, because of a C/N uptake ratio of 3.1. This situation is not exceptional and has also been encountered in zone 2, when the nitrogen stock concentration was non-limiting (see Table 2). This suggests an active uptake of nitrogen by the heterotrophic community. The relative preference index (RPI) shows, furthermore, that both ammonium and nitrate are in fair equilibrium with their respective availabilities (Table 1).

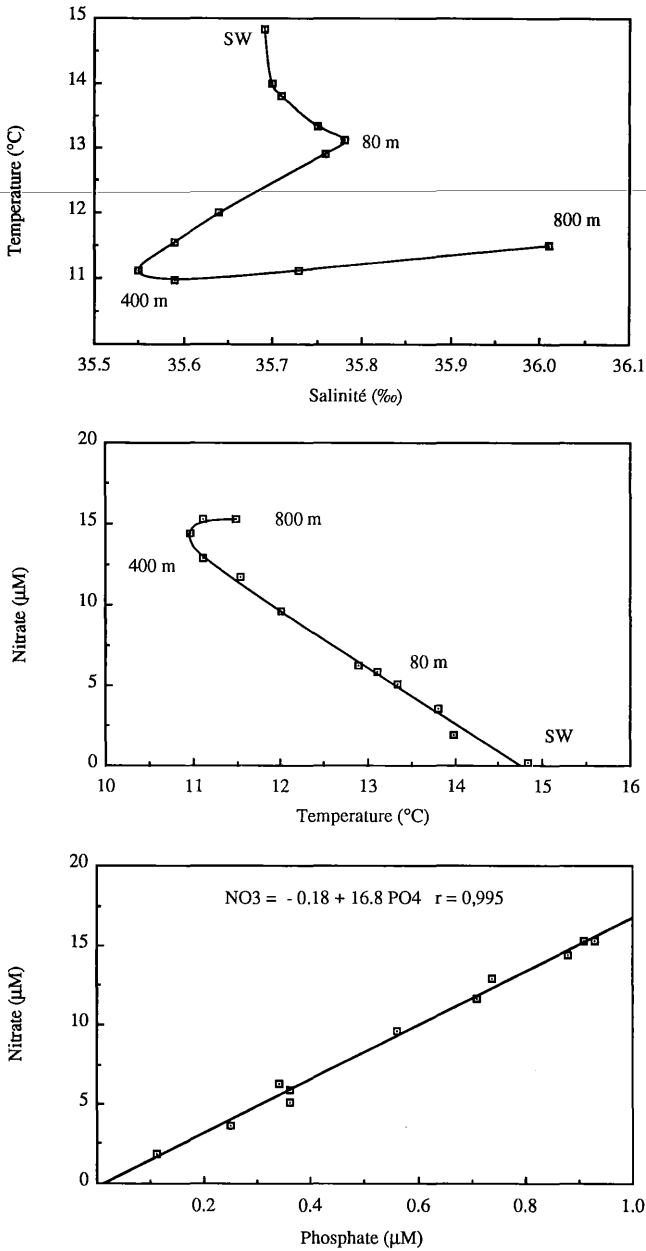


Fig. 7. – Hydrologic structure of the water column at a near-shore station (July 1990) in the upwelling region of the Northern coastal area of Spain: (A) T,S diagram, (B) and (C) variation of nitrate with temperature and phosphate.

Table 2
C/N/P uptake rates in the Gulf of Biscay during July 90

	Depth (m)	Chl. <i>a</i> ($\mu\text{g l}^{-1}$)	^{14}C uptake ($\text{nmole l}^{-1}\text{h}^{-1}$)	^{15}N uptake ($\text{nmole l}^{-1}\text{h}^{-1}$)	^{32}P uptake ($\text{nmole l}^{-1}\text{h}^{-1}$)	C/N	C/P	N/P
one 1	-10	2.2	393	36	1.7	10.9	231	21
3°25 N - 05°21 W	-40	1.3	236	44	0.63	5.4	374	70
one 2	-10	0.13	38	29	1.4	1.3	27	21
5°25 N - 08°00 W	-40	0.42	92	24	2.2	3.8	42	11
one 3	-10	5	587	190	3.4	3.1	172	56
2°43 N - 09°18 W								

4.- Phosphorus assimilation.

During July 1990, water samples collected in the offshore area (zone 2) were incubated under various conditions (figure 1). The uptake of ^{32}P with time was followed under artificial light, dark and in the presence of sodium azide. Figure 8 shows that the cumulative uptake of ^{32}P under constant light conditions increases more or less linearly with time. Furthermore, the rate of uptake after 30 hours reaches $\pm 40\%$ which is extremely high, suggesting that this particular nutrient must be regenerated fairly rapidly in order to sustain the high rate of incorporation. Another interesting observation is that the uptake of phosphorus occurs also under dark conditions at a relatively high rate, although the pathway of this transfer is not yet clear. The azide sample indicates that there is a small amount of adsorption taking place. The high rate of uptake under dark conditions indicates that phytoplankton is able to make use of phosphorus during the night. Field measurements have shown that phytoplankton continues to synthesize protein during the night at the expense of intracellular low molecular weight compounds, polysaccharides and lipids produced during the day (Morris *et al.*, 1981; Cuhel *et al.*, 1984). It is thus possible that phytoplankton may utilize phosphate to produce ATP and DNA in the absence of light. Alternatively, the high uptake of phosphate can also be attributed to bacterial activity.

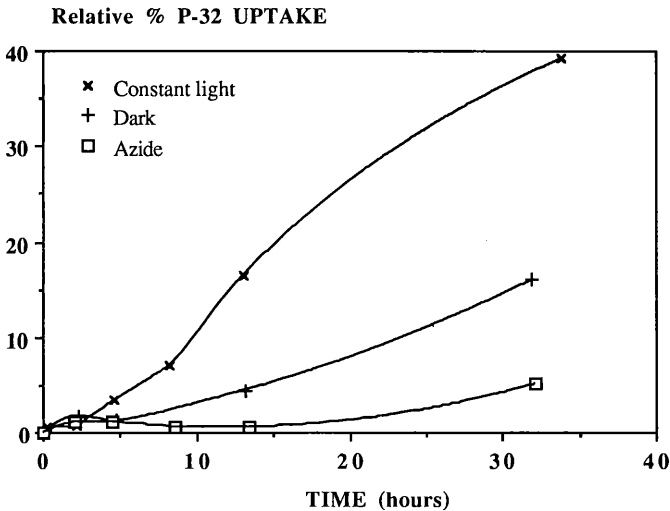


Fig. 8.- Relative uptake of ^{32}P under artificial light, dark and in the presence of sodium azide

During June 1991, the influence of the bacterial activity on the uptake of phosphorus has been investigated. The method involves the use of antibiotics such as Penicillin-G and Streptomycin sulfate. Penicillin is known to inhibit

synthesis of bacterial cell wall and Streptomycin inhibits 30S ribosome function (Stanier *et al.*, 1976). Two series of samples were incubated under constant artificial light conditions during 24 hours with various amount of ^{32}P added. One series was performed in the presence of antibiotics to inhibit the bacterial activity. The effect of antibiotic is demonstrated in figure 9, where the radioactivity in the solid phase is plotted against that in the dissolved phase. It is obvious that the addition of antibiotics lowered the percentage of ^{32}P incorporation by about 7%. Parallel experiments were also conducted in the presence of sodium azide. The results show that the uptake due to non-biological action never exceeds 2%.

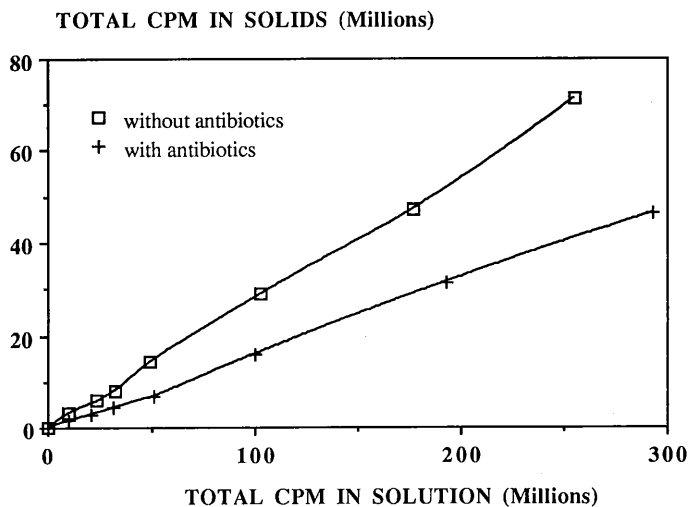


Fig. 9. – Comparison of ^{32}P under artificial light conditions in samples with and without antibiotics

Knowing the phosphate concentration of the sample, the absolute rate of phosphorus uptake has been calculated (Table 2). It is noteworthy that marine phytoplankton has a C/P ratio of about 106/1 and a N/P ratio of about 16/1. The results obtained in this study indicate that C/P uptake rates varies from 42 to 374 and N/P from 11 to 70. However, we are not able at present to evaluate quantitatively the role of bacteria in the uptake and regeneration of phosphorus. It is obvious that in the future, we have to determine the rates of transfer of phosphorus through various biological pathways.

5.— Conclusions.

Because of its geographical extension and the diversity of its hydrologic structure, the Gulf of Biscay is an important area for the study of exchange processes at the ocean margins. Although there is a gradual decrease of primary production along a transect crossing the shelf edge from shallow to deep basin regions, spatial variation of primary production are best related to the outlines of the summer thermal front (Ushant front) which follows almost the haline fronts pointed out by Morin *et al.* (1991). Despite a difference of about two months between the sampling periods, it is interesting to note the similarities regarding the nitrogen and carbon assimilation rates, the fluctuations of the C/N uptake ratios and the f -ratio values observed in this study and those reported for the Bay of Brest by Dauchez *et al.* (1991). The apparent time-scale difference in the growth season maturity may be related to the establishment of a haline or thermal stratification which has been demonstrated to be important for the initiation of the phytoplankton development. Supporting this view, Morin *et al.* (1991) have shown that the nutrient assimilation and phytoplankton development take place sequentially on the Armorican shelf and that a time-lag of nearly three months may exist between the initiation of the bloom in South Brittany and in the central part of the continental shelf.

To summarize, the global trend of the studied ecosystem has shown the major importance of nitrate assimilation, a property which is in agreement with the observed high nitrate concentrations and the corresponding low ammonium availabilities. Nevertheless, on the shelf edge, the available nitrate stock was often depleted in the summer and, subsequently, primary production was fueled with recycled nitrogen, mainly ammonium. The C/N/P uptake ratios exhibit great spatial variability that can reflect variations in the nutrient status of phytoplankton during its growth. Interestingly, we note that the interval of fluctuations (minimum and maximum values) for C/N (1.3–10.9) and C/P (42–374) is of the same order of magnitude. This can be ascribed that to the fact that the uptake rates of nitrogen and phosphorus occur through various biological pathways including the auto- and heterotrophic communities. Large variations in C/P (47–115) have been reported previously for the Weddel-Scotia Seas by Tréguer *et al.* (1991). On the other hand the deviations of the N/P ratios from the Redfield one might suggest a temporary imbalance in the regeneration rate of both nutrients. Our data suggest that mineralization of phosphate might be higher than nitrogen as indicated by the general tendency for a low photic N/P ratio observed in the Gulf of Biscay. It is obvious that in the future, we have to determined the regeneration rates of both nitrogen and phosphorus through isotopic dilution techniques.

Acknowledgements.

The authors would like to thank J.H. Hecq and C. Lejaer (ULg) for their measurements of chlorophyll *a* during the Global Change cruise of September 89. We are also indebted to A. Pollentier and J. Backers (MUMM) for the acquisition and treatment of the basic hydrographic data. This work was supported by the Belgian State—Prime Minister's Service—Science Policy Office in the frame work of the Impulse Programme "Global Change" Contracts no. GC/11/009 to ULB, GC/03/010 to VUB and GC/12/011 to ULg.

References.

- CARPENTER, E.J. and DUNHAM, S. (1985). Nitrogenous nutrient uptake, primary production, and species composition of phytoplankton in the Carmans river estuary, Long Island, New York, *Limnol. Oceanogr.*, 30:513–526.
- CODISPOTI, L.A. (1989). *Phosphorus vs. nitrogen limitation of new and export production*, in: W.H. Berger, V.S. Smetacek, G. Wefer (Editors), *Productivity of the ocean: present and past*, J. Wiley & Sons, Chichester, pp. 377–394.
- COLLOS, Y. and SLAWYK, G. (1980). *Nitrogen uptake and assimilation by phytoplankton*, in: P.G. Falkowski (Editor), *Primary Productivity in the Sea*, *Environ. Sci. Res.*, 19:159–211.
- CUHEL, R.L., ORTNER, P.B. and LEAN, D.R.S. (1984). Night synthesis of protein by algae, *Limnol. Oceanogr.*, 29:731–744.
- DAUCHEZ, S., QUÉGUINIER, B., TRÉGUER, P. and ZEYONS, C. (1991). A comparative study of nitrogen and carbon uptake by phytoplankton in a coastal eutrophic ecosystem (Bay of Brest, France), *Oceanologica Acta*, 14:87–95.
- DUGDALE, R. and GOERING, J.J. (1967). Uptake of new and regenerated forms of nitrogen in primary productivity, *Limnol. Oceanogr.*, 12:196–206.
- ELSKENS, I. and ELSKENS, M. (1989). *Handleiding voor de bepaling van nutriënten in zeewater met een Autoanalyzer II™ systeem*, Vrije Universiteit Brussel, 50 pp.
- EPPLEY, R.W. (1989). *New production: history, methods, problems*, in: W.H. Berger, V.S. Smetacek, G. Wefer (Editors), *Productivity of the ocean: present and past*, J. Wiley & Sons, Chichester, pp. 85–97.
- EPPLEY, R.W. and PETERSON, B.J. (1979). Particulate organic matter flux and planktonic new production in the deep ocean, *Nature*, 282:677–680.
- GOEYENS, L., STICHELBOU, L., POST, E. and BAEYENS, W. (1985). Preparation method for solid samples with low nitrogen content for spectrometric nitrogen-15 analysis, *The Analyst*, 110:135–139.
- GOLDMAN, J.C. (1988). *Spatial and temporal discontinuities of biological processes in pelagic surface waters*, in: B.J. Rothschild (Editor), *Towards a theory on biological-physical interactions in the world ocean*, Kluwer Academic Publishers, NATO ASI Series C, 239:273–296.

- HARRISON, W.G. (1983). *Use of isotopes*, in: E.J. Carpenter and D.G. Capone (Editors), *Nitrogen in the Marine Environment*, Academic Press, New York, pp. 763–807.
- HARRISON, W.G., PLATT, T. and LEWIS, M.R. (1987). *f*-ratio and its relationship to ambient nitrate concentration in coastal waters, *J. Plankt. Res.*, 9:235–248.
- HENRIKSEN, K. and KEMP, W.M. (1988). *Nitrification in estuarine and coastal marine sediments*, in: T.H. Blackburn and J. Sørensen (Editors), *Nitrogen Cycling in Coastal Marine Environments*, J. Wiley & Sons, Chichester, *SCOPE*, 33:207–249.
- JICKELLS, T.D. (1991). *What determines the fate of materials within ocean margins*, in: F.C. Mantoura, J.M. Martin and R. Wollast (Editors), *Ocean Margin Processes in Global Change*, J. Wiley & Sons, Chichester, pp. 211–234.
- KNAUER, G.A. (1993). *Productivity and new production of the oceanic system*, in: R. Wollast, F.T. Mackenzie and L. Chou (Editors), *Interactions of C, N, P and S Biogeochemical Cycles and Global Change*, Springer-Verlag, Berlin, NATO ASI Series I, 4:211–231.
- KOROLEFF, F. (1969). Direct determination of ammonia in natural waters as indophenol blue, *Int. Counc. Explor. Sea*, C.M., 9:19–22.
- MCCARTHY, J.J., TAYLOR, W.R. and TAFT, J.L. (1977). Nitrogenous nutrition of the plankton in the Cheapeake Bay. 1: Nutrient availability and phytoplankton preferences, *Limnol. Oceanogr.*, 22:996–1011.
- MORIN, P., LE CORRE, P., MARTY, Y. and L'HELGUEN, S. (1991). Spring evolution of nutrients and phytoplankton on the Armorican shelf (North-West European shelf), *Oceanologica Acta*, 14:263–280.
- MORRIS, I., SMITH, A.E. and GLOVER, H.E. (1981). Products of photosynthesis in phytoplankton of the Orinocco River and in the Caribbean Sea, *Limnol. Oceanogr.*, 26:1034–1044.
- PAASCHE, E. (1988). *Pelagic primary production in nearshore waters*, in: T.H. Blackburn and J. Sørensen (Editors), *Nitrogen Cycling in Coastal Marine Environments*, J. Wiley & Sons, Chichester, *SCOPE*, 33:33–57.
- PARSONS, T.R., TAKAHASHI, M. and HARGRAVE, B. (1984). *Biological Oceanographic Processes*, Pergamon Press, 330 pp.
- PINGREE, R.D., PUGH, P.R., HOLLIGAN, P.M. and FORSTER, G.R. (1975). Summer phytoplankton blooms and red tides along tidal fronts in the approaches to the English Channel, *Nature*, 258:672–677.
- PROBYN, T.A. and PAINTING, S.J. (1985). Nitrogen uptake by size-fractionated phytoplankton population in Antarctic surface waters, *Limnol. Oceanogr.*, 30:1327–1332.
- QUÉGUINIER, B. and TRÉGUER, P. (1986). *Freshwater outflow effects in a coastal, macrotidal ecosystem as revealed by hydrological, chemical and biological variabilities (Bay of Brest, western Europe)*, in: S. Skreslet (Editor), *The Role of Freshwater Outflow in Coastal Marine Ecosystems*, NATO ASI Series G, 7:129–230.
- SOROKIN, Y.I. (1985). Phosphorus metabolism in planktonic communities of the eastern tropical Pacific Ocean, *Mar. Ecol. Progr. Ser.*, 24:87–97.

- STANIER, R.Y., INGRAHAM, J.L., WHEELIS, M.L. and PAINTER, P.R. (1986). In: *General Microbiology*, Prentice-Hall, Englewood Cliffs, New Jersey, 689 pp.
- TRÉGUER, P., LINDNER, L., VAN BENNEKOM, A.L., LEYNAERT, A., PANOUSE, M. and JACQUES, G. (1991). Production of biogenic silica in the Weddell-Scotia Seas measured with ^{32}Si , *Limnol. Oceanogr.*, 36:1217–1227.
- VELDHUIS, M.J.W., COLIJN, F. and ADMIRAAL, W. (1991). Phosphate utilization in *Phaeocystis Pouchetii* (Haptophyceaea), *Mar. Ecol.*, 12:53–62.
- WOLLAST, R. (1991). *The coastal carbon cycle: fluxes, sources and sinks*, in: F.C. Mantoura, J.M. Martin and R. Wollast (Editors), *Ocean Margin Processes in Global Change*, J. Wiley & Sons, Chichester, pp. 365–382.
- WOLLAST, R. (1993). *Interactions of carbon and nitrogen cycles in the coastal zone*, in: R. Wollast, F.T. Mackenzie and L. Chou (Editors), *Interactions of C, N, P and S Biogeochemical Cycles and Global Change*, Springer-Verlag, Berlin. NATO ASI Series I, 4:195–210.

Seawater $p\text{CO}_2$ Distribution and Air-Sea CO_2 Exchanges on the Atlantic European Shelf

Michel FRANKIGNOULLE¹, Marc ELSKENS²,
Michèle LOIJENS³ and Patrick DAUBY¹

¹ Laboratoire d'Océanologie, University of Liège

² Laboratorium voor Analytische Scheikunde, Vrij Universiteit te Brussel

³ Laboratoire d'Océanographie chimique, Université libre de Bruxelles

Abstract.

Continental shelves and coastal areas are sites of several processes which can drastically influence the surface seawater $p\text{CO}_2$ distribution and result in relatively important air-sea CO_2 fluxes. We present here some data obtained in the English Channel, in the Gulf of Biscay and in the Celtic Sea which illustrate the effect of those coastal processes. It is in particular pointed out that upwelling and riverine input, which generate relatively important primary production, can also be sources of CO_2 to the atmosphere.

1.- Introduction.

Air-sea CO_2 exchange is an important process in the global carbon cycle because it determines the amount of anthropogenic carbon which enters the ocean. The buffering capacity of the ocean with respect to the atmospheric CO_2 excess is in fact a subject of controversy (see Tans *et al.*, 1990; Watson *et al.*, 1991). While oceanic water is most often close to the atmospheric equilibrium, in terms of CO_2 level, and then site of quite low air-sea exchange, it is now often suggested that coastal areas could be sites of relatively important fluxes (Walsh, 1988; Wollast, 1989; Walsh, 1991; Frankignoulle and Gattuso, 1993; Frankignoulle *et al.*, submitted). Indeed, coastal ocean has particular properties (riverine inputs, coastal upwellings, high productivity, ecosystems diversity, ...) which can induce a drastic change in surface water CO_2 level and then generate very high local CO_2 fluxes. In spite of this observation, the coastal ocean is never considered when modelling the oceanic carbon cycle, mainly due to the deficiency of field data.

The CO_2 flux at the air-sea interface is given by

$$(1) \quad F = K\alpha(p\text{CO}_2(\text{Water}) - P\text{CO}_2(\text{Air})) = K\alpha \Delta P\text{CO}_2$$

where K is the gas exchange coefficient (piston velocity), α is the CO_2 solubility coefficient in seawater, $p\text{CO}_2(\text{Water})$ and $P\text{CO}_2(\text{Air})$ are the partial CO_2 pressure in both phases. While the direction of the flux is then given by the sign of the gradient through the interface, its magnitude is function of both the gradient and the exchange coefficient. The latter depends on physical environment, that can be very complex [wind speed, turbulence, bubbles, surface film, ... see Liss (1983)] and the role of which is not yet fully understood. Wind speed is nevertheless recognised as the preponderant parameter controlling the gas exchange coefficient value (Liss and Merlivat, 1986; Wannikhof, 1992). Because the CO_2 level in the low atmosphere is quite homogeneous throughout the world, the partial CO_2 pressure in surface seawater is a key parameter which determines the direction of the air-sea CO_2 flux.

In this paper, we briefly review the effect that biological activity could induce on seawater $p\text{CO}_2$ distribution, we discuss some $p\text{CO}_2$ data which have been obtained in the Gulf of Biscay together with chlorophyll and primary production ones and we finally present air-sea CO_2 exchange measurements made in the Celtic Sea.

2.- Material and methods.

$p\text{CO}_2$ is calculated from experimental determination of both pH and total alkalinity (Talk). The later is obtained from classical Gran electrotitration on GF/C filtered samples. Talk calculation is made with corrections for fluoride and sulphate according to Hansson and Jagner (1973). The accuracy has been checked to be 0.05% (1 $\mu\text{eq/kg}$).

pH is measured using an electrochemical cell calibrated to take into account the effect of the ionic strength. The pH sensor, built to minimize and keep constant the junction potential, is calibrated by titrating $\text{NaCl}-\text{Na}_3\text{PO}_4$ solutions and is finally tested against NBS buffers (Frankignoulle and Distèche, 1984; Frankignoulle *et al.*, in preparation). The error on the absolute pH value is estimated to be about 0.006 pH unit.

$p\text{CO}_2$ and the complete speciation is calculated according to the Mole/kg NBS pH scale using the CO_2 acidity constants from Mehrbach *et al.* (1973), the CO_2 solubility coefficient from Weiss (1974), the borate acidity constant from Hansson (1973) and the water dissociation constant from Lyman (1957). The total borate molality is calculated using the Culkin (1973) ratio to salinity. The error on $p\text{CO}_2$ has been established to be less than 8 ppmV.

Chlorophyll *a* concentrations are determined using the spectrophotometric method (Lorenzen and Jeffrey, 1978).

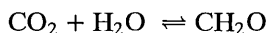
Primary production is determined as explained by Elskens *et al.* (this volume).

$\delta^{13}\text{C}$ on the total suspended matter (collected as explained by Dauby *et al.*, this volume), expressed relative to the PDB standard, is measured by Isotope Ratio Mass Spectrometry after combustion of the sample with the method described by Sofer (1980).

Air-sea CO_2 exchanges are estimated using the bell method, which consist to deploy an air incubator on the sea surface and to detect the initial variation of CO_2 in the air phase (Frankignoulle, 1988).

2.- Seawater $p\text{CO}_2$ distribution versus biological activity.

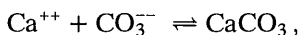
Biological activity can be roughly divided into two main processes, both of which having an important effect on the CO_2 level in surrounding water: the organic carbon metabolism (photosynthesis/respiration) and the inorganic carbon metabolism (calcification/dissolution). The first process can be summarized by



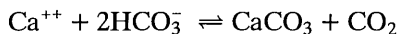
and the production of organic matter results in an uptake of dissolved CO_2 level and a decrease of the partial CO_2 pressure which can be simply calculated using the so-called REVELLE factor

$$\beta = \frac{\delta \ln T\text{CO}_2}{\delta \ln p\text{CO}_2} \simeq 10,$$

(see Sundquist, 1981). The calcification process can be written



or



and the uptake of carbonate ion (first equation) or the release of dissolved CO_2 (second equation) results in an increase of the partial CO_2 pressure in surrounding water. Contrary to organic metabolism, calcification is a process which favours the escape of CO_2 from seawater to the atmosphere (Ware *et al.*, 1992; Frankignoulle and Gattuso, 1993). Ware *et al.* (1992) have estimated, using speciation calculation, that the ratio *released CO_2 / precipitated CO_3^{--}* is about 0.6 and have suggested that coral reefs, which are sites of intensive calcification, could act globally as source of carbon dioxide to the atmosphere. Gattuso *et al.* (submitted) have recently performed air-sea CO_2 measurements on a Polynesian coral atoll and did observe a diel variation of the sign of the flux, with fluxes from air to sea during the day and fluxes from sea to air during the night, and

with a daily budget as a net flux from sea to air. Using buffer factors expressions developed by Frankignoulle (submitted), Frankignoulle *et al.* (submitted¹) have proposed an analytical expression which allows computation of the *released* CO_2 / *precipitated* CO_3^{2-} ratio and have shown that it increases with the dissolved CO_2 level in seawater and that the increasing atmospheric CO_2 level has a positive feedback with marine calcification.

When calcification occurs, it is obviously coupled to organic metabolism and the final impact on partial CO_2 pressure depends on the proportion of both processes. Frankignoulle (submitted) has proposed a REVELLE factor for simultaneous organic and inorganic metabolisms

$$\beta = \frac{\delta \ln p\text{CO}_2}{\delta \ln T\text{CO}_2} = -7.02 + 0.186\% C_{\text{org}},$$

where $\% C_{\text{org}}$ is the percentage of carbon uptake for organic metabolism.

As observed before, when calcification does not occur, primary production results in a decrease of seawater $p\text{CO}_2$. Watson *et al.* (1991) have recently plotted $p\text{CO}_2$ versus chlorophyll data obtained in the North Atlantic during Spring 1989. Depending on the investigated area, they have observed three kinds of linear relationship between both these parameters depending on present and past phytoplanktonic activity: the peak stage (bloom) linear regression is characterized by the fact that $p\text{CO}_2$ nearly intercepts the atmospheric equilibrium value as chlorophyll reaches 0 ($p\text{CO}_2 = 358 - 16.8[\text{Chl}a]$, $r = -0.79$), while the late stage of phytoplanktonic activity linear regression yields a lower intercept for 0 chlorophyll level ($p\text{CO}_2 = 299 - 6.6[\text{Chl}a]$, $r = -0.70$) because CO_2 , which can not be provided from deeper water through the seasonal thermocline, has to invade the surface layer from the atmosphere to recover the equilibrium value, and this is a relatively slow process.

Frankignoulle *et al.* (submitted²) have also determined the surface $p\text{CO}_2$ pattern in the English Channel in June 1992 and have obtained a distribution versus chlorophyll a which agrees well with the relationship proposed by Watson *et al.* (1991) for phytoplanktonic peak stage. On another hand, data they have obtained in the Southern Bight of the North Sea clearly show that riverine input can produce locally very high production but associated to a high $p\text{CO}_2$ level: in the area under the influence of the Scheldt Estuary, while the chlorophyll a concentration is as high as $7.99 \mu\text{g l}^{-1}$, $p\text{CO}_2$ is 407 ppmV, due to the high alkalinity value of Scheldt water. This coastal site thus acts together as an important sink of carbon, via primary production, and as a source of CO_2 to the atmosphere. Riverine input can be studied by the determination of the $\delta^{13}\text{C}$ in the total suspended matter and the figure 1 gives an example of results obtained in the English Channel in June 1991 (see Dauby *et al.*, submitted). In this area, the natural carbon sources are:

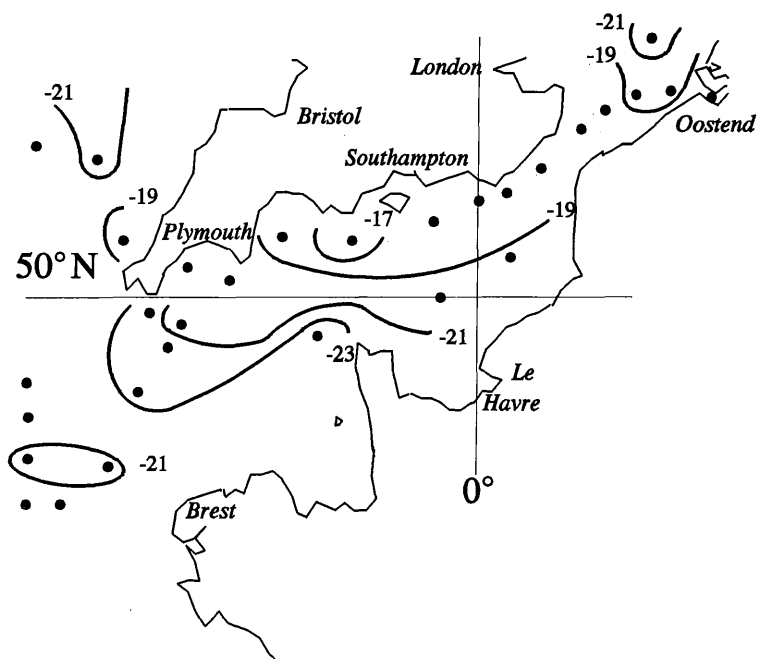


Fig. 1.— Distribution of $\delta^{13}\text{C}$, in ‰, observed in June 1991 in the English Channel.

- 1) phytoplankton, with temperature dependant $\delta^{13}\text{C}$ values [about -23‰ in our conditions (Fontugne and Duplessy, 1981)],
- 2) marine plants, with higher $\delta^{13}\text{C}$, ranging from -10 to -20‰ [seaweeds and seagrasses (Dauby, 1989)],
- 3) terrestrial plant material ($\delta^{13}\text{C} \simeq -27\text{‰}$).

As can be seen on figure 1, maximum $\delta^{13}\text{C}$ values (about -17‰) are observed near Solent River Mouth. This could be explained by an input of carbon originating either from marine macrophytes or from human industrial activities, which are particularly developed in the Southampton area. This “pollution effect” could moreover explain the gap in dissolved oxygen values observed in this area (Frankignoulle *et al.*, submitted²). On both sides of that maximum, $\delta^{13}\text{C}$ in suspended matter progressively decreases to reach values (especially South-westerly) expected for a phytoplankton-based oceanic system. Data measured in the Southern Bight of the North Sea reflect a mixture of planktonic production, anthropogenic and terrigenous inputs.

To illustrate the influence of biological activity and coastal processes on the distribution of surface seawater $p\text{CO}_2$, we present here data which have been obtained during transects along the Gulf of Biscay in 1989 and 1990. Table 1 gives, for 6 stations from the Ushant front to Vigo (Spain), the primary

Table 1

Distribution of surface $p\text{CO}_2$ (in ppmV) along a transect through the Gulf of Biscay, together with surface chlorophyll a contents (in $\mu\text{g l}^{-1}$) and integrated over depth and time primary production (in $\mu\text{g C m}^{-2} \text{d}^{-1}$)

Date	Site	Location	Chl. a	Pr. Prod.	$p\text{CO}_2$
13/9/89	Ushant front	N 490332 W 051230	1.41	884	268
7/7/90	Ushant front	N 485911 W 060138	1.18	900	291
3/7/90	Gulf of Biscay	N 510489 W 011996	0.33	153	338
3/7/90	Gulf of Biscay	N 503026 W 003862	0.13	141	337
15/9/89	Gulf of Biscay	N 471950 W 083130	0.11	47	310
10/7/90	Vigo	N 424095 W 092214	4.91	1431	444

production, the chlorophyll a contents and the partial CO_2 pressure of surface water. Primary production is integrated over time and depth, taking into account the depth of the mixed layer (density), the nutrients concentration (2 incubation depths), the solar radiation profile (quantameter profile, production calibrated *versus* radiation) and a correction factor (production in dark condition) to calculate production over a 24 hours period. Results given in table 1 can be discussed as follows:

- the Ushant front is characterized by a relatively high chlorophyll a concentration and production rate. The associated $p\text{CO}_2$ values are quite far from atmospheric equilibrium (presently about 355 ppmV) as a consequence of dissolved CO_2 use for organic metabolism. This frontal area then acts as sink for atmospheric CO_2 .
- the Gulf of Biscay itself has low chlorophyll a content and primary production. The observed $p\text{CO}_2$ are higher than those obtained in the frontal area and nearer the atmospheric equilibrium value.
- the near-shore station (Vigo) is characterized by high chlorophyll a content and important primary production. In spite of this important biological activity, surface $p\text{CO}_2$ is also very high and far from atmospheric equilibrium. This is obviously due to the important coastal upwelling which takes place along the Spanish and Portuguese Atlantic coast. Such high primary production site is then also an important source of CO_2 to the atmosphere. As discussed by Frankignoulle *et al.* (submitted²), some other coastal areas are also characterized by high production rate associated to high surface $p\text{CO}_2$ values: the Southern Bight of the North Sea which is influenced by water coming from the Scheldt displayed, in June 1992, chlorophyll concentration as high as $7.55 \mu\text{g l}^{-1}$, due to eutrophication, and $p\text{CO}_2$ value of 407 ppmV, due to the alkalinity of Scheldt water.

3.- Air-sea CO_2 exchange measurements.

Air-sea CO_2 fluxes have been estimated, during diel cycles, using the bell method in June 1992 in the Celtic Sea, above both the continental shelf and slope. Obtained data are reported in figure 2. At the slope station, important fluxes, especially the first day, are observed from air to sea in good agreement with the sign of the CO_2 gradient. At the shelf station, fluxes are about five times lower than the first day at the slope station. During those measurements, the pH has been monitored in surface water and, in both cases the partial CO_2 pressure is quite constant (± 5 to 10%) during the whole experiment. The observed CO_2 gradients can thus explain neither the variation of measured fluxes observed on the slope station from the first day to the second, nor the difference between both stations. According to the CO_2 gradients, fluxes at the slope station

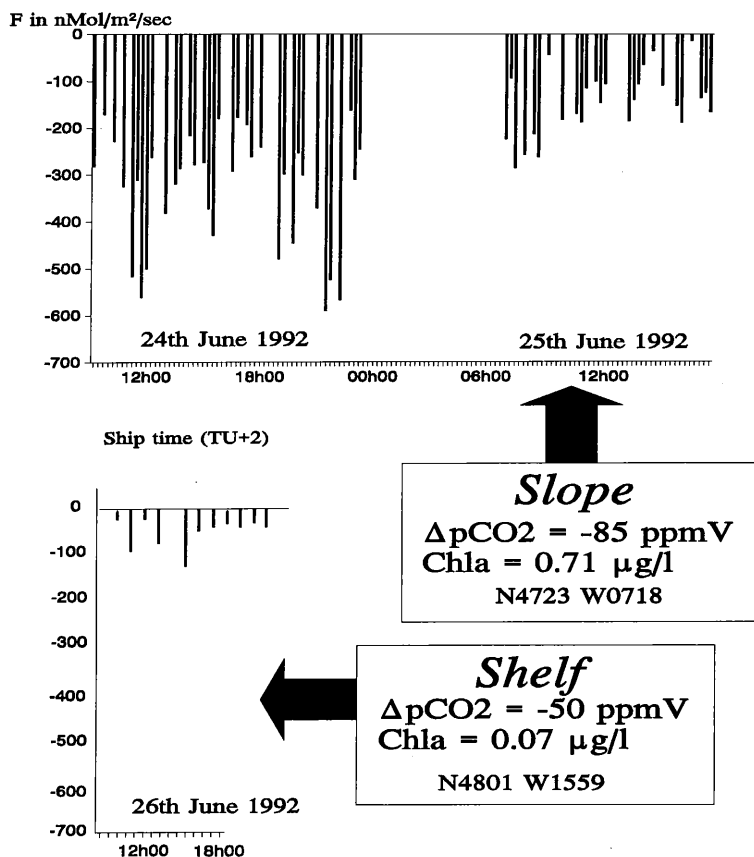


Fig. 2.- Measured air to sea CO_2 fluxes in the Celtic Sea in June 1992. Negative flux values do correspond to air to sea flux [cf. equation (1)]

should be about twice those at the shelf station. This is roughly observed by considering only the second day at the slope station. As shown on figure 3, high fluxes detected at the slope station are in fact related to the wind speed

Air-sea CO₂ exchange (Celtic Sea, Continental slope)

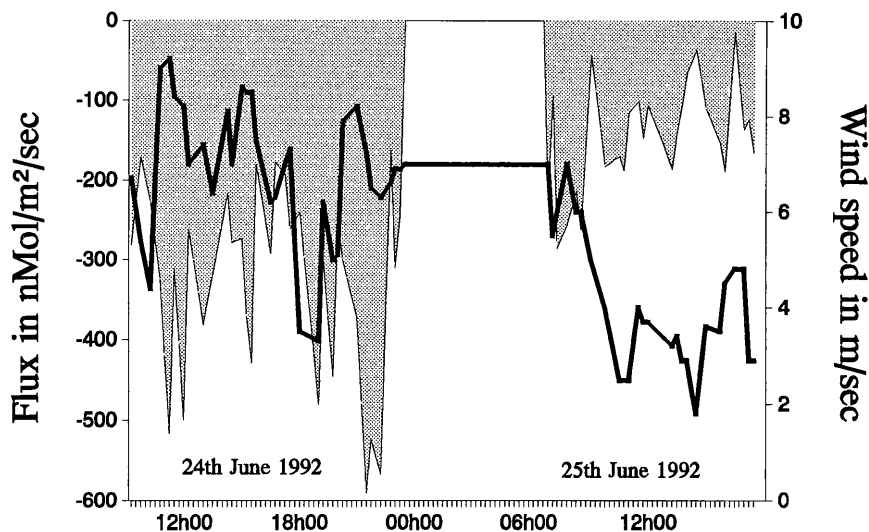


Fig. 3.— Measured CO₂ fluxes (area) at the slope station as a function of wind speed line

which is nearly always higher than 5 m s^{-1} , with peaks up to 9 m s^{-1} , at the slope station from the beginning of the experiment till about 9 a.m. the second day. Wind speed at the shelf station is lower than 3 m s^{-1} . Figure 3 clearly shows that air-sea flux maxima are correlated to wind speed ones. The effect of wind on air-sea exchange have been investigated by wind-tunnel experiments (see *e.g.* Liss and Merlivat, 1986; Wanninkhof, 1992), according to which the gas exchange coefficient [*cf.* equation (1)] is quite constant for wind speed lower than 5 m s^{-1} but increases exponentially for higher values. The variation of wind speed during the experiment can thus explain the one observed for air-sea CO₂ flux and results presented here illustrate well the relative importance of both the gradient and the wind speed on the exchanges. It is worth noticing that the used method to detect air-sea fluxes does suppress the direct wind effect on the exchange, due to the presence of the bell. Frankignoulle (1988) has anyway pointed out that the bell takes into account the global turbulence induced by wind in the upper layer and results obtained in the North Sea have shown that flux obtained using the bell is in good agreement with results from wind-tunnel within about 30%.

4.- Conclusions.

Coastal areas can be sites of processes which have a drastic effect on the surface seawater $p\text{CO}_2$ distribution and hence on air-sea CO_2 exchange. Data obtained in the Gulf of Biscay show that the Atlantic coastal upwelling (Spain) induces both important biological activity and high $p\text{CO}_2$ value in the surface layer. In other locations of the Gulf, primary production is associated to low $p\text{CO}_2$ level in good agreement with the expected effect of production alone. Depending on the river type, riverine input can also generate high production and $p\text{CO}_2$ oversaturation. The use of $\delta^{13}\text{C}$ as a tracer for terrestrial input should be improved by the knowledge of $\delta^{13}\text{C}$ associated to anthropogenic compounds. Air-sea CO_2 flux measurements carried out in the Celtic Sea have pointed out that wind speed has, as expected, a preponderant effect on the magnitude of the flux.

Acknowledgements.

The authors would like to thank Prof. Roland Wollast, cruise chief scientist, as well as Prof. A. Distèche for fruitful discussions, Captain and crews of the *R.V. Belgica* for helpful collaboration, A. Pollentier and J. Backers, from MUMM, for providing CTD and meteo data, R. Biondo and J.M. Théate for technical support.

This work has been funded by the *Fonds National Belge de la Recherche Scientifique* (Belgium), with which Michel Frankignoulle is a *Chercheur Qualifié*, by the *Service de la Politique Scientifique de Belgique* (Programme d'impulsion Global Change, conventions GC/12/011, GC/11/009 & GC/03/010), by the *Communauté Française de Belgique* (Programme Actions Concertées, convention 89/94-131) and by the Commission of the European Community (MAST Programme, numbers 0019 & 0022).

References.

- CULKIN, F. (1965). *The major constituents of seawater*, in: Riley, J.P. and Skirrow G. (Editors), *Chemical Oceanography*, Academic press, 2:121–161.
- DAUBY, P. (1989). The stable carbon isotope ratios in benthic foodwebs of the Gulf of Calvi, Corsica, *Continental Shelf Res.*, 9:181–195.
- DAUBY, P., GOBERT, S., FRANKIGNOULLE, M. and BOUQUEGNEAU, J.M. (Submitted). Particulate Al, Cd, Cr, Cu, Pb, Ti, Zn and $\delta^{13}\text{C}$ in the English Channel and adjacent areas, submitted to *Oceanol. Acta*.
- DAUBY, P., BABYENS, W., BOUQUEGNEAU, J.M., CHOU, L., COLLETTE, O., DEHAIRS, F., ELSKENS, M., FRANKIGNOULLE, M., LOIJENS, M., PAUCOT, H. and WOLLAST, R. (This Volume). *Trace elements in the Northeastern Atlantic: distribution in the suspended matter and transfert from the dissolved to the particulate phase*.

- ELSKENS, M., CHOU, L., DAUBY, P., FRANKIGNOULLE, M., GOEYENS, L., LOIJENS, M. and WOLLAST, R. (1993). *Primary production of the Gulf of Biscay*, this volume.
- FONTUGNE, M.R. and DUPLESSY, J.C. (1981). Organic carbon isotopic fractionation by marine plankton in the temperature range -1 to 31°C , *Oceanol. Acta*, 4:85–90.
- FRANKIGNOULLE, M. (1988). Field measurements of air-sea CO_2 exchange, *Limnol. Oceanogr.*, 33 (3):313–322.
- FRANKIGNOULLE, M., CANON, C. and GATTUSO, J.P. (Submitted¹). Marine calcification as a source of carbon dioxide with a positive feedback to increasing atmospheric CO_2 level, submitted to *Limnol. Oceanogr.*
- FRANKIGNOULLE, M. and GATTUSO, J.P. (1993). *Air-sea CO_2 exchanges in coastal ecosystems*, in: Wollast, R., Mackenzie, F.T. and Chou, L. (Editors), *Interactions of the carbon, nitrogen, phosphorus and sulphur biogeochemical cycles and Global Change*, Springer-Verlag, NATO ASI Series, 14:233–248.
- FRANKIGNOULLE, M., CANON, C. and DAUBY, P. (Submitted²). Distribution of partial CO_2 pressure in the English Channel. Relation with biological indicators and corresponding air-sea CO_2 fluxes, submitted to *Oceanol. Acta*.
- FRANKIGNOULLE, M. (Submitted). A complete set of buffer factor for acid/base CO_2 system in seawater, submitted to *Deep Sea Res.*
- GATTUSO, J.P., PICHON, M., DELESALLE, B. and FRANKIGNOULLE, M. (1993). Community metabolism and air-sea CO_2 fluxes in a coral reef ecosystem (Moorea, French Polynesia), in press in *Mar. Ecol. Prog. Ser.*
- HANSSON, I. (1973). A new set of acidity constants for carbonic acid and boric acid in sea water, *Deep Sea Res.*, 20:461–478.
- HANSSON, I. and JAGNER, D. (1973). Evaluation of the accuracy of GRAN plots by means of computers calculations, *Anal. Chim. Acta*, 65:363–373.
- LISS, P. (1983). *Gas transfer: experiments and geochemical implications*, in: Liss, P.S. and Slinn, W.G. (Editors), *Air-sea exchanges of gases and particles*, Reidel, NATO ASI Series, 241–298.
- LISS, P. and MERLIVAT, L. (1986). *Air-sea gas exchange rates: introduction and synthesis*, in: Buat-Ménard, P. (Editor), *The role of air-sea exchanges in geochemical cycling*, Reidel, NATO ASI Series, 113–128.
- LORENZEN, C.J. and Jeffrey, S.W. (1978). *Determination of chlorophyll in seawater*, Unesco Technical Paper in Marine Science, 35.
- LYMAN J. (1957). Ph. D. Thesis, Los Angeles.
- MEHRBACH C., CULBERSON, C.H., HAWLEY J.E. and PYTKOWICZ, R.M. (1973). Measurements of the apparent dissociation constants of carbonic acid in seawater at atmospheric pressure, *Limnol. Oceanogr.*, 18:897–907.
- SUNDQUIST E.T. and PLUMMER, L.N. (1981). Carbon dioxide in the ocean surface: the homogenous buffer factor, *Science*, 204:1203–1205.

- SOFER, Z. (1980). Preparation of carbon dioxide for stable carbon isotope analysis of petroleum fractions, *Anal. Chem.*, 52:1389–1391.
- TANS, P.P., FUNG I.Y. and TAKAHASHI, T. (1990). Observational constraints on the global atmospheric CO_2 budget, *Science*, 247:1431–1438.
- WALSH, J.J. [Editor] (1988). *On the nature of continental shelves*, Academic Press.
- WALSH, J.J. (1991). Importance of continental margins in the marine biogeochemical cycling of carbon and nitrogen, *Nature*, 350:53–55.
- WANNINKHOF, R. (1992). Relationship between wind speed and gas exchange over the ocean, *J. Geophys. Res.*, 97:7373–7382.
- WARE, J.R., SMITH, S.V. and REAKA-KUDLA, M.L. (1992). Coral reefs: sources or sinks of atmospheric CO_2 ?, *Coral reefs*, 11:127–130.
- WATSON, A.J., ROBINSON, C., ROBERTSON, J.E., WILLIAMS P.J. and FASHAM, J.R. (1991). Spatial variability in the sink for atmospheric carbon dioxide in the North Atlantic, *Nature*, 350:50–53.
- WEISS R.F. (1974). Carbon dioxide in water and seawater: the solubility of a non-ideal gas, *Mar. Chem.*, 2:203–215.
- WOLLAST, R. (1989). *The Scheldt Estuary*, in: Salomons, W., Bayne, B.L., Duursma, E.K. and Forstner, U. (Editors), *Pollution of the North Sea, an assessment*, Springer-Verlag, 183–193.

Distribution of particulate trace elements in the Northeastern Atlantic

Patrick DAUBY¹, Willy BAEYENS³, Renzo BIONDO¹,
Jean-Marie BOUQUEGNEAU¹, Lei CHOU², Olivier COLLETTE³,
Frank DEHAIRS³, Marc ELSKENS³, Michel FRANKIGNOULLE¹,
Michèle LOIJENS², Hugues PAUCOT² and Roland WOLLAST²

¹ Laboratoire d'Océanologie, Université de Liège

² Laboratoire d'Océanographie Chimique, Université Libre de Bruxelles

³ Laboratorium voor Analytische Scheikunde, Vrije Universiteit Brussel

Abstract.

From 1989 to 1992, five cruises were conducted in an area covering the English Channel, the Celtic Sea and the Gulf of Biscay. During these campaigns, suspended matter was collected by different techniques in order to analyze the spatial and vertical distribution of several particulate trace elements in relation to the global biogeochemical cycle of carbon. It appears that horizontal distribution varies strongly from one element to another and is mainly influenced either by anthropogenic and terrigenous inputs or by scavenging processes. On the other hand, the vertical distribution seems mainly linked to the primary production. In parallel to these trace element measurements, experiments were carried out to estimate the transfer rates of these elements from the dissolved to the particulate phase using radioactive tracers. The results clearly indicate that biological activity plays an important role in these transfers.

1.- Introduction.

Very little attention has been paid until now to the trace element content of suspended matter in the water column. Trace metals are however known to be enriched in the particulate phase, and their contents in the suspended materials or sediments often reflect the history of surrounding environments with respect to pollution. In the photic zone for example, passive or active sorption processes occur onto the organic matter produced by the organisms, and they are responsible for the transfer of many elements from the dissolved to the particulate phase. As suspended matter is one of the main sources of carbon either for pelagic or for benthic food webs, its elemental composition also directly alters heavy metal concentrations in high trophic levels.

The present paper describes results of trace element measurements performed on suspended matter collected during the Global Change cruises (1989 to 1992) by the Belgian team. One of the objectives of the Global Change programme is to study the processes controlling the transfer of trace elements related to the carbon cycle between both particulate and dissolved phases. The sampling area covers a wide range of zones with different dynamics: (i) the English Channel, characterized by complex hydrological processes due to bottom profile and strong tidal currents, (ii) the Celtic Sea, on both sides of the continental margin, (iii) the center of the Gulf of Biscay, a deep (> 4,000 m) oligotrophic area, and (iv) the Northwestern Spanish coast which is the center of an intense upwelling.

With respect to the goals of the Global Change programme, the mechanisms and rates of transfer of trace metals from the dissolved to the particulate phase in the oceanic system were also investigated. Radioactive trace metals have been used successfully in previous studies in order to evaluate the distribution coefficient and the rate of transfer of trace elements from the dissolved to the particulate phase in sea-water (Balistrieri & Murray, 1983; Li *et al.*, 1984; Nyffeler *et al.*, 1984; Buchholtz *et al.*, 1985; Santschi *et al.*, 1986; Jannasch *et al.*, 1988). Most of these measurements were made during laboratory experiments using artificial suspensions of sediments mixed with sea-water or in mesocosm systems mimicking the natural environment. The results indicate a very fast initial sorption of the radiotracers followed by a much slower uptake. This suggests that there is a rapid adsorption at the surface of the particles followed by a slower transfer process which may be due to physico-chemical or biological processes.

Mouchel & Martin (1990) were the first to propose the use of radiotracer uptake experiments carried out immediately on samples collected in rivers, estuaries and marine systems. The results obtained during these experiments were in fact very similar to those obtained in the laboratory and are characterized by an important and rapid initial transfer. These authors have suggested to use this method to define a fast distribution coefficient (K_D), easily evaluated by comparing the radioactivity of the solid collected after an initial stage, usually limited to 24 hours, with the radioactivity remaining in solution. This coefficient is very useful because it allows one to characterize the capacity of the suspended matter to induce scavenging of trace elements in the system considered. These short time measurements may also be used to understand the behaviour of trace metals in rapidly changing environments like estuaries or coastal zones.

Two of us have suggested (Wollast & Loijens, 1991) to improve this method by performing incubation experiments with natural samples spiked with radioactive trace metals similarly to the incubation experiments carried out with ^{14}C labelled HCO_3^- to measure primary production. By comparing the uptake of trace metals incubated under natural or controlled light conditions or in the dark,

with or without inhibitors of the biological activity, it is possible to understand and to evaluate the contribution of the biological activity in the transfer of trace metals from the dissolved to the particulate phase. It is well known that many trace metals act as oligo-elements essential for the metabolic activity of living organisms. They often exhibit a nutrient like behaviour in aquatic systems indicating that the organisms can act as major scavenging agents of trace elements in sea-water.

2.— Sampling methods. Intercomparison.

Samples of total suspended matter (TSM) were collected during the following cruises on board the *R/V Belgica*: campaign 89/21 (September 11th to 26th, 1989) and campaign 90/18 (July 2nd to 18th, 1990) in the English Channel, Western Biscay and Northwestern Spanish Shelf areas (● in figure 1); campaign 91/16 (June 24th to July 9th, 1991) in the Channel, Northern Biscay and Celtic Sea areas (■ in figure 1); campaign 92/23 (October 8th to 23rd, 1992) in the Northern Biscay shelf break area (La Chapelle Bank, ▲ in figure 1). The position of the stations and corresponding TSM amounts in surface waters are listed in Table 1.

TSM was sampled using three different techniques, depending on whether horizontal distributions or vertical profiles were investigated. Sample preparation for trace metal determination also differed according to sampling technique. Comparisons of the results obtained by the three following methods will be discussed further.

- (i) For horizontal distribution pattern determination (1991 cruise), TSM was sampled by continuous centrifugation of surface seawater pumped forward at 3 m depth while the ship was making headway; sampling periods ranged from 3 to 8 hours (courses from 45 to 160 km). TSM concentrations measured by this method are listed on Table 1. Samples were stored in petri-dishes and deep frozen. For the analysis of trace metals (Al, Cd, Cr, Cu, Pb, Ti, Zn) suspended matter was mineralized in a mixture (1:1) of 65% nitric acid and 37% hydrochloric acid at about 75°C during 12 hours. Elemental determinations were made by ICP-AES (A.R.L. 3510).
- (ii) Vertical distribution of particulate trace elements was investigated using 30 l Niskin bottles (1990 to 1992 cruises). Immediately after sampling, these bottles were pressurized with filtered air (0.3 bar) and seawater was filtered with Nuclepore membranes (0.45 µm). Niskin bottles were slightly adapted to fit the filterholders onto the lower lid instead of the original outlet, allowing the collection of rapidly settling particles. Membrane samples were air dried and kept at room temperature. For analysis, a preliminary mineralization and dissolution is made using a fusion technique with lithium

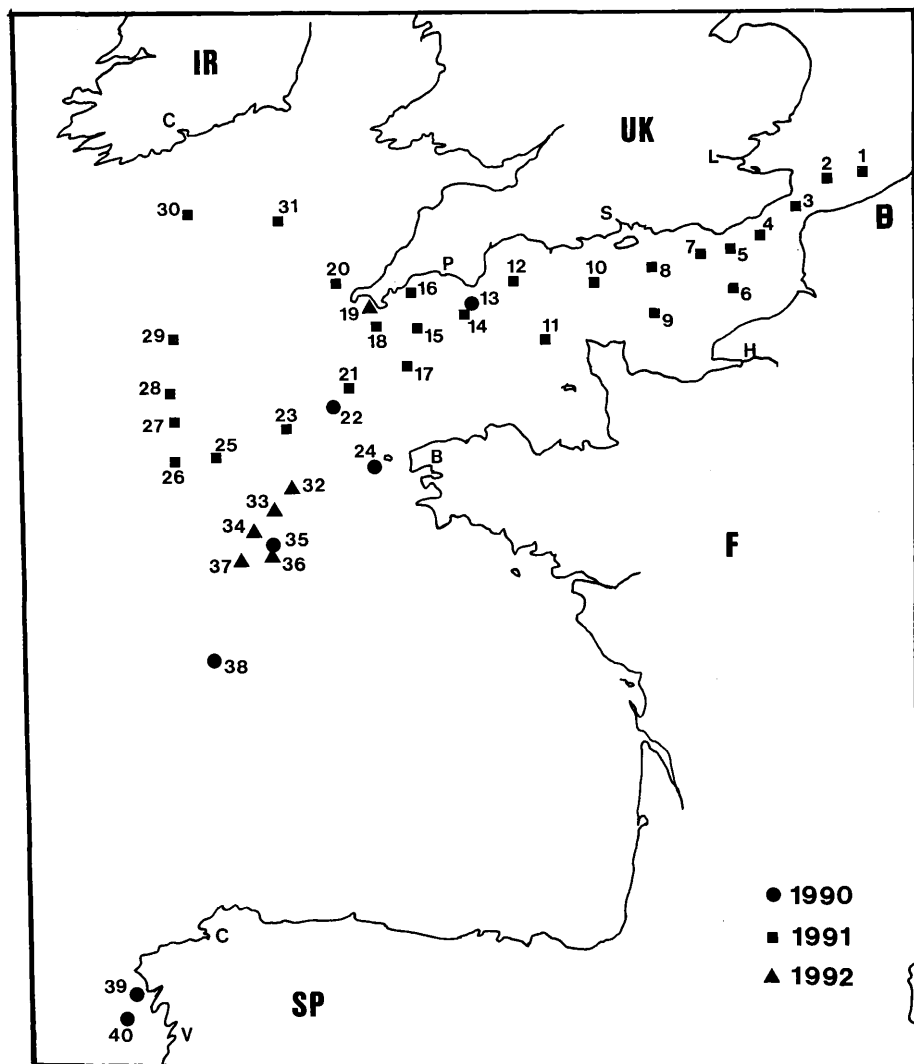


Fig. 1.— Position of the TSM sampling sites for the 1990, 1991 and 1992 cruises

metaborate as the flux. Elemental determinations were also performed with ICP-AES (Jobin-Yvon-48).

- (iii) Collection of larger amounts of TSM along vertical profiles was performed with a Stand Alone Pump (SAP), an *in situ* particle sampler, housed with a polycarbonate 30 cm filter holder fitted with a 1 μ m Nuclepore membrane. This device allows the filtration of a large volume of seawater (up to 2,000 l) at great depths (down to 5,000 m), and thus the collection of sufficient

Table 1
Sampling dates and locations, bottom depths, and TSM concentrations
(sampling by centrifugation)

Station #	Position	Depth (m)	Date	TSM (mg/l)
1	51°23'N–03°00'E > 51°20'N–02°30'E	11	91–Jun	4.10
2	51°20'N–02°30'E > 51°20'N–02°08'E	24	91–Jun	1.97
3	51°20'N–01°50'E > 50°50'N–01°00'E	34	91–Jun	1.92
4	50°50'N–01°00'E > 50°40'N–00°30'E	29	91–Jun	2.78
5	50°41'N–00°30'E	28	91–Jun	2.60
6	50°25'N–00°57'E > 50°01'N–00°04'W	41	91–Jul	3.79
7	50°41'N–00°30'E > 50°30'N–00°39'W	41	91–Jun	1.17
8	50°30'N–00°39'W > 50°20'N–01°35'W	52	91–Jun	1.34
9	50°00'N–00°15'W > 50°02'N–01°40'W	60	91–Jul	0.84
10	50°20'N–01°35'W > 50°15'N–02°30'W	52	91–Jun	1.62
11	50°00'N–01°49'W > 49°30'N–03°30'W	86	91–Jul	1.94
12	50°15'N–02°30'W > 50°05'N–03°30'W	58	91–Jun	1.58
13	50°00'N–03°50'W	72	90–Jul	2.75
14	50°05'N–03°30'W > 49°44'N–04°20'W	66	91–Jun	2.01
15	50°00'N–06°00'W > 49°30'N–03°30'W	101	91–Jul	1.31
16	50°08'N–05°05'W	10	91–Jun	1.62
17	49°44'N–04°22'W > 49°25'N–05°04'W	87	91–Jun	1.70
18	49°25'N–06°30'W > 50°06'N–05°00'W	77	91–Jun	1.77
19	50°03'N–05°19'W	28	92–Oct	1.31
20	50°15'N–05°40'W > 50°00'N–06°00'W	48	91–Jul	1.26
21	49°25'N–05°04'W > 49°05'N–06°10'W	107	91–Jun	1.95
22	49°00'N–06°00'W	120	90–Jul	1.89
23	48°56'N–06°01'W > 48°20'N–06°30'W	127	91–Jun	1.06
24	48°25'N–05°21'W	110	90–Jul	1.13
25	48°20'N–06°30'W > 48°09'N–08°14'W	340	91–Jun	1.38
26	48°09'N–08°20'W	1200	91–Jun	1.74
27	48°09'N–08°29'W > 49°00'N–08°33'W	475	91–Jun	1.10
28	49°00'N–08°22'W	155	91–Jul	0.53
29	49°04'N–08°11'W > 50°30'N–08°30'W	130	91–Jul	0.59
30	50°30'N–08°30'W > 51°45'N–08°20'W	65	91–Jul	0.64
31	51°45'N–08°15'W > 50°15'N–05°40'W	65	91–Jul	1.02
32	48°12'N–06°44'W	160	92–Oct	0.71
33	47°57'N–06°59'W	171	92–Oct	0.69
34	47°42'N–07°11'W	169	92–Oct	0.69
35	47°35'N–07°00'W	205	90–Jul	0.61
36	47°30'N–07°00'W	510	92–Oct	0.70
37	47°25'N–07°16'W	2000	92–Oct	0.72
38	46°25'N–08°00'W	4800	90–Jul	0.32
39	42°43'N–09°19'W	123	90–Jul	4.24
40	42°30'N–09°30'W	1230	90–Jul	4.21

quantities of suspended matter in waters of low particulate load. For each sample collected, metal concentrations (Cd, Cr, Co, Cu, Mn, Ni,

Pb, Zn) were measured using a Varian SpectrAA-400 Zeeman graphite furnace spectrometer. The analytical method involves direct injection of solid samples without the intermediate digestion step, as developed by Hoenig *et al.* (1989). Particulate Si and Al were also measured following the method described in Hoenig *et al.* (1991 a, b).

In order to control the reliability of metal determination, the entire analytical procedure was tested against standard reference sediments supplied by the National Institute of Standards and Technology (NIST), International Atomic Energy Agency (IAEA), Bureau Communautaire de Référence (BRC, EEC) and National Research Council of Canada (NRCC).

Table 2

Intercomparison of trace element data obtained by the three different sampling and analytical techniques in various geographical areas

Areas (station #)	Elements	<i>In situ</i> pump 1990 data	Centrifugation 1991 data	Niskin 1992 data
2, 3, 4, 5	Al (mg/g)	5.5	5.2	8.3
5, 7, 8			5.9	6.1
8, 10			7.8	9.3
12, 14			5.4	4.1
15, 21			1.1	0.9
25, 26, 27, 28	Cd (µg/g)	0.32	0.42	0.41
13, 14		0.61	0.6	
13, 14		20.3	15.3	
13, 14		25.3	23.2	
13, 14		25.3	17.7	
13, 14	Zn (µg/g)	47.5	58.3	

As different TSM collection techniques and metal determination methods were used, it is necessary to compare the results for the same water masses, *i.e.* for similar locations during the same sampling period, and ideally at the same depths. Unfortunately, few data are available for such a comparison because of the “weather at sea” which obliged us to use preferentially one sampling technique against another. Despite this drawback, concentrations obtained by different methods and laboratories on TSM collected at same sites and depths during the summer are very similar (Table 2). Intercomparison of these results allows us to control the quality of our data. The trace metal concentrations of TSM obtained in this study, regardless of the sampling and analytical techniques, are furthermore in good agreement with those obtained by Dehairs *et al.* (1985) and Baeyens *et al.* (1987) for similar sampling areas.

For experiments designed to study the transfer rate of trace metals from the dissolved to the particulate phase, the water samples were usually collected in

surface waters at depths corresponding to the maximum of fluorescence or of dissolved oxygen as recorded during the lowering of the CTD rosette. Samples were immediately spiked with the radionuclides and incubated under constant light conditions, at the surface seawater temperature. A few experiments were also carried out under variable light conditions. In order to reduce the perturbations of the natural conditions during the incubation experiment, the concentration of the carrier was kept at a low level. The final concentration obtained after addition of radionuclides is equal to 10 nmol l^{-1} for Mn, Co, Zn and 5 nmol l^{-1} for Cd. The influence of the amount of spike solution on the uptake of the radionuclide was investigated during a preliminary experiment. After incubation, samples were filtered on Sartorius $0.4 \mu\text{m}$ membranes and rinsed with pre-filtered seawater. Preliminary tests have shown that absorption of radionuclides onto the Sartorius cellulose filter was negligible. The activities were measured with a HPGE Canberra detector with a relative efficiency of 20% and a multichannel spectrometer serie 20 Model 2802. The activities recorded on the filters after incubation of open-sea water samples are often of the order 0.1 dpm and requires long counting times. The minimum number of counts was fixed at 1,000 to reduce the statistical error related to counting.

3.— Results and discussion.

3.1.— Horizontal surface distribution.

3.1.1.— Results from centrifugation (Table 3 and Figure 2).

Aluminium.

The distribution of the particulate Al concentrations is roughly correlated with that of particulate load. This is not surprising since particulate aluminium is mainly present in the sea as terrigenous aluminosilicates via riverine or atmospheric input. Observed concentrations are very similar all along the English Channel (from 3 to $16 \mu\text{g l}^{-1}$, from 2 to 7.5 mg g^{-1} TSM), with, however, higher values near the English coasts; these data are slightly lower than those of Dehairs *et al.* (1985) for the Eastern Channel, and are significantly below values measured in the Southern Bight of the North Sea by Duinker & Nolting (1977) and Dauby *et al.* (1993) who found concentrations up to 1.2 mg Al l^{-1} . In the Celtic Sea, concentrations are much lower, averaging $0.3 \mu\text{g l}^{-1}$ (0.4 mg g^{-1}), because the TSM in that region is mainly composed of organic matter. In the center of the Gulf of Biscay, concentrations decrease below $0.2 \mu\text{g l}^{-1}$ but rise sharply (up to $50 \mu\text{g l}^{-1}$) when approaching the Spanish coast.

Particulate metal concentrations in surface seawater ($\mu\text{g/l}$ or mg/l) and in TSM collected by centrifugation ($\mu\text{g/g}$ or mg/g) during the June 1991 cruise

Station #	Al		Cd		Cr		Cu		Pb		Ti		Zn	
	($\mu\text{g/l}$)	(mg/g)	(ng/g)	($\mu\text{g/l}$)	(ng/g)	($\mu\text{g/l}$)	(ng/g)	($\mu\text{g/l}$)	(ng/g)	($\mu\text{g/l}$)	(ng/g)	($\mu\text{g/l}$)	(ng/g)	($\mu\text{g/l}$)
1	27.3	6.7	16.9	4.13	166	40.5	152	37.1	470	114.7	287	70	1549	377.9
2	11.0	5.6	4.3	2.20	51	25.8	67	34.2	79	40.3	159	80	487	247.1
3	8.6	4.5	1.1	0.59	18	9.5	27	14.1	15	7.9	71	37	101	52.7
4	16.0	5.8	3.6	1.30	48	17.2	176	63.2	94	34.0	176	63	272	97.9
5	12.8	4.9	2.9	1.11	39	14.9	102	39.3	80	30.6	90	34	237	91.1
6	8.4	2.2	0.5	0.14	54	14.3	67	17.7	35	9.3	134	35	82	21.8
7	6.2	5.3	1.6	1.37	19	16.1	58	49.6	35	30.2	45	38	103	87.8
8	10.0	7.5	2.2	1.66	28	20.9	134	99.7	52	38.7	63	47	181	135.1
9	3.8	4.5	0.4	0.53	15	18.0	19	22.5	16	18.8	52	61	38	44.9
10	13.0	8.1	0.7	0.44	32	19.6	29	17.8	33	20.3	78	48	92	57.1
11	2.8	1.4	0.6	0.32	21	10.9	36	18.5	25	13.0	42	21	54	28.0
12	7.9	5.0	1.9	1.20	24	15.3	30	18.8	28	17.8	69	43	104	65.8
14	11.4	5.7	1.2	0.60	31	15.3	47	23.2	36	17.7	60	30	117	58.3
15	1.6	1.2	0.7	0.56	21	15.8	31	23.4	13	10.0	26	20	64	48.6
16	8.8	5.5	1.3	0.83	29	17.6	39	24.1	33	20.5	40	25	117	72.1
17	6.5	3.8	1.4	0.84	28	16.4	60	35.5	35	20.6	25	15	135	79.3
18	3.7	2.1	1.5	0.84	36	20.1	37	20.7	17	9.7	24	13	126	71.0
20	2.7	2.1	0.9	0.72	68	54.2	33	26.3	27	21.8	39	31	84	67.0
21	1.7	0.9	2.2	1.10	34	17.3	44	22.8	16	8.0	21	11	141	72.1
23	5.4	5.1	1.5	1.38	46	43.6	89	83.9	70	65.6	61	57	214	201.7
25	1.0	0.8	0.9	0.66	12	9.0	21	15.1	13	9.3	13	10	40	29.3
26	0.9	0.5	1.7	0.97	21	12.3	22	12.4	14	7.8	13	7	53	30.7
27	0.2	0.2	1.8	1.60	19	17.6	23	21.3	11	10.2	2	2	38	34.9
28	0.1	0.2	0.3	0.63	8	14.9	15	28.6	1	0.9	2	3	13	24.2
29	0.4	0.7	0.3	0.52	99	167.6	16	27.3	7	11.6	3	4	27	45.4
30	0.2	0.3	0.3	0.46	14	21.4	12	18.7	1	1.6	2	3	23	36.6
31	0.5	0.5	0.4	0.38	85	83.7	17	16.7	14	13.7	9	9	55	54.3
soils*		71		0.35		70		30		35		5000		90
rivers*		94		(1)		100		100		100		5600		250

* Data for mean soils and river particulate material from Martin & Meybeck, 1979.

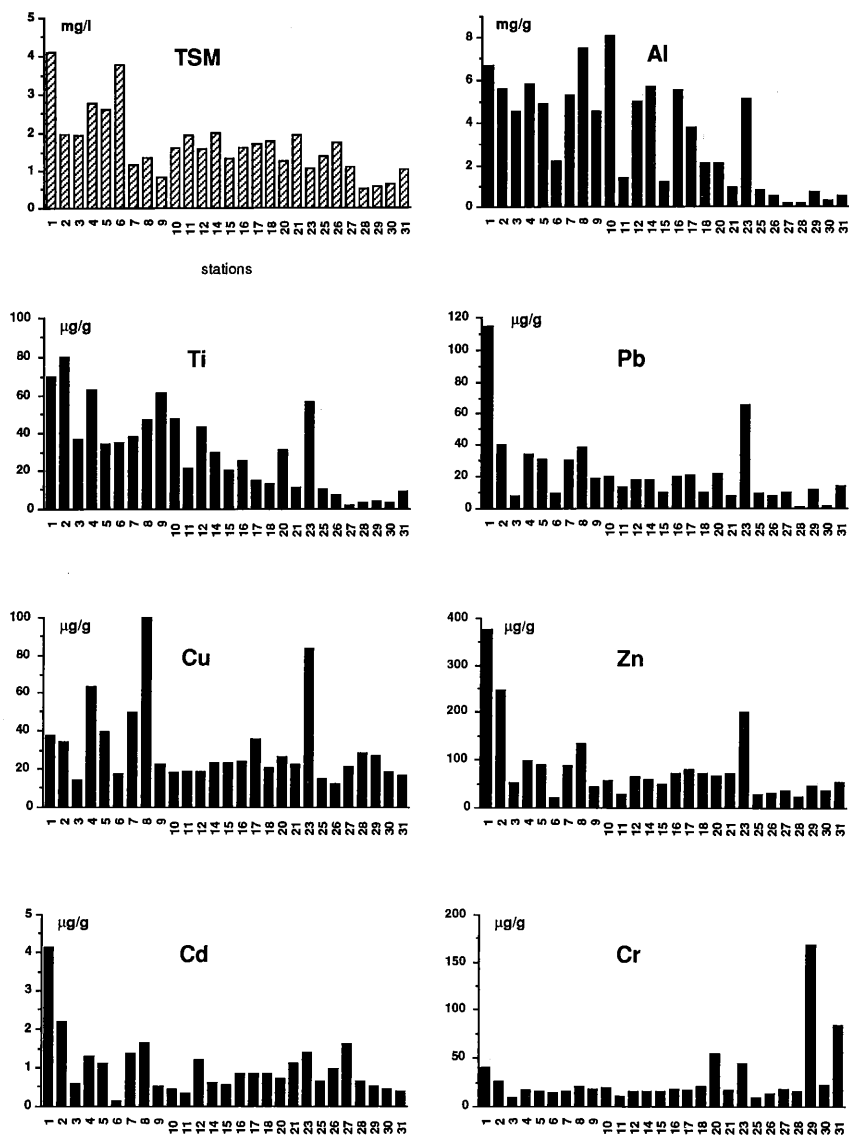


Fig. 2.— TSM concentrations in surface waters sampled by centrifugation during the June 1991 cruise, and heavy metal concentrations in this TSM.

Titanium.

The distribution of Ti associated with TSM is similar to that of aluminium, as this element is also a tracer of terrestrial material. The concentrations are nevertheless particularly high ($\geq 70 \mu\text{g g}^{-1}$) in the Southern Bight (where

Nolting & Eisma, 1988, have found up to 2 mg Ti g^{-1}) and the Strait of Dover, and could be attributed to the presence of several recent dumping sites of titanium dioxide production waste; these dumps, if now theoretically stopped, should progressively release this metal and are probably responsible for the observed concentrations.

Copper.

The measurements of Cu concentration in the TSM show minimum values in the whole Celtic Sea (except for Station 23) and in the Western Channel, about $25 \text{ } \mu\text{g g}^{-1}$ on the average. In the Eastern Channel, concentrations increase, especially along the English coast, indicating a land source of Cu, likely related to the large industrial complexes of the Southeastern UK. It is also worth noting that there is no correlation between TSM concentration in surface seawater and Cu concentration in TSM, and that thus this metal seems to be associated with particulate matter inputs, either terrigenous or resuspended. The observed concentrations are in good agreement with those obtained by Dehairs *et al.* (1985) in the same area.

Zinc.

Among the elements analyzed in TSM, zinc is the one (after Al) which presents at all the stations (except the 6th) the highest concentrations, as also previously observed by Dehairs *et al.* (1985) and Baeyens *et al.* (1987). In the Southern Bight, values are peculiarly high, going beyond mean crustal or riverine values; this could be attributed to the drastic influence of Scheldt River and to the resuspension processes related to shallowness and tidal mixing. In the Channel, two relative maxima ($> 200 \text{ } \mu\text{g g}^{-1}$) are observed, on both the western and eastern parts of the English coast, probably related to industrial activities. In the Celtic Sea, values are much lower (between 30 and $55 \text{ } \mu\text{g g}^{-1}$), except for Station 23 where high concentrations of copper and lead are also observed; the unexpectedly high metal concentrations observed there could be the result of a recent local sewage release.

Lead.

The relative distribution of particulate Pb in the area studied is very similar to that of Zn, with a maximum (nearly $115 \text{ } \mu\text{g g}^{-1}$) close to the Belgian coast (input from the Scheldt River) and high values (around $40 \text{ } \mu\text{g g}^{-1}$) on the English coast of the Eastern Channel. As for both the latter metals, no apparent correlation could be found between TSM concentrations in seawater and metal concentrations in TSM, suggesting a passive sorption of metal on suspended matter.

Cadmium.

This metal is relatively peculiarly abundant in the waters off the Belgian coast, near the Scheldt Mouth, as was also described by Baeyens *et al.* (1987), Bouqueneau *et al.* (1992) and Dauby *et al.* (1993); this is not surprising as Belgium is the largest Cd consumer in Western Europe. In the Channel, concentrations range from 0.4 to 1.3 $\mu\text{g g}^{-1}$ along the English coast, with a maximum observed off Southampton. The French side and the Western Channel are less contaminated, with values around 0.3 $\mu\text{g g}^{-1}$. Concentrations observed in the Celtic Sea waters are low (about 0.3 ng l^{-1}), but are relatively high in the corresponding TSM (about 1 $\mu\text{g g}^{-1}$), suggesting a process of high metal uptake (see further) by suspended matter in these oligotrophic waters.

Chromium.

Particulate Cr concentrations in the water are nearly constant throughout the whole Channel (about 20 $\mu\text{g g}^{-1}$), and present two maxima: one in the Southern Bight, probably related to riverine discharge, and another one of lower importance in the Celtic Sea. This second maximum appears, however, much more important when considering the Cr concentrations in TSM (figure 2) that reach, in that area, 5 to 10 times (up to 167 $\mu\text{g g}^{-1}$) the concentrations observed elsewhere. TSM thus seems to have a high affinity for chromium, and this scavenging process is confirmed by the inverse exponential relationship between Cr/TSM ratios and TSM concentrations in seawater.

3.1.2.— Results from *in situ* pumping.

As was also observed for centrifugation samples, the particulate Al concentrations in all the SAP samples are well below 70 mg g^{-1} which is the value found in soils (Martin & Whitfield, 1983), suggesting that the particulate material collected has a high organic content. Suspended matter sampled in waters close to the coastal area (Stations 13, 24 and 39) contains higher Al, implying continental inputs of terrigenous material. It should be pointed out that Station 39, located right at the Spanish coast in an area where there are many Rias estuaries, has the highest particulate Al contents.

The surface distribution of particulate trace metals are shown in figure 3. It is interesting to point out that particulate Mn shows spatial distribution very similar to that observed for particulate Al. This suggests that these two elements are intimately linked with a correlation coefficient of 0.81 and have the same origin. There is a particularity regarding Station 38 compared to Station 24, both situated in the Gulf of Biscay. Indeed, Station 38 is far from the continent and thus likely receives the least terrestrial inputs as indicated by the lowest Al contents. However, when normalized with respect to Al, the suspended matter

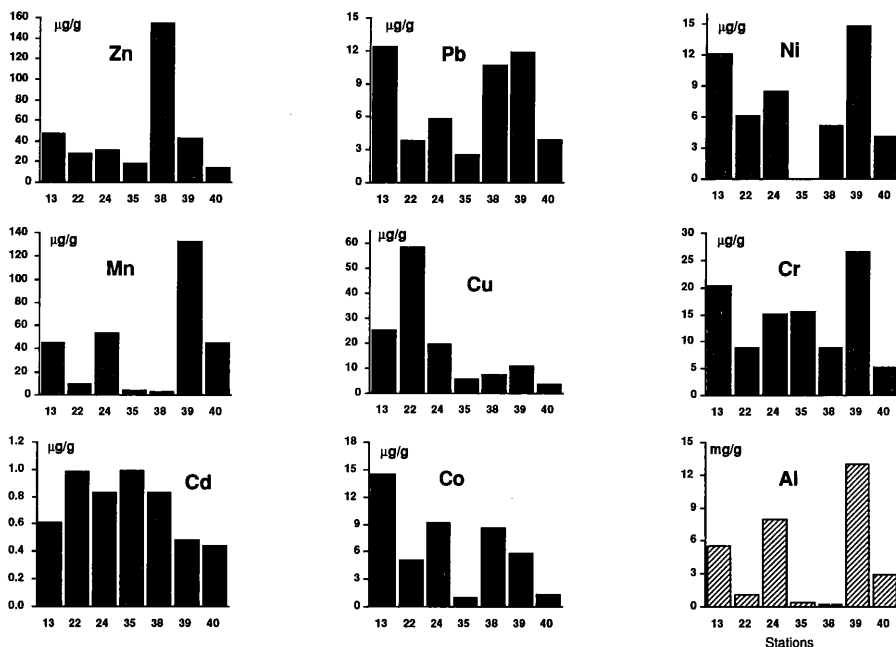


Fig. 3.— Trace element concentrations in surface water TSM sampled by *in situ* pumping during the July 1990 cruise.

collected at Station 38 is enriched in several trace metals, especially Pb, Co, Cu and Zn compared to Station 24. This implies that these metals are enriched mainly in the planktonic phase, and that an active scavenging process likely occurs in these oligotrophic waters, what is confirmed by the data obtained for trace metals in TSM with the centrifugation technique. Furthermore, it has been recognized that phytoplankton generally plays an important role in the biogeochemical cycling of trace elements in the aquatic environment (Morel & Hudson, 1985; Price & Morel, 1990), and that trace metals tend to be scavenged by organic matter due to their strong complexation with organic ligands. Therefore, in areas of high productivity, seasonal variations can be observed and correlated with the annual production cycle (Bacon *et al.*, 1985).

3.2.— Vertical distribution.

3.2.1.— Results from *in situ* pumping (Figures 4 to 6).

During the 1992 cruise (\blacktriangle in figure 1), TSM was collected in the northern part of the Gulf of Biscay, on both sides of the continental slope, but only the results obtained for Stations 32 and 37 will be presented here. Vertical distribution of particulate trace metal concentrations were determined and the

Table 4

Summary of results on the particulate trace metal concentrations of TSM collected at Stations 32 and 37 by *in situ* pumping during the October 1992 cruise

Depth (m)	Al (mg/g)	Zn (μ g/g)	Ni (μ g/g)	Cr (μ g/g)	Mn (μ g/g)	Cu (μ g/g)	Cd (μ g/g)	Pb (μ g/g)	Co (μ g/g)	Fe (mg/g)	POC (%)
Station 32											
10	2.4	108.1	19.1	41.8	81.5	20.8	2.46	10.3	0.66	1.3	
40	9.9	184.3	34.9	78.4	185.8	66.7	3.96	15.7	1.09	5.3	
80	23.9	94.6	23.7	52.9	327.7	24.7	0.96	22.8	2.07	11.2	
110	10.1	47.3	14.8	49.9	146.8	14.3	0.93	11.4	0.84	4.5	
Station 37											
20	4.2	120.9	15.0	42.6	192.3	16.3	2.78	11.9	0.84	1.5	9.8
50	5.9	123.0	15.6	29.3	226.2	20.3	1.56	14.0	0.75	3.1	5.0
80	27.5	155.4	75.6	84.8	537.5	38.0	1.35	38.1	2.93	13.2	2.5
140	27.5	122.3	38.4	62.7	690.0	38.1	3.05	23.0	2.85	12.7	1.7
200	10.1	102.1	24.1	40.0	325.4	31.3	0.85	25.5	1.37	4.3	2.1
500	20.1	169.5	53.2	145.7	550.8	54.3	1.68	43.5	2.73	10.7	1.0
600	25.4	167.7	34.9	62.4	543.6	55.1	0.34	43.1	3.55	12.9	0.65
800	13.2	98.1	22.0	38.7	245.5	31.9	0.83	23.9	1.94	5.4	0.67
1000	14.4	153.6	50.3	57.4	240.5	86.2	1.57	42.2	1.44	7.0	0.41

results are summarized in Table 4 where the particulate Al and organic carbon contents are also indicated. Vertical profiles of temperature and salinity are shown in figure 4. The *T/S* diagramme reveals clearly that four different water masses (surface, 200 m, 600 m, bottom) can be identified for Station 37, located on the deepest edge of the slope.

Contaminants such as heavy metals are usually accumulated in the fine fractions of sediments or suspended materials containing elements like Al, Fe and organic matter (ICES, 1988). Normalization of particulate trace metal concentrations has been a subject of discussion (Loring, 1988; Windom *et al.*, 1989). Application of appropriate normalization procedure may help in deciphering the data. Particulate Al is a good indicator of fine terrestrial origin such as clays. Therefore, it can be considered as a suitable candidate to be used for normalization purpose. Figure 5 shows the vertical distribution of Al and organic carbon for Stations 32 and 37. It is worth noticing that particulate organic carbon content of the suspended matter decreases exponentially with depth indicating a very fast remineralization of organic matter during settling. At the same time, the particulate Al content is the lowest in the photic zone suggesting a dilution of this element by biogenic material due to primary production.

The vertical distribution of particulate trace metals (normalized with respect to Al) are shown in figure 6 where the particulate Ba/Al is also indicated. A general trend is observed for most trace metals investigated except for Fe and Ba.

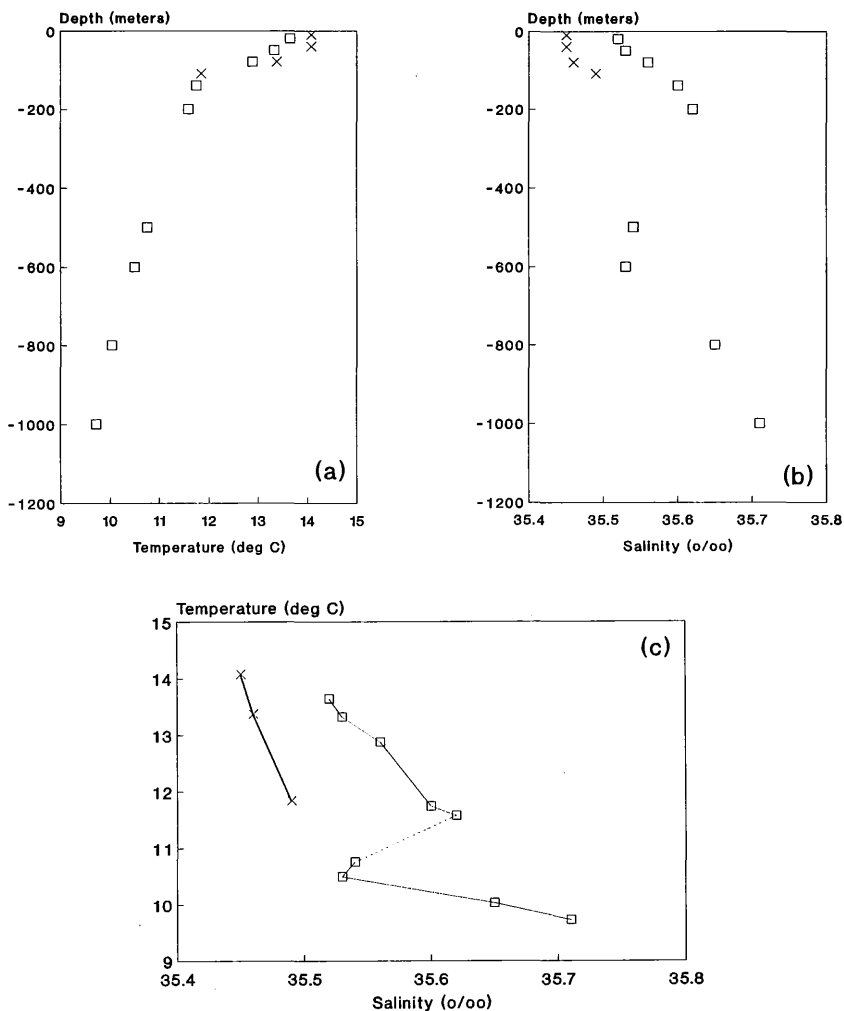


Fig. 4.— Temperature, Salinity, and T/S diagramme for Station 32 (x) and Station 37 (□) for October 1992 cruise.

There is an enrichment in the photic zone, especially for Cd. This is probably due to an uptake of trace elements by phytoplankton via biological and/or physico-chemical pathways. The variations in particulate trace metal concentrations with respect to Al below the photic zone seem to be related to different water masses existing that have all different particulate trace metal chemistry. Particulate Ba shows a different vertical profile compared to other metals. Its behaviour strongly influenced by biological activity will be discussed in detail in the following section. It is finally interesting to point out that particulate Fe/Al remains fairly constant

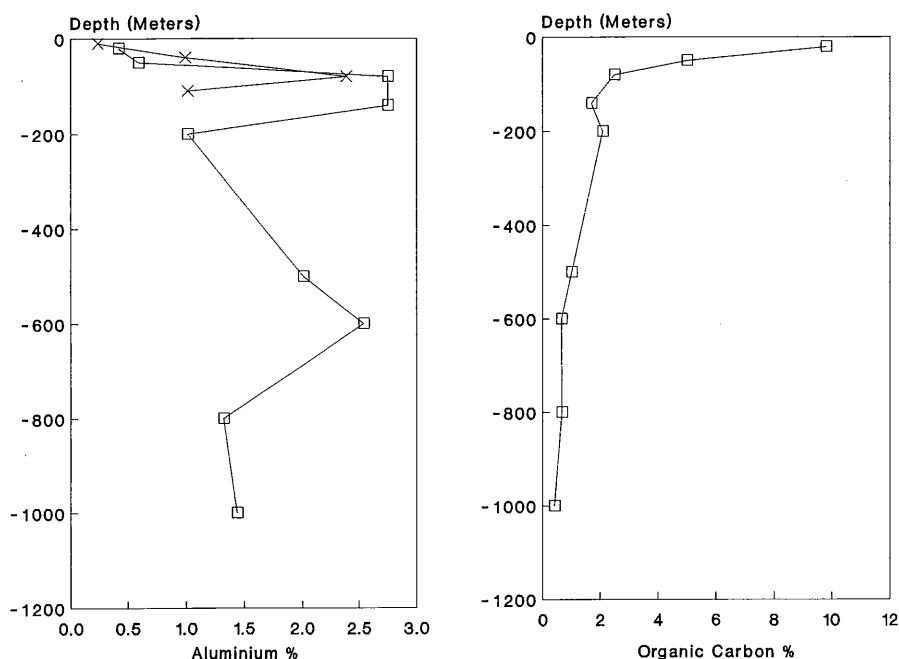


Fig. 5.— Vertical distribution of particulate Al and organic carbon in the TSM collected by *in situ* pumping during the October 1992 cruise for Station 32 (x) and Station 37 (□).

at a ratio close to 0.49 throughout the water column. This ratio is typically found for atmospheric dust over the North Atlantic (Duce *et al.*, 1991).

3.2.2.— Results from Niskin sampling – Ba distribution (Figures 6 to 8).

It is known that the main carrier of particulate Ba in suspended matter is Ba-barite (Dehairs *et al.*, 1980). The fraction of the Ba associated with aluminosilicates in suspended matter was calculated using the Ba/Al ratio for mean crust (Al: 82 mg g⁻¹; Ba: 500 µg g⁻¹; Bowen, 1979) and the Al content of the sample:

$$(\text{Al})_{\text{sample}} * (\text{Ba/Al})_{\text{crust}} = (\text{Ba})_{\text{sample associated with aluminosilicates}}$$

This exercise showed that the highest fraction of Ba in aluminosilicates are usually below 25% of the total Ba concentrations. Such values can occur in surface and bottom waters. Atmospheric deposition and sediment resuspension may be responsible for this observation. For the rest of the water column, the fraction of Ba in aluminosilicates is generally less than 10%. It follows that the vertical distribution of particulate Ba, normalized with respect to Al content, shows a substantial enrichment in Ba especially at depths ranged between 100 and 600 m (figure 6). This points towards another component as the main Ba carrier.

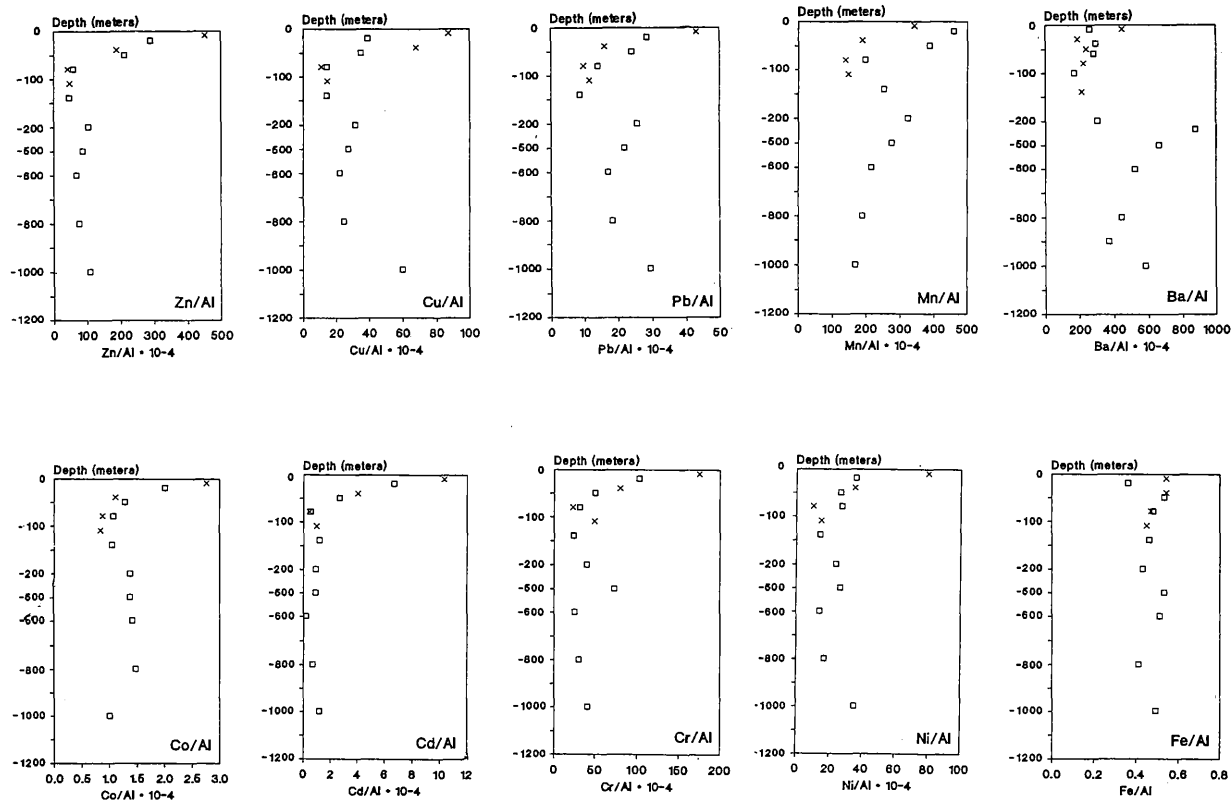


Fig. 6.— Vertical distribution of particulate trace metals in the TSM collected by *in situ* pumping during the October 1992 cruise for Station 32 (x) and Station 37 (□)

It has been known for some time that particulate Ba-barite in the oceanic water column and the sediments reflects production in the surface layers (Bishop, 1989; Dymond *et al.*, 1992; Dehairs *et al.*, 1980, 1990). These studies have revealed that Ba is incorporated by the biota (it is not known whether this process is active or passive) and precipitates thereafter as BaSO_4 (barite) within aggregates of biogenic detritus. These aggregates form the suitable micro-environments wherein barite saturation conditions are likely to be fulfilled (Bishop, 1988; Stroobants *et al.*, 1991; Dehairs *et al.*, 1980). Such barite micro-crystals account for the largest fraction of total particulate Ba at mesopelagic depths (Dehairs *et al.*, 1980). Furthermore, investigations in the Southern Ocean indicate that the occurrence of Ba-barite at mesopelagic depths is related to the type of production (*i.e.* new *versus* recycled) in the euphotic layer, with significant mesopelagic barite accumulation reflecting predominance of new, or export production (Dehairs *et al.*, 1992).

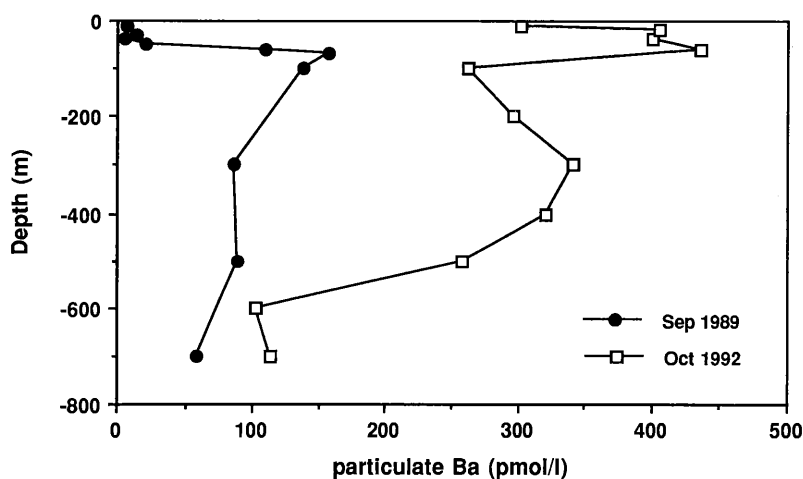


Fig. 7.— Vertical profiles of total particulate barium in the upper 600 m of water column at Station 45°00' N–8°28' W (September 1989 cruise) and at Station 37 (October 1992 cruise).

To investigate the spatial and temporal variability of new and recycled production in the Gulf of Biscay, the distribution of mesopelagic Ba-barite was systematically studied. During September 1989 and June 1990, generally low mesopelagic Ba-barite concentrations were observed. A typical profile at a station located in the deep basin region (45°00' N, 8°28' W) is shown in figure 7. Despite the relatively low Ba concentrations (maxima are close to 200 pmol l^{-1}) the broad Ba maximum in the 100 to 400 m depth range is clearly visible. Such relatively low concentrations were also observed during spring and summer in the marginal ice zone (MIZ) of the Scotia-Weddell Confluence and in the

coastal and continental shelf (CCSZ) area of Prydz Bay (Dehairs *et al.*, 1991, 1992). In these areas the low mesopelagic Ba-barite concentrations coincided with high biomasses and primary productivities. Values of net production vary between 600 and 1400 mg C m⁻² d⁻¹ (Mathot *et al.*, 1992). However, the primary production was observed to be mainly ammonium sustained (f -ratio < 0.5; Goeyens *et al.*, 1991; Dehairs *et al.*, 1992), reflecting predominance of recycling over export. On the contrary, the low barite concentrations in the Gulf of Biscay correspond to low productivities. Primary production in this zone ranges from 47 to 220 mg C m⁻² d⁻¹ (Elskens *et al.*, this volume). The nitrogen assimilation experiments indicate that, during spring, the ecosystem evolves from a first phase of about 2 months where new production predominates into a second one dominated by regenerated production (f -ratio ranging from 0.1 to 0.9). In this case, it is thus possible that both effects (low productivities and limited export production) contribute to the low observed mesopelagic barite.

During June and October 1992 at the ocean margin of the Gulf of Biscay (La Chapelle Bank), the situation was quite different. At these stations, significant concentrations of mesopelagic Ba-barite are observed (maximal Ba concentrations up to 580 pmol l⁻¹ at 200 m; Station 47°25' N, 7°18' W). Figure 7 shows the profile for October, 1992. Such high concentrations were observed mainly in the ice free open ocean zone (OOZ) of the Antarctic Circumpolar Current (ACC), both in the Atlantic and Indian Ocean sectors (Dehairs *et al.*, 1990, 1991). These latter systems, though generally less productive than the MIZ and CCSZ systems, are characterized by increased relative importance of the new *versus* recycled production (f -ratio ≥ 0.5).

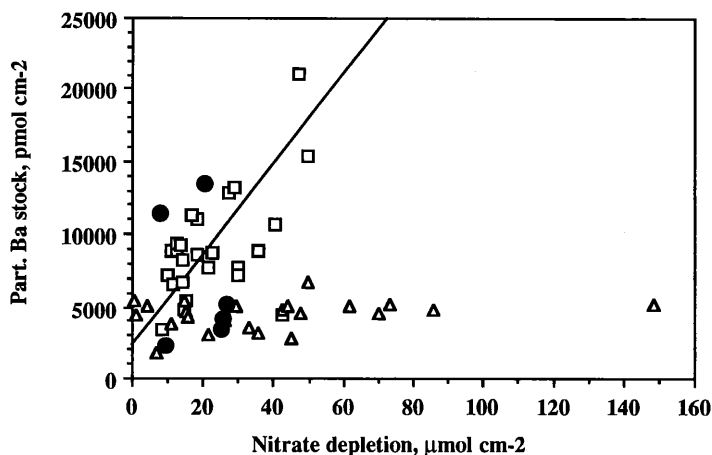


Fig. 8.— Stocks of total particulate Ba (pmol cm⁻²) at mesopelagic depth (*i.e.* between 100 to 500 m depth) *versus* nitrate depletion (11 μmol cm⁻²) for Southern Ocean Ooz (□) and MIZ + CCSZ stations (△) as given in Dehairs *et al.* (1992) and Gulf of Biscay (●; this study).

To visualize the difference between the two situations, Ba-barite stocks in the 60 to 500 m depth interval were plotted *versus* nitrate depletion over the season (figure 8). Ba stocks represent the integrated Ba amount, in nmol m^{-2} , over the depth interval considered. As previously mentioned in Elskens *et al.* (this volume), nitrate depletion is the integrated difference between the winter nitrate concentration and the observed *in situ* concentration in the mixed layer. It represents a conservative estimate of the nitrate consumed over the season, nitrate being either exported to the deep or recycled to a large degree. In figure 8, the data obtained in the Southern Ocean have also been reproduced. For the Southern Ocean, stations in the MIZ and the CCSZ typically have a wide range of nitrate depletion, but only a narrow range of low Ba-barite stocks. On the other hand, the OOOZ of the ACC shows generally much larger Ba-barite stocks for similar nitrate depletions and positive correlation between barite stocks and nitrate depletions is observed (figure 9). The stations sampled during 1989 and 1990 in the Gulf of Biscay fit the MIZ and CCSZ barium-nitrate depletion picture, while the stations of 1992 fit the OOOZ situation. This behavior suggests that export during 1992 have been significant while it was not in 1989 and 1990.

What differentiates these years? During 1989, 1990 and 1991, the surface waters (upper 60 m) have generally low stocks of particulate Ca, Sr and Si. Data in Table 5 show maximum stock concentrations of 742, 5.6 and 149 nmol cm^{-2} for Ca, Sr and Si respectively. During 1992, both in June and October, particulate Ca, Sr and Si stocks in the upper 60 m increased about tenfold, to reach a maximum of 4833, 47.4 and $2100 \text{ nmol cm}^{-2}$, respectively. This significant increase in Ca, Sr and Si contents during 1992 was not paralleled by a similar increase in POC. In June 1992 the stock concentrations of POC was $82 \mu\text{mol cm}^{-2}$, while in October it was $20 \mu\text{mol cm}^{-2}$, similar to the values observed during the previous years. The phytoplankton community thus appear to have been quite different in 1992 with predominance of CaCO_3 secreting species (Coccolithophoridae) and also diatoms. This difference in phytoplankton composition has probably resulted in very large Ba uptake in the euphotic layer (stock concentrations of Ba in surface water during June is up to $28,946 \text{ pmol cm}^{-2}$!) but also in the build-up of larger mesopelagic Ba-barite stocks (Table 5). Thus increased contribution of skeleton forming groups in the phytoplankton community of 1992 has increased the relative importance of export production, probably as the result of increased particle density.

3.3.— Dissolved to particulate transfer experiments.

One of the aim of our study is also to understand the mechanism and to quantify the kinetics of the transfer of dissolved trace metals from the dissolved phase to the particulate phase. The vertical distribution of the concentration

Table 5

Stock concentrations in the upper 60 m of water column for POC, PN, Chlorophyll *a*, particulate Al, Ca, Sr, Si and Ba. Concentrations of Ca, Sr, Si and Ba have been corrected for the fraction carried by the terrigenous aluminosilicate fraction using crustal compositions as given by Bowen, 1979. Stocks represent depth-integrated concentrations of the respective elements over the thickness of the mixed layer. Nitrate depletion over the season were calculated according to Elskens *et al.* (this volume). Mesopelagic Ba stocks are depth-integrated concentrations between 100 and 500 m depth.

Position	St.	Date	POC $\mu\text{mol}/\text{cm}^2$	PN $\mu\text{mol}/\text{cm}^2$	Chl. <i>a</i> $\mu\text{g}/\text{cm}^2$	Al nmol/cm^2	Ca nmol/cm^2	Sr nmol/cm^2	Si nmol/cm^2	Ba pmol/cm^2	NO ₃ depletion $\mu\text{mol}/\text{cm}^2$	Mesopelagic Ba pmol/cm^2
47°17'N 8°37'W		Sep-89	14.9	2.4	1.6	13.2	738	5.6	119	65	24.9	3395
46°00'N 8°29'W		Sep-89	18.6	2.5	1.6	6	466	3.4	163	59	25.4	4230
45°00'N 8°28'W		Sep-89	20.4	2.8	1.1	9.6	589	4.3	149	113	26.8	5172
46°25'N 8°00'W	38	Jul-90	30.6	4.4	2.6	15.9	742	4.6	—	67	9.2	2310
47°23'N 7°18'W		Jun-92	82.1	9.2	5.7	200	4833	47.4	1630	28946	20.6	13416
47°25'N 7°15'W	37	Oct-92	19.7	2.5	6.3	46.3	3465	22.1	2100	2378	7.8	11415

of trace elements normalized with respect to Al clearly indicate their relative enrichment in the photic zone suggesting a possible influence of the biological activity during this transfer. This is confirmed by the fact that the vertical distribution of dissolved metals often exhibits a nutrient like profile, where the metals are strongly depleted in the photic zone (Bruland & Franks, 1983). For some metals like for example Zn, Mn or Fe, their metabolic role is known and their role as essential oligo-elements well established. Others like Cd have no active role in the metabolism of organisms, but the dissolved species are also strongly depleted in the photic zone and the composition of the particles exhibits a relative enrichment of this metal in the surface ones. One may thus assume that besides the active uptake of trace elements by the plankton, there may be also passive adsorption of some other elements by the solid-liquid interface created during the production of particulate organic matter.

In order to gain a better understanding of the behaviour of the trace metals in the euphotic zone, we have first investigated the influence of the concentration of the metal on its rate of uptake by using radiotracers supported by concentration of the stable isotope slightly higher than the natural concentration. Thus in the following experiments 1 nCi represents between 50 and 100 pmol of the non-radioactive metal.

The influence of the amount of radionuclide added to the sample on its transfer from the dissolved to the particulate phase is shown in figure 9. Since the amount transferred to the solid phase represents no more than 5% and is usually less than 1% of the total radioactivity of the system, one may consider that the activity of the aqueous and thus the concentration of the metal phase remain constant during the experiment. As shown in the figure, the experimental results are well described by a Langmuir type adsorption isotherm where

$$(1) \quad X^* = \frac{S_T x^*}{x^* + \frac{1}{K}}$$

x^* and X^* are respectively the activities of the aqueous and solid phases, S_T is the total amount of adsorption sites and K is the equilibrium constant of the adsorption reaction

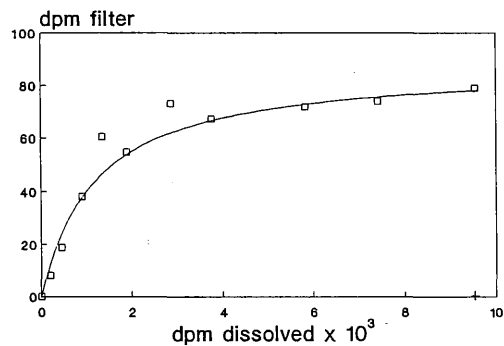
$$(2) \quad x^* + S_o = X^*$$

where S_o is a non-occupied site of the solid phase.

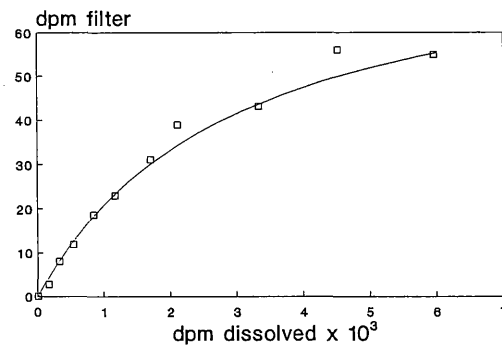
It is however important to note that this equation may also represent the uptake resulting from a biological activity governed by a Menten-Michaelis kinetic process, where the rate equation is given by

$$(3) \quad r = \frac{k_{\max} x^*}{K_m + x^*}$$

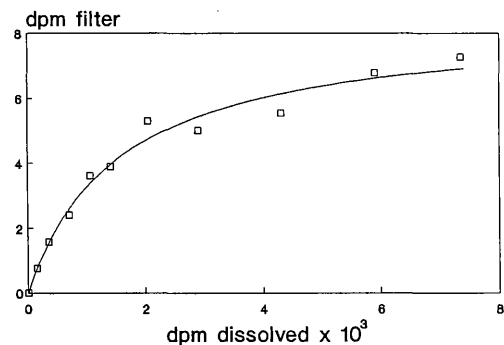
MANGANESE



ZINC



COBALT



CADMIUM

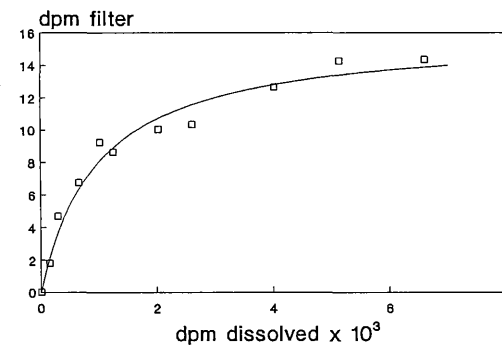


Fig. 9.- Activity of the particles as a function of the remaining activity of the aqueous solution after 24 hours of reaction. Activities corresponding to a sample of 600 ml of seawater taken at Station 21.

where k_{\max} is the maximum rate of uptake of a substrate and K_m the Michaelis constant. In fact, equations (1) and (3) are similar expressions and it is impossible to distinguish the two mechanisms by considering the influence of the concentration of the metal in the dissolved phase on its transfer to the solid phase. We have thus performed other experiments in order to better define the role of organisms in this transfer.

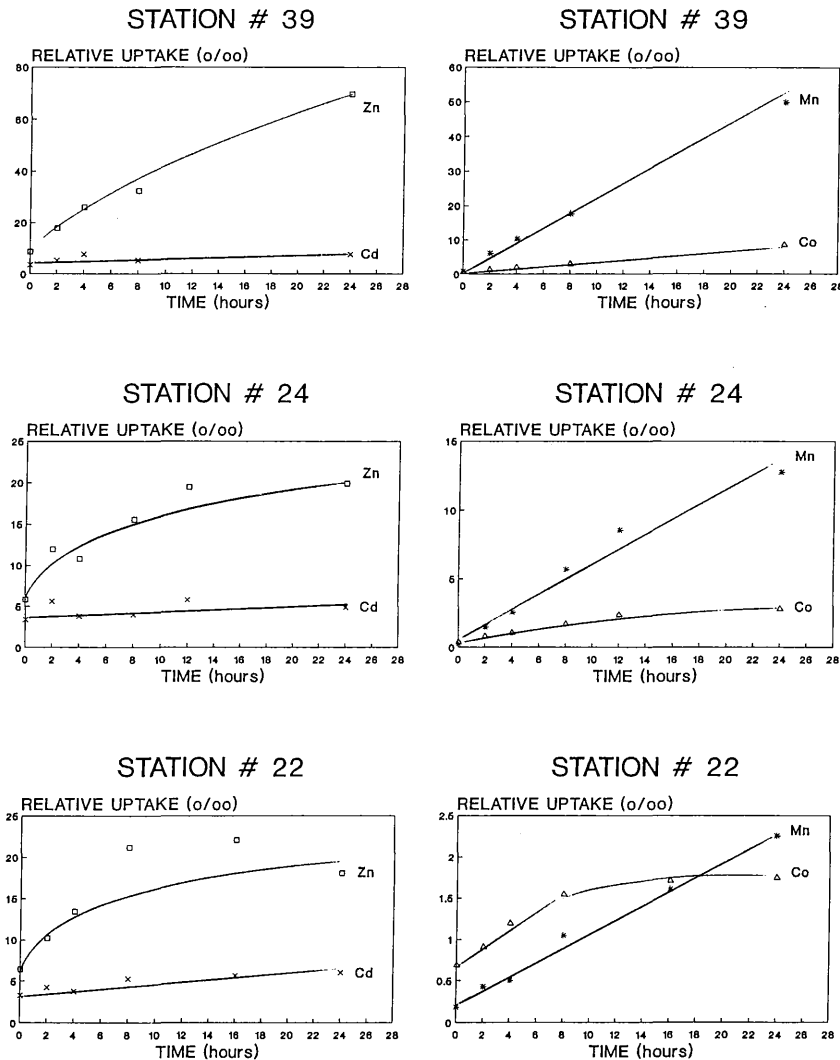


Fig. 10.– Comparison of the kinetics of transfer of radionuclides at three stations corresponding to various primary productions (#22: 457, #24: 900, #39: 2100 mg C m⁻² d⁻¹). The results are expressed in terms of activity of the solid phase divided by the total activity of the sample, in ‰.

In the following kinetic experiments, the spikes have been adjusted in order to obtain an initial radioactivity of the aqueous phase close to 1000 dpm per 100 ml seawater for all the radionuclides. We will first compare rates of uptake of the radionuclides obtained during 24 hours incubation experiments under constant light conditions at three stations with contrasting productivities. At station 22 on the continental shelf the ^{14}C measured productivity was $457 \text{ mg C m}^{-2} \text{ d}^{-1}$. The uptake of radionuclides as a function of time is given in figure 10.

The results are expressed in terms of relative uptake which represents the radioactivity of the solid phase after a given reaction time divided by the total radioactivity of the spiked seawater sample (dissolved + particulate). The kinetic behaviour of the various radionuclides is very similar to what has been observed in the English Channel and the Mediterranean (Wollast & Loijens, 1991). In the case of Zn and Cd, an important instantaneous uptake of radionuclides is observed, followed by a slower transfer. In the case of Zn, the concentration of sorbed element reaches rapidly a maximum and even starts to decrease. Mn and Co on the other hand are only very slightly adsorbed during the initial stage but are transferred at a rate which remains almost constant during the 24 hours of the experiment.

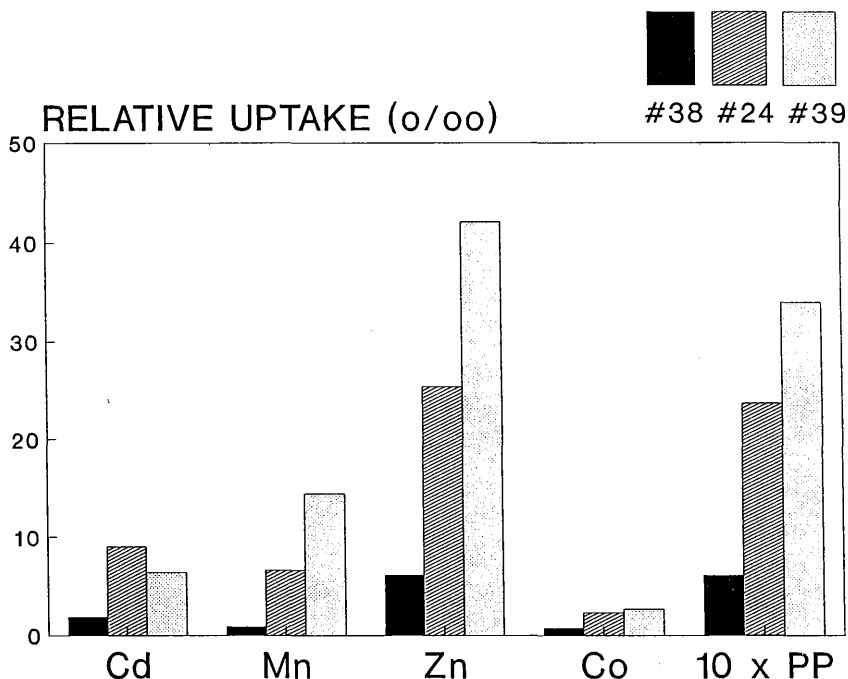


Fig. 11.— Comparison of the uptake of radioactive trace elements and radiocarbon (PP) during incubation experiments of 12 hours under natural light conditions.

The results obtained are rather different at station 39 which is situated in the upwelling region along the Spanish coast. The measured ^{14}C productivity was $2100 \text{ mg m}^{-2} \text{ d}^{-1}$. (Elskens *et al.*, this volume). There is still a rather high initial uptake of Cd and Zn during the incubation experiment (figure 10) but there is also a continuous and linear increase of the amount transferred to the solid phase for all the elements except maybe for Cd. The uptake after 24 hours is also significantly higher for Mn, Zn and Co as compared with the experiment carried out at the previous station. This result suggests that the transfer due to the photosynthetic activity might be predominant in this upwelling area. The role of biological activity is also confirmed by the results obtained at Station 24 for which an intermediate primary production was observed ($900 \text{ mg C m}^{-2} \text{ d}^{-1}$).

The influence of primary production on the transfer of trace metals is also well demonstrated by an incubation experiment under natural light conditions performed at Stations 38, 24 and 39, corresponding to areas of increasing productivity. As shown in figure 11, there is an excellent correlation between the C_{inorg} uptake and the trace metals fixations.

The influence of biological activity on the transfer of trace metals from the dissolved to the particulate phase was also investigated by using different conditions during the incubation experiment. Three spiked seawater samples were incubated respectively under constant light, in the dark and after addition of sodium azide to inhibit biological activity. The results of one of these experiments performed at Stations 38, 24 and 39 are shown on figure 12. The effect of these various conditions on the rate of transfer is the largest for Station 39 which is the station exhibiting the highest productivity. At Station 38 located in the Biscay oligotrophic area with a primary production of $142 \text{ mg C m}^{-2} \text{ d}^{-1}$, the uptake of trace elements is limited and the influence of the various conditions on the relative uptake is strongly reduced.

The influence of these conditions is also less pronounced at Station 24, characterized by an intermediate primary production ($900 \text{ mg C m}^{-2} \text{ d}^{-1}$). This station is however under the influence of the French coast and the Channel entry. The solid phase thus probably contains a significant fraction of inorganic detrital particles of continental origin.

Finally a few long term experiments were also performed, where the transfer of trace elements during incubation experiments carried out in the dark were followed for a few months. The results obtained at Station 7 located in the English Channel are shown as an example in figure 13. This station is strongly under the influence of continental input as indicated by its high Al content (see above).

The behaviour of the trace metals shown here is very similar to what has been observed during the laboratory experiments of Li *et al.* (1984) Nyffeler *et al.* (1984), Jannasch *et al.* (1988) or during mesocosm experiments (Santschi *et*

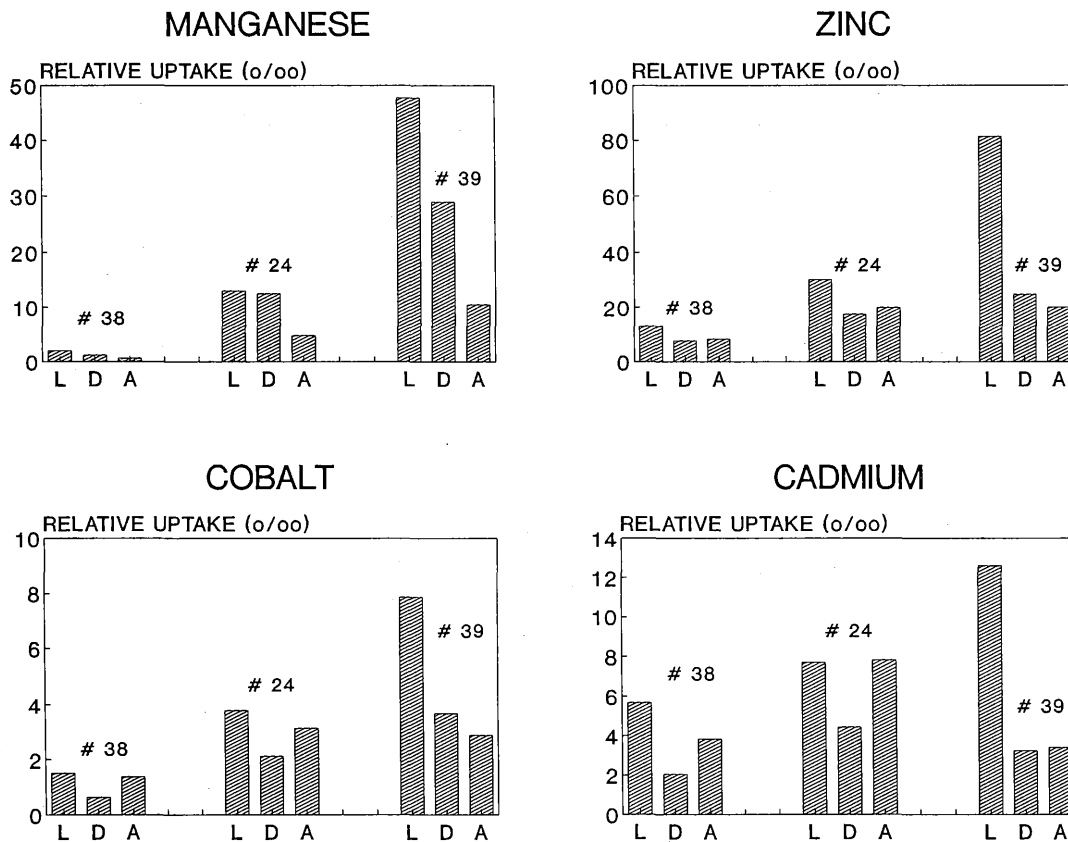


Fig. 12.— Influence of the incubation conditions on the transfer of radionuclides. Incubation during 24 hours under constant light (L), in the dark (D), and with samples inhibited with sodium azide (A). The primary productions are as for figure 11.

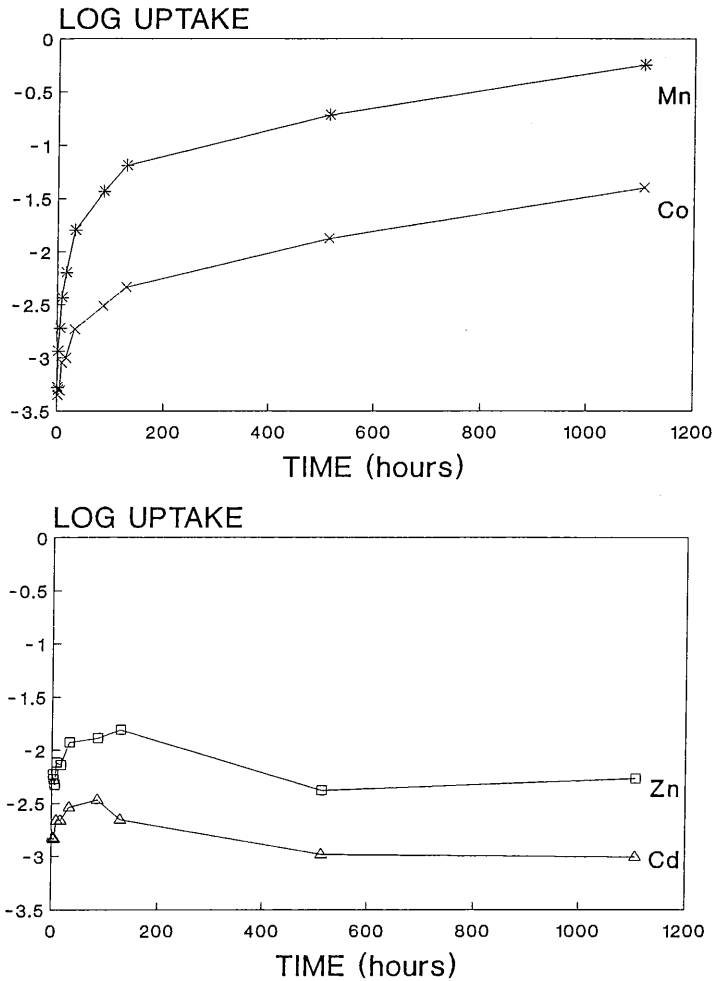


Fig. 13.— Relative uptake of radionuclides during long term experiments performed in the dark at Station 7 which is dominated by the presence of detrital material.

al., 1986). However differences can be distinguished. For Co and Mn, there is a slow and continuous uptake of the dissolved elements which is still going on after two months. A very large fraction of the Mn added to the system has been removed from the aqueous solution after two months (56%). In the case of Cd and Zn, the uptake reaches a maximum after a few days and the radionuclides are then released back to the aqueous solution. The uptake of Zn and Cd after two months represents only 5‰ and 1‰ of the initial spike respectively. In this case it may be assumed that the system is close to equilibrium since the activities of the two metals have reached a steady concentration.

4.- Conclusions.

The distribution of particulate trace metals in the Southern Bight of the North Sea, the English Channel and the Gulf of Biscay reflects well the origin of the suspended matter and allows one to distinguish between the detrital fraction of continental origin and the biogenic material produced in the water column. As one may expect, the relative importance of the biological fraction is gradually increasing from the North Sea to the Gulf of Biscay. Abnormally high values have been detected, which can be attributed to anthropogenic effects.

The vertical distribution of the particulate trace metals in the water column is strongly influenced by the uptake of nutrient like elements in the euphotic zone. Most of the trace elements are strongly enriched in the particles of the surface waters, but seem rapidly released during the remineralization process in the deeper waters.

The use of radiotracers during incubation experiments carried out on natural seawater samples has been proven to be a very successful method to investigate the mechanism and the rate of transfer of trace elements from the dissolved to the particulate phase. The results obtained during the Belgian Global Change Programme indicate that biological activity plays an important role in the transfer of trace metals in the area investigated. The importance of this transfer explains well the enrichment observed for most of the trace metals in the particles present in the euphotic zone. There is however also a rapid chemical sorption process which is especially important for zinc and cadmium. The use of inhibitors of the biological activity indicates that a positive uptake is superposed to active biological process. In the case of manganese, the transfer is largely dominated by the biological uptake and there is furthermore a strong positive influence of light on the transfer.

As shown by several authors, this method can be used successfully to evaluate distribution coefficients of trace metals in the marine environment. One may hope that this method will also provide Redfield ratios for trace elements which will be used to evaluate quantitatively the contribution of biological activity to the scavenging of trace metals in the ocean.

Acknowledgements.

We would like to thank the Crews of the *R/V Belgica* and both A. Pollentier and J. Backers for their cooperation during the different cruises. We are also grateful to D. Bajura, N. Canu, J.P. Clément and J.M. Théate for their help during sampling and measurements. This work was funded by the Belgian State—Prime Minister's Service—Science Policy Office in the framework of the Impulse Programme "Global Change" (contracts nrs. GC/11/009, GC/12/011 and GC/03/010), and by the French Community of Belgium (Actions de Recherches Concertées, convention 89/94-131). Frank DEHAIRS and Michel Frankignoulle are Research Associates at the Belgian National Fund for Scientific Research (FNRS).

References.

- BACON M.P., HUH C.A., FLEER A.P., DEUSER W.G. (1985). Seasonality in the flux of natural radionuclides and plutonium in the deep Sargasso sea, *Deep-Sea Res.*, 32:273–286.
- BAEYENS W., GILLAIN G., DECADT G., ELSKENS I. (1987). Trace metals in the eastern part of the North Sea. I. Analyses and short term distribution, *Oceanol. Acta*, 10:167–179.
- BALISTRIERI L.S., MURRAY J.W. (1983). Metal solid interactions in the marine environment: Estimating the apparent equilibrium binding constants, *Geochim. Cosmochim. Acta*, 47:1091–1098.
- BISHOP J.K.B. (1988). The barite-opal-organic carbon association in oceanic particulate matter, *Nature*, 332:341–343.
- BISHOP J.K.B. (1989). *Regional extremes in particulate matter composition and flux: effects on the chemistry of the ocean interior*, in: W.H. Berger, V.S. Smetacek and G. Wefer (eds.), *Productivity of the Ocean. Present and Past*, John Wiley, New York, pp. 117–137.
- BOUQUEGNEAU J.M., GOBERT S., FRANKIGNOULLE M., DAUBY P. (1992). La matière en suspension de la couche de surface du plateau continental nord-ouest européen. II. Teneurs en métaux lourds et transfert dans la chaîne trophique, *Bull. Soc. roy. Sci. Liège*, 61:155–162.
- BOWEN H.J.M. (1979). *Environmental Chemistry of the Elements*, Academic Press, London, 333 pp.
- BRULAND K.W., FRANKS R.P. (1983). *Mn, Ni, Cu, Zn and Cd in the Western North Atlantic*, in: C.S. Wong, E. Boyle, K.W. Bruland, J.D. Burton and E.D. Goldberg (eds.), *Trace metals in Seawater*, NATO Conference Series, IV: Marine Sciences, Plenum Press, New York, pp. 395–414.
- BUCHHOLTZ M.R., SANTSCHI P.H., BROECKER W.S. (1985). *Comparison of radio-tracer K_d values from batch equilibration experiments with in-situ determinations in the deep sea using the MANOP lander: The importance of geochemical mechanisms in controlling ion uptake and migration*, in: *Proc. Scientific Seminar on the Application of Distribution Coefficients to radiological Assessment Models*, CEC, Brussels.
- DAUBY P., GOBERT S., FRANKIGNOULLE M., BOUQUEGNEAU J.M. (1993). Distribution of particulate Al, Cd, Cr, Cu, Pb, Ti, Zn and $\delta^{13}\text{C}$ in the English Channel and adjacent areas, *Oceanol. Acta*, submitted.
- DEHAIRS F., CHESSELET R., JEDWAB J. (1980). Discrete suspended particles of barite and the barium cycle in the open ocean, *Earth Planet. Sci. Lett.*, 49:528–550.
- DEHAIRS F., GILLAIN G., DEBONDT M., VANDENHOUT A. (1985). *The distribution of trace and major elements in Channel and North Sea suspended matter*, in: R. Van Grieken and R. Wollast (eds.), *Progress in Belgian Oceanographic Research*, Antwerp University Press, pp. 136–146.
- DEHAIRS F., GOEYENS L., STROOBANTS N., BERNARD P., GOYET C., POISSON A., CHESSELET R. (1990). On suspended barite and the oxygen minimum in the Southern Ocean, *Global Biogeochem. Cycles*, 4:85–102.

- DEHAIRS F., STROOBANTS N. and GOEYENS L. (1991). Suspended barite as a tracer of biological activity in the Southern Ocean, *Mar. Chem.*, 35:399–410.
- DEHAIRS F., BAEYENS W., GOEYENS L. (1992). Accumulation of suspended barite at meso-pelagic depths and export production in the Southern Ocean, *Science*, 258:1332–1335.
- DUCE *et al.* (1991). The atmospheric input of trace species to the world ocean, *Global Biogeochem. Cycles*, 5:193–259.
- DUINKER J.C., NOLTING R.F. (1977). Dissolved and particulate trace metals in the Rhine estuary and the Southern Bight, *Mar. Pollut. Bull.*, 8:65–71.
- DYMOND J., SUESS E., LYLE M. (1992). Barium in deep-sea sediment: a geochemical proxy for paleoproductivity, *Paleoceanogr.*, 7:163–169.
- ELSKENS M., CHOU L., DAUBY P., FRANKIGNOULLE M., GOEYENS L., LOIJENS M. and WOLLAST R. (1993). *Primary production of the Gulf of Biscay*, this volume.
- GOEYENS L., SORENSSON F., TRÉGUER P., MORVAN J., PANOUSE M., DEHAIRS F. (1991). Spatio-temporal variability of inorganic nitrogen stocks and assimilatory fluxes in the Scotia-Weddell Confluence area, *Mar. Ecol. Progr. Ser.*, 77:7–19.
- HOENIG M., REGNIER P., WOLLAST R. (1989). Automated trace metals analyses of slurried solid samples by GFAAS with application to sediments and suspended matter collected in natural waters, *J. Anal. Atom. Spectrom.*, 4:631–634.
- HOENIG M., REGNIER P., CHOU L. (1991a). Determination of the high aluminium content in suspended matter samples collected in natural waters by slurry sampling – Electrothermal Atomic Absorption Spectrometry, *J. Anal. Atom. Spectrom.*, 6:273–274.
- HOENIG M., REGNIER P., CHOU L. (1991b). Dosage direct d'éléments majeurs dans des matières en suspension des eaux d'estuaires et marines par spectrométrie d'absorption atomique électrothermique, *Analysis*, 19:163–166.
- ICES (1988). *Studies of contaminants in sediments*, in: *Report of the ICES Advisory Committee on Marine Pollution*, Cooperative Res. Rep., Copenhagen, 160:83–85.
- JANNASCH H.W., HONEYMAN B.D., BALISTRIERI L.S., MURRAY J.W. (1988). Kinetics of trace element uptake by marine particles, *Geochim. Cosmochim. Acta*, 52:567–577.
- LI Y.H., BURKHARDT L., BUCHHOLTZ M., O'HARA P., SANTSCHI P.H. (1984). Partition of radiotracers between suspended particles and seawater, *Geochim. Cosmochim. Acta*, 48:2011–2019.
- LORING D.H. (1988). *Normalization of heavy metal data*, in: *Report of the 75th statutory Meeting of the WGMS in relation to pollution*, Annex 2, ICES Publ., Copenhagen, 19–42.
- MARTIN J.M., MEYBECK M. (1979). Elemental mass-balance of material carried by world major rivers, *Mar. Chem.*, 7:173–206.

- MARTIN J.M., WHITFIELD M. (1983). *The significance of the river input of chemical elements to the ocean*, in: C.S. Wong, E. Boyle, K.W. Bruland, J.D. Burton and E.D. Goldberg (eds.), *Trace metals in Seawater*, NATO Conference Series, IV: Marine Sciences, Plenum Press, New York, pp. 265–296.
- MATHOT S., DANDOIS J.M., LANCELOT C. (1992). Gross and net primary production in the Scotia-Weddel Sea sector of the Southern Ocean during spring 1988, *Pol. Biol.*, 12:321–332.
- MOREL F.M., HUDSON R.J. (1985). *The biogeochemical cycle of trace elements in aqueous systems: Redfield revisited*, in: W. Stumm (ed.), *Chemical Processes in Lakes*, John Wiley & Sons, New York, pp. 389–426.
- MOUCHEL J.M., MARTIN J.M. (1990). *Adsorption Behaviour of Several Trace Metals in the Changjiang Plume*, in: G.H. Yu, J.M. Martin and J.Y. Zhan (eds.), *Proc. Int. Symp. of the Changjiang Estuary and its Adjacent coastal waters of the East China Sea*, China Ocean Press, pp. 263–279.
- NOLTING R.F., EISMA D. (1988). Elementary composition of suspended particulate matter in the North Sea, *Neth. J. Sea Res.*, 22:219–236.
- NYFFELER U.P., LI Y.H., SANTSCHI P.H. (1984). A kinetic approach to describe trace element distribution between particles and solution in natural systems, *Geochim. Cosmochim. Acta*, 48:1513–1522.
- PRICE N.M., MOREL F.M. (1990). *Role of the extracellular enzymatic reactions in natural waters*, in: W. Stumm (ed.), *Aquatic Chemical Kinetics*, John Wiley & Sons, New York, pp. 235–257.
- SANTSCHI P.H., NYFFELER U.P., ANDERSON R.F., SCHIFF S.L., O'HARA P. (1986). Response of radioactive trace metals to acid-base titration in controlled experimental ecosystems: Evaluation of transport parameters for application to whole-lake radio-tracer experiments, *Can. J. Fish. aquat. Sci.*, 43:60–77.
- STROOBANTS N., DEHAIRS F., GOEYENS L., VANDERHEIJDEN N., VAN GRIEKEN R. (1991). Barite formation in the Southern Ocean water, *Mar. Chem.*, 35:411–421.
- WINDOM H.L., SHROPP S.J., CALDER F.D., RYAN J.D., SMITH R.G. Jr., BURNEY L.C., LEWIS F.G., RAWLINSON C.H. (1989). Natural trace metal concentrations in estuarine and coastal marine sediments of the South Eastern United States, *Environ. Sci. Technol.*, 23:314–320.
- WOLLAST R., LOIJENS M. (1991). *Study of the scavenging of trace metals in marine systems using radionuclides*, in: J. Kershaw and D.S. Woodhead (eds.), *Radionuclides in the Study of Marine Processes*, Elsevier, pp. 154–163.

Modelling the Coastal Ocean's Complex Ecohydrodynamics

A case study: the Northern Bering Sea

Jacques C.J. NIHOUL, P. ADAM and S. DJENIDI

GHER, University of Liège

É. DELEERSNIJDER

ASTR. University of Louvain

Abstract.

There is a need for three-dimensional biogeochemical/ecosystem models.

On the one hand, geochemical and ecological processes are strongly correlated with physical processes by the resonant interactions and subsequent scale matching of the ecohydrodynamic adjustment. On the other hand, ecosystems live on nutrient supplies which are partly regenerated in the water column—hence subjected to the caprices of the local hydrodynamics—, partly imported into the system through the boundaries (bottom-sediments, coasts, air-sea interface...) with a spatial variability which inevitably, is imprinted on the system's kinetics.

The complexity of the biogeochemical processes to take into account however raises the question of the feasibility and reliability of models with very sophisticated physics and biology. A compromise has to be found, incorporating enough of each discipline's sophistication to be realistic but little enough to keep the model between tractable bounds.

The role of the Ocean in the global balance of the Earth's biogeochemical cycles has long been recognized but it is only recently that one has begun to realize the cogent part played by shelf and coastal zones (the so-called "neritosphere") in the global environment's dynamics.

The neritosphere extends from the shore-lines, beaches and estuaries across continental shelves, to where exchanges and interactions occur with the ocean. Fundamentally different hydrodynamic regimes occur in the ocean, where flow in the interior is geostrophically balanced, and on the shelf where surface and bottom stresses associated with wind and tidal forcings, together with buoyancy inputs at the boundaries, tend to dominate the motion.

The study of the neritosphere is essential not only because it is particularly vulnerable to bifurcations of the global environment but mainly because the majority of terrestrial rejections, transiting through the neritosphere, are there reprocessed, so that neritic physical and biogeochemical mechanisms condition the form and rythm of global fluxes between land, atmosphere and ocean.

Neritic processes notably differ from oceanic processes, not only because biogeochemical reactions occur in different conditions (of pressure, pH ...) and in a range of concentrations and relative abundance of elements beyond compare with the ocean but mainly because the shelf hydrodynamics is specific.

Hydrodynamic processes the time scales of which correspond to the time scales of biological populations, capture these populations in their physical spatial structures and the frequency or persistence of the latter command the speed of the exchanges with the ocean or the atmosphere (Nihoul and Djenidi, 1991).

It is difficult to see how a *simple* model could be used to describe ecosystems and biogeochemical cycles. On the one hand, geochemical and ecological processes are strongly correlated with physical processes by the resonant interactions and subsequent scale matching of the ecohydrodynamic adjustment, on the other hand, they live on nutrient supplies which are partly regenerated in the water column—hence subjected to the caprices of the local hydrodynamics—, partly imported into the system through the boundaries (bottom-sediments, coasts, air-sea interface, ...) with a spatial variability which, inevitably, is imprinted on the system's kinetics.

A recent investigation of the Northern Bering Sea's Ecohydrodynamics (Nihoul and Djenidi, 1991; Nihoul *et al.*, 1992) has shown, for instance, that the variations in time and space of primary and secondary productions in the Northern Bering and Chukchi Seas and the export of carbon to the Arctic basin were entirely controlled by the persistence of an upwelling in the Anadyr Strait region and the subsequent advection to the Bering Strait and deployment in the Northern Bering Sea of the plume of nutrient-rich water carried along by the Anadyr Stream.

The model applied in this study was the GHER 3D Primitive Equation Model divided in two submodels (Nihoul *et al.*, 1989; Adam, 1991):

- (i) the hydrodynamic model, the state variables of which are the velocity vector \mathbf{v} , the pressure p , the temperature θ , the buoyancy b (or salinity), the turbulent kinetic energy k and the turbulent dissipation rate ϵ (or mixing length ℓ);
- (ii) the plankton ecosystem model, the state variables of which are the concentrations n_1, n_2, \dots of nutrients, the biomasses of phytoplankton φ ,

zooplankton z , bacteria β and the concentration of organic matter d (interactions with the benthic ecosystem are treated in the bottom boundary conditions).

Some representative results are discussed below. Comparison with observations (Adam, 1991; Brasseur and Haus, 1991) shows that this model—with fairly sophisticated hydrodynamics and comparatively simple ecodynamics—is able to reproduce the essentials of the Northern Bering Sea’s Ecohydrodynamics which earlier models and studies—with a more detailed ecodynamic insight and simpler physics—had failed to perceive.

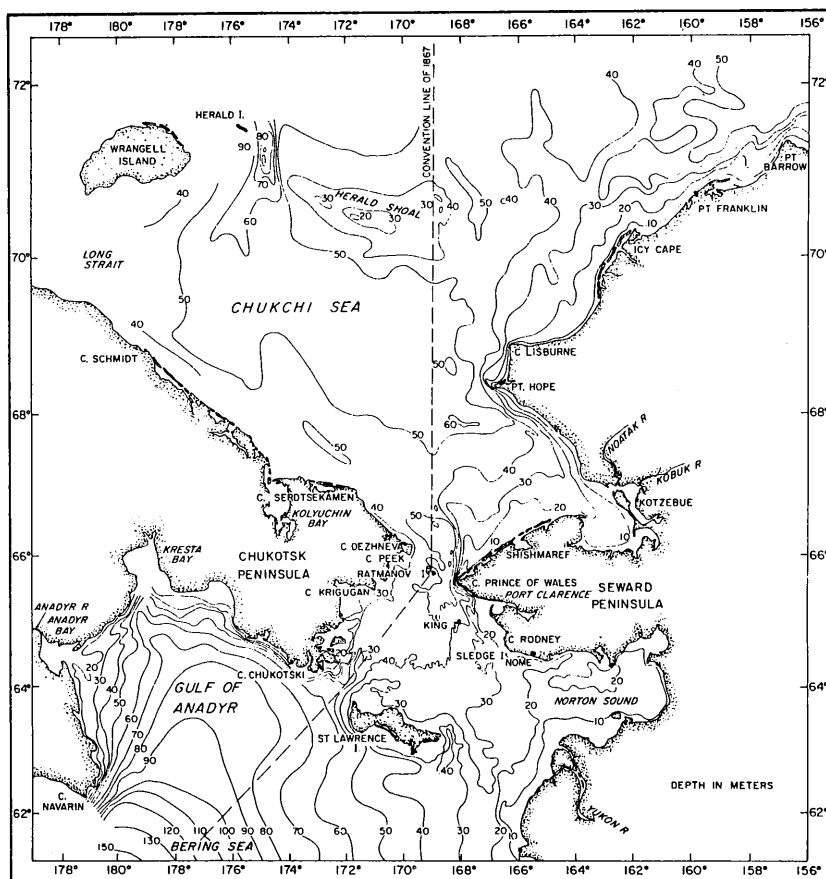


Fig. 1.— The Northern Bering Sea

3 D model of the Northern Bering's Sea ecohydrodynamics.

The Northern Bering Sea is a relatively shallow basin limited by the Bering Strait to the north and St. Lawrence Island to the south (figure 1). The flow passing through the Bering Strait, from the Pacific Ocean to the Arctic Ocean, penetrates the Northern Bering Sea through the Strait of Anadyr, to the west of St. Lawrence and through the Strait of Shpanberg, to the east. More than 60 % of the mean northward transport of water through the Bering Strait is derived from the "Anadyr Stream", a subsidiary of the Bering Slope Current which flows around the coasts of the Gulf of Anadyr, following the 60–70 isobaths, to the Anadyr Strait (Coachman *et al.*, 1975).

An extensive survey of the Northern Bering Sea was carried on for five years in the scope of the NSF ISHTAR Program. The observations were concentrated in the summer months with the objective of determining the main physical, chemical and biological characteristics of the system in typical summer situations (*e.g.* Walsh *et al.*, 1985, 1989).

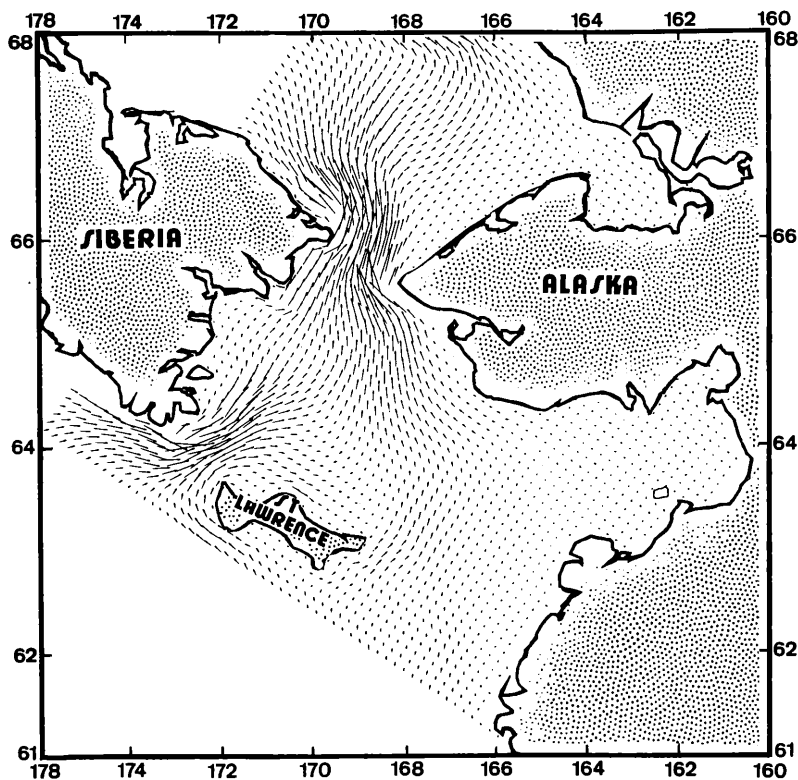


Fig. 2.— Total transport in the Northern Bering Sea calculated by the 3 D Model (Reference summer situation 1.8 Sv through Bering Strait).

The data were exploited—together with historical and climatic data—in simulation exercises, using the GHER 3D Model, aimed at the mathematical visualization of the general ecohydrodynamics of the Northern Bering Sea in the summer.

Figure 2 shows the total transport computed by the three-dimensional model. One can see the essential contribution of the “Anadyr Stream” flowing in through the Anadyr Strait and deploying in the Northern Bering Sea, in agreement with the observations.

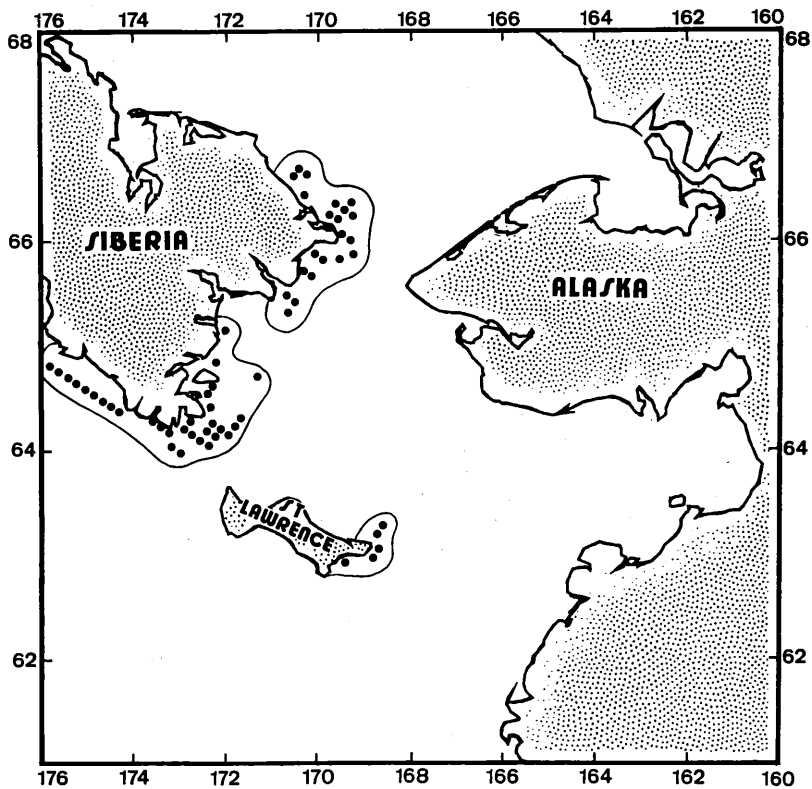


Fig. 3.— Upwellings/upsloping along the Siberian coast and the East coast of St. Lawrence’s Island indicated by grid points where the upwelling/upsloping vertical velocity is significantly high (as much as 4 m day^{-1} on the western side of the Anadyr Strait) [Reference summer situation].

Horizontal fields of the vertical velocity at different depths show marked upwellings and downwellings reflected in the horizontal and vertical buoyancy distributions (figures 3, 4, 5).

Figures 4 and 5 represent the buoyancy field at 5 m and 15 m depth. Regions of upwelling (along the Siberian coast and the east coast of St. Lawrence

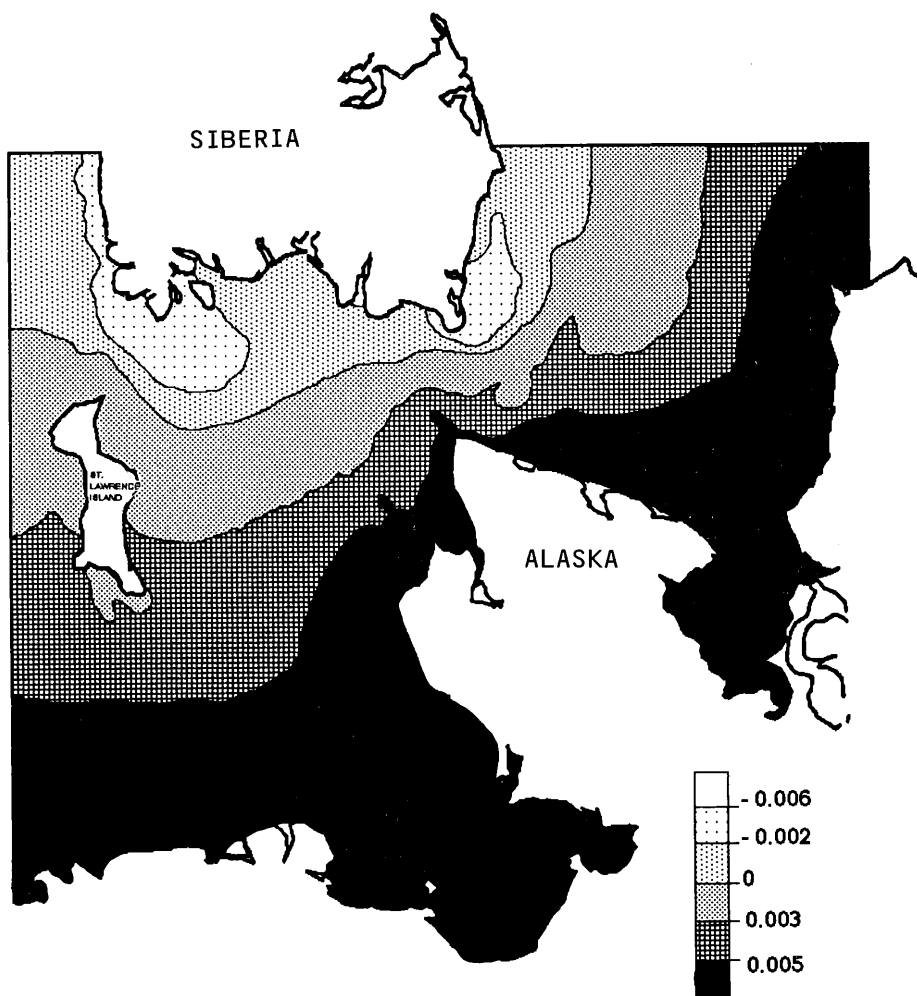


Fig. 4.- Buoyancy field in the Northern Bering Sea at 5 m depth (ms^{-2}) [Reference summer situation].

Island) and regions of downwelling (along the Alaskan coast and the west coast of St. Lawrence Island) are marked respectively by large negative values at the surface and large positive values at depth. Vertical advection and mixing in the Anadyr Strait are illustrated by the cross section distributions of buoyancy and turbulent kinetic energy shown in figure 6.

Horizontal distributions of buoyancy display non-negligible horizontal gradients and suggest the co-existence of different water masses. Schematically, one can discern three regions: the Anadyr Stream drawing along the nutrient-rich upwelled water of the Anadyr Strait into the Northern Bering and Chukchi

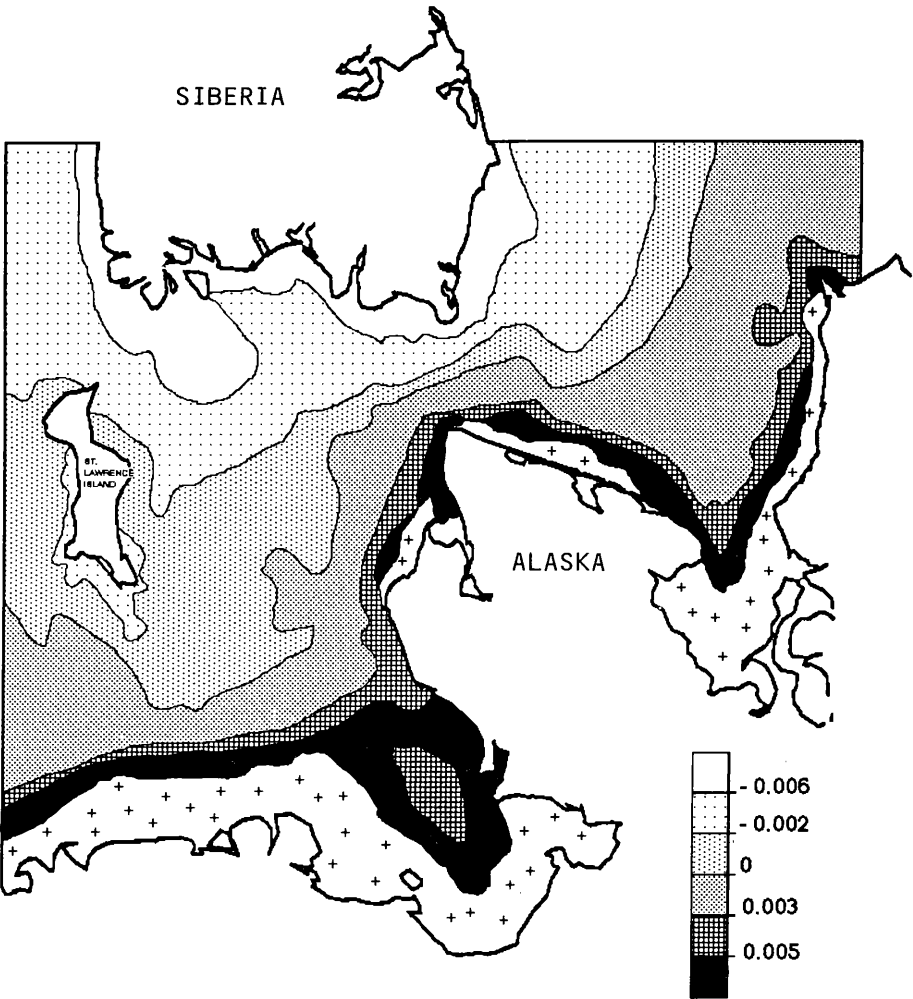


Fig. 5.– Buoyancy field in the Northern Bering Sea at 15 m depth (ms^{-2}) [Reference summer situation].

Seas, the Alaskan coastal waters filling the shallow eastern part and presumably overflowing the Anadyr Stream in the central region, an analogous riverine-influenced water mass off the Soviet coast denoted Siberian coastal water.

The separations between water masses have more or less pronounced frontal characteristics. The western front is the seat of occasional baroclinic instabilities giving rise to strong secondary flows in the form of eastwards propagating interleaving layers. These layers which have typically a width of 10 km, in the early stage of development, widen progressively as they flow eastwards, spreading the nutrient rich water over the Northern Bering Sea.

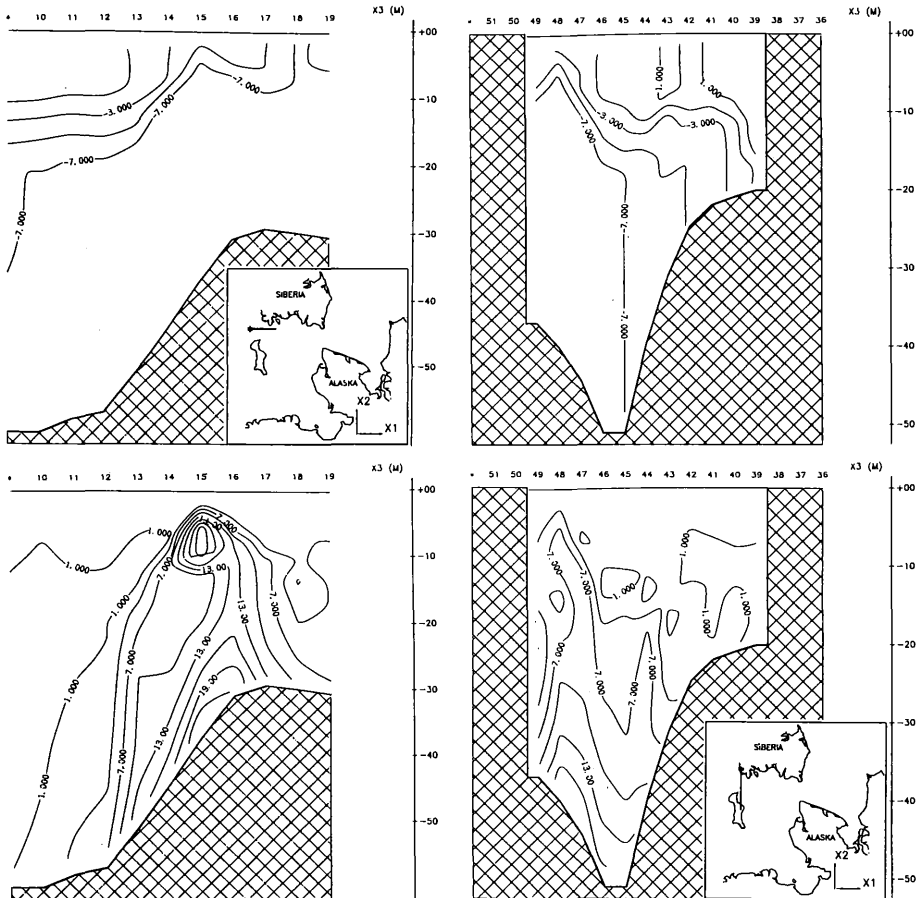


Fig. 6.— Distribution of buoyancy (in 10^{-3} m s^{-2}) [above] and turbulent kinetic energy (in $10^{-4} \text{ m}^2 \text{ s}^{-2}$) [below] in two perpendicular sections through the Anadyr Strait (Reference summer situation).

The formation of such layers can be explained by a baroclinic instability of the cold plume's frontal edge. Using the numerical results of the 3D Model, the stability analysis gives the characteristics of the incipient layers in good agreement with the observations.

The occasional occurrence of a marked upwelling plume swept along in the Northern Bering Sea as an unstable frontal current and the subsequent development of extruding layers, flowing eastwards, contribute, as the flow deployment described above, to the lateral diffusion of the nutrients and one may argue that the productivity of the Northern Bering Sea depends on the intensity and the variability of both the primary and secondary flows.

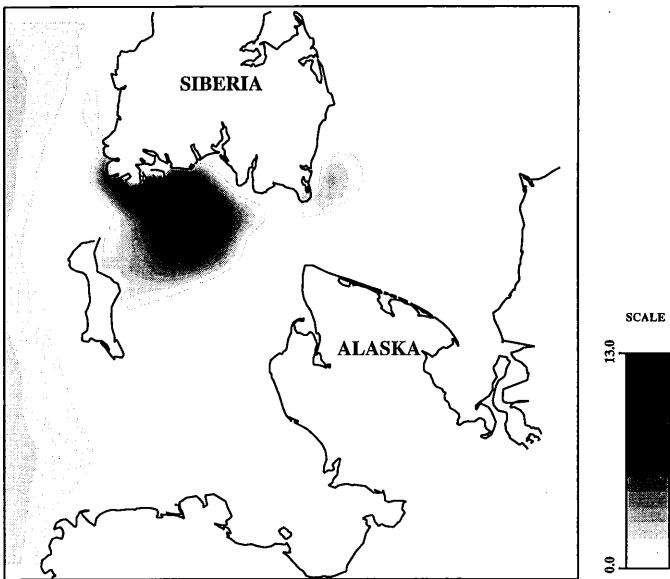


Fig. 7.– Sea surface distribution of nitrate in the Northern Bering Sea (in $\mu\text{atg N l}^{-1}$) [Reference summer situation].

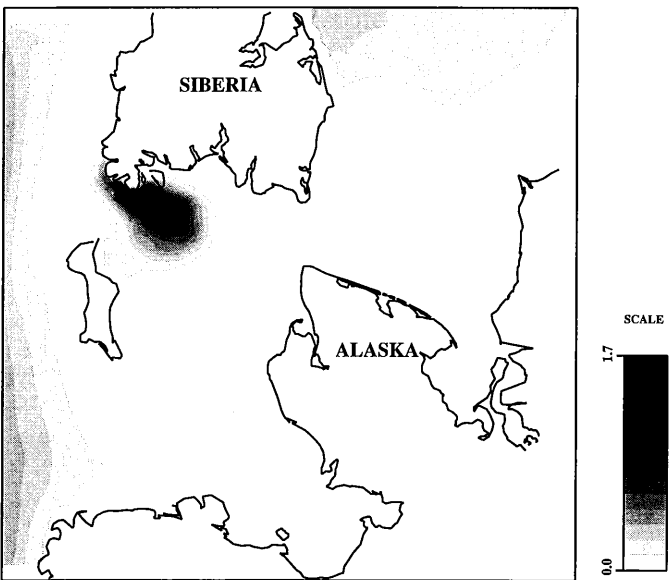


Fig. 8.– Sea surface distribution of ammonium in the Northern Bering Sea (in $\mu\text{atg N l}^{-1}$) [Reference summer situation].

The outputs of the hydrodynamic model can be used to compute horizontal and vertical velocities, velocity veerings, vertical buoyancy gradients, turbulent energy and dissipation rate, diffusivity coefficients, ... and these can be substituted in the plankton ecosystem model. The latter can then be solved with appropriate, "typical" boundary conditions induced from the observations.

Figures 7 and 8 show respectively the concentrations of nitrate and ammonium at the surface. They confirm the general transport of nutrients by the Anadyr Stream deploying in the Northern Bering Sea and the coastal upwellings/upslopings of nitrates. The nitrate distribution pattern however is indicative of a non-passive scalar dynamics. Nutrient uptake is evident and confirmed by the plankton distribution.

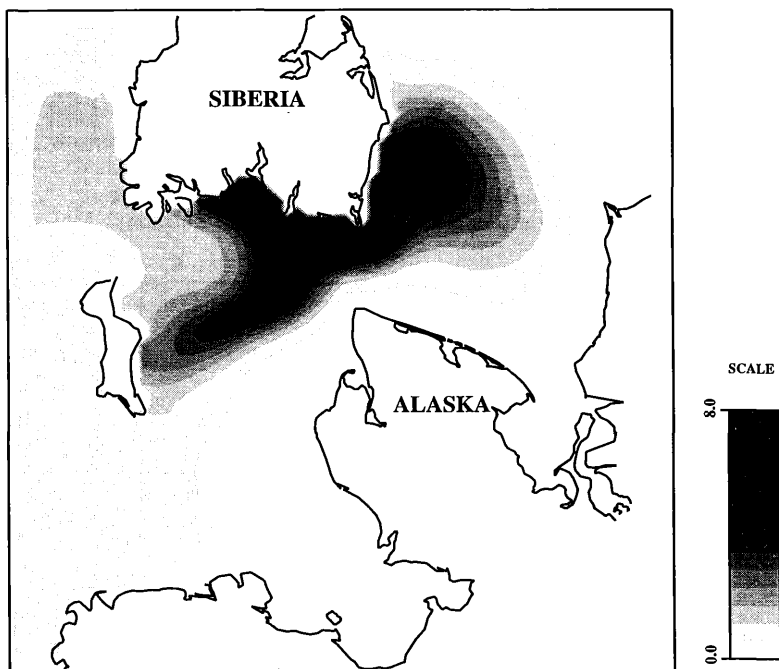


Fig. 9.— Sea surface distribution of phytoplankton in the Northern Bering Sea (in $\mu\text{atg NI}^{-1}$) [Reference summer situation].

Figures 9, 10 and 11 show respectively the surface distribution of phytoplankton, zooplankton and organic matter.

The lateral extension of primary production may be related to the occasional instability of the upwelling plume and the extrusion towards the east of nutrient rich layers of water. This is also reflected in the distribution of organic matter.

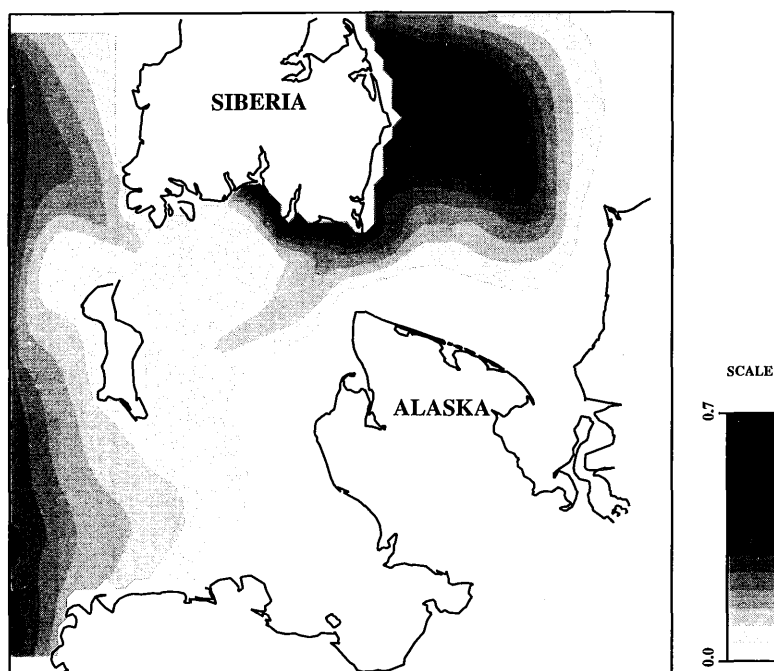


Fig. 10.— Sea surface distribution of zooplankton in the Northern Bering Sea (in $\mu\text{atg N l}^{-1}$) [Reference summer situation].

The secondary production maximum is relegated to the Chukchi basin as expected; grazing taking place progressively as phyto- and zooplankton populations are transported away by the Anadyr Stream.

Figure 12 shows the distribution of organic matter at 40 m depth.

The model of the Northern Bering Sea shows that organic matter fixed south of the Arctic Ocean and entrained north through the Bering Strait, together with a concomitant import of “new” dissolved nitrogen to the Chukchi and East Siberian shelves, can balance the carbon budgets of the polar basins.

Combining for instance the results of the hydrodynamic and ecohydrodynamic models, one estimates that the accumulated spring stock of nitrate in the Chukchi/East Siberian Seas is of the order of $\sim 1.2 \text{ atg NO}_3^- \text{ m}^{-2}$.

This accumulated stock must be removed by protein synthesis, during a carbon production (with a C/N ratio of 6/1) of $\sim 10^2 \text{ g C m}^{-2} \text{ yr}^{-1}$ over the next year, to avoid build-up of nitrate stocks from one year to the next. The amount of local primary production which is buried in the Chukchi sediments is unknown, and may constitute a significant sink. As an upper bound, however, this estimated new production, over the 10^{12} m^2 area of the Chukchi/East Siberian shelves, amounts to $\sim 10^{14} \text{ g C yr}^{-1}$.

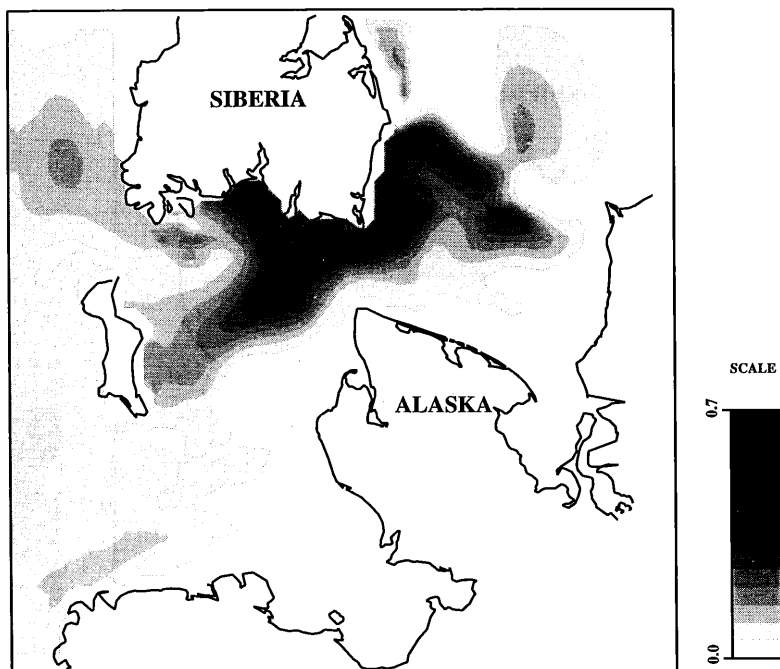


Fig. 11. – Sea surface distribution of organic matter in the Northern Bering Sea (in $\mu\text{atg N l}^{-1}$) [Reference summer situation].

Export of this new production, minus a small shelf burial loss, could today satisfy most of the AOU (“apparent oxygen utilization”) demands of the Arctic basins.

The role of the Arctic Ocean and adjacent shelves in global carbon budgets has thus far been neglected. Changes in deep-water formation and/or a decline of marine primary production at high latitudes, perhaps as a result of increased light limitation on geological time scales, is suspected to have been an important component of atmospheric CO_2 rise, and thus global control of warming trends, begun 15,000 yr ago. Simple box models of high latitude ecosystems, embedded within the global oceans, ignore the Arctic Ocean, however, assuming that ice cover curtails gaseous exchange between atmosphere and ocean.

Circumvention of this ice cover constraint on CO_2 exchange occurs by primary production within open waters of the Bering/Chukchi/East Siberian Seas, at the margins of the permanent ice pack in the Arctic Ocean. Satisfaction of present AOU demands leads to a brine-mediated, shelf input of $\sim 10^{14} \text{ g C yr}^{-1}$ to the halocline of the Eurasian and Canadian basins, for eventual southward export via Fram Strait. In terms of anthropogenic release of CO_2 of $\sim 5 \cdot 10^{15} \text{ g C yr}^{-1}$ to the atmosphere, such a present Arctic sink is small. If

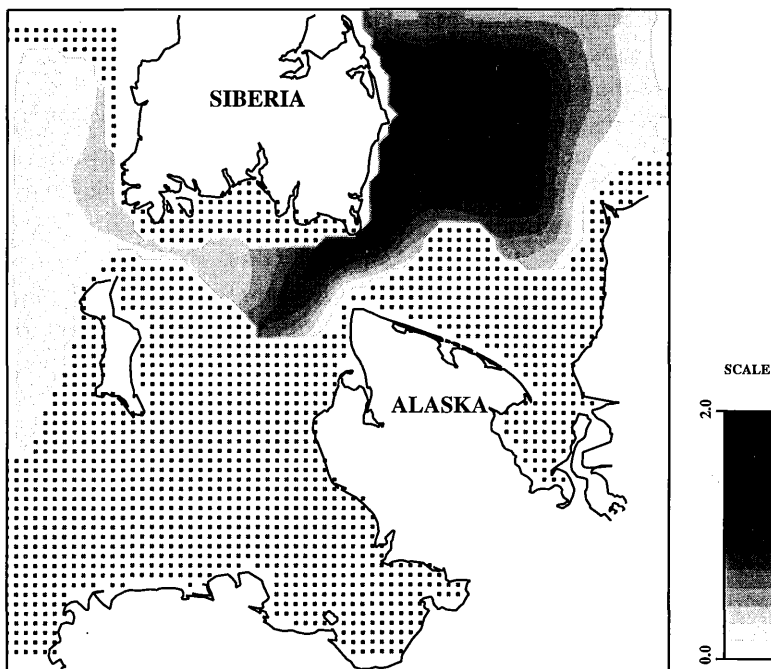


Fig. 12.— Organic matter in the Northern Bering Sea at 40 m depth (in $\mu\text{atg N l}^{-1}$) [Reference summer situation].

projected greenhouse warmings of more than 2°C were to melt most of the Arctic ice pack, however, a future organic carbon sink of at least $5 \cdot 10^{14} \text{ g C yr}^{-1}$ might ensue here, for eventual sequestration within deep water formation in either the Atlantic or Arctic Oceans.

The Northern Bering Sea's summer ecohydrodynamics is characterized by quasi-permanent, reproducible hydrodynamical phenomena which control resonant, ecohydrodynamically adjusted, essential ecological processes

- (i) the inflow, deployment and outflow of the Anadyr Stream in and out the basin,
- (ii) the strong upwelling/upsloping maintained by this flow at the Anadyr entrance,
- (iii) the entrainment of the nutrient rich upwelled waters by the Anadyr Stream into the Northern Bering and Chukchi Seas with the repartition along stream of successive maxima of primary and secondary productions,
- (iv) the cohabitation of the Anadyr water mass with the Alaskan coastal water mass, both converging — with some border overlapping — towards the Bering Strait,

- (v) the existence of fairly sharp horizontal gradients at the separation of the two water masses, exacerbated by the enhanced specificity of the Anadyr water trailing the upwelling/upsloping plume,
- (vi) the recurrent instabilities at the frontal separation of the Anadyr and Alaskan water masses with subsequent eastwards-propagating interleaving layers, increasing lateral mixing and creating the conditions of phytoplankton blooms along the front,
- (vii) the impact of the prevalent northbound flow through the Bering Strait on the ecohydrodynamics of the Southern Chuckchi Sea and on global biogeochemical transports from the Northern Pacific to the Arctic Mediterranean Sea.

References.

- ADAM, P. (1991). *Sensitivity Analysis of a 3D Mathematical Model of the Northern Bering Sea*, Dissertation, Mech. Eng. Dept, Liège University, 89 pp.
- BRASSEUR, P. and HAUS, J. (1991). Application of a Three-Dimensional Variational Inverse Model to the Analysis of Ecohydrodynamic Data in the Bering and Chuckchi Seas, *Journal of Marine Systems*, 1:383–401.
- COACHMAN, L.K., AAGAARD, K. and TRIPP, R.B. (1975). *Bering Strait. The Regional Physical Oceanography*, University of Washington Press, 172 pp.
- NIHOUL, J.C.J., DELEERSNIJDER, É. and DJENIDI, S. (1989). Modelling the General Circulation of Shelf Seas by 3D $k-\epsilon$ Models, *Earth Science Reviews*, 26:163–189.
- NIHOUL, J.C.J. and DJENIDI, S. (1991). Hierarchy and Scales in Marine Ecohydrodynamics, *Earth Science Reviews*, 31:255–277.
- NIHOUL, J.C.J., ADAM, P., BRASSEUR, P., DELEERSNIJDER, É., DJENIDI, S. and HAUS, J. (1992). Three-Dimensional General Circulation Model of the Northern Bering Sea's Summer Ecohydrodynamics, *Continental Shelf Research*, 13:509–542.
- WALSH, J.J., BLACKBURN, T.H., COACHMAN, L.K., GOERING, J.J., MC ROY, C.P., NIHOUL, J.C.J., PARKER, P.L., SPRINGER, A.M., TRIPP, R.B., WHITLEDGE, T.E. and WIRICK, C.D. (1985). The role of the Bering Strait in carbon/nitrogen fluxes of polar marine ecosystems, *Proceedings Fairbanks Conference on Marine Living Systems of the Far North*, May 1985.
- WALSH, J.J., MC ROY, C.P., COACHMAN, L.K., GOERING, J.J., NIHOUL, J.C.J., WHITLEDGE, T.E., BLACKBURN, T.H., PARKER, P.L., WIRICK, C.D., SHUERT, P.G., GREBMEIER, J.M., SPRINGER, A.M., TRIPP, R.D., HANSELL, D., DJENIDI, S., DELEERSNIJDER, É., HENRIKSEN, K., LUND, B.A., ANDERSEN, P., MULLER-KARGER, F.E. and DEA, K. (1989). Carbon and Nitrogen Cycling within the Bering/Chuckchi Sea: Source Regions for Organics Matter Affecting AOU Demands of the Arctic Ocean, *Progress in Oceanography*, 277–359.

The Westerschelde Estuary: two Food Webs and a Nutrient Rich Desert

O. HAMERLYNCK¹, J. MEES¹, J.A. CRAEYMEERSCH², K. SOETAERT²,
K. HOSTENS¹, A. CATTRIJSE¹ and P.A. VAN DAMME³

¹ Marine Biology Section, University of Gent

² Netherlands Institute for Ecology, Centre for Estuarine and Coastal Ecology

³ Laboratory for Ecology, University of Leuven

Abstract.

Hummel *et al.* (1988) hypothesised the concomitant existence of two separate food chains in the Westerschelde: a photo-autotrophic coastal food chain in the marine part and a heterotrophic chain in the brackish part. The present study intends to re-examine the hypothesis on the basis of recently published data. Biomass gradients of the important functional units along an estuarine transect were observed to differ from those reported by Hummel *et al.* (1988) in some important aspects. The bimodal primary production gradient reported by Spaendonck *et al.* (in press) does not resemble the phytoplankton biomass curve, gradually increasing from the sea to Antwerp proposed by Hummel *et al.* (1988). Estimates of mesozooplankton biomass were found to be about an order of magnitude lower than reported by Hummel *et al.* (1988) and to display a completely different and more complex spatial pattern. However, the new gradient found is more in line with the hypothesis of two food chains than the gradient reported by Hummel *et al.* (1988). In the macrobenthos the biomass peak in the brackish part reported by Hummel *et al.* (1988) could not be confirmed. This finding does not falsify the original hypothesis as the function of this detritus dependent macrobenthic fauna is largely taken over by the hyperbenthic mysids, a group of previously unknown importance in the system. The existence of two food chains is also supported by the gradients observed in fish and epibenthic invertebrates, functional units not addressed by Hummel *et al.* (1988). In the zone between the two different food chains the dominant animal groups of the pelagic system have only a low biomass, this is the nutrient rich desert of the title. The zone upstream of the Dutch-Belgian border supports no hyperbenthos, no epibenthos and no mesozooplankton because of the low dissolved oxygen concentrations (less than 40% saturation), but there is a prominent peak in the microzooplankton. Clearly, in the brackish part, the richness of most functional units can only be explained on the basis of an input of organic matter from outside, consumed through a heterotrophic food chain. A second, smaller peak is observed close to the mouth of the estuary and is dependent on the primary production in the marine part of the estuary. Even for individual species this clear bimodal pattern can be observed. This disqualifies simplistic physiological models of estuarine succession as a basis for the findings. In the oxygenated part of the system there is no good general correlation between macrobenthic biomass (mostly suspension-feeders)

and primary production. Macrobenthic biomass is highly variable in this zone, probably as a result of local differences in current velocity maxima. The new data confirm the view of Hummel *et al.* (1988) but it is concluded that these authors must have formulated their hypothesis intuitively and could not have done so from the data available at the time.

1.— Introduction.

There has recently been renewed emphasis on food web theory in ecological studies (Lawton, 1989). Much of the thinking on this subject has been severely hampered by the lack of appropriate data on enough components of reasonably complex food webs. The claim by Briand and Cohen (1987), that food chains in two-dimensional areas such as estuaries tend to be shorter, was not confirmed by a recent, relatively well documented, study of an estuarine food web (Hall and Raffaelli, 1991). However, in studies of the properties of food webs (*e.g.* chain length, degree of omnivory, connectance, etc.) of a large area encompassing a diversity of habitats, such as an estuary, care should be taken not to confound different food chains or “compartments” *sensu* Paine (1980). Besides the theoretical aspects of compartmented webs regarding system stability (Pimm and Lawton, 1980), the elucidation of web infrastructure is a prerequisite for a correct evaluation of web properties (Rafaelli and Hall, 1992).

With the increased research effort into the dominant role of bacteria in secondary production in marine and estuarine ecosystems (Cole *et al.*, 1988) more insight has been gained into the distinction between detritus based food chains, termed heterotrophic (Smith *et al.*, 1989; Findlay *et al.*, 1991), where respiration exceeds production and phytoplankton dominated food chains, termed autotrophic, where primary production exceeds respiration. Unlike previously thought, the bacterial production does not simply result in a remineralisation of nutrients but also opens up a loop towards the zooplankton through the protozoans (Billen *et al.*, 1990). In estuarine systems it is thought this loop may support an important food chain sustained by the detrital organic carbon imported from the riverine system. Care should be taken with the term autotrophic food chain as around hydrothermal vents, methane sources, hypoxic parts of estuarine systems and elsewhere chemo-autotrophic food chains exist (*e.g.* Conway and McDowell, 1990). Photo-autotrophic would be a better term for the food chains termed autotrophic by Findlay *et al.* (1991).

Hummel *et al.* (1988) hypothesised the concomitant existence of two separate food chains in the Westerschelde. Their hypothesis was based on scattered and comparatively old data from the literature. In the meantime a concerted research effort has been developed by Dutch and Belgian scientists which has begun to make available more systematically collected and more reliable recent data for different functional units (phytoplankton, zooplankton, hyperbenthos,

etc.) of the Westerschelde ecosystem. These data are now being used for the development and validation of an ecological model of the Westerschelde (Soetaert *et al.*, 1992; Herman *et al.*, unpublished). This paper will examine some of the input data for this model in relation to the Hummel *et al.* (1988) hypothesis. Additional data on the higher trophic levels in the Westerschelde, not to be included in the MOSES model are also presented.

2.- Materials and Methods.

The Westerschelde estuary (figure 1) is the lower part of the river Schelde. It is the last remaining true estuary of the Delta area and is characterised by a marked salinity gradient. The estuarine zone of the tidal system extends from the North Sea (Vlissingen) to Antwerp, 80 km inland. Further upstream the system can be termed riverine, though the tidal influence extends to Gent. The water in the estuarine part is virtually completely mixed and the residence time in the brackish part is rather high: about 60 days (Soetaert and Herman, submitted). Consequently fresh water (average inflow $100 \text{ m}^3 \text{ s}^{-1}$) dilution is gradual and downstream transport is relatively slow. Shifts in salinity zone distribution occur in accordance with seasonal variations in the freshwater inflow. The abiotic environment is discussed in Heip (1989) and Eck *et al.* (1991). The estuary carries high pollution loads, both in inorganic and organic contaminants. The riverine part is anoxic throughout most of the year (Herman *et al.*, 1991).

Spatially the estuarine system under consideration in the present study was divided into 12 compartments according to the MOSES model (Soetaert *et al.*, 1992). The MOSES model contains an extra compartment in the riverine system. Therefore the 12 estuarine compartments are numbered 2 to 13 when going from Antwerp to the North Sea (figure 1). Functionally the units considered are phytoplankton (Spaendonk *et al.*, in press), zooplankton comprising meso-zooplankton, benthic larvae and part of the microzooplankton, *i.e.* Rotatoria and *Noctiluca miliaris* (Soetaert and Rijswijk, in press), macrobenthos (Craeymeersch *et al.*, 1992), hyperbenthos (Mees and Hamerlynck, 1992; Mees *et al.*, in press a), epibenthos and fish (Hamerlynck *et al.*, in press). The reader is referred to these publications for detailed descriptions of the sampling methodologies. Table 1 shows a matrix of the spatial compartments and the functional units for which data were available.

The primary production data are based on fortnightly measurements taken in 1989 (Spaendonk *et al.*, in press). The zooplankton data are annual means from approximately fortnightly samples from April 1989 through March 1991 (Soetaert and Rijswijk in press). The macrobenthos data refer to a stratified random sampling in the autumn of 1990 according to the grid shown in figure 2.

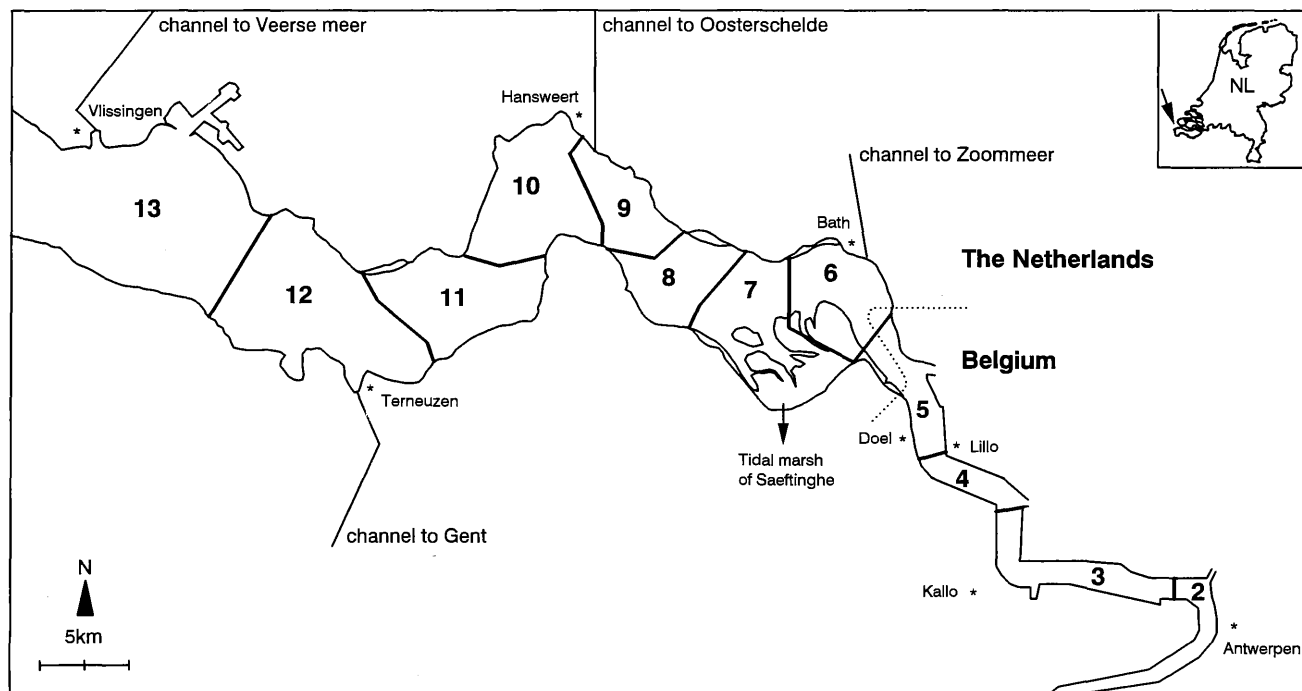


Fig. 1.

Table 1

Compartment	2	3	4	5	6	7	8	9	10	11	12	13
Zooplankton	•	•	•	•	•	•	•	•	•	•	•	•
Primary production	•		•	•	•	•		•	•	•	•	•
Macrobenthos					•	•	•		•	•	•	•
Hyperbenthos	•	•	•	•	•	•	•	•	•	•	•	•
Epibenthos & fish			•	•	•	•	•	•	•	•	•	•

The strata were intertidal, subtidal and gully (more than 10 m below Mean Tidal Level) stations. During the macrobenthos survey no data were collected upstream of compartment 6, but it is known that in the upstream (hypoxic) zone only some oligochaetes survive (P.M. Meire, pers. comm.). For the hyperbenthos the data are the averages per station of the 1990 seasonal data reported in Mees *et al.* (in press a). The area upstream of compartment 6 was explored for hyperbenthos in March, April and May 1990 and in August 1991 but no animals were found. The epibenthos and fish data are annual means based on monthly samples collected in 1989. The data in compartments 4 and 5 refer to samples collected from the intake screens of Doel power station. Between April and July virtually no fish were recorded in this area (P.A. Van Damme, unpublished).

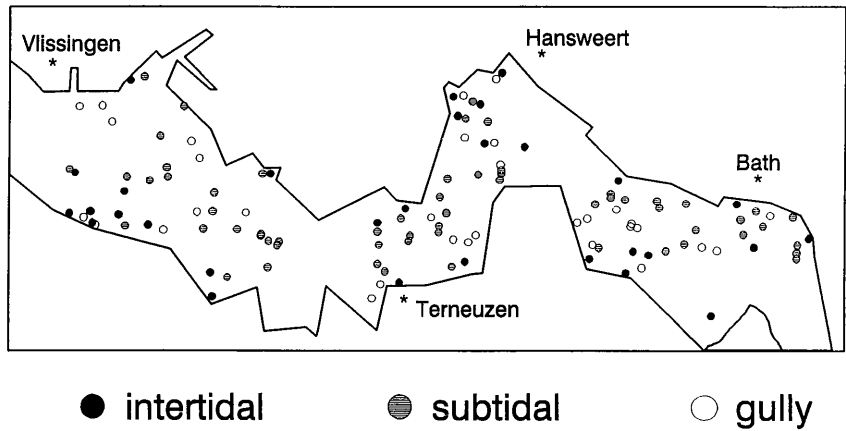


Fig. 2.

Values reported as Ash-free Dry Weight (ADW) were converted to g C using the same 0.4 conversion factor as in Hummel *et al.* (1988). Dry Weight data from the zooplankton study (Soetaert and Rijswijk, in press) were first converted to ADW by subtracting 10%.

3.- Results and discussion.

The results of the present data compilation and the biomass patterns reported by Hummel *et al.* (1988) are shown in Figs. 3 through 7.

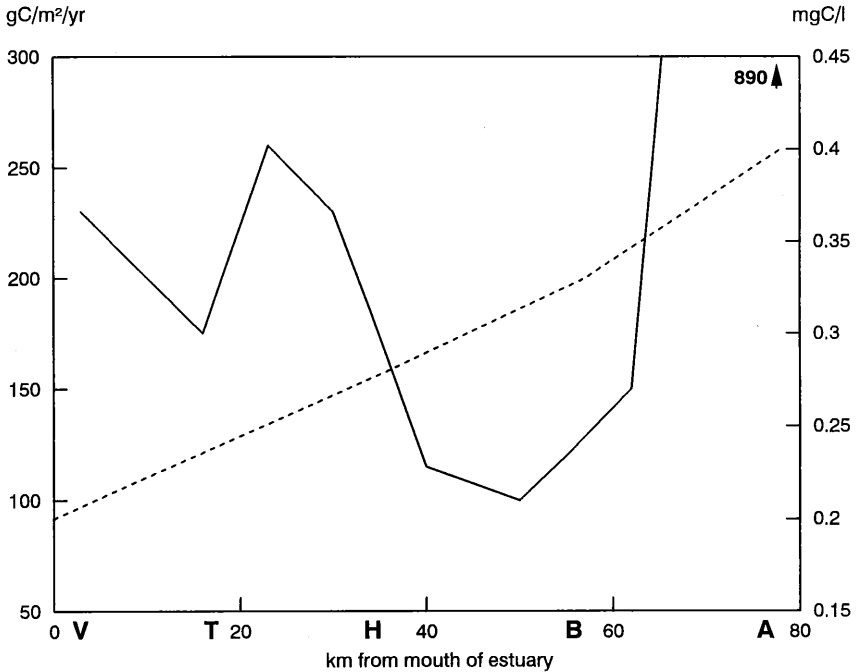


Fig. 3.

Besides proposing the two food chain hypothesis Hummel *et al.* (1988) also split the tidal part of the river into three zones: a fresh water tidal zone from Gent to Antwerpen which falls outside the scope of the present study, a brackish tidal zone (Antwerpen to Hansweert) and a marine tidal zone (Hansweert to Vlissingen). This second division was confirmed in the community structure of the zooplankton (Soetaert and Rijswijk, in press), the macrobenthos (Meire *et al.*, 1991), the hyperbenthos (Mees and Hamerlynck, 1992; Mees *et al.*, in press a) and the epibenthic invertebrates and fishes (Hamerlynck *et al.*, in press) and therefore seems very robust.

Though it is difficult to compare chlorophyll *a* concentrations from Hummel *et al.* (1988) with production figures given in Spaendonck *et al.* (in press), these authors also provide peak concentrations of chlorophyll *a* at a few stations which broadly confirm the link between phytoplankton biomass, expressed as chlorophyll *a* concentrations and primary production. Peak concentrations in

the marine part (Hansweert) are higher than in the brackish part (Bath), but the biomass peak in Antwerpen is 10 to 20 times higher than those peaks (Spaendonk *et al.*, in press). In the Hummel model phytoplankton biomass was essentially increasing from the mouth up to Antwerpen even if they also stated that primary production was low in the turbid brackish zone (figure 3). According to Spaendonk *et al.* (in press) the high primary production around Antwerpen in 1989 was mostly due to salinity intolerant freshwater species that would not survive transport to the turbid brackish zone. In the rest of the estuary primary production was found to be essentially light limited. However, as there may be a high variability in the patterns of chlorophyll *a* and primary production among years, more data are still required to come to more robust conclusions regarding this functional unit in the Westerschelde.

For the zooplankton (which in their definition corresponds to the mesozooplankton) Hummel *et al.* (1988) also reported a gradual increase in biomass from Vlissingen to Antwerpen (and a steep decline further upstream). Besides the fact that the biomass reported by Hummel *et al.* (1988) seems an order of magnitude too high (figure 4a) (they even reported more zooplankton than phytoplankton in the brackish part, possibly their zooplankton data refer to the spring bloom only?), a very clear bimodal pattern in mesozooplankton biomass could be found with the peak in the brackish part (predominantly *Eurytemora affinis*) about double (figure 5a) the peak at the mouth of the estuary (a mixture of coastal species). The mesozooplankton decreases rapidly east of Bath as a consequence of hypoxia. The peak in primary production and the peak in *Eurytemora affinis* are separated by about 30 km. In between (figure 5b) there is a clear peak in the microzooplankton – as quantified by Soetaert and Rijswijk (in press) –, which in this part of the system consists mostly of Rotifera, a group relatively resistant to hypoxia and an essential link for opening up the microbial loop (Azam *et al.*, 1983) for higher trophic levels. According to Fenchel (1988) the bacterial production is consumed by heterotrophic nanoflagellates and protozoans (all associated to the particulate detritus), which in turn are taken by ciliates, heterotrophic dinoflagellates and Rotifera.

A clear representative of the coastal food chain in the zooplankton are the meroplankton (planktonic larvae of benthic animals) which decrease gradually from the mouth to the brackish part (figure 5c).

A trend line through the macrobenthos biomass (figure 4b) would more or less conform to the bimodal pattern reported by Hummel *et al.* (1988) except that the average biomass in the marine part reported in the present study is about four times higher than the biomass in the brackish part. Hummel *et al.* (1988) reported a 1.5 times higher mean biomass in the brackish part than in the marine part. Even going back to the original data used by Hummel *et al.* (1988) this higher peak in the brackish zone could not be retrieved. It is well documented

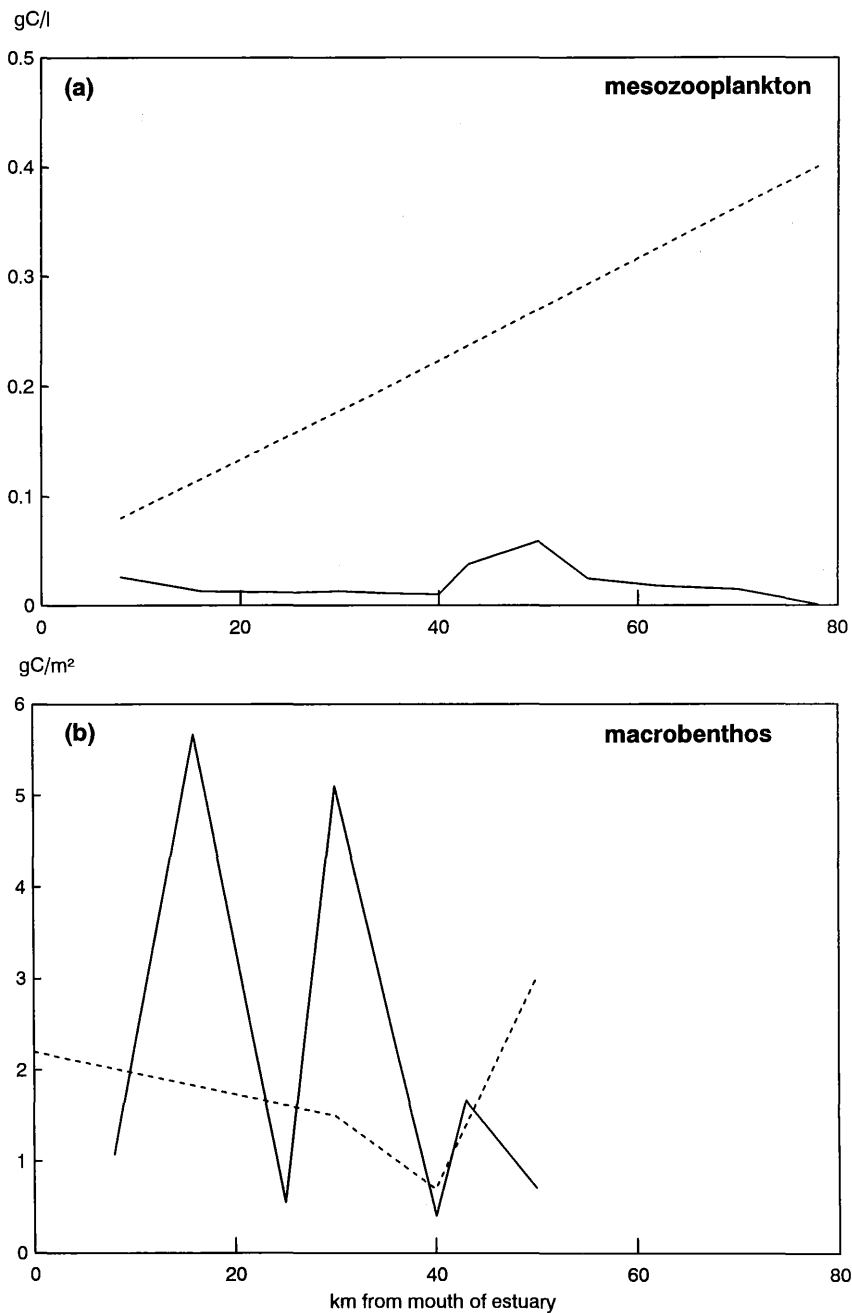


Fig. 4.

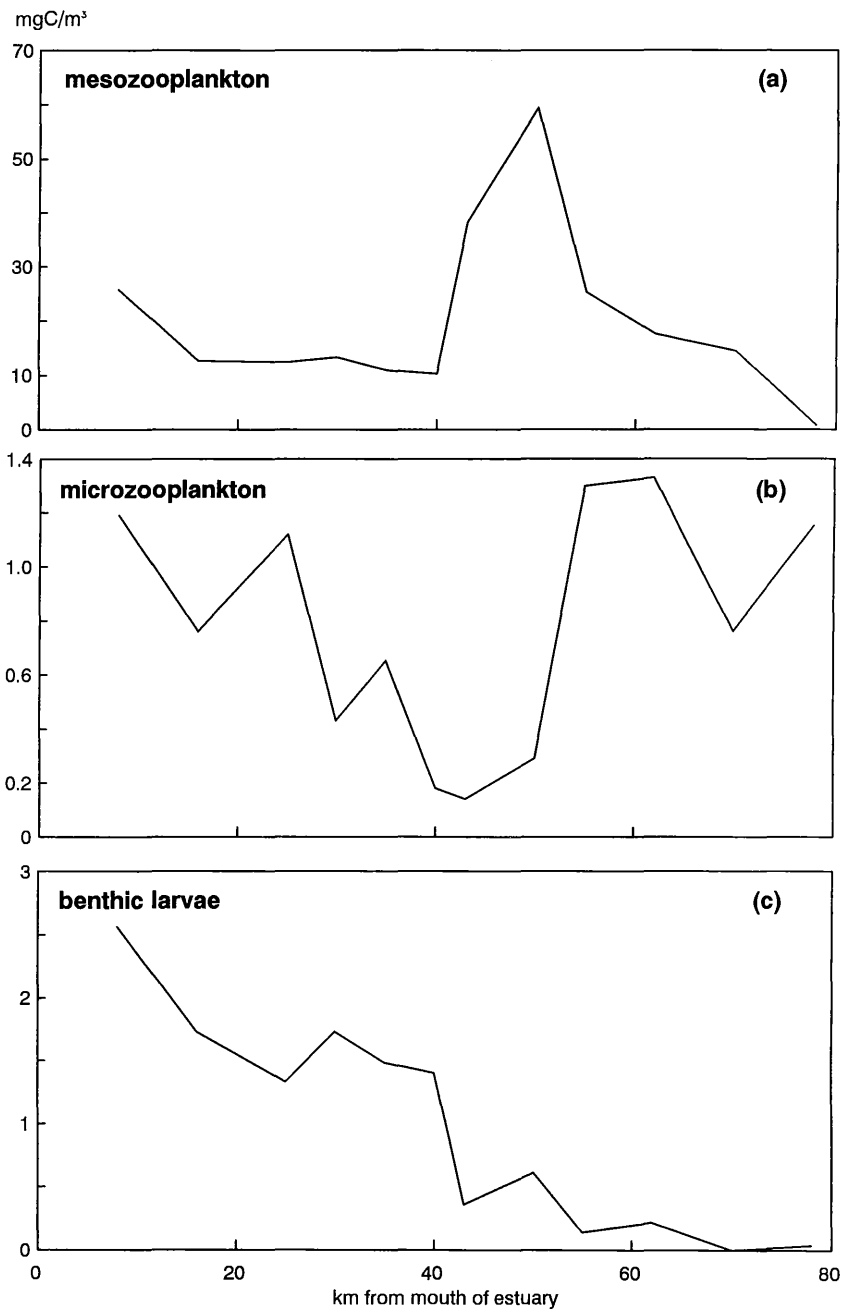


Fig. 5.

that the macrobenthos in the brackish part is dominated by deposit-feeders dependent on sedimenting detritus for their food supply (Meire *et al.*, 1991). In the marine part the suspension-feeders dominate and these depend mostly on primary production filtered from the water column (Herman and Scholten, 1990). In spite of this, there does not seem to be a good correlation between primary production and macrobenthic biomass in the marine part. Though both rise steeply west of Hansweert there is a primary production peak spatially coinciding with a deep macrobenthic biomass trough at about 25 km from the mouth, east of Terneuzen. The variability in macrobenthic biomass in the marine part seems to be extremely high and would at first sight seem to make any conclusions about this functional unit impossible. However, suspension-feeders do not only need primary production, they also need relatively stable sediments and not too many indigestible particles in the water column. They therefore prefer areas with current velocities below 0.6 m s^{-1} (Dijkema, 1988). Preliminary data from the 2D hydrodynamical model of the Westerschelde (Portela *et al.*, 1992) suggest the two peaks coincide with two compartment subareas (both at the outer curve of a relatively sharp turn in the main ebb channel) where current velocities are consistently lower than in other parts of the marine zone (Ramiro Nevez, pers. comm.).

The hyperbenthos has only recently been discovered to be an important component of the Westerschelde ecosystem, both structurally (Mees and Hamerlynck, 1992; Mees *et al.*, in press a) and functionally (Mees *et al.*, submitted a). Most of the biomass pattern shown in figure 6a consists of Mysidacea. Coming from the sea a first peak in hyperbenthos biomass occurs in the vicinity of Hansweert. A second, larger peak coincides with the trough in primary production and the copepod peak in the vicinity of Bath. It is at present unclear what may be the cause of the bimodality within the peak in the brackish part. Some of this may be smoothed out when true annual means, based on the monthly samples taken (Mees, unpublished) instead of the seasonal data reported here, become available. Alternatively the presence of the large tidal marsh of Saeftinghe or some aspect of the hydrodynamics in the brackish part may be involved. Within some species groups a clearly bimodal pattern, with a peak close to the mouth of the estuary and a second peak in the brackish part, can be observed, an example are the gammaridean amphipods (figure 6b).

Data on fish and epibenthic invertebrates were also not available to Hummel *et al.* (1988). The brown shrimp *Crangon crangon* is the dominant epibenthic invertebrate in the system (Hamerlynck *et al.*, in press) and both the adult shrimp (figure 7a) and the hyperbenthic living juvenile postlarval shrimp of less than 20 mm total length (figure 6c) display a clearly bimodal pattern with a smaller peak close to the mouth of the estuary and a large peak in the brackish part. The biomass pattern of the demersal fish is rather similar to the pattern in the adult

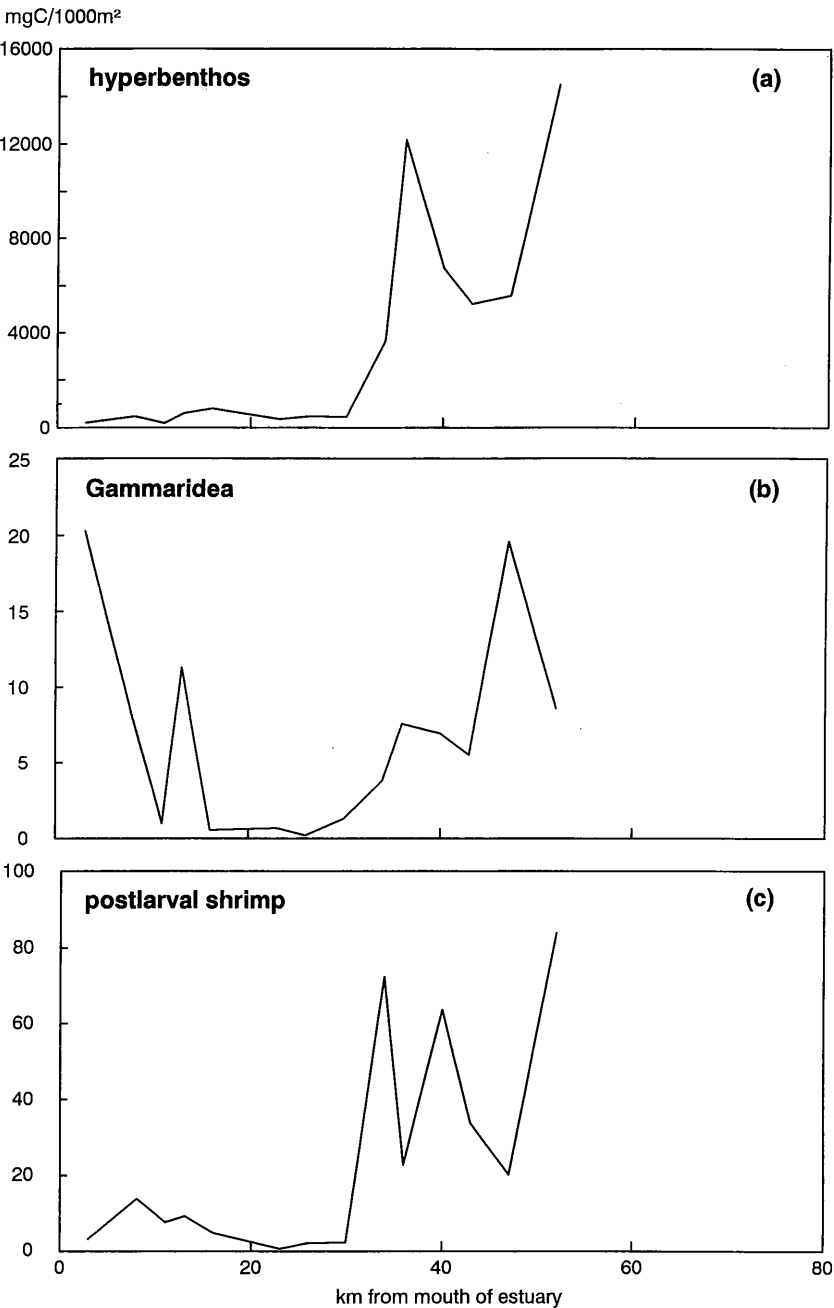


Fig. 6.

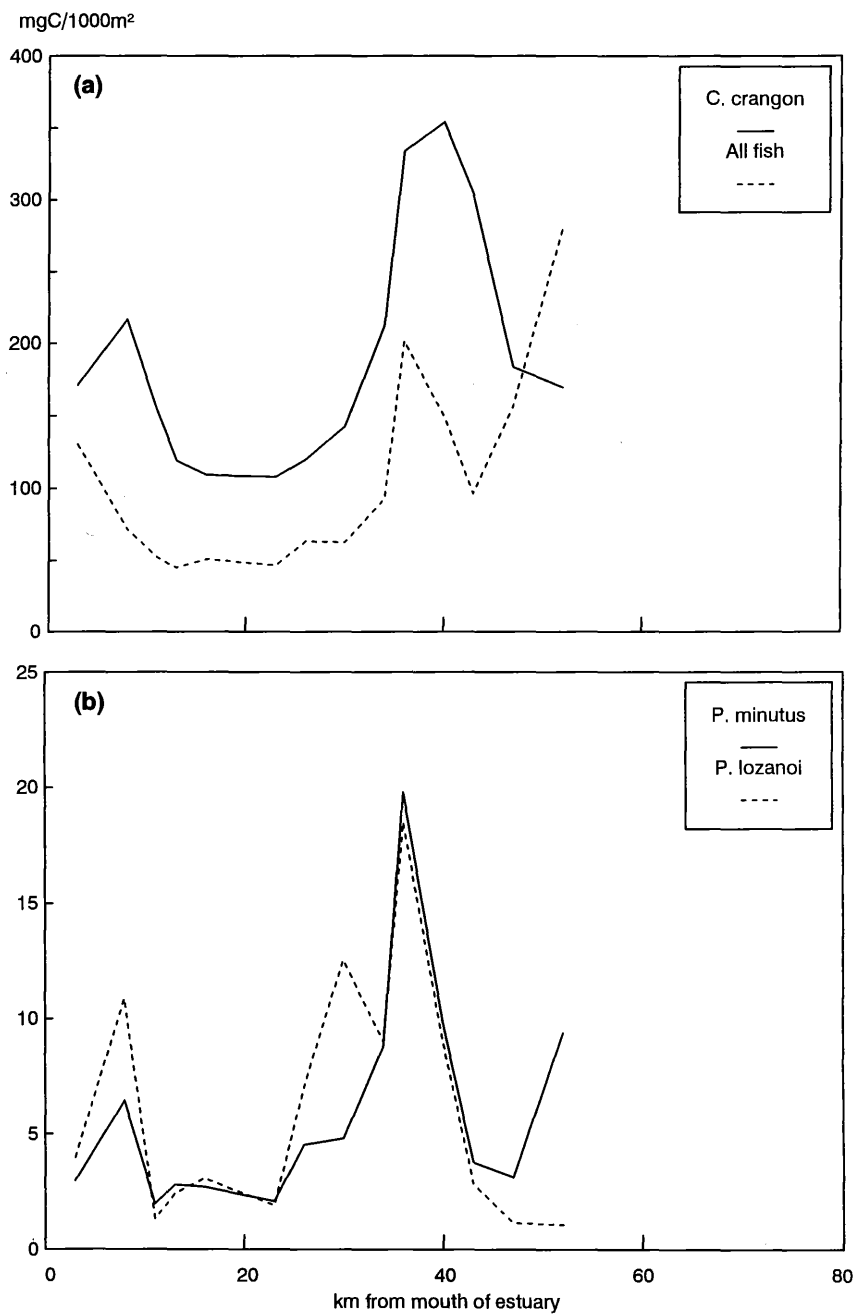


Fig. 7.

shrimp (figure 7a). The two-peaked structure within in the brackish part is very similar to the observed pattern in the hyperbenthos (figure 6a). Possibly the fish fauna is entirely dependent on the hyperbenthos in this part of the system. Within the fish the dominant components are flatfish and gobies (Hamerlynck *et al.*, in press). Within the gobies the bimodal pattern is clear, both in *Pomatoschistus minutus* and *Pomatoschistus lozanoi* (figure 7b).

At present there are insufficient data on piscivorous birds to extend the analysis to that unit (Stuart *et al.*, 1990). Also, though anecdotal observations suggest seals are predominantly recorded around the Hooge Platen close to the mouth and on the Plaat van Valkenisse in the brackish part, as for the birds, coverage in the middle part of the estuary is too low to allow any firm conclusions to be drawn at present.

The results of the present study suggest that there are indeed two separate food chains in the Westerschelde as suggested by Hummel *et al.* (1988) and that a bimodal pattern of biomass distribution along the estuarine gradient is present, at least in the pelagic functional units. This pattern propagates through to the higher trophic levels. It is unclear how Hummel *et al.* (1988) arrived at their hypothesis from the data they had compiled. Hummel *et al.* (1988) stated that most of the biomass trends found show an increase from the sea to Antwerpen and that this may seem contradictory. They claim this contradiction will be explained in § 3.3.1 of their paper, but such a section can not be found.

There seems to be no gradual transition between the two purported food chains and they are separated by an intermediate "desertic" zone of over 20 km width. As an explanatory mechanism it is suggested, in accordance with Hummel *et al.* (1988), that the richness of brackish part is supported by a detritus based food chain. Virtually all of the non-refractory organic material in this zone would be either re-mineralised by the intense heterotrophic bacterial activity (Goossen *et al.*, 1992) or consumed by the zooplankton and the hyperbenthos, either directly or through the microzooplankton. Part of the material also settles on the bottom and sustains the deposit-feeding macrofauna. Possibly part of the energy requirements of shrimp are also sustained directly by detritus (or detritus plus bacteria and other micro-heterotrophs). This "second trophic level" in turn supports the rich community of epibenthic invertebrates (crabs and shrimp) and fish.

In the "desertic" zone the remaining organic matter is presumably mainly refractory. There is still a surplus of nutrients available and primary production is relatively high. Possibly as a consequence of high current velocities this primary production cannot be used very efficiently by the macrobenthos, except in a few relatively low turbulence sites where the suspension-feeders thrive. Still, it remains unclear why the zooplankton is not capable of exploiting the primary production in this zone.

Towards the mouth of the estuary primary production remains high and a coastal food chain flourishes. At the second trophic level species composition differs substantially in some groups, *e.g.* the zooplankton (Soetaert and Rijswijk, in press) and the hyperbenthos (Mees *et al.*, in press b). At the next trophic level the dominant species in both food chains are rather similar. That the observed bimodal pattern is caused by the underlying food chains and not by the physiologic limits of the respective organisms can be seen from the distribution in shrimp and gobies where the bimodal pattern can be observed within single species. Secondary support for the subordinate (if any) role of physiological limitation is provided by the fact that *Neomysis integer* has its peak distribution at much higher salinities in the Westerschelde than in the other European estuaries (Mees *et al.*, submitted b). Fecundity and growth in the Westerschelde are comparable or higher than those recorded in the other areas (Mees *et al.*, submitted b) indicating that the animals are not particularly stressed.

The role of the tidal marshes within the brackish part is less clear at present. At high tide they are intensively used by both hyperbenthic crustaceans (Cattrijsse *et al.*, in press; Mees *et al.*, in press b) and juvenile stages of fishes (Cattrijsse, unpubl.; Frid and James, 1988) and may thus form an integral part of the food web of the estuary. Logically, as tidal marshes are sinks for mud they should be net importers and not net exporters of organic matter. This high input of organic matter may be one of the attractants for the mobile fauna. Presumably added to that there is a substantial primary production by the diatom phyto-benthos in the sheltered tidal creeks. It is also possible that there may be a qualitative edge to foraging in a tidal marsh related to the characteristic lipid quality reported for a nearby coastal marsh by Hemminga *et al.* (1992). Several mysid species, both coastal zone species and estuarine endemics, move into the tidal marshes to release their larvae (Mees *et al.*, in press b). In view of the high densities of fish and shrimp in the marsh (Cattrijsse, unpublished), instead of being a strategy of predator avoidance, this behaviour may also be related to food quality.

The obvious next step for a better understanding of the system and especially of its characteristic heterotrophic food chain in the brackish part is the detailed investigation of the link between the bacterial production and the higher trophic levels. Are it really the detritus-associated bacteria that form the basis of the food chain and are they consumed as such by the next links, *i.e.* the mesozooplankton and the mysids? It seems unlikely that copepods and mysids, in view of their short and uncomplicated digestive systems are able to incorporate unmodified plant detrital material with its characteristic C/N ratio to a great extent. However, it is also known that mysids possess cellulases (Mann, 1988) so the alternative hypothesis, namely that bacteria and metazoa compete for the same detritus can as yet not be ruled out. The heavily polluted Westerschelde may be a particularly

interesting system for the analysis of the energy transfers under consideration here because some of the important functional units are spatially segregated due to the gradient in dissolved oxygen (and not as a result of transport processes because of the high residence time of the water). This should facilitate the analysis of the underlying processes.

4.- Conclusions.

Except for the bimodality in the macrobenthos biomass reported by Hummel *et al.* (1988) none of the patterns in their other functional units were suggestive of the existence of two separate food chains. They have therefore probably proposed their model intuitively. As is often the case they were right but for the wrong reasons.

Acknowledgements.

This research was supported by the European Community, contract no. MAST-0024-C (JEEP 92 project), by the Belgian FKFO project 32.0086.88. Kris Hostens and André Cattrijsse acknowledge a grant from the Institute for the Encouragement of Scientific Research in Industry and Agriculture (IWONL). Contribution no. 648 of the Centre for Estuarine and Coastal Ecology, Netherlands Institute of Ecology, Yerseke.

References.

- AZAM, F., FENCHEL, T., FIELD, J.G., GRAY, J.S., MEYER-REIL, L.A. and THINGSTAD, F. (1983). The ecological role of water-column microbes in the sea, *Mar. Ecol. Progr. Ser.*, 10:257-263.
- BILLEN, G., JOIRIS, C., MEYER-REIL, L. and LINDEBOOM, H. (1990). Role of bacteria in the North Sea ecosystem, *Neth. J. Sea Res.*, 26:265-293.
- BRIAND, F. and COHEN, J.E. (1987). Environmental correlates of food chain length, *Science*, 238:956-960.
- CATTRIJSE, A., MEES, J. and HAMERLYNCK, O. (in press). The hyperbenthic amphipoda and isopoda of the Voordelta and the Westerschelde estuary, *Cah. Biol. Mar.*
- COLE, J.J., FINDLAY, S. and PACE, M.L. (1988). Bacterial production in fresh and saltwater ecosystems: a cross-system overview, *Mar. Ecol. Progr. Ser.*, 43:1-10.
- CONWAY, N. and MCDOWELL, J. (1990). *The use of biochemical indicators in the study of trophic interactions in animal-bacteria symbioses: Solemya velum, a case study*, in: M. Barnes and R.N. Gibson (Editors), *Trophic relationships in the marine environment*, Aberdeen University Press, 553-564.

- CRAEYMEERSCH, J.A., BRUMMELHUIS, E.B.M., SISTERMANS, W. and STIKVOORT, E.C. (1992). *Het macrobenthos van de Westerschelde, de Oosterschelde, het Veerse Meer en het Grevelingenmeer. Najaar 1990*, Internal Report NIOO-CEMO, Yerseke, 44 pp. (in Dutch).
- DIJKEMA, R. (1988). Shellfish cultivation and fisheries before and after a major flood barrier construction project in the southwestern Netherlands, *J. Shellfish Res.*, 7:241–252.
- ECK, G.T.M. van –, DE PAUW, N., LANGENBERGH, M. Van den – and VERREET, G. (1991). *Emissies, gehalten, gedrag en effecten van (micro)verontreinigingen in het stroomgebied van de Schelde en het Schelde-estuarium*. *water*, 60:164–180 (in Dutch).
- FENCHEL, T. (1988). Marine plankton food chains, *Annu. Rev. Ecol. Syst.*, 19:19–38.
- FINDLAY, S.F., PACE, M.L., LINTS, D., COLE, J.J., CARACO, N.F. and PEIERLS, B. (1991). Weak coupling of bacterial and algal production in a heterotrophic system: The Hudson River estuary, *Limnol. Oceanogr.*, 36:268–278.
- FRID, C.L.J. and JAMES, R. (1988). The role of epibenthic predators in structuring the marine invertebrate community of a British coastal salt marsh, *Neth. J. Sea Res.*, 22:307–314.
- GOOSSEN, N., RIJSWIJK, P. van –, PEENE, J. and KROMKAMP, J. (1992). *Annual patterns of bacterial production in the Scheldt estuary (SW-Netherlands)*, in: P.M.J. Herman (Editor), *JEEP 92: Major biological processes in European Tidal Estuaries*, Internal Report Netherlands Institute of Ecology, 109–113.
- HAMERLYNCK, O., HOSTENS, K., ARELLANO, R.V., MEES, J., VAN DAMME, P.A. (in press). The mobile epibenthic fauna of soft bottoms in the Dutch Delta (south-west Netherlands): spatial structure, *Neth. J. Aquat. Ecol.*
- HEIP, C.H.R. (1989). *The ecology of the estuaries of Rhine, Meuse and Scheldt in the Netherlands*, in: J.D. Ross (Editor), *Scient. Mar.*, 53:457–463.
- HEMMINGA, M.A., KLAP, V.A., SOELEN, J. van – and LEEUW, J. de – (1992). Shifts in seston characteristics after inundation of a European coastal salt marsh, *Limnol. Oceanogr.*, 37:1559–1564.
- HERMAN, P.M.J. and SCHOLTEN, H. (1990). *Can suspension-feeders stabilise estuarine ecosystems?*, in: M. Barnes and R.N. Gibson (Editors), *Trophic relationships in the marine environment*, Aberdeen University Press: 104–116.
- HERMAN, P.M.J., HUMMEL, H., BOKHORST, M. and MERKS, G.A. (1991). *The Westerschelde: interaction between eutrophication and chemical pollution?*, in: M. Elliott and J.-P. Ducrotoy (Editors), *Estuaries and Coasts: Spatial and temporal intercomparisons*, Olsen and Olsen, 359–364.
- HUMMEL, H., MOERLAND, G. and BAKKER, C. (1988). The concomitant existence of a typical coastal and a detritus food chain in the Westerschelde estuary, *Hydr. Bull.*, 22:35–41.
- LAWTON, J.H. (1989). *Food webs*, in: J.M. Cherrett (Editor), *Ecological concepts*, Blackwell Scientific, 43–78.

- MANN, K.H. (1988). Production and use of detritus in various freshwater, estuarine, and coastal marine ecosystems, *Limnol. Oceanogr.*, 33:910–930.
- MEES, J. and HAMERLYNCK, O. (1992). Spatial community structure of the winter hyperbenthos of the Schelde-estuary, the Netherlands, and the adjacent coastal waters, *Neth. J. Sea Res.*, 29:357–370.
- MEES, J., DEWICKE, A. and HAMERLYNCK, O. (in press a). Seasonal composition and spatial distribution of hyperbenthic communities along estuarine gradients in the Westerschelde, *Neth. J. Aquat. Ecol.*
- MEES, J., CATTRIJSSE, A. and HAMERLYNCK, O. (in press b). Distribution and abundance of shallow-water hyperbenthic mysids (Crustacea, Mysidacea) and euphausiids (Crustacea, euphausiacea) in the Voordelta and the Westerschelde, south-west Netherlands, *Cah. Biol. Mar.*
- MEES, J., ABDULKERIM, Z. and HAMERLYNCK, O. (submitted a). Life history, growth and production of *Neomysis integer* (Leach, 1814) in the Westerschelde estuary (S.W. Netherlands).
- MEES, J., FOCKEDEY, N. and HAMERLYNCK, O. (submitted b). Comparative study of the hyperbenthos of three European estuaries.
- MEIRE, P.M., SEYS, J.J., YSEBAERT, T.J. and COOSEN, J. (1991). *A comparison of the macrobenthic distribution and community structure between two estuaries in SW Netherlands*, in: M. Elliott and J.-P. Ducrotoy (Editors), *Estuaries and Coasts: Spatial and temporal intercomparisons*, Olsen and Olsen, 221–230.
- PAINE, R.T. (1980). Food webs: linkage, interaction strength and community infrastructure, *J. Anim. Ecol.*, 49:667–685.
- PIMM, S.L. and LAWTON, J.H. (1980). Are food webs divided into compartments?, *J. Anim. Ecol.*, 49:879–898.
- PORTELO, L., MONTEIRO, J. and NEVES, R. (1992). *Numerical modelling of tidal flow and salinity transport in the Westerschelde (The Netherlands): first results*, in: P.M.J. Herman (Editor), *JEEP 92: Major biological processes in European Tidal Estuaries*, Internal Report Netherlands Institute of Ecology, 149–157.
- RAFAELLI, D. and HALL, S.J. (1992). Compartments and predation in an estuarine food web, *J. Anim. Ecol.*, 61:551–560.
- SOETAERT, K. and HERMAN, P.M.J. (submitted). Estimating estuarine residence times in the Westerschelde (The Netherlands) using a simple box model.
- SOETAERT, K. and RIJSWIJK, P. van – (in press). Spatial and temporal patterns of the zooplankton in the Westerschelde estuary, *Mar. Ecol. Progr. Ser.*
- SOETAERT, K., HERMAN, P.M.J. and SCHOLTEN, H. (1992). *MOSES: Model of the Scheldt estuary*, in: P.M.J. Herman (Editor), *JEEP 92: Major biological processes in European Tidal Estuaries*, Internal Report Netherlands Institute of Ecology, 137–148.
- SMITH, S.V., HOLLIBAUGH, J.T., DOLLAR, S.J. and VINK, S. (1989). Tomales Bay, California: A case for carbon-controlled nitrogen cycling, *Limnol. Oceanogr.*, 34:37–52.

- SPAENDONK, A.J. van -, KROMKAMP, J. and VISSCHER, P. (in press). Primary production of phytoplankton in the turbid, coastal plain estuary the Westerschelde (the Netherlands), *Neth. J. Sea Res.*
- STUART, J.J., MEININGER, P.L. and MEIRE, P.M. (1990). *Watervogels van de Westerschelde*, Internal Report Universiteit Gent—Rijkswaterstaat Dienst Getijdewateren, 175 pp. (in Dutch).

Modelling Approach of the Planktonic Vertical Structure in Deep Austral Ocean

The Example of the Ross Sea Ecosystem

J.-H. HECQ¹, P. BRASSEUR¹, A. GOFFART¹,
G. LACROIX¹ and L. GUGLIELMO²

¹ University of Liège ² University of Messina, Italy

Abstract.

Hydrological, chemical and biological data obtained during a Vth Ross Sea ITALI-ANTARTIDE cruise have confirmed that the most important factors regulating the Antarctic pelagic food chain are physical processes operating within the circumpolar marginal ice zone during the ice melting period. As a typical characteristic of the Ross Sea, the ice free surface is propagating from the South to the North, with an increase of the water surface exposed to the sunlight. The diversity of pattern of water characteristics vertical profiles in Ross sea area seems due to specific local constraints more than diversity of ecosystem. First, the ice edge melting is not simultaneous for the whole region, the central and southern part being opened sooner than the lateral part. Secondly, the areas of depth shallower than 500 m seems to be inaccessible to krill which is strongly influencing the utilisation of primary production. Finally, The Western part of the Ross Sea is richer in phytoplankton than the eastern side probably because the different ice algae content of the ice pack.

First steps in coupling a 1D physical and a biological model in the Ross Sea are presented. Following pattern is proposed: ice algae are liberated by melting ice, growth and sediment in the upper mixed layer, are influenced by light and turbulence and are grazed by zooplankton and later other planktonic populations are regenerated.

1.- Introduction.

The condition of low biomass in spite of high nutrients has often been referred as a major "paradox" of the Southern Ocean (El-Sayed, 1984). However, there are frequent exceptions to this generality, and massive blooms higher than

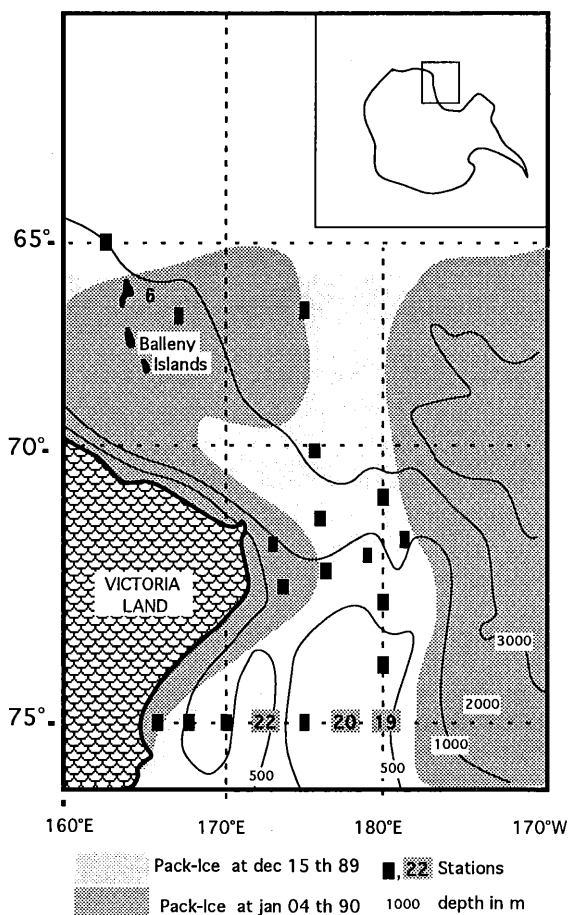


Fig. 1.— Sampling area and position of stations of the Vth Italian antarctic expedition. Ice edge extension during the cruise.

$10 \mu\text{g l}^{-1}$ of Chlorophyll *a* have been observed in some restricted regions (Nelson and Smith, 1986; Holm Hansen *et al.*, 1989; Mitchell and Holm Hansen, 1991).

In the Ross Sea area, for example, important phytoplankton concentrations have been observed directly (Smith and Nelson, 1985) or by remote sensing (Comiso, 1991). In that area, the characteristic extension of the marginal ice front seems to be responsible of the high productivity. As a typical characteristic of the Ross Sea, the ice free surface is propagating from the South to the North, with an early increase of the ice free water surface exposed to the sunlight (polynia) and also an increase of the length of the ice edge, as shown by weekly remote sensing pictures (Hecq *et al.*, 1992, 1993; Guglielmo *et al.*, 1993).

The evolution of the superficial water column ecosystem is governed by biological constraints but also physical constraints like insolation, water temperature, vertical thermohaline stratification, wind stress, turbulence, etc.

An interdisciplinary approach of the Ross Sea ecosystem has been realized on the base of the data acquired during the Vth ITALIANTARTIDE (*RV Cariboo*) expedition, South of the Antarctic Convergence, in December 1989 and January 1990 (figure 1).

In order to estimate the effects of hydrodynamics on spatial distribution of biological components, a coupling between an hydrodynamic model and a biological model have been enterprised (Hecq *et al.*, 1993).

2.- Summary of experimental results.

Using vertical profiles of phytopigments (chlorophylls, xanthophylls and phaeophorbids) detected by HPLC on GF/F filters (0.45 μm), biomasses and physiological state of the phytoplanktonic communities have been identified (Hecq *et al.*, 1992, 1993; Hecq and Goffart, 1991). Vertical profiles of zooplankton have been done by BIONESS nets from coastal to offshore area (Guglielmo *et al.*, 1993). Krill informations have been acquired by acoustic detections (Azzali *et al.*, 1992).

In the Ross Sea, along the ice edge and in the area of just broken pack-ice, phyto-pigments concentrations of the water column show strong maxima in the upper layers (from 2 to 6 $\mu\text{g l}^{-1}$ of chl. *a*) [figure 2a, st. 6]. Such concentrations could be attributed to the liberation of ice phytoplankton by melting ice. In this area, analysis performed on ice algae from the ice-snow interface reveal phytopigments concentrations from 80 to 250 $\mu\text{g l}^{-1}$ of chl. *a*. This is in good agreement with the hypothesis that organic matter is intensively produced in the marginal ice zones (El-Sayed, 1984; Smith and Nelson, 1985; Nelson and Smith, 1986).

Various hypotheses can explain the enhancement of phytoplankton biomass along the ice-edge. Ice edge upwelling, stratified condition related to critical depth and releasing of ice algae in the water column after melting process (Smith and Nelson, 1985) could act as a synergy for phytoplankton blooms. As a general rule, the strong hydrodynamical constraints associated to the main frontal systems and to the areas of increased stability influence the distribution and productivity of plankton organisms (Goffart and Hecq, 1988, 1989; Goffart *et al.*, 1992).

In that ice-edge area, phaeophorbids, which are produced by chlorophyll degradation during grazing, are absent in the water column, revealing a reduced

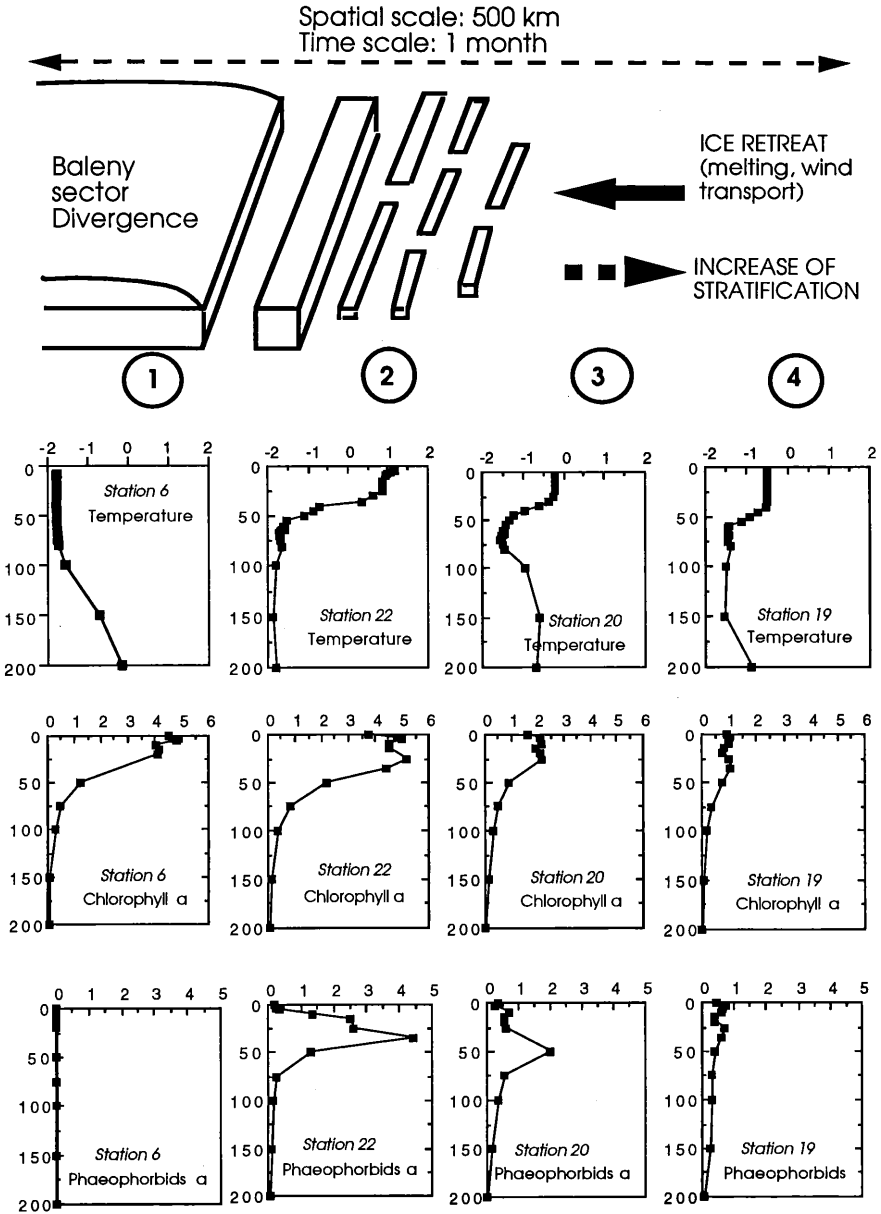


Fig. 2a.- Vertical distribution of temperature (data from Artegiani), chlorophyll *a* and phaeophorbids *a* (HPLC), from 0 to 200 m, at four stations, from the ice edge to offshore (depth < 500 m).

zooplankton activity. Mesozooplankton is characterized by a scarce density in the whole water column. This situation corresponds to the beginning of the

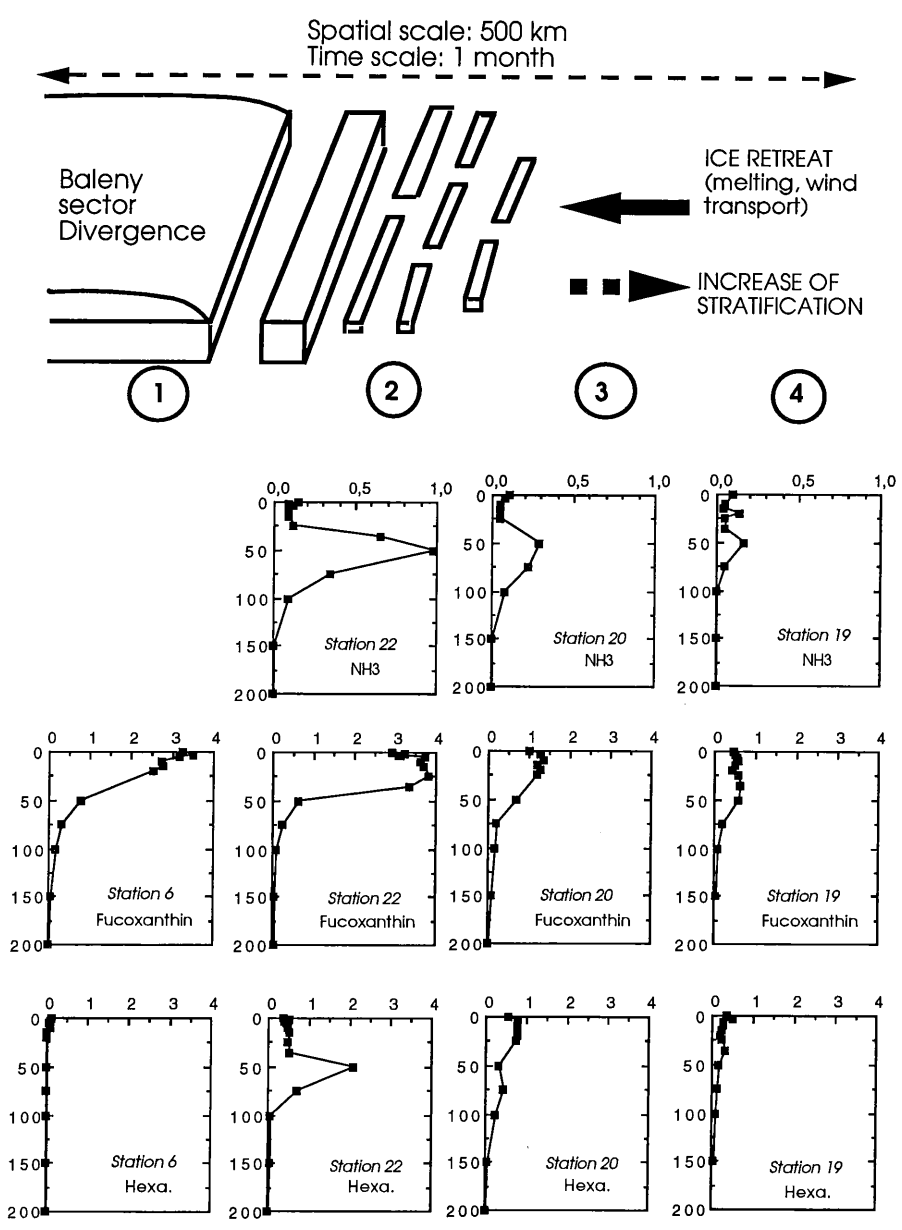


Fig. 2b.- Vertical distribution of ammoniac, fucoxanthin and hexanoyloxyfucoxanthin (HPLC), from 0 to 200 m, at four stations, from the ice edge to offshore (depth < 500 m).

phytoplankton bloom when the populations of herbivorous zooplankton have not developed yet.

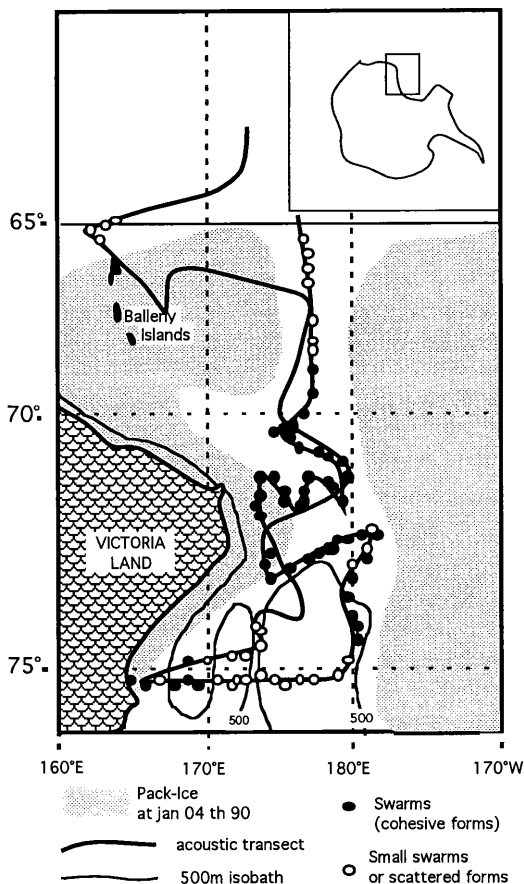


Fig. 3.— Distribution of Krill (from Azzali, in Hecq *et al.*, 1993).

However, few individuals of krill (*Euphausia superba*) were grazing actively on the ice algae through a series of canals that were spotted in the ice pack.

In open ice-free waters, the total chloro-pigments *a* concentration is quite the same as in ice edge area. However, chlorophyll *a* is often replaced by high concentrations of phaeophorbids *a* (2 to $3 \mu\text{g l}^{-1}$) which correspond to high grazing activity of herbivorous zooplankton. The maximum values of phaeophorbids are generally recorded between 40 and 70 meters and corresponds to maxima of copepods, chaetognaths and krill observed between 0 and 80 m and also to the distribution of NH_4 which confirms grazing and excretion activities.

As far as the secondary production is concerned, two different ecosystem diagrams can be distinguish according to the bottom topography.

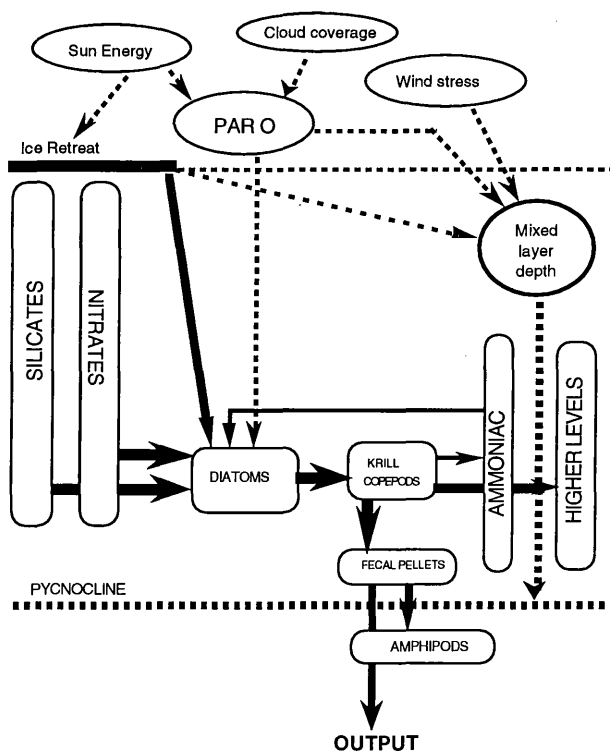


Fig. 4a.– Conceptual diagram of Ross Sea pelagic ecosystem (Hecq *et al.*, 1993).

In the central part of the Ross Sea, outside the shelf where waters are deeper than 500 m, the chlorophyll *a* is strongly reduced. This reduction corresponds to areas where pack ice has disappeared for a long time (about 20 days), as shown by remote sensing. Numerous and dense aggregations of *Euphausia superba* were detected by echosurveys (Azzali *et al.*, 1992) in central and northern parts of the Ross Sea, west off Cape Adare, and do not confirm the opinion that Pacific sector of Antarctic is poor with krill [figure 3] (Guglielmo *et al.*, 1993; Hecq *et al.*, 1993). Visual observations of high concentrations of predators (mainly birds like Antarctic petrel) near krill aggregates confirm active energetic flow across *E. superba* in the Ross Sea food web (figure 4a).

In the south western part of Ross Sea, corresponding to depths shallower than 500 m, but ice free waters, krill is quite absent and replaced by other herbivorous like copepods distributed between 50 and 100 m depth. That corresponds to high values of chlorophyll *a* in the euphotic layer; phaeophorbids and ammoniac are more vertically distributed in relation to various zooplankton components. Moreover the distribution of secondary pigments suggests that

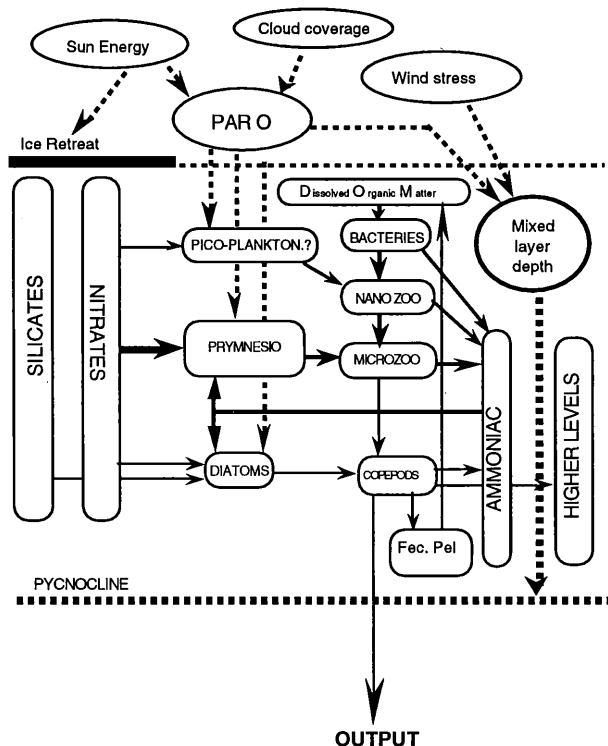


Fig. 4b.— Conceptual diagram of Ross Sea Shelf ecosystem (Hecq *et al.*, 1993).

diatoms (characterised by fucoxanthin) are not the dominant phytoplankton species and prymnesiophyceae (hexanoyl-oxyfucoxanthin), cryptophyceae, etc. occur also in the bottom of euphotic zone (figure 2b). Moreover, a succession of various zooplankton species occurs (Guglielmo *et al.*, 1993) and confirms the existence of different pathways through which a major part of the available energy may be flowing (figure 4b).

3.— The model.

The different characteristic areas recognized in the Ross Sea during this spring period are not to be taken as different ecosystems but more really as different temporal steps of a typical ecosystem progressing from pack ice to ice free waters.

Results confirm the idea that biomass, composition and productivity of plankton ecosystem during the spring, in the Ross Sea depends essentially on the time after the waters become ice free.

The following pattern is proposed: ice algae are liberated by melting ice, sediment in the water column, are grazed by zooplankton and later new planktonic populations are regenerated.

Actually many authors accord to a common spatio-temporal sequence of events in the water column at a receding ice-front (Smith and Nelson, 1985; Hecq *et al.*, 1990; Lancelot *et al.*, 1992): melt water and epontic algae are introduced into the surface layer during ice melting. Certain species of epontic algae are able to growth in the melt water lens. A stable layer of meltwater retards vertical mixing and thus allows the algal species to accumulate and to form a local biomass maximum. The meltwater lens is continuously being degraded at its seaward edge by vertical mixing. This results in phytoplankton at location seaward of the meltwater lens having the same elemental and species composition as within it, but at lower absolute concentrations and mixed over a greater vertical extend. These cells may or may not continue to grow in the more deeply mixed water column. Recently the role of U.V. on smallest phytoplanktonic cells growth have been argued (El-Sayed *et al.*, 1990).

Some hypotheses about the important decrease of phytoplankton biomass in the water column after the ice edge retreat have been presented. Iron which may be depleted will be limiting for the primary production (Martin *et al.*, 1990) and grazing is reducing the phytoplankton biomass more than the productivity (Bidigare *et al.*, 1986). For example, in offshore area, where krill is the dominant herbivorous, the biomass of diatoms can be depleted in a few days or a few hours in some area, In the contrary, where krill is generally absent, copepods, pteropods, salps, etc. are the dominant herbivores, so that, grazing on nanophytoplankton and particularly on diatoms is reduced.

Moreover the major part of picoplankton ($< 2 \mu\text{m}$), not usable by krill and macrozooplankton is consumed by microzooplankton as small copepodites, larvae and protozoans (tintinnids, etc.). The unicellular heterotrophic flagellates also consume bacterial components. The plankton biomass and production in this part of Austral Ocean, is far from the general picture of a near oligotrophic system (Jacques and Treguer, 1986).

If all those processes controlling the ecosystem have their own importance, they are influenced by physical structure of the water column. Moreover, they are non linear and impossible to experiment.

An integrated modellistic approach based on field data more than on theoritical concept is necessary to simulate numerically the effect of various hypothesis concerning ecosystem control presented by field experts. First steps

Table 1
Hydrodynamic equations system (from Lacroix and Djenidi, 1992)

$$\begin{aligned} \nabla \cdot \mathbf{u} + \frac{\partial u_3}{\partial x_3} &= 0 \\ \frac{\partial \mathbf{u}}{\partial t} + \mathbf{u} \cdot \nabla \mathbf{u} + u_3 \frac{\partial \mathbf{u}}{\partial x_3} + f \mathbf{e}_3 \wedge \mathbf{u} &= -\nabla q + \frac{\partial}{\partial x_3} \left(\tilde{\nu} \frac{\partial \mathbf{u}}{\partial x_3} \right) \\ \frac{\partial T}{\partial t} + \mathbf{u} \cdot \nabla T + u_3 \frac{\partial T}{\partial x_3} &= \frac{\partial}{\partial x_3} \left(\tilde{\lambda}^T \frac{\partial T}{\partial x_3} \right) \\ \frac{\partial S}{\partial t} + \mathbf{u} \cdot \nabla S + u_3 \frac{\partial S}{\partial x_3} &= \frac{\partial}{\partial x_3} \left(\tilde{\lambda}^S \frac{\partial S}{\partial x_3} \right) \\ \frac{\partial k}{\partial t} + \mathbf{u} \cdot \nabla k + u_3 \frac{\partial k}{\partial x_3} &= \tilde{\nu} \left\| \frac{\partial \mathbf{u}}{\partial x_3} \right\|^2 - \tilde{\lambda}^b \frac{\partial b}{\partial x_3} - \varepsilon + \frac{\partial}{\partial x_3} \left(\tilde{\nu}^k \frac{\partial k}{\partial x_3} \right) \end{aligned}$$

where

$$\begin{aligned} \nabla &= \mathbf{e}_1 \frac{\partial}{\partial x_1} + \mathbf{e}_2 \frac{\partial}{\partial x_2} ; \quad q = \frac{p}{\rho_0} + g x_3 ; \\ \frac{\partial q}{\partial x_3} &= b ; \quad b = -\frac{\rho - \rho_0}{\rho_0} g = b(T, S) ; \end{aligned}$$

$\mathbf{u} = (u, v)$ is the horizontal velocity; T the temperature; S the salinity; k the turbulent kinetic energy; $\tilde{\nu}, \tilde{\lambda}^b$ the turbulent diffusion coefficients; b the buoyancy; g the gravitational acceleration; ρ the density and ε the dissipation rate of the turbulent kinetic energy by viscosity.

in coupling a 1D physical and a biological model are presented in relation to data acquired during the Vth Italianartide Expedition (1989–1999).

The physical model is a simplified version of the GHER general 3D model to a 1D vertical model with a turbulent $k - \varepsilon$ closure [Table 1] (Nihoul, 1984; Nihoul *et al.*, 1989; Lacroix and Djenidi, 1992). The simulation of the temporal evolution of the physical structure of the upper layer is done in order to provide depth of upper mixed layer and pycnocline, and turbulent diffusion coefficient profiles necessary to force the biological model. Figure 5 presents the simulation of the formation of the thermocline with different wind conditions. Turbulence induced by wind stress is an important physical element governing the establishment and decay of the thermocline and the turbulent diffusion of non-migrating biological variables (nutrients, phytoplankton, microzooplankton and suspended particles).

The biological model, especially built to study, in the future, the vertical distribution of phyto-pigments, is based on classical following equations for the primary production, and grazing (Saksaug *et al.*, 1991; Svanson, 1991; Hecq *et al.*, 1993). The variation of biological variables B is governed by a single equation as a sum of production, destruction, sedimentation and turbulent diffusion

$$(1) \quad \frac{\partial B}{\partial t} = \frac{dB}{dt} - w_z \cdot \frac{\partial B}{\partial z} + \frac{\partial}{\partial z} \left[\tilde{\nu} \cdot \frac{\partial B}{\partial z} \right]$$

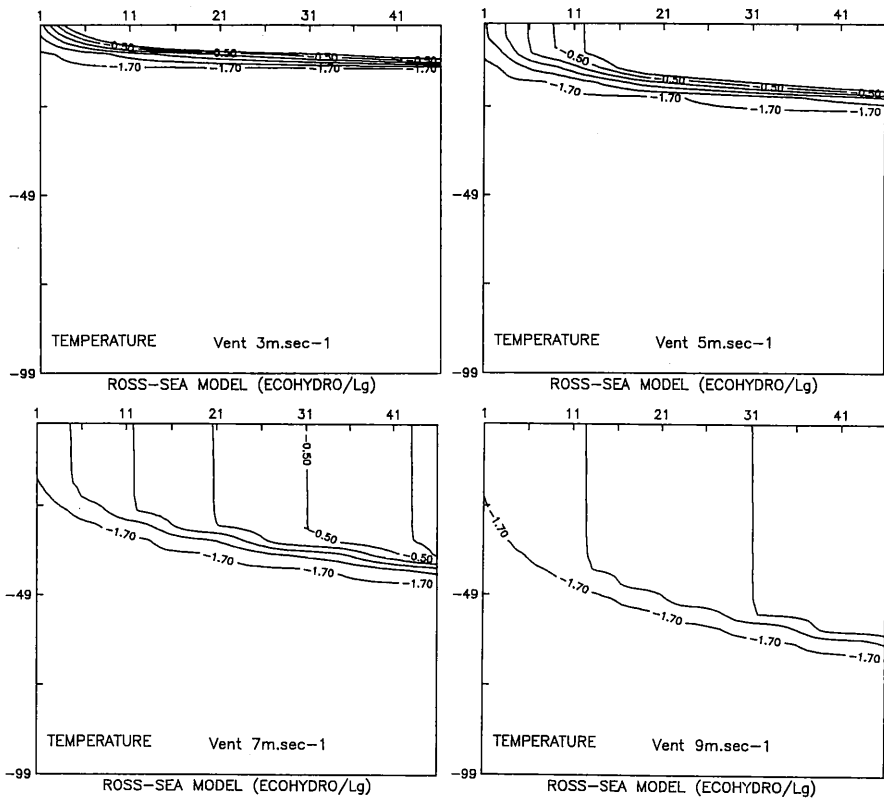


Fig. 5.— Simulation of thermocline formation with various wind conditions.

where w_z and $\tilde{\nu}$ are the coefficients of sedimentation and of turbulent diffusion. For example the diatom/krill/fecal pellets food web have been simulated for the northern part of the Ross Sea. In this step of the work, the basic equation for diatom production is considered only light limited and influenced by grazing by krill and by diffusion

$$(2) \quad \frac{\partial D}{\partial t} = P_{\max}^B \cdot I_{\lim} \cdot D - \left[\zeta_{\max} \cdot \frac{D - D_s}{k_{sD} + D} \right] \cdot Kr - w_z \cdot \frac{\partial D}{\partial z} + \frac{\partial}{\partial z} \left[\tilde{\nu} \cdot \frac{\partial D}{\partial z} \right]$$

where P_{\max}^B is the maximum photosynthetic rate and I_{\lim} the limitation by light, D is the diatoms biomass and D_s a threshold value for grazing. Kr represent the krill concentration and ζ_{\max} is the maximum grazing rate. I_{\lim} is a function of the initial slope (α) and P_{\max}^B of the P/I curve and of available light. The coefficients used in the diatoms equation model have been determined by Mitchell and Holm-Hansen (1991), in similar conditions:

$$(3) \quad I_{\text{lim}} = 1 - \exp \left(- \frac{\alpha \cdot \text{PAR}_{(z)}}{P_{\text{max}}^B} \right)$$

$$(4) \quad \text{PAR}_{(z)} = \text{PAR}_{(0^+)} \cdot \tau \cdot \exp(-\text{KPAR} \cdot z)$$

$$(5) \quad \text{KPAR} = 0.078 + 0.0136(\text{chl. } a + \text{phaeo. } a)$$

where $\text{PAR}_{(z)}$ and $\text{PAR}_{(0^+)}$ are the photosynthetic active radiation at the depth z and above the surface; τ is the coefficient of penetration of light across the interface.

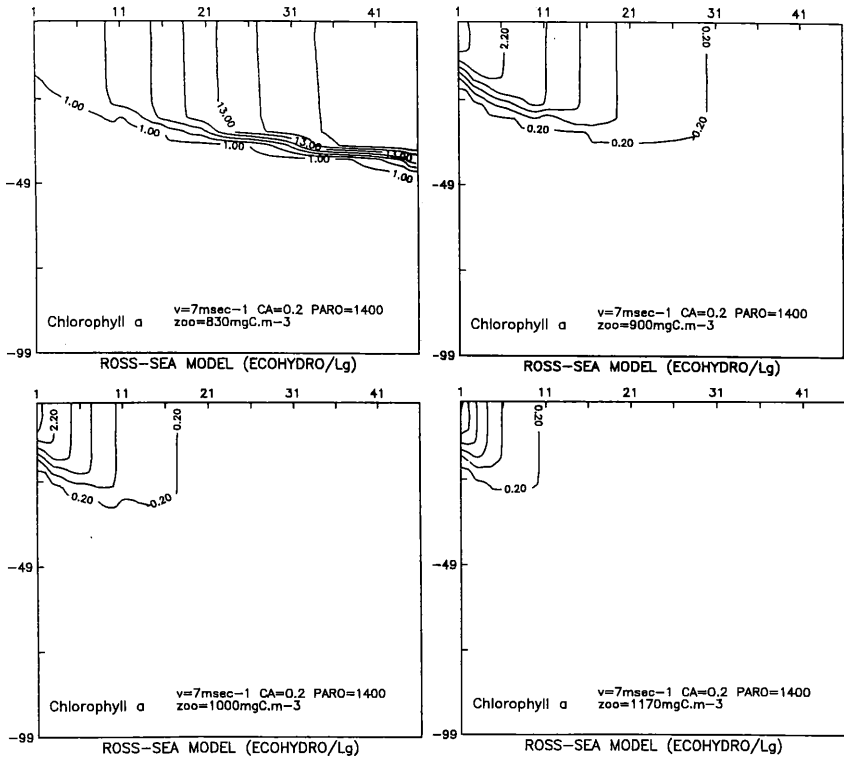


Fig. 6. – Simulation of diatoms vertical profiles variations in function of diverse krill concentration.

For the Krill (Kr), the growth depends on the coefficient of assimilation of ingested food (κ_{max}) and on excretion, eggs production, predation and mortality

$$(6) \quad \frac{\partial Kr}{\partial t} = Kr \cdot \left[\kappa_{\text{max}} \cdot \left(\zeta_{\text{max}} \cdot \frac{D - D_s}{k_{sD} + D} \right) - (r_{Kr} + e_{Kr} + c_{Kr} + m_{Kr}) \right]$$

The krill fecal pellets reach sedimentation speed of 200 m D^{-1} . The effect of turbulence is neglected:

$$(7) \quad \frac{\partial F_{Kr}}{\partial t} = (1 - \kappa_{\max}) \left[\zeta_{\max} \cdot \frac{P - P_s}{k_{sP} + P} \right] \cdot Kr - w_{F_{Kr}} \cdot \frac{\partial F_{Kr}}{\partial z}$$

Assuming that diatoms are realised by ice melting in the mixed layer and grazed by krill, the biomass of phytoplankton is plotted in function of depth and of time. A simulation is done with diverse krill concentrations and shows the decrease of the diatoms after a period of few days with concentrations of 900 mC m^{-3} of krill, independently of nutrients which are not limiting factor. A complete depletion of diatoms can occur where krill is present.

4.- Conclusions.

The diversity of pattern of water characteristics vertical profiles in Ross sea area seems influenced by specific properties. First, the ice edge melting is not simultaneous for the whole region, the central and southern part being opened sooner than the lateral part. Secondly, the areas of depth shallower than 500 m seems to be inaccessible to krill which is strongly influencing the utilisation of primary production. Finally, the Western part of the Ross Sea is richer in phytoplankton than the eastern side this is probably due to the different content in ice algae of the ice pack. For those reason a coupled 1D model of first trophic levels is realist and only influenced by initial conditions and by external stresses like wind and light. However, if the Ross Sea area need to be modelled as an integrated ecosystem, some state variables and control functions concerning upper trophic layers have to be taken into account:

- the ice free water surface and the ice edge length variations during the season and the vertical structure of the water column will influence the primary production and need to be considered in relation to the ice system in terms of wind stress and turbulence.
- the phytoplanktonic variables begin to be understood but an effort must be done on the influence of different class sizes of phytoplankton.
- zooplanktonic variables, however do not have the same spatial and temporal scales than phytoplankton and differences exist between species. Moreover, following the spatial related to the shelf, two species of macrozooplankton krill or amphipods, exist and will consume the same phyto-planktonic communities but these two zooplanktonic groups does not have the same vertical distribution on the water column and will be or not accessible to marine birds. This factor probably orientates the switch {Fishes \Leftarrow Zooplankton \Rightarrow Birds} and influences the distribution of higher trophic levels and also the distribution of all planktonic organic material.

— on the other hand, following the migrating processes of zooplankton, the quantity of fecal pellets varies strongly in function of the depth and in the whole the organic material is transferred to an other scale.

For all these reasons, in the future, the efforts have to be pointed on an adapted experimentation and modelling on interacting processes between primary, secondary and tertiary producers. Not only standing stocks but especially processes of grazing, ammonium excretion, fecal pellets production, sedimentation, nutrient recycling and vertical migrations have to be taken in account in relation to physical processes of ice melting and retreat.

The strategy of the cruise must be orientated to selected long term stations characteristic of a temporal state of the ecosystem more than a spatial numerous data acquisition.

Acknowledgements.

This work is a part of the Belgian Research Program in Antarctic founded by the Science Policy Office (SPPS Project Antar 06, Brussels, Belgium) in connection to National Italian Research Project in Antartide (ENEA and CNR). Jean-Henri Hecq is Senior Research Assistant from FNRS (National Foundation for Scientific Research) and Pierre Brasseur is Research Assistant from FNRS.

References.

- AZZALI, M., KALINOWSKI, J., COSIMI, G. and CASTAGNANI, R. (1992). *Distribution of krill biomass in the Ross Sea, December 89–January 90*, Nat. Sc. Com. Ant., Ocean. Camp. Data rep., II:469–507.
- BIDIGARE, R.R., FRANK, T.J., ZASTROW, C. and BROOKS, J. (1986). The distribution of algal chlorophylls and their degradation products in the Southern Ocean, *Deep Sea Research*, 33:923–937.
- COMISO, J.C. (1991). Satellite remote sensing of the Polar Oceans, *Journal of Marine Systems*, 2:395–434.
- EL-SAYED, S. (1984). *Productivity of Antarctic waters. A reappraisal*, in: O. Holm Hansen, L. Bolis, R. Gilles (Editors), *Marine Phytoplankton and Productivity*, Springer Verlag, Berlin, pp. 19–34.
- EL-SAYED, S.Z., STEPHENS, F.C., BIDIGARE, R.R. and ONDRUSEK, M.E. (1990). *Effect on Ultraviolet radiation on Antarctic Marine phytoplankton*, in: K.R. Kerry and G. Hempel (Editors), *Antarctic Ecosystems, Ecological Change and Conservation*, pp. 379–385.
- GOFFART, A. and HECQ, J.-H. (1988). Distribution of phytoplanktonic parameters in the Indian sector of the Southern Ocean during Indigo III cruise, *Proceedings of the Belgian National Colloquium on Antarctic Research*, Brussels, October 20, 1987, Prime Ministers Service Science Policy Office, 147–166.

- GOFFART, A. and HECQ, J.-H. (1989). *Zooplankton Biochemistry and Ecodynamics*, in: S. Caschetto (Editor), *Belgian Scientific Research Programme on Antarctica. Scientific Results of Phase One (Oct. 85–Jan. 89)*, Vol. I: *Plankton Ecology*, Belgian Prime Minister's Services Sciences Policy Office, Brussels, Belgium, 2:1–60.
- GOFFART, A., CATALANO, G., MAGAZZU', G. and HECQ, J.H. (1992). *Some examples of the influence of hydrodynamical constraints on phytoplanktonic biomass and productivity in the Southern Ocean*, in: V.A. Gallardo, O. Feretti and H.I. Moyano (Editors), *Processes of the "Oceanografia in Antartide" International Workshop 7–9 march 1991*, Concepcion, Chile, pp. 265–271.
- GUGLIELMO, L., HECQ, J.H., ARTEGANI, A., BENEDETTI, F., CATALANO, G., DECEMBRINI, F., FABIANO, M., GOFFART, A., INNAMORATI, M., LAZZARA, L., NUCCIO, C. and PASCHINI, E. (1993). Ecohydrodynamical approach of the planktonic ecosystem during the Vth ITALIANTARTIDE expedition in the Pacific sector of the Southern Ocean (1989–1990), *Journal of Marine Systems*, (submitted).
- HECQ, J.H. and GOFFART, A. (1991). *Results of phytospigments analysis by high performance liquid chromatography (HPLC) during the Vth ITALIANTARTIDE expedition (1989–1990)*, Nat. Sc. Com. Ant., Ocean .Camp., Data Report, Part II:123–152.
- HECQ, J.H., MAGAZZU', G., GOFFART, A., CATALANO, G., VANUCCI, S. and GUGLIELMO, L. (1992). Distribution of planktonic components related to structures of water masses in the Ross Sea area during the Vth ITALIANTARTIDE expedition, *Atti del 9° Congresso A.I.O.L.*, S. Margherita, Ligure, 665–678.
- HECQ, J.H., GOFFART, A., AZZALI, M., AZZOLINI, R., CATALANO, J., GUGLIELMO, L., MAGAZZU', G., POVERO, P. and VANUCCI, S. (1993). Ecohydrodynamical approach of the planktonic ecosystem during the Vth ITALIANTARTIDE expedition in the Pacific sector of the Southern Ocean (1989–1990), *Journal of Marine Systems*, (submitted).
- HOLM HANSEN, O., MITCHELL, B.G., HEWES, C.D. and KARL, D.M. (1989). Phytoplankton blooms in the vicinity of Palmer Station, Antarctica, *Polar Biology*, 10:49–57.
- JACQUES, G. and TREGUER, P. (1986). *Écosystèmes pélagiques marins*, Masson Éd., Paris, 243 pp.
- LACROIX, G. and DJENIDI, S. (1992). *Extending the GHER 3D model to the modelling of ecosystems in western mediterranean coastal zones: results from an exploratory study*, Comptes Rendus EROS 2000 Program Mast, 89–104.
- LANCELOT, C., VETH, C. and MATHOT, S. (1991). Modelling of the ice Edge phytoplankton bloom in the Scottia Weddell Sea sector of the Southern Ocean, *Journal of Marine System*, 2(3/4):333–346.
- MARTIN, J.H., GORDON, R.M. and FITZWATER, S. (1990). Iron in Antarctic waters, *Nature*, 345:156–158.
- MITCHELL, B.G. and HOLM HANSEN, O. (1991). Observation and modeling of the Antarctic phytoplankton crop in relation to mixing depth, *Deep Sea Research*, 38:981–1007.

- NELSON, D.M. and SMITH, W.O. (1986). Phytoplankton bloom dynamics of the western Ross Sea ice edge. / II. Meso-scale cycling of nitrogen and silicon, *Deep Sea Research*, 33:1389–1412.
- NIHOUL, J.C.J. (1984). A three-dimensional general marine circulation model in a remote sensing perspective, *Annales Geophysicae*, 2 (4):433–442.
- NIHOUL, J.C.J., DELEERSNIJDER, É. and DJENIDI, S. (1989). Modelling the General Circulation of Shelf Seas by 3D $k - \epsilon$ Models, *Earth-Science Reviews*, 26:163–189.
- SAKSHAUG, E., SLAGSTAD, D. and HOLM HANSEN, O. (1991). Factors controlling the development of phytoplankton blooms in the Antarctic Ocean—a mathematical model, *Marine Chemistry*, 35:259–271.
- SMITH, W.O. and NELSON, D.M. (1985). Phytoplankton bloom produced by a receding ice edge in the Ross Sea: Spatial Coherence with the density field, *Science*, 227:163–166.
- SVANSON, A. (1991). A simple primary production model for the NW Weddell Sea, *Marine Chemistry*, 35:347–354.

Control of Phytoplankton Development by Nitrate Availability in the Liguro-Provençal Basin (Western Mediterranean)

Anne GOFFART and J.H. HECQ*

Unité d'Écohydrodynamique, University of Liège

Abstract.

Ten years of mesoscale oceanographic studies in the Liguro-Provençal basin (Corsican area) have emphasized that phytoplankton communities distribution is characterized by a high spatial and temporal heterogeneity. The phytoplankton organization is greatly influenced by the presence of the Liguro-Provençal front whose functioning contributes significantly to increase the local productivity. The role of the front in the phytoplankton productivity enhancement is important all through the year but is much more effective from March to May. In the entire basin, a crucial moment for phytoplankton communities is encountered during summer, when surface waters are nutrient exhausted. The characteristic response of the primary producers is to sink below the surface mixed layer and to develop deep chlorophyll maxima (DCM). Their formation and maintenance are discussed. During the stratified period, all data support the view that phytoplankton distribution is primarily controlled by nitrate availability.

1.- Introduction.

For a long time, the primary production of the Mediterranean had the reputation to be among the lowest in the world and has been compared to the Sargasso Sea (Sournia, 1973). Paradoxically, fishing activities have been going on for centuries and are at present increasing (FAO, 1985). The annual yield of marine animals, both pelagic and demersal, amounts to 300 to 400 kg of fish per km² of sea (Margalef, 1985). Moreover, large numbers of marine mammals, mainly dolphins, long-finned whale and porpoises, are regularly observed (Viale *et al.*, 1986; personal observations).

* Senior Research Assistant from FNRS, Belgium.

Recently, remote sensing data acquisition allows a synoptic mapping of algal pigments and a reappraisal of the mean annual carbon fixation rate. For the Western Mediterranean, it has been estimated at $94 \text{ g C/m}^2\text{.year}$ (Morel and André, 1991).

On the basis of these contradictions and because the large populations of higher trophic levels depend ultimately on phytoplankton as the base of the food web, accurate understanding of the main environmental factors controlling phytoplankton production is essential to the estimate of the real fertility of the Mediterranean.

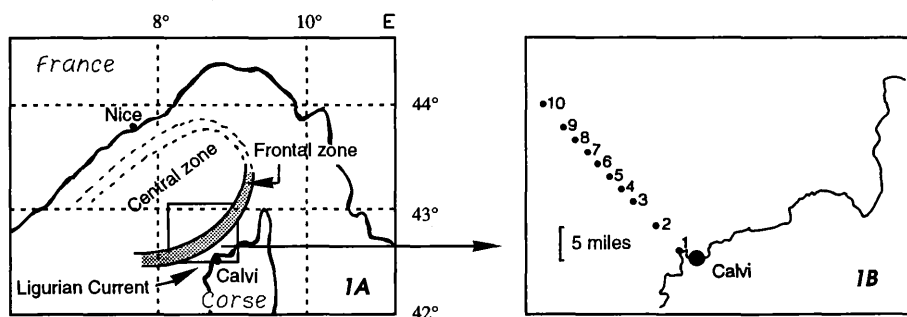


Fig. 1.— Map of the Liguro-Provençal basin showing the position of the main hydrological structures (1a) and the location of the stations (1b).

As a contribution to this general objective, oceanographic cruises were carried out in the Liguro-Provençal basin between 1982 and 1991. A schematic representation of the investigated area is presented at figure 1a. It shows the relative position of the main hydrological structures of the area, whose Liguro-Provençal front is the most important feature. Sampling stations were located across the front, along the Calvi-Nice axis from the Corsican coast to 30 miles offshore (figure 1b). Results are reported in Hecq *et al.* (1983), Goffart and Hecq (1985), Licot (1985), Hecq *et al.* (1986), Brohée *et al.* (1989), Goffart and Hecq (1990), Hecq and Goffart (1990) and Goffart (1992).

Field experience has emphasized that phytoplankton communities distribution is characterized by a high spatial and temporal heterogeneity and that the Western Mediterranean is far to be uniformly poor. Examples are shown to illustrate that the dynamics of phytoplankton is highly controlled by nutrients availability, itself dependent on hydrological constraints.

2.- Contribution of the Liguro-Provençal front (Corsican area) to the phytoplankton production.

The Liguro-Provençal front is a frontal structure resulting from the existence of a permanent cyclonic circulation of the coastal surface waters (Ligurian Current) around the central zone of the Liguro-Provençal basin. It is a permanent geostrophic front separating the light coastal waters from the denser offshore water masses. Accurate descriptions of the Ligurian current and of the frontal zone dynamics, including the vertical circulation, are provided in Boucher *et al.* (1987), Béthoux *et al.* (1988) and Sournia *et al.* (1990).

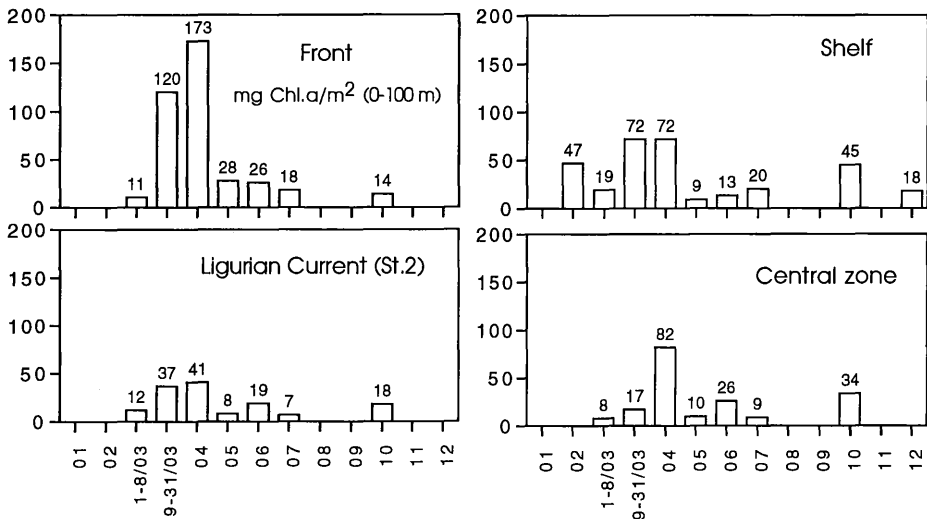


Fig. 2.- Temporal evolution of integrated chlorophyll *a* (0–100 meters, mg/m²) when averaged within each of typical hydrological zone encountered from the Corsican coast to 30 miles offshore. Results were obtained between 1982 and 1991. Number of cruises per zone and per period varies between 1 and 5. From Goffart (1992).

As emphasized in Hecq *et al.* (1986), Goffart (1992), Hecq *et al.* (1992) and Goffart *et al.* (in preparation), the divergence associated with the frontal system brings nutrients from deep water into the photic layer, allowing a continuous “new” phytoplankton production. Ten years of investigations on phytoplankton ecology in the Liguro-Provençal area have shown that the role of the front in enhancing phytoplankton biomass and primary production is important all through the year but is much more effective from March to May (figure 2). As a consequence, a marked contrast between the productive frontal zone and the low standing crops of the adjacent areas, including the shelf, is observed.

3.— Seasonal organization of phytoplankton populations.

In the entire Liguro-Provençal basin, winter mixing brings up deep water and leads to a relative nutrients enrichment of the surface layers. Offshore of Calvi, surface nitrate pre-bloom concentrations are of about 1, 3–5 and 5 μM for the Ligurian Current, the frontal zone and the central part of the basin respectively. However, the surface mixed layer is deeper than the euphotic zone (winter euphotic depth varies from 30 to 40 meters) and phytoplankton is alternately carried into and out of the lighted layers (figure 3). In these conditions, phytoplankton cells spend on average too much time in inadequately illuminated water that no net growth occurs.

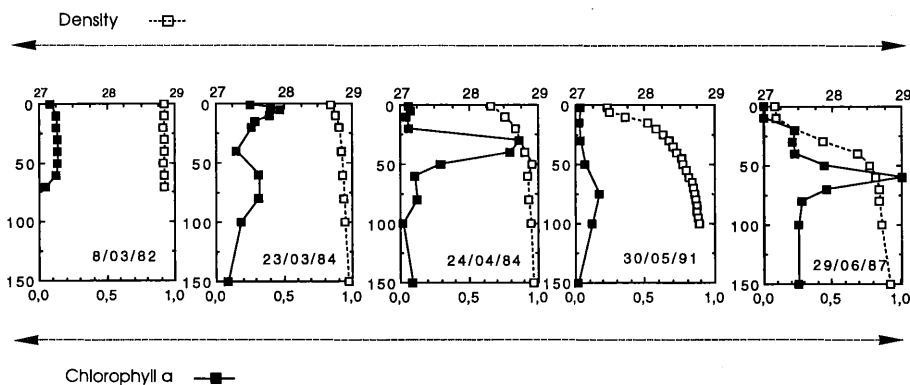


Fig. 3.— Seasonal evolution of the vertical distribution of density σ_θ and chlorophyll a (mg/m^3) in the Ligurian Current, 5 miles offshore of Calvi (station 2).

The spring bloom occurs after the winter nutrient supply, when turbulent mixing intensity reduces, allowing the early stratification of the water column (figure 3). On the shelf, it starts usually in February while it is observed quite one month later offshore. Phytoplankton communities, diatoms dominated, develop in the upper part of the water column and lead to a rapid exhaustion of surface nutrients.

From the beginning of April, an oligotrophic layer develops at the surface. Low nitrate concentrations prevail in the surface layer ($< 0.3 \mu\text{M}$ between 0 and 20 meters) and a subsurface chlorophyll maximum appears, in relation with nutrient impoverishment of the mixing layer (figure 3).

As spring and early summer progress, insolation increases and wind mixing in the upper layers of the euphotic zone induces the establishment of the seasonal thermocline. The density gradient imposes a rigorous constraint on the vertical flux of nitrate from deep water (Lewis *et al.*, 1986) and new production leads to the complete winter nitrate exhaustion in the mixing layer (figure 4).

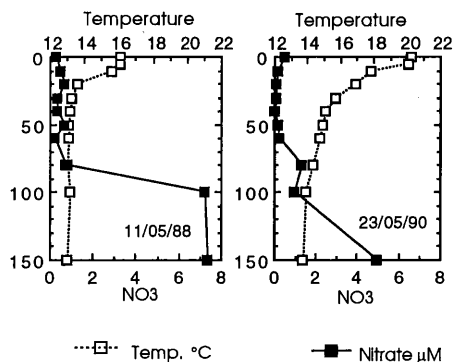


Fig. 4.– Early summer vertical distribution of temperature (°C) and nitrate (μM) in the Ligurian Current (Station 2).

In response to this nutrient stress, and during all the stratified period, the primary producers sink below the thermocline and develop a pronounced deep chlorophyll maximum (figure 3), still within the euphotic zone, at depths ranging from 40 to 100 meters (Goffart, 1992).

Table 1
Depth of the DCM in the Mediterranean

Area	Period	Depth of the DCM (meters)	Reference
Catalano-Balearic front	May	40 m	Estrada and Margalef, 1988
Mallorca-Menorca channel	May	60 m	Estrada and Margalef, 1988
Algerian coast (Mediterranean water between 1 and 3°E)	May	62 m	Lohrenz <i>et al.</i> , 1988
Catalan coast (Barcelona)	July	40–80 m	Estrada, 1985
Tyrrhenian	Summer	50–75 m	Marino <i>et al.</i> , 1984
Israeli coast	Summer	75–125 m	Berman <i>et al.</i> , 1984
Ionian Sea	July	90 m	Berland <i>et al.</i> , 1988
Creto-African area	July	100 m	Berland <i>et al.</i> , 1988
Levant basin	June	90–120 m	Berland <i>et al.</i> , 1988

The existence of widespread deep chlorophyll maxima (DCM) is a common feature in the oligotrophic waters of the Mediterranean and has been reported by numerous authors (table 1).

In the Liguro-Provençal basin, the most evident feature is that the position of the deep chlorophyll maximum is closely associated with the nitrite maxima and with the nitracline that occurs well below the largest vertical gradient in temperature and density (figure 5). The vertical distribution of phytoplankton

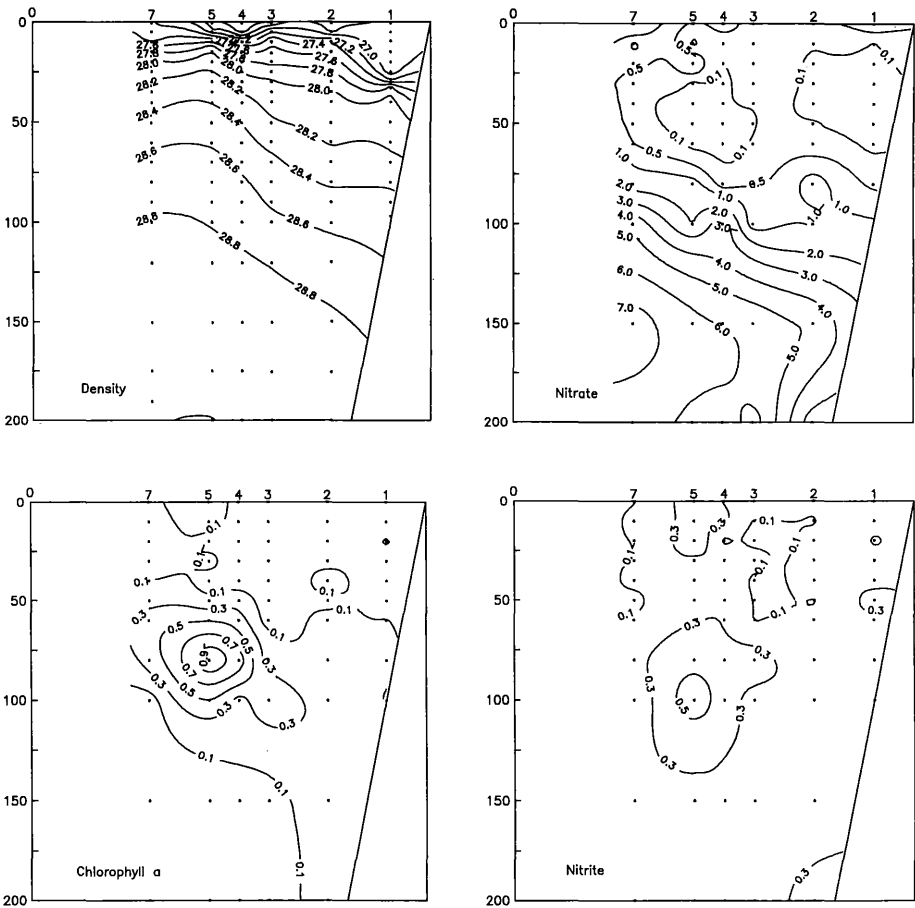


Fig. 5. – Upper 200 meters distribution of density σ_θ , nitrate (μM), HPLC chlorophyll *a* (mg/m^3) and nitrite (μM) from the Corsican coast (station 1) to 20 miles offshore (station 7). [23 and 26 May 1990]

is thus under the control of both light and nutrients and the position of the chlorophyll maximum in the water column is determined by the opposing gradients of light and nitrate rather than by isopycnals constriction and stability maximum. As proposed by Lohrenz *et al.* (1988), the interactive relationship between nutrient supply and phytoplankton *in situ* growth seems to be primarily responsible for the formation and location of chlorophyll maxima. Even if phytoplankton productivity is low at the level of the DCM, because of light limitation, the primary production in these maxima [$0.1\text{--}0.5 \text{ mg C}/\text{m}^3 \cdot \text{h}$ (Cahet *et al.*, 1972; Estrada, 1985)] is particularly important during summer because consists for a high proportion in a new production, derived from a net conversion of nitrate to plant biomass (Estrada *et al.*, 1985; Goffart, 1992). Moreover, it is the upward

nutrient flux, and not the ambient nutrient levels, that determines the magnitude of the *in situ* new production (e.g. Sournia, 1973; Eppley *et al.*, 1979; King, 1986; Lewis *et al.*, 1986).

Table 2

Mean chlorophyll *a* concentration, mean phytoplankton abundance and mean chlorophyll *a* content per 10^6 cells in samples taken in the area extending from the Catalan coast to the channel between Mallorca and Menorca (July 1982). Standard errors of the means are indicated and the number of observations in each case is given in parentheses. From Estrada (1985).

Depth range	Chlorophyll <i>a</i> (mg/m ³)	Total phytoplankton (cells/ml)	µg chl. <i>a</i> /10 ⁶ cells
Above the DCM	0.12 ± 0.01 (64)	46.7 ± 2.6 (66)	3.13 ± 0.44 (64)
DCM	0.90 ± 0.21 (8)	212.8 ± 102.4 (8)	9.11 ± 2.74 (8)
Below the DCM	0.18 ± 0.03 (42)	27.2 ± 5.1 (44)	8.21 ± 0.88 (42)

Other mechanisms, such as increase in cellular chlorophyll content rather than higher cell abundance, are also proposed to explain the formation of deep chlorophyll maxima (Cullen and Eppley, 1981; Venrick, 1982; Prieur and Legendre, 1988). In the western Mediterranean, average chlorophyll *a* content per cell appears to be effectively higher in the deeper part of the euphotic zone (table 2) but in many of the cases, an increased phytoplankton abundance contributes significantly to the deep chlorophyll maximum (Estrada, 1985; Estrada *et al.*, 1985).

Depth differential grazing may also be a cause for chlorophyll maxima (Cullen and Eppley, 1981; Prieur and Legendre, 1988) and control the vertical distribution of phytoplankton. Phaeophorbids *a*, the main chlorophyll *a* degradation products found in fecal pellets, are the result of the breakdown of chlorophyll *a* by the enzymatic activity of the herbivorous zooplankton digestive system. They are apparently not assimilated and can be used as a conservative tag for heterotrophic activity producing fecal material (Jeffrey, 1974; Welschmeyer and Lorenzen, 1985; Hecq *et al.*, 1992). In the Liguro-Provençal basin, preliminary studies on phaeophorbids distribution have shown a tight coupling between phytoplankton abundance and zooplankton grazing (figure 6). However, populations highly dominated by 19'hexanoyloxyfucoxanthin, a Prymnesiophytes pigment, seem to be less degraded by grazing activity. As a consequence, grazing could change the relative composition of phytoplankton populations and lead to a shift in species and/or size fractions composition.

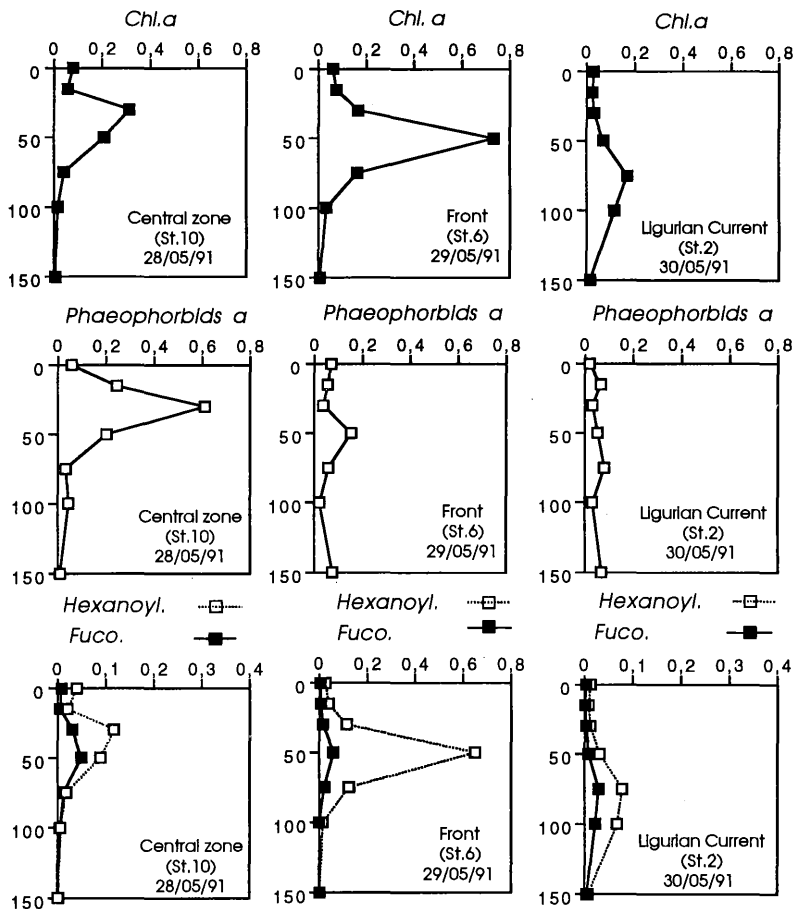


Fig. 6.— Summer vertical distribution of chlorophyll *a*, phaeophorbids *a*, fucoxanthin and 19'hexanoyloxyfucoxanthin ($\mu\text{g/l}$) in the different hydrological zones of the Liguro-Provençal basin. All pigments were detected by HPLC.

4.— Conclusions and perspectives.

Observational case studies have emphasized that the distribution of phytoplankton biomass in the Liguro-Provençal basin is sharply discontinuous in space and time, with restricted periods of high standing crops in a general oligotrophic environment. As a consequence, the heterogeneity in the distribution of food must play an important role in the trophic organization of the ecosystem.

Among the factors responsible for this heterogeneity, processes controlling nitrate availability are prevalent and govern the dynamics of the phytoplankton communities. Nitrate supply in the photic zone is entirely under hydrodynamical

control (*i.e.* winter mixing, instabilities at frontal interfaces, vertical turbulent transport at the nitracline) while new phytoplankton production leads to a progressive impoverishment of the surface layers. On account of resonant interactions between physical and biological processes of similar time- and length-scales, the ecosystem adapts optimally to the spatial variability and takes maximum benefit of the environmental conditions (Nihoul and Djenidi, 1991). Examples of the Liguro-Provençal frontal system and of the formation and maintenance of the DCM are given in illustration.

Actually, in order to calibrate coupled hydrodynamical/biological models of nitrogen circulation in the Mediterranean, following processes need to be determined *in situ*:

- the fluxes of nitrogen assimilation by phytoplankton communities, especially during the stratified period (nutrient fluxes through the nitracline) and the associated ratio of new and regenerated production,
- the fluxes of nitrogen regeneration by the food web dynamics,
- the atmospheric inputs and their impact on local productivity,
- the rate of export of organic nitrogen from the surface layer.

References.

- BERLAND, B.R., BENZHITSKI, A.G., BURLA-KOVA, Z.P., GEORGIEVA, L.V., IZMESTIEVA, M.A., KHOLODOV, V.I. and MAESTRINI, S.Y. (1988). Conditions hydrologiques estivales en Méditerranée, répartition du phytoplancton et de la matière organique, *Oceanol. Acta*, n° spéc., 163–177.
- BERMAN, T., TOWNSEND, D.W., EL SAYED, S.Z., TREES, C.C. and AZOV, Y. (1984). Optical transparency, chlorophyll and primary productivity in the Eastern Mediterranean near the Israeli coast, *Oceanol. Acta*, 7:367–372.
- BÉTHOUX, J.P., PRIEUR, L. and BONG, J.H. (1988). Le courant Ligure au large de Nice, *Oceanol. Acta*, n° spéc., 59–67.
- BOUCHER, J., IBANEZ, F., PRIEUR, L. (1987). Daily and seasonal variations in the spatial distribution of zooplankton populations in relation to the physical structure in the Ligurian front, *J. Mar. Res.*, 45:133–173.
- BROHÉE, M., GOFFART, A., FRANKIGNOULLE, M., HENRI, V., MOUCHET, A. and HECQ, J.H. (1989). Variations printanières des communautés planctoniques en baie de Calvi (Corse) en relation avec les contraintes physiques locales, *Cah. Biol. Mar.*, 30:321–328.
- CAHET, G., FIALA, M., JACQUES, G. and PANOUSE, M. (1972). Production primaire au niveau de la thermocline en zone néritique de Méditerranée Nord-Occidentale, *Mar. Biol.*, 14:32–40.

- CULLEN, J.J. and EPPLEY, R.W. (1981). Chlorophyll maximum layers of the Southern California Bight and possible mechanisms of their formation and maintenance, *Oceanol. Acta*, 4:23–32.
- EPPLEY, R.W., RINGER, E.H. and HARRISON, W.G. (1979). Nitrate and phytoplankton in southern California coastal waters, *Limnol. Oceanogr.*, 24:483–494.
- ESTRADA, M. (1985). *Deep phytoplankton and chlorophyll maxima in the Western Mediterranean*, in: M. Moraitou-Apostolopoulou and V. Kiortis (Editors), *Mediterranean Marine Ecosystems*, Plenum Press, 1–8:247–277.
- ESTRADA, M., VIVES, F. and ALCARAZ, M. (1985). *Life and the productivity of the open ocean*, in: R. Margalef (Editor), *Western Mediterranean*, Pergamon Press, 148–197.
- ESTRADA, M. and MARGALEF, R. (1988). Supply of nutrients to the Mediterranean photic zone along a persistent front, *Oceanol. Acta*, n° spéc., 133–142.
- FAO (1985). *Bulletin CGPM*, 6.
- GOFFART, A. (1992). *Influence des contraintes hydrodynamiques sur la structure des communautés phytoplanctoniques du bassin Liguro-Provençal (secteur Corse)*, Thèse de doctorat, Université de Liège, Belgique, 163 pp.
- GOFFART, A. and HECQ, J.H. (1985). Influence du front Liguro-Provençal — secteur Corse — sur la production planctonique (1983–1984), *Rapp. Comm. int. Mer Médit.*, 29 (9):133–134.
- GOFFART, A. and HECQ, J.H. (1990). Stabilité interannuelle de la distribution de la production planctonique associée au front Liguro-Provençal (secteur Corse), *Rapp. Comm. int. Mer Médit.*, 32 (1):P-II3.
- GOFFART, A., HECQ, J.H. and PRIEUR, L. (en préparation). Contrôle de la distribution des biomasses phytoplanctoniques par le front Liguro-Provençal (secteur Corse), *Oceanol. Acta*.
- HECQ, J.H., LICOT, M. and GOFFART, A. (1983). Relation entre la structure verticale de la colonne d'eau et la distribution du phytoplancton en baie de Calvi (Corse), *Rapp. Comm. int. Mer Médit.*, 28 (9):77–78.
- HECQ, J.H., BOUQUEGNEAU, J.M., DJENIDI, S., FRANKIGNOULLE, M., GOFFART, A. and LICOT, M. (1986). *Some aspects of the Liguro-Provençal frontal ecohydrodynamics*, in: J.C.J. Nihoul (Editor), *Marine Interfaces Ecohydrodynamics*, Elsevier, *Oceanogr. Ser.*, 42:257–271.
- HECQ, J.H. and GOFFART, A. (1990). *Le système frontal Liguro-Provençal et ses implications biologiques sur le plateau continental corse au large de Calvi*, Programme « Flux Océaniques » (France – JGOFS), *Rapp. n° 8 : Frontal*, 104–107.
- HECQ, J.H., MARTY, J.C., CLAUSTRE, H. and PRIEUR, L. (1992). *Distribution des produits de dégradation de la chlorophylle a durant la campagne Almofront, I. Processus et bilans dans les fronts géostrophiques*, Marseille-Luminy 20–22 octobre 1992, *Frontal* (France – JGOFS), 116–118.
- JEFFREY, S.W. (1974). Profiles of photosynthetic pigments in the ocean using thin-layer chromatography, *Mar. Biol.*, 26:101–110.

- KING, D.K. (1986). The dependence of primary production in the mixed layer of the eastern tropical Pacific on the vertical transport of nitrate, *Deep-Sea Res.*, 33:733–754.
- LEWIS, M.R., HARRISON, W.G., OAKLEY, N.S., HEBERT, D. and PLATT, T. (1986). Vertical Nitrate Fluxes in the Oligotrophic Ocean, *Science*, 234:870–873.
- LICOT, M. (1985). *Étude écohydrodynamique du front Liguro-Provençal au large de la Corse*, Thèse de doctorat, Université de Liège, Belgique, 131 pp.
- LOHRENZ, S.E., WIESENBERG, D.A., DEPALMA, I.P., JOHNSON, K.S. and GUSTAFSON, D.E. (1988). Interrelationships among primary production, chlorophyll and environmental conditions in frontal regions of the Western Mediterranean Sea, *Deep-Sea Res.*, 35:793–810.
- MARGALEF, R. (1985). *Introduction to the Mediterranean*, in: R. Margalef (Editor), *Western Mediterranean*, Pergamon Press, 1–16.
- MARINO, D., MODIGH, M. and ZINGONE, A. (1984). *General features of phytoplankton communities and primary production in the Gulf of Naples and adjacent waters*, in: O. Holm-Hansen, L. Bollis and R. Gilles (Editors), *Lecture Notes on Coastal and Estuarine studies: Marine phytoplankton and productivity*, Springer Verlag, 8:89–100.
- MOREL, A. and ANDRÉ, J.M. (1991). Pigment distribution and primary production in the Western Mediterranean as derived and modeled from Coastal Zone Color Scanner observations, *J. Geophys. Res.*, 96:12.685–12.698.
- NIHOUL, J.C.J. and DJENIDI, S. (1991). Hierarchy and scales in marine ecohydrodynamics, *Earth Sci. Rev.*, 31:255–277.
- PRIEUR, L. and LEGENDRE, L. (1988). *Oceanographic criteria for new phytoplankton production*, in B.J. Rothschild (Editor), *Toward a Theory on Biological-Physical Interactions in the World Ocean*, Kluwer Academic Publishers, 71–112.
- SOURNIA, A. (1973). La production primaire planctonique en Méditerranée. Essai de mise à jour, *Bulletin de l'étude en commun de la Méditerranée*, Monaco, n° spéc., 5, 128 pp.
- SOURNIA, A., BRYLINSKI, J.M., DALLOT, S., LE CORRE, P., LEVEAU, M., PRIEUR, L., FROGET, C. (1990). Fronts hydrologiques au large des côtes françaises : Les sites-ateliers du programme Frontal, *Oceanol. Acta*, 13:413–438.
- VENRICK, E.L. (1982). Phytoplankton in oligotrophic ocean: observations and questions, *Ecological Monographs*, 52:129.
- VIALE, D., MORIAZ, C., PALAZZOLI, I. and VIALE, C. (1986). Repérage aérien de Cétacés en Mer Ligure, *Rapp. Comm. int. Mer Médit.*, 30 (2):245.
- WELSCHMEYER, N.A. and LORENZEN, C.J. (1985). Chlorophyll budgets: zooplankton grazing and phytoplankton growth in a temperate fjord and the Central Pacific Gyres, *Limnol. Oceanogr.*, 30:1–21.

The State of the Art of Plankton Research in two Hyperhaline Bodies of Water, the Levantine Basin and the Arabian Gulf

J. GODEAUX*

University of Liège

Abstract.

In this report are presented some of the results of the investigations carried out either separately or in collaboration by members of the Plankton Committee of ICSEM (International Commission for the Scientific Exploration of the Mediterranean Sea, Monaco) both in the Levantine Basin and in the Arabian (Persian) Gulf. Owing to the limited number of pages and the abundance of the matter, a few well known groups of animals have been selected with the aim to stress the peculiarities and the original features of these two bodies of water as compared with the neighbouring seas.

1.— The Levantine Basin.

The Mediterranean, a partially enclosed sea, is connected at 36°N to the warm temperate Atlantic Ocean through the Straits of Gibraltar, a narrow channel, 25 km wide and 320 m deep. The salinity and the temperature of the incoming water are respectively 36‰ and 13.5°C.

This sill is a barrier preventing the inflow of the cold deep atlantic waters and is responsible for the homothermy of the Mediterranean (from 100 m depth to the bottom). The Straits of Gibraltar also impede the entry of bathypelagic species; exceptions are scarce and usually disappear promptly. This explains the type of the Mediterranean settlements.

The Mediterranean itself is divided into a western and an eastern basin at the level of the Straits of Sicily at 12°E. This strait is 145 km wide with a maximum depth of 330 m. It acts as a geographic, hydrologic and climatic barrier, reenforcing the sieve effects of the Straits of Gibraltar.

* President of the Plankton Committee of ICSEM (International Commission for the Scientific Exploration of the Mediterranean Sea, Monaco).

The eastern basin may also be divided into two sectors by a line joining Greece to Cirenaica at 22°E. The western sector or central Mediterranean remains poorly known and seems of little interest to the biologists (except the Ionian and Adriatic Seas). Just a few papers can be cited concerning Chaetognatha (Furnestin, 1974), Appendicularia (Onciu, 1988), Thaliacea (Godeaux, 1988a).

The easternmost sector of the Mediterranean or Levantine Basin is a kind of cul-de-sac, the ecology of which is controlled by different forcing factors. It is a concentration basin, surrounded by warm and arid countries where rains are rare and fresh water discharges limited: the water budget is negative.

Along the coasts, mostly in the south eastern part (and around the islands), the depth is less than 1,000 m. In the central area, the sea is deeper, locally down to 4,000 m and more.

Water circulation in the Levantine Basin is complex (Robinson *et al.*, 1992) but from the biological point of view the anticlockwise surface North African current along the southern and the eastern coasts is the most important.

The surface salinity, already reaching 37‰ at the Straits of Sicily, is permanently above 39‰ in the coastal waters of the Middle East, and above 38.5‰ elsewhere. The surface temperature varies from 17°C in winter to 30–32°C during summer, a long dry season (Lakkis, 1990).

The Levantine Basin is submitted to the effects of two man-made artefacts: the Suez Canal and the Great Aswan Dam.

The Suez Canal, opened in 1869, is just a capillary tube (365 m wide at the surface, 14.5 m deep) linking two seas, but its biological importance is obvious. Thanks to a quasi-permanent northward current, many aggressive Eritrean (Indopacific) species – the lessepsian migrants (Por, 1978, 1989) – have succeeded in crossing the waterway, invading the Levantine Basin, and either intermingling with the autochthonous populations or more simply expelling them, so altering the biological landscape of the whole Eastern Mediterranean.

For millenaries, the summer Nile floods poured tons of fresh water and sediments into the sea. Already reduced by the progressive damming of the river from the beginning of this century (the discharge diminishing from 100 km³/year to 35 km³/year in mean during the last decade), the outflow of fresh water is now limited to some 4 km³/year since the completion of the Great Aswan Dam in 1965. This also means the end of the sediment input and therefore no more nutrients, no more phytoplankton blooms, no food for the sardines, and a drastic drop of the catches from 18,000 tons/year to 500 tons/year (now the yield of the fisheries is rising again with an increased run off of nutrient-rich water). Moreover the missing fresh water is replaced by an equal volume of imported sea water, what somewhat contributes (combined with the intense evaporation) to the increase of the surface salinity.

Briefly the Levantine Basin exhibits subtropical or even tropical characteristics: it is indeed "a sea within a sea" (Galil, 1992).

The upper layers of the Eastern Mediterranean waters display highly oligotrophic characters and the primary production is very low (Weikert, 1988), half that of the other Basin (Oren after Kimor, 1983); phosphate is the limiting factor. On the contrary the waters below 450 m (nutricline) are relatively richer in nutrients. These waters can be carried upwards into the euphotic layer thanks to certain hydrological features and the primary production becomes locally more important. An example is given by a relatively large-scale cyclonic gyre observed between Rhodes and Cyprus, in the northern part of the Basin, which is responsible for a permanent upwelling of deep waters. The primary production reaches $60 \text{ g C/m}^2 \cdot \text{year}$ in the central part of the gyre ($33 \text{ g C/m}^2 \cdot \text{year}$ in the related anticyclone): chlorophyll *a* is high (maximum around 100 m depth) and zooplankton is present in large quantities (Salihoglu *et al.*, 1990; see also Pancucci-Papadopoulou *et al.*, 1992). On the other hand a large warm core eddy, detected south of Cyprus, has been investigated at the point of view new production. During winter, a vertical mixing of the upper layers (down to 450 m) increases the input in nutrients into the euphotic zone; most of the nutrients are derived from the decomposition of the previous year's primary production. The phytoplankton produced biomass is $70 \text{ mg Chl. } a/\text{m}^2$ (Krom *et al.*, 1992).

A comparative study of the phytoplankton communities in the near-surface waters (NSW) and in the deep chlorophyll maximum layer (DCM, $\pm 100 \text{ m}$ = base of the euphotic zone) has shown that the monads (nanoplankton: 1–3 m) followed by the coccolithophorids (picoplankton: 10–20 m) are largely dominant in both layers. Diatoms, dinoflagellates and the other groups represent just a small percentage of the assemblages. Although pennate diatoms are dominant in the DCM and the centric diatoms in the NSW, the gross compositions of the two phytoplankton populations are similar; nevertheless, the intracellular chlorophyll concentration is significantly higher in the DCM communities (Kimor *et al.*, 1987).

Concerning the zooplankton, the filter effects of the two straits result in an impoverishment of the epipelagic and mesopelagic populations (both in number of species and in number of individuals), and a deficiency, if not a lack, of bathypelagic species.

The populations are a mixture of eurythermous euryhaline species and of thermophilic metahaline species, often missing or rare in the Western Basin.

That can be illustrated by a few examples:

- a) Chaetognatha: the chaetognaths (arrow-worms) are planktonic worms which are important as predators, food for young fishes and parasite carriers. Numerous species have been identified in the Mediterranean, but the distribution of some of them is uneven. *Krohnitta subtilis*, *Sagitta serrato-dentata*

are present in the eastern sector and also in the associated Tyrrhenian Sea. *Pterosagitta draco*, *Sagitta tasmanica* and *S. planctonis* are limited to the western basin, mainly off the African coast. *Sagitta enflata*, an eurythermous ubiquitous species is found in the whole sea. *Sagitta friderici* also very common, is only known from the Levantine Basin (Furnestin, 1953, 1970; Casanova, 1970; Lakkis, 1990). *Sagitta neglecta* observed near Alexandria is an Eritrean migrant (Halim, 1990).

- b) Thecosomatous pteropods. These pelagic mollusks are provided with a thin and fragile shell. Of the 25 species identified with certainty in the whole sea, a few are limited to the east. *Creseis chierchae*, a tropical species, is only known from the Levantine Basin; *Hyalocylis striata* and *Cavolinia gibbosa gibbosa* (Indian form), species of warm and saline waters, frequent and abundant in the Eastern Basin, are rare in the Western one, especially north of 40°N. *Cavolinia inflata* is characteristic of the western sector. Other pteropods are common to both sectors: e.g. the thermophilic *Spiratella* (*Limacina*) *trochiformis*, *Creseis virgula virgula* and *Styliola subula*, mainly present in the warmer Algerian waters in the west. No pteropod seems to have crossed the Suez Canal (Rampal, 1968, 1970).
- c) Tunicata. Most of the commonest thaliacean species are present in both sectors. The others are rare or missing. *Thalia orientalis* present in the Atlantic Ocean waters off the Straits of Gibraltar invaded the Mediterranean in the early fifties (Bernard, 1958). It seems still rare in the Western Basin, but forms swarms in the Levantine Basin, mixed with its subspecies provided with "balancers", and with *Thalia democratica*. *Salpa fusiformis*, the second in rank of the salps, is common in the whole Mediterranean, but the aggregate form (blastozoid) displays less truncal muscle fibres in the Eastern Basin (as seen in the tropical waters), an influence of the temperature which looks similar to that observed on herring backbone. *Cyclosalpa pinnata* is accompanied in the Eastern Basin by the related but different species, *C. polae* missing in the west (Godeaux, 1988a). No salp has crossed the Suez Canal but species living in the Red Sea as *Thalia cicar* and *Salpa cylindrica*, two tropical cosmopolitan species, and *Thalia rhomboides*, an Indopacific tropical species, could successfully settle in the Levantine Basin.

Some 20 species of Appendicularians have been reported by different authors (Fenaux, 1967, 1970; Halim *et al.*, 1974; Lakkis and Zeidane, 1985; Onciu, 1988) from the Eastern Basin but they are also present in the other one. Those missing are rare or less frequent in the Western Mediterranean. The depauperation seems to be relatively insignificant in this case (Por, 1989).

Many other groups have also been taken into consideration, e.g. the coelenterates and the copepods at the points of view either of their bathymetric distribution or their affinities with the Indopacific fauna.

Very few investigations have been done yet on the vertical distribution of plankters above depths of 3,000 m and more. The first exhaustive survey was done by Kimor and Wood (1975) especially focused on the algae and microzooplankton (Rhodes Deep, maximum depth 4,400 m). They recorded different species below 2,000 m: several Siphonophora as *Bassia bassensis*, *Chelophyes appendiculata*, *Eudoxoides spiralis*, etc., the Ostracods *Conchoecia elegans* and *Philomedes globosa*.

The hydrologic conditions prevailing in the entire water column are quite abnormal with a temperature exceeding 13.5°C and a salinity always above 38.6‰ (Kimor and Woods 1975). Similar conditions can only be observed in the enclosed Red Sea, but not in the open waters.

Using a Moccuss device, equipped with closing nets, Weikert and Trinkaus (1990) have followed the quantitative vertical distribution and the diurnal migrations of the mesozooplankton, the macrozooplankton and the micronekton down to 4,250 m in a deep hole south of Crete. Below 2,000 m, number of specimens and biomass decrease steadily. The decrease of the biomass in relation with the depth is faster than in the oceanic open waters: this could be explained by a low vertical flux of particular organic matter and by the surrounding temperature enhancing bacterial recycling (Weikert, 1990a, b).

Although the mesopelagic plankters submerge deeper than usual, they cannot replace the missing bathypelagic species.

The copepods are dominant with a majority of species concentrated in the upper layers. Three genera are found extremely dominant in successive depth ranges of the water column down to 4,000 m: *Haloptilus*, *Eucalanus* and *Lucicutia* with local peaks of abundance. Some other groups yet unidentified have also been observed: ostracods, tunicates, ... (Weikert and Trinkaus, 1990).

The vertical distribution of the copepods and other plankters in the Cretan Sea was also examined by Pancucci-Papadopoulou *et al.* (1992) using a 200 m WP-2 closing net, with somewhat different results (e.g. abundance of cyclopoid copepods, etc.).

More studies are obviously needed, combining catches with closing nets and direct observations of the fragile species (e.g. *Ctenophora lobata*) from manned submersibles (Cyana, Johnston-sea-link).

The lessepsian migrations initiated very early with the arrival in Port Saïd in 1899 of the crab *Portunus pelagicus* now sold on the markets in Egypt. Especially since the completion of the Aswan Dam, the migrations from the Red Sea to the Levantine Basin are increasing. They mainly concern fish [about 50 species (Golani, 1990)], decapods [some 37 species, many of great commercial value: penaeids and crabs (Galil, 1992)], benthic molluscs, polychaetes, and ascidians. The Levantine Basin is undergoing a progressive evolution into an appendage of the Red Sea as a Lessepsian province.

Concerning the plankton, it is necessary to be extremely critical owing to the total lack of old documentation on the populations. It is now accepted that numerous species are relicts of the former Tethys which outlined the dry out periods of the sea (Por, 1989; Goy *et al.*, 1990). Moreover only epipelagic species are concerned.

To be identified as a lessepsian migrant, a species must have been found both in the Levantine Basin, the Red Sea and in the Suez Canal.

Nevertheless different species are obviously recent migrants: dinoflagellates [*Ceratium egyptiacum* (Halim, 1990)], the chaetognath *Sagitta neglecta* (Halim, 1990), the copepods *Calanopia elliptica*, *C. media*, *Acartia centrura* and more recently *Paracalanus aculeatus* and *Calocalanus pavo*, etc. (Berdugo, 1968, 1974; Kimor, 1983; Halim, 1990; Lakkis, 1990). Among the medusae, some fifty percent of those recorded from the Lebanese coasts are cosmopolitan; just a few belong to the Indo-pacific fauna but may be relicts (Goy *et al.*, 1990, 1991). Among the Scyphomedusae, three are recent Eritrean invaders: *Cassiopea andromeda*, *Phyllorhiza punctata* and especially *Rhopilema nomadica*, the umbrella of which can reach a 60 cm diameter (Galil *et al.*, 1990); this species is very harmful to man. But curiously enough, the euryhaline neritic cladocera *Penilia avirostris* present for a long time in the Suez Canal and also recorded from the Gulf of Suez and from the Western Mediterranean and the Black Sea does not pass beyond Port Saïd. Other plankters display the same behaviour. The reason is not known.

Owing to the importance of this biogeographic phenomenon, a continuous survey of the area is undoubtedly of considerable interest.

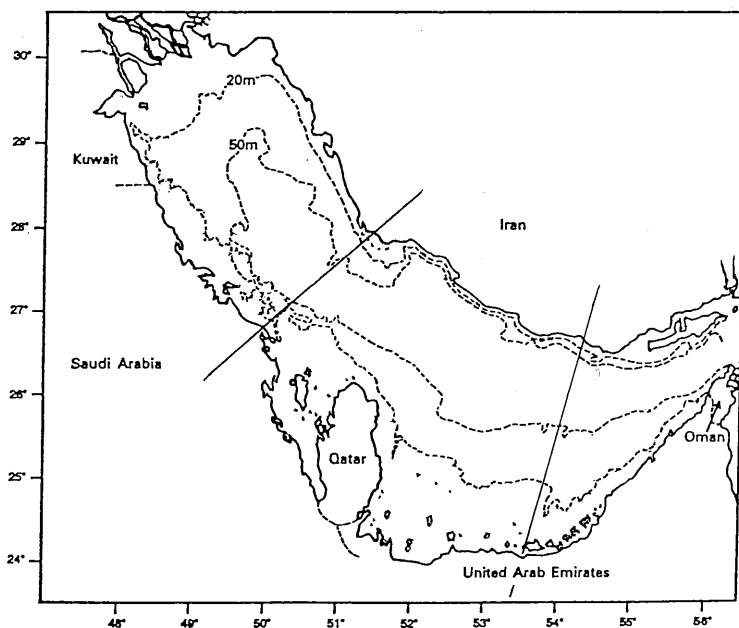
2.— The Arabian (Persian) Gulf.

The Arabian Gulf is a sedimentary basin displaying the shape of a shallow lagoon, 1,000 km long and 300 km wide at the maximum.

The Gulf is connected at 26°30'N to the Gulf of Oman and the northern Arabian Sea through the bottle necked Straits of Hormuz outlining the Musandam Peninsula.

The Gulf of Oman is more than 3,000 m deep at its eastern side but the steeply slope of bottom rises to about 80 m deep at the Straits of Hormuz. There is no real sill.

The maximum depth of the Arabian Gulf is less than 120 m, with about 35 m in mean. The deepest part (> 50 m) is off the Iranian coast, stretching along the main axis of the lagoon. Therefore most of the Gulf belongs to the euphotic zone. The Arabian coast is lined by a continental shelf with varying width and less than



Arabian Gulf and its divisions after Emery (1956). Isobaths in meters.

20 m deep. There is no continental edge. This coast is also the most damaged by oil pollution.

Surrounded by arid and warm countries and submitted to an intense evaporation, the Gulf is a concentration basin. The only important input of fresh water is the Shatt el-Arab but its influence remains limited to the innermost part of the Gulf. The surface salinity, about 36.5‰ at the Straits, gradually increases up to 40–42‰ or even more in the shallow bays (e.g. between Qatar and Trucial Coast). An anticlockwise surface current runs along the Iranian coast: with the density increase, the water sinks to the bottom, flows out through the Straits of Hormuz and finally contributes to the dense layer observed about 300 m deep in the Arabian Sea. The surface temperature varies according to the season and the zone of the Gulf considered: 22°C at the inlet and only 14°C at the far end (due to cold northerly winds) in winter, but 30 to 35°C everywhere in summer. Salinity and temperature gradients are opposite.

Information regarding the origins of the Gulf and the local hydrodynamics is given by Sheppard *et al.* (1992).

The Gulf is submitted (as the Red Sea) to the NE monsoon, responsible for an important drift of open sea plankters of Indopacific origin. Concerning the plankton and its ecology, the Gulf remains relatively less investigated. It was neglected by the International Indian Ocean Expedition if one excepts a

three-day cruise of the French ship *Commandant Robert Giraud* in May 1961 [10 stations operated (Frontier, 1963a)]. Later on a Japanese cruise [*Umitaku-Maru* in December 1967 (Yamazi, 1974)] explored the shallow zone along the Arabian coast and an American cruise [*Atlantis II* in March 1977 (Grice and Gibson, 1978; Gibson *et al.*, 1980)] prospected the deepest part of the Gulf. But the most intensive investigations were done by Michel *et al.* from September 1979 to August 1980 (Michel *et al.*, 1982, 1986a, b), mainly in the Kuwait waters and above a 20 m depth. Halim (1984) also compiled the information on the plankton of the Gulf and the Red Sea.

The two last campaigns are complementary but unfortunately the collections remain still partly sorted out and only a few groups have been exhaustively studied.

The Gulf has been divided into three parts following the sediments composition (Emery, 1953), divisions maintained by the planktonologists.

The American expedition identified some 105 species of protists, mainly algae (spring bloom), say Diatoms 55, Dinoflagellates 30, Coccolithophoridae 7. A few species are dominant: *e.g.*, *Nitzschia delicatissima*, *N. closterium*, *Rhizosolenia alata* var. *indica*, *Coscinodiscus gigas* (500 μ m diameter), *Coccolithus* (*Emiliana*) *huxleyi*, *Calcisolenia murrayi* and *Gephyrocapsa oceanica*. Local swarms of Foraminifera and Radiolaria were also noted. The phytoplankton primary production is high during summer and fall, very low during spring (Al Abdulkader, 1990).

In the zooplankton, the copepods, the ostracods and the cladocera are dominant, followed by the coelenterates, the chaetognaths, the thecosomatous pteropods and the tunicates (appendicularians, doliolids and salps).

The copepods have been identified by Yamazi, Michel *et al.* and Gibson *et al.*, the ostracods by Michel *et al.*

- a) Cladocera. They represent a variable proportion of the total catches, ranging from 0 to 26% between Qatar and Trucial Coast. *Penilia avirostris*, a neritic and euryhaline species, is the most abundant followed by *Evadne tergestina*, an open sea species. A third species, *Podon* sp., is rarer. In the shallow Gulf of Suez, rather similar to this Gulf, *Evadne spinifera* replaces *E. tergestina* only observed in summer in the deep Gulf of Aqaba. According to Michel *et al.* (1986b), *Penilia* and *Evadne* are mutually exclusive having their peaks at different moments of the year.
- b) Chaetognatha. The number of species is relatively important (Casanova, pers. communic.) and some of them are frequent, in descending order: *Sagitta bedoti* and *S. enflata*, especially present in the eastern part, *S. neglecta* and *Krohnitta pacifica* in the innermost part, *S. ferox* in the centre, and *S. bedfordii* in the whole basin. Five more species are less common: *S. pulchra*, ... (Michel *et al.*, 1986b). *S. pacifica*, a mesopelagic species, is limited by

the 200 m isobath, and does not penetrate into the Gulf (Furnestin and Codaccioni, 1968).

- c) Thecosomatous pteropods. Just a few species are present in the lagoon. *Creseis virgula* is recorded from the three sectors with the less frequent *Creseis acicula*. *Cavolinia globulosa* is present at the limits of the 2nd and the 3rd sectors (Rampal, pers. communic.). Moreover a few specimens of *Limacina inflata* were caught in the eastern sector and of *Hyalocypris striata* in the strait proper (Frontier, 1963b). *Cavolinia longirostris* was also observed in the Kuwait waters (Michel *et al.*, 1986a, b).

Except *Limacina inflata*, none of these pteropods is present in the Gulf of Suez where they are replaced by four other species (Rampal, 1990). All these species are the most frequent and abundant ones encountered in the Arabian Sea (Frontier, 1963b). *Desmopterus papilio*, a nude cosmopolitan species was also collected. Numerous veliger larvae of gastropods and lamellibranchs were also observed, with a few Atlantidae and larvae of gymnosomatous pteropods (Clionidae).

d) Tunicata.

- Appendicularia: they constitute a small fraction of the plankton, often less than 5% or even 1%, except at a station (*Atlantis II*) of the eastern sector off the Trucial Coast where they amounted to 22.5% of the total. *Oikopleura longicauda*, the most frequent species, *O. rufescens* and *Fritillaria formica* f. *digitata* are caught in the three sectors of the Gulf. *O. fusiformis* is limited to the innermost part whereas *Fritillaria pellucida* f. *omani* and two large species, *Stegosoma magnum* and *Megalocercus huxleyi* are found from the Straits of Hormuz to the south-eastern bay of the Gulf. All these species are also known from the Gulf of Oman, where they form the bulk of the 13 local species (Fenaux, 1964 and pers. communic.).
- Doliolids: the five species present are cosmopolitan. All the stages of development were observed. The dominant species is *Doliolum denticulatum*. Curiously enough, *D. nationalis*, a neritic species, is rare in the catches of *Atlantis II*; it was commoner in those of the *Cd Robert Giraud* (Godeaux, 1988b). The second species in importance is *Dolioletta tritonis* (with *D. gegenbauri*). The genus *Doliolina* is only represented by a few characteristic larvae as probably the other small forms escape the nets. No specimen of *Doliolina indicum* characteristic of the Indian Ocean has been observed.

The distribution of the doliolids is very irregular in *Atlantis II* catches: absent or almost absent in the stations near the Straits of Hormuz and in the western part of the Gulf, and very common proportionally elsewhere (from 2 to 20% of the catches).

- Salps: As previously observed (Godeaux, 1988b), just two species were identified: the very common *Salpa (Wheelia) cylindrica*, widely distributed throughout the tropical waters, and *Thalia rhomboides*, an Indo-pacific species often mistaken for *Thalia democratica* (Michel *et al.*, 1986a). The catches of the salp *Pegea confoederata* off the Kuwait coast is interesting, as this large salp lives in the oceanic waters.

The presence of these herbivora, often of a small size, is an indirect proof of the existence of tiny protists grazed by them.

The Arabian Gulf is inhabited by an impoverished Indo-pacific fauna. Only the most frequent epipelagic plankters present in the Arabian Sea and the Gulf of Oman succeed in settling in the Gulf. Settlement is proved by the existing successive stages of development of different species.

It must be emphasized that the specimens of *Cavolinia longirostris*, *Sagitta bedfordii*, *Krohnitta subtilis* and *Pegea confoederata* caught in the northwestern part of the Gulf, were in an excellent condition. That means that the anticlockwise circulation is faster than previously stated (Michel, pers. communic.).

Nevertheless the Arabian Gulf remains underinvestigated up to now. The determinations of the species must be extended, and their annual cycles and successions followed. Probably the estimation of effects of recent oil spills on these insufficiently known populations will be difficult. A comparison with the similar Gulf of Suez is just being initiated and will be pursued.

References.

- AL-ABDULKADER, K.A. (1990). *Phytoplankton ecology of the western arabian Gulf* (Abstract of a thesis, Texas A.M. University).
- BERDUGO, V. (1968). See KIMOR, B. (1983).
- BERDUGO, V. (1974). See KIMOR, B. (1983).
- BERNARD, M. (1958). *Systématique et distribution saisonnière des Tuniciers pélagiques d'Alger*. Rapp. Comm. int. Mer Médit., Monaco, 14:211–231.
- CASANOVA, J.P. (1970). *Indicateurs hydrologiques et écologiques en Méditerranée*, Journées Étud. planctonol. C.I.E.S.M., Monaco, 29–33.
- EMERY, K.D. (1956). Sediments and water of Persian Gulf, *Bull. Amer. Assoc. Petr. Geol.*, 40:2354–2383.
- FENAUX, R. (1964). Les Appendiculaires de la troisième campagne du « Commandant Robert Giraud » en mer d'Arabie, *Bull. Inst. océanogr.*, Monaco, 62 (n° 1302), 14 pp.
- FENAUX, R. (1967). *Les Appendiculaires des mers d'Europe et du Bassin méditerranéen. Faune de l'Europe et du Bassin méditerranéen*, 2, Masson et Cie eds, Paris, 116 pp.

- FENAUX, R. (1970). Sur les Appendiculaires de la Méditerranée orientale, *Bull. Museum nat. Histoire nat.*, Paris, 42 (6, ser. 2):1208–1211.
- FRONTIER, S. (1963a). Zooplancton récolté en mer d'Arabie, golfe Persique et golfe d'Aden (3^e campagne océanographique du « Commandant Robert Giraud »). I. – Données générales — Répartition quantitative, *Cahiers « O.R.S.T.O.M. »*, 3:17–30.
- FRONTIER, S. (1963b). Zooplancton récolté en mer d'Arabie, golfe Persique et golfe d'Aden. II. – Pteropodes : systématique et répartition, *Cahiers « O.R.S.T.O.M. »*, 6:233–254.
- FURNESTIN, M.L. (1953). Sur quelques Chaetognathes d'Israël, *Bull. Sea Fish. Res. Stn. Haifa*, 16:411–414.
- FURNESTIN, M.L. (1970). *Chaetognathes des campagnes du « Thor » (1908–11) en Méditerranée et en mer Noire*, Dana Report, 79:3–46.
- FURNESTIN, M.L. (1974). *Chaetognathes de la partie sud-occidentale du Bassin oriental de la Méditerranée*, Rapp. Comm. int. Mer Médit., Monaco, 22 (9):135–137.
- FURNESTIN, M.L. and CODACCIONI, J.C. (1968). Chaetognathes du nord-ouest de l'océan Indien (golfe d'Aden-mer d'Arabie-golfe d'Oman-golfe Persique), *Cahiers « O.R.S.T.O.M. »*, 6:143–171.
- GALIL, B.S. (1992). Eritrean Decapods in the Levant. Biogeography in motion, *Bull. Inst. océanogr.*, Monaco, n° s., 9:115–123.
- GALIL, B.S., SPANIER, E. and FERGUSON, W.W. (1990). The Scyphomedusae of the Mediterranean coast of Israël, including two lessepsian migrants new to the Mediterranean, *Zool. Mededeling.*, 64:95–105.
- GIBSON, V.R., GRICE, G.D. and GRAHAM, S.J. (1980). *Zooplankton investigations in Gulf waters north and south of the Straits of Hormoz*, in: *Proceed. Symp. coastal and marine Environm. in Red Sea, Gulf of Aden and tropical western Indian Ocean*, Karthoum, 501–517.
- GODEAUX, J. (1988a). Thaliacés méditerranéens : une synthèse, *Bull. Soc. roy. Sci. Liège*, 57 (4–5):359–377 (Bibliography).
- GODEAUX, J. (1988b). Thaliacés récoltés en mer d'Arabie, dans le golfe Persique et dans le golfe d'Aden par le « N.O. Commandant Robert Giraud », *Bull. Séanc. Acad. r. Sci. Outre-Mer*, Bruxelles, 34 (2):301–324.
- GOY, J., LAKKIS, S. and ZEIDANE, R. (1990). Les méduses de la Méditerranée orientale, *Bull. Inst. océanogr.*, Monaco, 11, n° s., 7:79–88.
- GOY, J., LAKKIS, S. et ZEIDANE, R. (1991). Les méduses (*Cnidaria*) des eaux libanaises, *Ann. Inst. océanogr.*, Paris, 67 (2):99–128.
- GOLANI, D. (1990). Environmentally-induced meristic changes in Lessepsian fish migrants. A comparison of source and colonizing populations, *Bull. Inst. océanogr.*, Monaco, n° s., 7:143–152.

- GRICE, G.D. and GIBSON, V.R. (1978). *General biological oceanographic data from the Persian Gulf and Gulf of Oman*, Woods Hole Oceanogr. Institution, Rep. B-WHOI-78-38, 35 pp.
- HALIM, Y. (1984). Plankton of the Red Sea and the Arabian Gulf, *Deep-Sea Res.*, 31 (6-8A):969-982.
- HALIM, Y. (1990). On the potential migration of Indo-pacific plankton through the Suez Canal, *Bull. Inst. océanogr.*, Monaco, n° s., 7:11-28 (Bibliography).
- HALIM, Y., ABOUL-EZZ, S. et GUERGUESS, S.K. (1974). *Appendiculaires de la mer d'Alexandrie et des eaux avoisinantes*, Rapp. Comm. int. Mer Médit., Monaco, 22 (9): 113-114.
- KIMOR, B. (1983). Distinctive features of the plankton of the Eastern Mediterranean, *Ann. Inst. océanogr.*, Paris, 59 (2):97-106 (Bibliography).
- KIMOR, B., BERMAN, T. and SCHNELLER, A. (1987). Phytoplankton assemblages in the deep chlorophyll maximum layers off the Mediterranean coast of Israel, *J. Plankton Res.*, 9 (3):433-443.
- KIMOR, B. and WOOD, E.J.F. (1975). A plankton study in the Eastern Mediterranean Sea, *Marine Biology*, 29:321-333.
- KROM, M.D., BRENNER, S., KRESS, N., NEORI, A. and GORDON, L.I. (1992). Nutrient dynamics and new production in a warm-core eddy from the eastern Mediterranean Sea, *Deep-Sea Res.*, 39 (3-4):467-480.
- LAKKIS, S. (1990). Vingt ans d'observations sur le plancton des eaux libanaises : structure et fluctuations interannuelles, *Bull. Inst. océanogr.*, Monaco, n° s., 7:51-66 (Bibliography).
- LAKKIS, S. et ZEIDANE, R. (1985). *Les appendiculaires des eaux néritiques libanaises. Observations faunistiques et écologiques*, Rapp. Comm. int. Mer Médit., Monaco, 29 (9):287-288.
- MICHEL, H.B., BEHBEHANI, M., HERRING, D., ARAR, M. and SHOUSHANI, M. (1982). *Zooplankton diversity, distribution and abundance in Kuwaiti waters*, in: R. Halwegy, D. Clayton and M. Behbehani (eds), *Marine Environment and Pollution*, The Alden Press Oxford, 53-68.
- MICHEL, H.B., BEHBEHANI, M. and HERRING, D. (1986a). Zooplankton of the western Arabian Gulf south of Kuwait waters, *Kuwait Bull. mar. Sci.*, 8:1-36.
- MICHEL, H.B., BEHBEHANI, M., HERRING, D., ARAR, M., SHOUSHANI, M. and BRAKONIECKI, T. (1986b). Zooplankton diversity, distribution and abundance in Kuwait waters. *Kuwait Bull. mar. Sci.*, 8:37-105.
- ONCIU, T. (1988). *Données concernant les appendiculaires des eaux libyennes*, Rapp. Comm. int. Mer Médit., Monaco, 31 (2):239.
- OREN, O.H. (1970), after KIMOR (1983).
- PANCUCCI-PAPADOPOULOU, M.-A., SIOKOU-FRANGOU, I., THEOCHARIS, A. and GEORGOPOULOS, D. (1992). Zooplankton vertical distribution in relation to the hydrology in the NW Levantine and SE Aegan Seas (spring 1986), *Oceanologica Acta*, 15 (4):365-381.

- POR, F.D. (1978). *Lessepsian migration. The influx of Red Sea biota into the Mediterranean by way of the Suez Canal*, Springer Verlag, Ecological Studies, 23, 228 pp.
- POR, F.D. (1989). *The legacy of Tethys. An aquatic biogeography of the Levant*, Kluwer Acad. Publ., Dordrecht, Monographiae Biologicae, 63, 214 pp.
- RAMPAL, J. (1968). *Les ptéropodes thécosomes en Méditerranée*, C.I.E.S.M. (Plancton), Monaco, 142 pp.
- RAMPAL, J. (1970). *Ptéropodes thécosomes indicateurs d'eau d'origine orientale en Méditerranée occidentale*, in : *Journées d'Études planctonologiques*, C.I.E.S.M. (Plancton), Monaco, 49–52.
- RAMPAL, J. (1990). Les thécosomes de la mer Rouge, *Bull. Inst. océanogr.*, Monaco, n° s., 7:103–107.
- ROBINSON, A.R., MALANOTTE-RIZZOLI, P., HECHT, A. *al.* (1992). General circulation of the Eastern Mediterranean — The POEM group, *Earth Science Reviews*, 32:285–309.
- SALİHOĞLU, I., SAYDAM, C., BASTÜRK, Ö., YILMAZ, K., GÖÇMEN, D., HATİPOĞLU, E. and YILMAZ, A. (1990). Transport and distribution of nutrients and chlorophyll—a by mesoscale eddies in the northeastern Mediterranean, *Marine Chemistry*, 29:375–390.
- SHEPPARD, C., PRICE, A. and ROBERTS, C. (1992). *Marine ecology of the Arabian region. Patterns and processes in extreme tropical environments*, Academic Press. Publ., London, 359 pp.
- WEIKERT, H. (1988). *New information on the productivity of the deep Eastern Mediterranean and Red Sea*, Rapp. Comm. int. Mer Médit., 31 (2):305.
- WEIKERT, H. (1990a). A proposal vertical distribution pattern of micronekton in the deep Levantine Sea, Eastern Mediterranean, and its applicability to the Red Sea, *Bull. Inst. océanogr.*, Monaco, n° s., 7:39–50.
- WEIKERT, H. (1990b). *Vertical distribution of zooplankton and micronekton in the deep Levantine Sea*, Rapp. Comm. int. Mer Médit., Monaco, 32 (1):199.
- WEIKERT, H. and TRINKAUS, S. (1990). Vertical mesozooplankton abundance and distribution in the the deep Eastern Mediterranean Sea SE of Crete, *J. Plankton Res.*, 12 (3):601–628.
- YAMASI, I. (1974). *Analyses of the data on temperature, salinity and chemical properties of the surface water, and the zooplankton communities in the Arabian Gulf in December 1968*, in: *Arabian Gulf Fishery-Oceanography Survey*, December 1968, 1:26–51.

List of Participants

Mr. Joan BACKERS
Management Unit of Mathematical Models
% Mijenbestrijdingsschool
3^e & 23^e Linierregimentsplein
8400 OOSTENDE

Dr. W. BAEYENS
Lab. voor Analytische Chemie
VUB
Pleinlaan, 2
1050 BRUSSEL

Dr. Jean-Marie BECKERS
GHER
Université de Liège
Sart-Tilman B5
4000 LIÈGE

Mrs. Sylvie BECQUEVORT
Groupe de Microbiologie des
Milieux Aquatiques
ULB – Campus de la Plaine
Boulevard du Triomphe – CP 221
1050 BRUXELLES

Miss Myriam BEGHYN
Marine Biology Section
University of Ghent
Ledeganckstraat, 35
9000 GENT

Mr. Andrea BELGRANO
Institute of Zoology
Marine Biology Section
University of Ghent
Ledeganckstraat, 35
9000 GENT

Mr. Samy BELKHIRIA
Écohydrodynamique
Université de Liège
Sart Tilman B5
4000 LIÈGE

Prof. Gilles BILLEN
Groupe de Microbiologie des
Milieux Aquatiques
ULB – Campus de la Plaine
Boulevard du Triomphe – CP 221
1050 BRUXELLES

Dr. J. BOISSONNAS
Commission Communautés Européennes
DGXII MAST
Rue de la Loi, 200
1049 BRUXELLES

Dr. BOHLE-CARBONNEL
Commission Communautés Européennes
DGXII MAST
Rue de la Loi, 200
1049 BRUXELLES

Miss Isabelle BOURGE
Service d'Océanologie
Université de Liège
Sart Tilman B6
4000 LIÈGE

Eng. Pierre BRASSEUR
GHER
Université de Liège
Sart Tilman B5
4000 LIÈGE

Dr. Louis CABIOCH
Station Biologique
F-29682 ROSCOFF Cedex (France)

Dr. André CATTRIJSSE
Marine Biology Section
University of Ghent
Ledeganckstraat, 35
9000 GENT

Dr. Lei CHOU
Laboratoire d'Océanographie
ULB
Campus de la Plaine – CP 208
1050 BRUXELLES

Mr. Olivier COLLETTE
 Dienst Analytische Chemie ANCH
 VUB
 Pleinlaan, 2
 1050 BRUSSEL

Dr. Peter COUTTEAU
 Laboratory for Aquaculture
 State University of Ghent
 Rozier, 44
 9000 GENT

Dr. Marc DE BATIST
 Renard Centre of Marine Geology
 State University of Ghent
 Krijgslaan, 281 – S8
 9000 GENT

Miss Lieve DE BOCK
 Department of Chemistry
 U.I.A.
 Universiteitsplein, 1
 2610 ANTWERP (Wilrijk)

Prof. Guy DE MOOR
 Lab. Physical Geography
 University of Ghent
 Krijgslaan, 281
 9000 GENT

Mr. Geert DE SCHAEPMEESTER
 Lab. Physical Geography
 University of Ghent
 Krijgslaan, 281
 9000 GENT

Dr. Frank DEHAIRS
 Dienst Analytische Chemie
 VUB
 Pleinlaan, 2
 1050 BRUSSEL

Eng. Marleen DEHASQUE
 Dept. Aquaculture
 State University of Ghent
 Rozier, 44
 9000 GENT

Dr. K. DELBEKE
 Lab. voor Ecologie
 VUB
 Pleinlaan, 2
 1050 BRUSSEL

Dr. Éric DELEERSNIJDER
 Unité ASTR
 Université Catholique de Louvain
 Chemin du Cyclotron, 2
 1348 LOUVAIN-LA-NEUVE

Eng. Éric DELHEZ
 GHER
 Université de Liège
 Sart Tilman B5
 4000 LIÈGE

Mr. Stéphane DESGAIN
 Océanologie
 Université de Liège
 Sart Tilman B6
 4000 LIÈGE

Mr. Guy DE SMET
 Marine Biology Section
 University of Ghent
 Ledeganckstraat, 35
 9000 GENT

Miss Salud DEUDERO COMPANY
 Morphologie & Systematiek der Dieren
 University of Ghent
 Ledeganckstraat, 35
 9000 GENT

Mr. Dirk DEWEIRD
 Management Unit of Mathematical Models
 % Mijnenbestrijdingsschool
 3^e & 23^e Linierregimentsplein
 8400 OOSTENDE

Miss Ann DEWICKE
 Lab. Marine Ecology
 University of Ghent
 Ledeganckstraat, 35
 9000 GENT

Miss Els DE WINNE
 Lab. Physical Geography
 University of Ghent
 Krijgslaan, 281
 9000 GENT

Dr. Philippe DHERT
 Lab. for Aquaculture
 Artemia Reference Center
 State Univ. of Ghent
 Rozier, 44
 9000 GENT

Prof. Albert DISTÈCHE
Océanologie
Université de Liège
Sart Tilman B6
4000 LIÈGE

Dr. S. DJENIDI
GHER
Université de Liège
Sart Tilman B5
4000 LIÈGE

Mr. Abderrahman EL BEKALI
Océanologie
Université de Liège
Sart Tilman B6
4000 LIÈGE

Eng. Marc ELSKENS
Dienst Analytische Chemie
VUB
Pleinlaan, 2
1050 BRUSSEL

Miss Élisabeth ETASSE
Observatoire du Littoral
Manche Sud Mer du Nord
BP 2035
Rue du Palais Rihour, 5
F-59014 LILLE Cedex (France)

Dr. Th. FICHEFET
Astronomie et Géophysique
Institut G. Lemaître
Université Catholique de Louvain
Chemin du cyclotron, 2
1348 LOUVAIN-LA-NEUVE

Mrs. Nancy FOCKEDEV
Marine Biology Section
University of Ghent
Ledeganckstraat, 35
9000 GENT

Dr. Michel FRANKIGNOULLE
Océanologie
Université de Liège
Sart Tilman B6
4000 LIÈGE

Mr. Marco A. GALICIA PEREZ
GHER
Université de Liège
Sart Tilman B5
4000 LIÈGE

Mr. M. GERLACHE
Océanologie
Université de Liège
Sart Tilman B6
4000 LIÈGE

Prof. Jean GODEAUX
Institut de Zoologie
Lab. de Biologie Marine
Université de Liège
Quai Van Beneden, 22 I1
4020 LIÈGE

Dr. Anne GOFFART
Écohydrodynamique
Université de Liège
Sart Tilman B5
4000 LIÈGE

Dr. Peter GRANDSARD
Management Unit of Mathematical Models
% Mijnenbestrijdingsschool
3^e & 23^e Linie regimentsplein
8400 OOSTENDE

Dr. Olivier HAMERLYNCK
Marine Biology Section
University of Ghent
Ledeganckstraat, 35
9000 GENT

Dr. Jean-Henri HECQ
Écohydrodynamique
Université de Liège
Sart Tilman B5
4000 LIÈGE

Prof. Carlo HEIP
Netherlands Inst. of Ecology Center
MIOO – CEMO
Vierstraat, 28
NL-4401 EA YERSEKE
(The Netherlands)

Dr. Peter HERMAN
Netherlands Inst. of Ecology Center
Vierstraat, 28
NL-4401 EA YERSEKE
(The Netherlands)

Miss HERZL
Lab. d'Océanographie
ULB – Campus de la Plaine
Boulevard du Triomphe – CP 208
1050 BRUXELLES

Dr. Kris HOSTENS
Marine Biology Section
University of Ghent
Ledeganckstraat, 35
9000 GENT

Prof. Patric JACOBS
Renard Centre of Marine Geology
University of Ghent
Krijgslaan, 281 – S8
9000 GENT

Miss Wendy JAMBERS
Department of Chemistry
U.I.A.
Universiteitsplein, 1
2610 ANTWERP (Wilrijk)

Dr. C. JANSSEN
Lab. Biological Research Aquatic Pollution
University of Ghent
Plateauststraat, 27
9000 GENT

Dr. Edmonde JASPERS
IZWO
Inst. of Marine Scientific Research
Victorialaan, 3
8400 OOSTENDE

Miss Célia JOAQUIM-JUSTO
Écohydrodynamique
Université de Liège
Sart Tilman B5
4000 LIÈGE

Prof. C. JOIRIS
Lab. voor Ecotoxicologie
VUB
Pleinlaan, 2
1050 BRUSSEL

Dr. Elisabeth KOPCZYNSKA
Analytical Chemistry
VUB
Pleinlaan, 2
1050 BRUSSEL

Miss Geneviève LACROIX
Lab. d'Écologie du Plancton Marin
LEPM
Université Pierre et Marie Curie
BP 28 – La Darse
F-06230 VILLEFRANCHE-SUR-MER
(France)

Dr. Christiane LANCELOT
Groupe de Microbiologie des
Milieux Aquatiques
ULB – Campus de la Plaine
Boulevard du Triomphe – CP 221
1050 BRUXELLES

Dr. Jean LANCKNEUSS
Lab. Physical Geography
University of Ghent
Krijgslaan, 281
9000 GENT

Mr. Didier LARDINOIS
Institut de Zoologie
Service Prof. Jeuniaux
Université de Liège
22, Quai Van Beneden I1
4020 LIÈGE

Dr. Patrick LAVENS
Lab. for Aquaculture
Artemia Reference Center
State University of Ghent
Rozier, 44
9000 GENT

Mr. Dirk LE ROY
Lange Nieuwstraat, 43
2000 ANTWERPEN

Miss Natascha LEFEVRE
Marine Biology Section
University of Ghent
Ledeganckstraat, 35
9000 GENT

Mrs. Michèle LOIJENS
Océanographie Chimique
ULB – Campus de la Plaine
Boulevard du Triomphe – CP 208
1050 BRUXELLES

Miss Géraldine MARTIN
GHER
Université de Liège
Sart Tilman B5
4000 LIÈGE

Mrs. Sylvie MATHOT
Groupe de Microbiologie des
Milieux Aquatiques
ULB – Campus de la Plaine
Boulevard du Triomphe – CP 221
1050 BRUXELLES

Mr. Jan MEES
Marine Biology Section
University of Ghent
Ledeganckstraat, 35
9000 GENT

Miss Greet MERCHIE
Lab. for Aquaculture
Artemia Reference Center
State University of Ghent
Rozier, 44
9000 GENT

Mr. Mark MOENS
Management Unit of Mathematical Models
Gulledelle, 100
1200 BRUSSELS

Mr. Tom MOENS
Marine Biology Section
University of Ghent
Ledeganckstraat, 35
9000 GENT

Prof. Florentina MOSORA
Biomécanique
Université de Liège
Sart Tilman B5
4000 LIÈGE

Prof. Jacques C.J. NIHOUL
GHER
Université de Liège
Sart Tilman B5
4000 LIÈGE

Mr. Alain NORRO
Océanologie
Université de Liège
Sart Tilman B6
4000 LIÈGE

Eng. José OZER
Management Unit of Mathematical Models
Gulledelle, 100
1200 BRUSSELS

Mr. H. PAUCOT
Lab. d'Océanographie Chimique
ULB – Campus de la Plaine
Boulevard du Triomphe – CP 208
1050 BRUXELLES

Dr. Georges PICHOT
Management Unit of Mathematical Models
Gulledelle, 100
1200 BRUSSELS

Eng. André POLLENTIER
Management Unit of Mathematical Models
% Mijnenbestrijdingsschool
3° & 23° Linierregimentsplein
8400 OOSTENDE

Mr. Pierre REGNIER
Dept. d'Océanographie
ULB – Campus de la Plaine
Boulevard du Triomphe – CP 208
1050 BRUXELLES

Prof. François RONDAY
Météorologie
Université de Liège
Sart Tilman B5
4000 LIÈGE

Mrs. Véronique ROUSSEAU
Groupe de Microbiologie des
Milieux Aquatiques
ULB – Campus de la Plaine
Boulevard du Triomphe – CP 221
1050 BRUXELLES

Mr. Kevin RUDDICK
Management Unit of Mathematical Models
Gulledelle, 100
1200 BRUSSELS

Mr. Koen SABBE
Lab. voor Morfologie, Systematiek en Ecologie van de Planten
University of Ghent
Ledeganckstraat, 35
9000 GENT

Miss SCHOEMANN
Groupe de Microbiologie des
Milieux Aquatiques
ULB – Campus de la Plaine
Boulevard du Triomphe – CP 221
1050 BRUXELLES

Mr. Roland SCHOENAUEN
GHER
Université de Liège
Sart Tilman B5
4000 LIÈGE

Dr. Jos SCHOOFS
Service de la Programmation de la Politique
Scientifique
Rue de la Science, 8
1040 BRUXELLES

Mrs. Danielle SCHRAM
Marine Biology Section
University of Ghent
Ledeganckstraat, 35
9000 GENT

Mr. Jan SCHRIJVERS
Marine Biology Section
University of Ghent
Ledeganckstraat, 35
9000 GENT

Miss Karine SOHET
Lab. de Biologie marine
ULB
Avenue F. Roosevelt, 50 – CP 160/15
1050 BRUXELLES

Mr. Ali TEMARA
Lab. de Biologie marine
ULB
Avenue F. Roosevelt, 50 – CP 160/15
1050 BRUXELLES

Prof. Neal THOMAS
Flow Research Evaluation Diagnostic (FRED)
University of Birmingham, U.K.

Mr. Franck TOURATIER
GHER
Université de Liège
Sart Tilman B5
4000 LIÈGE

Eng. C. VAN CAUWENBERGHE
Dienst der Kust Hydrografie
Administratief Centrum
Vrijhavenstraat, 3
8400 OOSTENDE

Miss Fabienne VANDEKERKOVE
Observatoire de l'Environnement Littoral
et Marin
BP 2035
5, rue du Palais Rihour
F-59014 LILLE Cedex (France)

Mr. Johan VAN DE VELDE
Marine Biology Section
University of Ghent
Ledeganckstraat, 35
9000 GENT

Mr. Dirk VAN GANSBEKE
Marine Biology Section
University of Ghent
Ledeganckstraat, 35
9000 GENT

Mr. Pieter VANHAUWAERT
Renard Centre of Marine Geology
State University of Ghent
Krijgslaan, 281 – S8
9000 GENT

Prof. R. VAN GRIEKEN
Departement Scheikunde
Universitaire Instelling
U.I.A.
Universiteitsplein, 1
2610 WILRIJK

Dr. Vera VAN LANCKER
Lab. Physical Geography
University of Ghent
Krijgslaan, 281
9000 GENT

Mr. Hans VAN MALDEREN
Department of Chemistry
U.I.A.
Universiteitsplein, 1
2610 ANTWERP (Wilrijk)

Mr. Kris VANNESTE
Renard Centre of Marine Geology
State University of Ghent
Krijgslaan, 281 – S8
9000 GENT

Dr. Ann VANREUSEL
Marine Biology Section
University of Ghent
Ledeganckstraat, 35
9000 GENT

Mr. Gilbert VAN STAPPEN
Lab. for Aquaculture
Artemia Reference Center
State University of Ghent
Rozier, 44
9000 GENT

Dr. Ramiro VARELA
GHER
Université de Liège
Sart Tilman B5
4000 LIÈGE

Prof. G. VERBEKE
Vaste Secretaris
Royal Academy of Belgium
Ducale Straat
1000 BRUXELLES

Mr. Dominick VERSCHELDE
Marine Biology Section
University of Ghent
Ledeganckstraat, 35
9000 GENT

Mr. Wim VERSTEEG
Renard Centre of Marine Geology
State University of Ghent
Krijgslaan, 281 – S8
9000 GENT

Prof. Magda VINCX
Marine Biology Section
University of Ghent
Ledeganckstraat, 35
9000 GENT

Miss Sophie WARNY
Océanologie
Université de Liège
Sart Tilman B6
4000 LIÈGE

Mr. Jan WITTOECK
Marine Biology Section
University of Ghent
Ledeganckstraat, 35
9000 GENT

Miss Anne-Françoise WOITCHIK
Dienst Analytische Chemie ANCH
VUB
Pleinlaan, 2
1050 BRUSSEL

Prof. R. WOLLAST
Lab. d'Océanographie Chimique
ULB – Campus de la Plaine
Boulevard du Triomphe – CP 208
1050 BRUXELLES

Program

Thursday January 21, 1993

- 9.00 9.15 Introduction to the Workshop
G. VERBEKE, Vaste Secretaris
Koninklijk Academie voor Wetenschappen, Letteren en Schone Kunsten
van België
- 9.15 10.15 Marine Science in the European Community
State-of-the-Art and Perspective
Dr. BOISSONNAS, European Community, General Direction XII/E
- 10.15 10.30 Coffee break
(Setting up of poster display)
- 10.30 12.30 **Session 1:** Chairman F.C. Ronday
- i) Nowcasting
Reconstruction of data fields and data assimilation
P. BRASSEUR, J.M. Brankart, J. Haus, J.C.J. Nihoul
 - ii) Forecasting
Results of metagnostic (system-oriented) and diagnostic (process-oriented) models
J.M. BECKERS, J. Haus, J.C.J. Nihoul, R. Schoenauen
 - iii) *Development of interdisciplinary models of ecosystems under weak or severe hydrodynamic constraints*
É. DELHEZ, G. Lacroix, G. Martin, J.C.J. Nihoul, R. Varela
 - iv) *Ecological models*
P. HERMAN, C.H.R. Heip
- General discussion on the modelling session
- The four lectures will be illustrated by case study applications to the North West European Continental Shelf, the Westerschelde, the Mediterranean Sea and the Bering Sea with presentation of a videofilm.
- 14.00 15.30 **Session 2:** Chairman R. Wollast
- i) *Morphodynamics and sediment dynamics in the Southern Bight*
J. LANCKNEUS, G. de Moor
 - ii) *Atmospheric deposition of heavy metals into the North Sea*
R. VAN GRIEKEN, J. Injuk, H. Van Malderen

iii) *Meiobenthos of the NE Atlantic*

A. VANREUSEL, M. Vincx, B.J. Bett, A. Dinet, T. Ferrero, A.J. Goo-
day, P.J.D. Lambshead, O. Pfannkuche, T. Soltwedel

15.30 16.00 Coffee break, Poster session

16.00 17.30 **Session 3:** Chairman R. Van Grieken

16.00 17.00 *Exchanges at the Ocean Margins*
(A belgian contribution to IGBP/Global Change)

R. WOLLAST, M. ELSKENS, M. FRANKIGNOULLE, P. DAUBY

i) *Exchanges between the Atlantic Ocean, the English Channel and the
North Sea*

ii) *Primary production and nutrient fluxes*

iii) *Carbon fluxes at the air-sea interface and in the water column*

iv) *Biogeochemistry of trace elements*

17.00 17.30 *Modelling and prediction of coastal eutrophication*

C. Lancelot, G. BILLEN, V. Rousseau

Friday January 22, 1993

9.00 11.00 **Session 4:** Chairman C.H. Heip

9.00 9.45 *Ecohydrodynamic processes in a local and global biogeochemical perspective*

S. DJENIDI, A. GOFFART, J.H. Hecq, G. Lacroix, J.C.J. Nihoul

9.45 10.15 *The Scheldt estuarial and coastal zones*

F.C. RONDAY, R. WOLLAST

10.15 11.00 i) *The structure and dynamics of estuarine endo-benthic communities*

M. VINCX, K. Soetaert, Li Jian

ii) *The structure and dynamics of estuarine epi- and hyper-benthic commu-
nities*

O. HAMERLIJNCK, J. Mees, K. Hostens, A. Cattrijse

11.00 11.30 Coffee break, Poster session

11.30 12.30 **Session 5:** Chairman J. Godeaux

i) *Control of phytoplanktonic production by zooplankton in deep oceans*

J.H. HECQ, P. Brasseur, A. Goffart, G. Lacroix

ii) *On the Antarctic paradoxes*

C. LANCELOT, S. Mathot, S. Becquevort, L. Goeyens, F. Dehairs

14.00 15.30 **SESSION 6:** Chairman G. de Moor

i) *Progress in zooplankton research*

J. GODEAUX

ii) *Progress in mariculture research*

P. SORGELOOS

iii) *How toxic are toxic residues. An ecotoxicological view*

C. JOIRIS, J.M. Bouquegneau

15.30 16.00 General conclusions
Chairman J.C.J. Nihoul

Lessons and perspectives
L. ONKELINX, Minister of Environment

16.00 Reception

Composition : Étienne RIGA
T_EX, L_AT_EX (partim), METAFONT

Achevé d'imprimer le 30 octobre 1993 sur la
presse offset d'Étienne RIGA, imprimeur-
éditeur, à La Salle, B-4120 NEUPRÉ

Téléphone + 32 41 71 58 10
Télécopie

